Sheffield Hallam University

A Sheffield Hallam University thesis
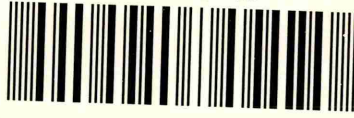
ProQuest Number: 10697316

ProQuest 10697316

LOW FREQUENCIES SOUND INSULATION IN DWELLINGS

Thesis submitted in accordance with the requirements of Sheffield Hallam University for the degree of Doctor in Philosophy by

Sophie Maluski

February 1999

1
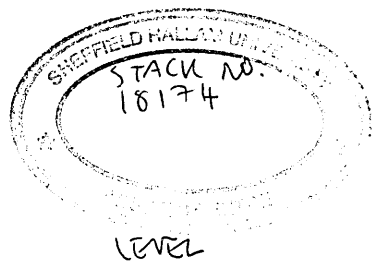
A MA MÈRE,

A LA MEMOIRE DE MON PÈRE

I WOULD LIKE TO DEDICATE THIS THESIS TO MY MOTHER AND TO THE MEMORY OF MY FATHER WHO WAS UNFORTUNATELY UNABLE TO SEE THE COMPLETION OF THIS WORK.

I WOULD ALSO LIKE TO THANK MY PARENTS FOR HAVING GENERALLY INTRODUCED ME TO THE SUBJECT OF ACOUSTICS, AS AN INTEREST WHICH I HAVE MAINTAINED FROM AN EARLY AGE TO THE PRESENT DAY.

2

ABSTRACT

Low frequency noise transmission between dwellings is an increasing problem due to home entertainment systems with enhanced bass responses. The problem is exacerbated since there are not presently available methods of measurement, rating and prediction appropriate for low frequency sound in rooms.

A review of the classical theory of sound insulation and room acoustics has shown that both theories are not applicable. In fact, the sound insulation of party walls at low frequencies is strongly dependent on the modal characteristics of the sound fields of the two separated rooms, and of the party wall. Therefore methods originally developed for measurement conditions where the sound field was considered diffuse, may not be appropriate for room configurations with volumes smaller than $50m^3$ and for frequencies where sound wavelengths are large.

An alternative approach is proposed using a Finite Element Method (FEM) to study the sound transmission between rooms. Its reliability depends on the definition of the model, which requires validating measurement. FEM therefore does not replace field or laboratory measurements, but provides complementary parametric surveys not easily obtainable by measurements.

The method involves modelling the acoustic field of the two rooms as an Acoustic Finite Element model and the displacement field of the party wall as a Structural Finite Element model. The number of elements for each model was selected by comparing the numerical eigenfrequencies with theoretical values within an acceptable processing time and error. The simulation of a single room and of two coupled rooms, defined by linking the acoustic model with the structural model, were validated by comparing the predicted frequency response with measured response of a 1:4 scale model.

The effect of three types of party wall edge condition on sound insulation was investigated: simply supported, clamped, and a combination of clamped and simply supported. It is shown that the frequency trends still can be explained in terms of the classical mechanisms. A thin masonry wall is likely to be mass controlled above 50Hz. A thick wall is stiffness controlled, below 100Hz. A clamped thin wall provides a lower sound insulation than a simply supported, whereas a clamped masonry wall provides greater sound level difference at low frequencies than a simply supported.

The sound insulation of masonry walls are shown to be strongly dependent on the acoustical modal characteristics of the connected rooms and of the structural modal characteristics of the party wall. The sound pressure level difference displays a sequence of alternating maxima and minima about a trend, dictated by the properties of the party wall. The sound insulation is lower in equal room than in unequal rooms, whatever the edge conditions and smaller wall areas provide higher sound insulation than large areas.

A correction factor is proposed as a function of room configuration and wall area and edge conditions. Attempts to quantify the factor were made using statistical and deterministic analyse, but further work is required.

3

AKNOWLEDGEMENTS

CONTENTS

FIGURES

10

TABLES

GLOSSARY OF SYMBOLS

A	absorption in the receiving room (m^2)
B	bending stiffness (N.m)
B	bending stiffness of the plate at the notch (N.m),
B_d:	measurement frequency band (Hz)
C	kinetic energy of the sound field
C	geometrical coupling matrix
C_w	Waterhouse correction factor in dB
CCCC	Name given for the clamped wall
D	damping coefficient per unit area of the wall
D_{nT}	standardised sound pressure level difference (dB)
E	total energy of the sound field
E	Young's Modulus (N.m^{-2}),
F	force applied on the surface of the panel
I_t	transmitted intensity (W.m^{-2})
K	stiffness coefficient per unit area of the wall
K_{N_1}	expansion coefficient.
[K]	acoustic stiffness matrix
[K_s]	wall stiffness matrix
L_1, L_p	space Averaged sound pressure level inside the source room (dB)
L_I	normal sound intensity (dB)
L_2	space-averaged sound pressure levels in the receiving room (dB)
L_{encl}	length of all the edges of the enclosure (m)
L_{2R}	spatial averaged sound pressure level inside the receiving room (dB)
L_{WR}	power level (dB)
L_y, L_z:	dimensions of the party wall (m)
L_x, L_y, L_z:	dimensions of the enclosure and transmission room (m)
M	Modal overlap
[M]	acoustic mass matrix
[M_s]	wall mass matrix
N	number of eigenmodes having frequencies less than f
N_1	modes of the source room of integers n_{x_1} n_y, n_z
N_2	modes of the receiving room of integers n_{x_2}, n_y, n_z
N	modes of integers n_y n_z of the panel
[N]	listing of shape functions
P	potential of the sound field
Q	Sound source function
R	Sound Reduction Index
R'	Apparent sound reduction index or standardised level difference (dB)
R_x, R_y, R_z	rotational displacement in three dimensions

S	surface area of the party wall (m²)
S_0	$S_0 = 1 m^2$ a reference value
S_{encl}	total area of the enclosure (m²)
SNR	Signal/ Noise Ratio
SCSC	name given for the wall with mixed edge conditions - simply supported/clamped/simply/clamped
SSSS	name given for the simply supported wall
T	reverberation time (s)
T_0	reference reverberation time , $T_0 = 0.05s$
T_1	reverberation time of the source room
T.L.	transmission loss (dB)
$T.L._o$	transmission loss at normal incidence (dB)
$T.L._{Diffuse}$	field incidence mass law
U_x, U_y, U_z	translational displacement in the three dimensions
V	room volume (m³)
V_1	volume of the source room (m³)
V_2	volume of receiving room (m³)
W_{inc}	sound power incident (W)
W_{trans}	sound power transmitted (W)
W_{rad}:	radiated sound power by the wall (W)
W_R	power emitted by the reference sound source (W)
W_0	reference power $W_0 = 10^{-12}$ (W)
Γ_1	sound field in the source room
Γ_2	sound field in the receiving room
$\Lambda.$	rotational stiffness of the plate
Λ'	rotational stiffness in terms of the unnotched plate stiffness
Ω_1	primary sound field in the source room
Ω_2	secondary sound field in the source room
Ψ	reverberation term
c_B	bending wave speed (m.s⁻¹)
c_L	longitudinal speed in wall (m.s⁻¹).
c_0	sound velocity in air (m.s⁻¹)
f	frequency (Hz)
f_c	critical frequency (Hz)
$f_{n_y n_z}$	natural frequency or eigenfrequency of the structural mode
f_{n_x, n_y, n_z}	natural frequency or eigenfrequency of acoustic modes (Hz)
Δf_i	bandwidth of a mode, i, (Hz)
h	thickness of the wall or the plate (m)
h_b	thickness of the notch (m)
k_b	free bending wavenumber
k_x, k_y, k_z:	wavenumber components in the x, y- and z-directions

$k_{N_1}^2$	eigenvalues corresponding to g_{N_1} in the source room
$k_{N_2}^2$	eigenvalues corresponding to g_{N_2} in the receiving room
Δl	width of the notch (m)
m	order of the sequence
n(f)	model density of a bending wave field
n_x, n_y, n_z:	integers
p_0	sound pressure amplitude
p_i	incident sound pressure
p_t	transmitted power (W)
$\{p\}$	pressure function in each element
$\{p\}_e$	nodal values of the pressure function associated with the element
t	time (s)
$v(y,z)$	normal vibration velocity distribution
$<v_n^2>$	normal of the space time average mean square vibration velocity
w	vibration displacement of the wall (m)

α	absorption coefficient of the surface material
$\varepsilon, \varepsilon_0$	frequency error, error ratio(%)
ε_v	volumetric strain
Υ	Period of the Maximum Length Sequence
η	loss factor of the party wall
λ_i	incident acoustic wavelength (m)
λ_c	critical wavelength (m)
λ_T	trace wavelength (m)
λ_b	bending wavelength (m)
ν	Poisson ratio.
θ	angle of incident sound wave
ρ_S	surface density (kg.m^{-2}),
ρ_0	air density (kg.m^{-3})
σ_{rad}:	radiation efficiency
τ	transmission coefficient of the party wall
υ	pressure velocity
ω	angular frequency (rad.s^{-1}).
ζ	Party wall velocity.
$\delta(x)$	Dirac function

Other terms are used and defined locally

1   INTRODUCTION

The last 50 years have shown a developing understanding of the sound transmission phenomena in dwellings [Kihlman (1991)]. This has been accompanied by an increasing requirement for high sound insulation for party walls and floors. More recently, the rapid development in mechanical and electrical domestic appliances has resulted in increasing numbers of domestic noise-related complaints [Brooks (1989), Murray (1995), Grimwood (1997)], which is also due to an increase in noise environmental awareness. Many of the complaints are due to the low frequencies originating, for example, from hi-fis, televisions and home-cinemas. Their frequencies often are below 100Hz [Brooks (1989), Mathys (1993), Leventhall (1995), Grimwood (1995 & 97)]. They are well above background noise and are not well controlled by the separating walls and floors between dwellings. Moreover, such noise, including infra-sound, can affect the health of the occupant [Berglung et al (1996), Mirowska (1997)]. Good sound insulation at low frequencies, therefore, is an important requirement in dwellings.

Laboratory measurements of sound insulation at low frequencies produce a poor repeatability [Farina (1997)]. Repeatability is qualitatively, the closeness of agreement between successive results obtained with the same test procedure on the same test specimen under the same conditions (same operator, apparatus, laboratory and short intervals of time between tests) [ISO 140 part 2 (1993)]. Measurements of sound insulation at low frequencies are also known to produce a poor reproducibility [Roland (1995), Goydke (1998)]. Reproducibility is qualitatively, the closeness of agreement between individual results obtained with the same method on identical test specimens but under different conditions (different operators, different apparatus, different laboratories and different times) [ISO 140 part 2 (1993)]. Recent investigations have shown that repeatability and reproducibility in laboratories can be improved by placing special absorption panels [Fuchs et al (1998)] at positions which correspond to acoustic modes [Pedersen (1997), Fuchs et al (1998)].

In the field, the room volumes in dwellings are smaller than those in laboratories; the

measurements at low frequencies also have poor repeatability and poor reproducibility.

The problem, stated in Chapters 2 and 3, is that the classical theory of sound fields and sound insulation and the measurement procedures and corrections which result from them, are not relevant to low frequencies. The theory does not apply when the sound wavelength is large compared with room and wall dimensions, and must be replaced with a modal characterisation of the sound field and of the wall vibration. A room mode or a structural mode is defined as an acoustic or a structural wave which travels along a path and comes back at its starting point.

Present methods of measurements of sound insulation are described in Chapter 4. It is confirmed that the methods of measurement and rating of walls and floors are tenuous below 100Hz.

Measurements of the vibrational field on typical brick walls, presented in Chapter 2, show that the wall edge conditions have a strong effect on the modal behaviour and therefore on the sound insulation at low frequencies. The need to include the edge conditions in the study is highlighted.

The core of this thesis is an investigation of the sound transmission between dwellings in the frequency range 25 - 200Hz. Since no accurate method is available for low frequency measurement, various methods of predicting the sound fields and the wall vibrations are described in Chapter 5 to find the best method.

A Finite Element Method (FEM) is proposed. The theories of the acoustic finite element and of the structural finite element methods are described in Chapters 6 and 8. Its implementation is described in Chapter 6, in particular, the number of elements required to model the rooms and party wall, accurately.

To use FEM for subsequent studies, the choice of the mesh models is validated in Chapter 7. The frequency response is measured in a 1:4 scale enclosure and then compared with the prediction obtained by the Acoustic Finite Element model.

The Acoustic Finite Element model then is extended to describe two rooms, separated

19

by a party wall, as described in Chapter 8. A Structural – Acoustic Finite Element model is created and is validated by comparing the predicted and measured sound pressure level differences. FEM is shown to be an appropriate method for predicting sound transmission at low frequencies between rooms of volumes less than or equal to $50m^3$.

A parametric survey is conducted of the effects of edge conditions and room configuration on the sound level difference in Chapter 9. The effects of edge conditions and room configuration are studied.

In Chapter 10, an attempt is made to find a form of correction factor to field level difference from the deterministic and statistical survey.

Concluding statements and suggested topics for further work are given in Chapter 11.

1.1 REFERENCES

Berglund, B. and Hassmen, P., (1996): *'Sources and effects of low frequency noise'*, Journal of the Acoustical Society of America, Vol.99 (5), 2985-3002

Brooks, J. R., Attenborough, K., (1989): *'The implication of measured and estimated domestic source levels for insulation requirements'*, Proceeding of I.O.A., Vol.11 (11), 19-27

Farina, A., Fausti, P., Pompoli, R. and Scamoni, F., (1997): *'Intercomparison of laboratory measurements of airborne sound insulation of partitions pompoli'*, Proceeding of Inter-Noise 97, 881-886

Fuchs, H.V., Zha, X., Spah, M. and Pommerer, M., (1998): *'Qualifications of small freefield and reverberation rooms for low frequencies'*, Proceeding of Euro-Noise 98, Vol.2, 657-662

Goydke, H., (1998): *'Investigations on the precision of laboratory measurements of sound insulation of building elements according to the revised Standard ISO 140'*, Proceeding of Inter-Noise 98, 480

Grimwood, C., (1995): *'Complaints about poor sound insulation between dwellings'*, Bulletin of the Institute of Acoustics, Vol.20 (4), 11-16

Grimwood, C., (1998), *'Occupant opinion of sound insulation in converted and refurbished dwellings in England and the implication for national building Regulations'*, Proceeding of Euro-Noise 98, Vol.2 (2), 705-710

ISO 140 (1978): *'Measurement of sound insulation in buildings and building elements* Part 2: *Statement of precision requirements'*

Kihlman, T., (1991): *'Fifty years of development in sound insulation of dwellings'*, Proceeding of Inter-Noise 91, 3-15

Knudsen, V.O., (1932): *'Resonance in small rooms'*, Journal of the Acoustical Society, July 1932, 21-37

Leventhal, H.G., (1995): *'The role of low frequency noise and infrasound in sound quality'*, Proceeding of Inter-Noise 95, 933-935

Mathys, J., (1993): *'Low frequency noise and acoustical standards'*, Applied Acoustics, 185-204

Mirowska, M., (1997): *'Low frequency noise in domestic environment: Measurement*

results and assessment of annoyance', 5th International Congress on Sound and Vibration, 15-18 December, Adelaide, South Autralia

Murray, I., (1995): '*Noisy neighbours*', Journal THE TIMES, Monday 14 August 1995, 1-7

Pedersen, D.B., (1997), '*Laboratory measurement of the low frequency sound insulation*', DAGA 97, Kiel, 105-106

Roland, J, (1995): '*Adaptation of existing test facilities to low frequencies measurements*', Proceeding of Inter-Noise 95, 1113- 1115

2 SOUND INSULATION OF PARTY WALLS AT LOW FREQUENCIES

2.1 INTRODUCTION

In Chapter 1, it has been highlighted that airborne sound insulation is difficult to measure at low frequencies. In this chapter, it is shown that classical theories of sound fields in enclosures and the transmission of sound through panels are not applicable because the modal behaviour of the sound fields and of the panel are not described. This will be demonstrated by first describing sound insulation of an infinite wall using classical theory. Then, sound insulation of a finite wall is described for both diffuse and non diffuse sound fields. The modal behaviour of the party wall and of the sound field will be observed to control the sound transmission. Measurements of the structural modes of two brick walls are described and the effects of edge conditions are observed to control the eigenfrequencies, and hence the bending wave modal distribution.

2.2 SOUND TRANSMISSION OF AN INFINITE WALL

2.2.1 Transmission Loss

In classical theory, the wall is assumed thin, isotropic, flat and infinite in extent [London(1949), Sewell (1970), Beranek (1992), Bies et al (1996)]. An incident sound wave strikes the surface of the wall at an angle θ. Part of the sound energy is reflected, part of it is absorbed and part of it is transmitted. The determination of the energy transmitted through the wall is defined by the transmission coefficient τ, given [Beranek (1992)], as;

$$\tau(\theta,\omega) = \frac{W_{trans}(\theta,\omega)}{W_{inc}(\theta,\omega)} \qquad (2.1)$$

where τ (θ,ω) is the transmission coefficient of the party wall at incident angles θ and angular frequency ω, $W_{inc\ (\theta,\omega)}$ is the sound power incident on the source side and $W_{trans(\theta,\omega)}$ is the sound power transmitted to the receiver side.

The transmission can be expressed in terms of the transmission loss (T.L.) in dB, also known as the sound reduction index (R), given by;

$$\text{T.L.} = 10\log\left(\frac{1}{\tau(\theta,\omega)}\right) \tag{2.2}$$

2.2.2 Classical theory of sound insulation

The sound insulation is often described by the approximate equation [Crocker et al (1982)];

$$\text{T.L} = 10\log\left(\frac{D_1^2 + (\omega\rho_S - K/\omega)^2}{4\rho_0^2 c_0^2 / \cos^2\theta}\right) \tag{2.3}$$

where $D_1^2 = D + 2\rho_0 c_0 / \cos\theta$, D is the damping coefficient per unit area, **K** is the stiffness coefficient per unit area, ρ_S is the mass per unit area, ρ_0 is the air density, c_0 is sound velocity in air. Equation 2.3, however, does not include the effects of the higher order panel resonances and wave coincidence, which have been observed experimentally.

The transmission loss against frequency, presented in Figure 2.1, is deduced partly from theoretical and experimental considerations. Five regions are distinguished:

1. Bending stiffness control
    The wall acts as a spring, the stiffness of which controls the sound transmission, to give;

$$T.L. = 10\log\left(\frac{K/\omega}{4\rho_0^2 c_0^2 / \cos^2\theta}\right) \qquad (2.4)$$

The sound transmission loss decreases with frequency increase, at -6dB/octave, until the first panel resonance is excited [Bies et al (1996)]. Transmission loss is dependent on the incident angle and the medium fluid.

2. Wall resonance

The wall resonates at frequencies where the mass and the stiffness controlled mechanisms cancel. This phenomenon is described in detail in section 2.4.2.

3. Mass control

The sound transmission is controlled by the mass of the wall, according to;

$$T.L. = 10\ \log\left(\frac{(\rho_s\,\omega)^2}{4\rho_0^2 c_0^2 / \cos^2\theta}\right) \qquad (2.5)$$

where the terms are as in Equation 2.3. The wall in this region behaves as a limp wall. **K** and D are negligible. The transmission loss also depends on the angle of incidence, θ.

For normal incidence, when θ = 0,

$$T.L._0 = 20\ \log\left(\frac{\rho_s\omega}{2\rho_0 c_0}\right) \qquad (2.6)$$

Also, if the wave strikes the wall at grazing incidence (θ =90°), the sound is assumed to transmit through the wall without attenuation. If the superficial mass, m, is doubled or if the frequency is doubled, the sound insulation increases by 6dB. This is known as the mass law, and a thick single wall therefore has a greater sound transmission loss than a thin wall.

25

If all incident angles are included to give a random incidence value, the Equation 2.5 is rewritten as follows;

$$T.L._{Random} = T.L._0 - 10 \log(0.23\, T.L._0) \tag{2.7}$$

If angles from the normal to 78^0 are included ($T.L._0 > 15dB$), the Equation 2.7 becomes [Beranek (1992)];

$$T.L._{Diffuse} = T.L._0 - 5 \tag{2.8}$$

where $T.L._{Diffuse}$ is known as the field incidence mass law

4. Coincidence region

The coincidence region starts from the critical frequency, f_c, when the bending wave speed (see Section 2.4.1) equals the sound speed.

When the wall is excited by an incident acoustic wave, λ_i, at an angle θ, a trace wave of wavelength λ_T, is generated, where

$$\lambda_T = \lambda_i / \sin\theta \tag{2.9}$$

When the trace wavelength matches free bending wavelength, λ_b, wave coincidence occurs and $\lambda_b = \lambda_i / \sin\theta$. Critical coincidence takes place at grazing incidence (i.e. $\theta = 0$). Subsequent wave coincidences occur at non-grazing angles, up to the damping control region.

5. Damping control

The sound transmission is controlled by the damping of the wall, which is mainly due to the transfer of energy through the junctions to other parts of the buildings [Craik (1981)]. Transmission loss is given by;

$$T.L. = T.L._0 + 10 \log(f/f_c - 1) + 10 \log\eta - 2 \tag{2.10}$$

26

where η is the loss factor of the party wall. In this region, the transmission loss increases at 9dB per octave till the mass law performance is recovered at 6dB/octave.

2.3   SOUND TRANSMISSION OF A FINITE WALL

2.3.1 Sound insulation in a diffuse field

An isotropic wall of dimensions greater than the incident sound wavelength is considered. Bending wave resonances are allowed at specific frequencies, dictated by the wall dimensions. However, the predicted transmission loss for infinite walls often applies to finite walls. The sound pressure level on the source side, L_1, forces the panel to vibrate, which then radiates to the receiving side creating a sound pressure level, L_2. The transmission loss is then obtained from the two sound pressure levels, the surface of the party wall, S, and the absorption in the receiving room, A, giving;

$$T.L. = L_1 - L_2 + 10\log\left(\frac{S}{A}\right) \qquad (2.11)$$

Such relationships are however only applicable for frequencies well above the first bending-wave resonance of the panel where the wavelength is small compared with the party wall dimensions [Bhattacharya (1971)]. The edge conditions are assumed not to be influential, whereas the real edge conditions of the party wall are found to have a strong influence on the coincidence region [Kihlman (1970), Kihlman (1972), Bies et al (1996)]. The coincidence region tends also to be not observable when the thickness of the party wall is large such as for masonry walls [Bergasolli (1970)]. The damping region is strongly influenced by edge damping and internal damping. Despite those highlighted problems, Equation 2.11 is the accepted theoretical basis for standard measurements.

2.3.2 Sound insulation when wavelength is equal to panel dimensions

The same thin, flat, isotropic wall is considered. The sound wavelength, now, is equal or greater than the panel dimensions. Two types of sound pressure fields are considered:

1) The sound field consists of a large number of excited room modes in the measurement band (often one-1/3 octave). An example of this is the sound fields in large rooms at low frequencies

2) The sound field consists of a small number of excited room modes. An example of this is the sound fields in small rooms.

In the first case, the sound transmission loss deviates from the mass law, whatever the panel dimensions [London (1949), Sewell (1970), Nilsson (1972), Mulholland (1973), Novikov (1998), Gargliadini (1990-91)]. The panel radiates like a piston [Heckl (1981)]. Nilsson [1972] defined a new relationship which takes into account the non-statistical behaviour of the sound field and the modal behaviour of the panel, including edge conditions. Novikov [1998] defined a correction factor including the area of the plate and of the laboratory wall where the panel is placed. Utley [1968] and others [Nilsson (1972), Bhattacharya (1972)] showed that the discrepancies depend on the configuration of the transmission rooms (dimensions, aspect ratio, etc.).

The second case is illustrated by Figure 2.2. The transmission loss shows the same trend as a mass law trend, but displays alternating maxima and minima due to acoustic couplings between rooms. The phenomenon has been observed by many authors [Heckl (1958), Utley (1968.), Mulholland (1973), Sharp (1978), Kropp (1994), Osipov (1996-97), Pietrzyk (1997),]. The number of excited room modes is much less than that in a diffuse sound field and the sound is transmitted by forced vibration of the wall [Josse and Lamure (1964), Sharp (1978)]. The room modes force the surface of the wall to take the same mode shape which then radiates into the receiving room. These strong variations tend to cancel each other out when 20 modes at least are excited in a third octave band [Mulholland (1973), Halliwell et al (1985)].

If the thin isotropic wall is replaced by a thick isotropic wall, the structural modal density is then small at low and mid frequencies [Warburton (1953), Bergassoli (1970),

Pietrzyk (1997)]. Again, the sound is transmitted by forced vibration of the wall [Josse and Lamure (1964), Sharp (1978)]. Acoustic-structural couplings occur, which also create alternating maxima and minima in transmission loss. The forced transmission is seen as the most important phenomenon of transmission rather than the transmission at resonance [Josse and Lamure (1964), Mulholland (1973)].

To summarise, the transmission loss at low frequencies is strongly influenced by both the acoustical and the structural modal characteristics.

2.4 VIBRATIONAL BEHAVIOUR OF A FINITE WALL

2.4.1 Thin Wall

A finite wall is assumed where thickness is small compared with the airborne and structure borne wavelengths. Various structural waves are generated when a force is applied to the surface of the wall or a force applied to all surfaces [Fahy (1985)]. They include shear, torsional and compressional waves. Shear waves are identified as transverse waves with displacements normal to the plane of the wall. Torsional waves are also shear waves, but are characterised by a torsional displacement. The direction of particle displacement of compressional waves is in the direction of wave propagation. The three waves are regrouped into one flexural wave; the bending wave which depends on the thickness of the wall. A wall cannot be considered as thin when the thickness is greater than a sixth of the bending wavelength [Cremer (1953 & 88)].

The bending stiffness, B, is defined as follows;

$$B = \frac{Eh^3}{12(1-v^2)} \qquad (2.12)$$

where E is the Young's Modulus (N.m^{-2}), h is thickness of the wall (m) and v is the Poisson ratio.

Bending waves control the surface displacement of the wall. They are easy to excite due to their low input impedance, and are good sound radiators because their motion is normal to the plate surface.

Bending wave speed, c_B, is given by;

$$c_B = \left(\frac{B\omega^2}{\rho_S} \right)^{1/2} \qquad (\text{m.s}^{-1}) \qquad (2.13)$$

where ρ_S is the surface density of the wall (kg.m^{-2})

The speed of the bending wave increases with the square root of the frequency. It is dependent upon the thickness of the wall, where the lowest propagation speed is obtained for the thinnest wall. The bending wave speed is smaller than the velocity of sound in air at frequencies below the critical frequency and greater above the critical frequency. Such differences in velocity explain the radiation and control of the sound transmission through the wall.

2.4.2 Masonry wall

When a thick wall i.e. a wall with a thickness greater than 1/6 of the bending wavelength, is excited by an acoustic wave, bending waves and shear waves are excited. Resonance and radiation efficiency are then different from a wall where only bending waves are excited [Heckl (1958 & 81), Llungren (1991-a&b), Rindel (1988)].

Rindel [1988] developed an expression for wall radiation, which combines the bending wave and shear wave speeds. He showed that at low frequencies, speed of transverse waves is asymptote to the bending wave speed. The wall radiation is therefore controlled by the bending wave speed only. Llungren [1991] investigated analytically the airborne sound transmission of thick walls. He also showed that the solution agrees with the bending wave solution at low and medium frequencies. He showed that the classical theory of thin plate can be extended to three times the thickness of the wall.

30

That idea, however, is not developed here. Consequently, the thick wall can be expressed by the classic thin plate theory [Cremer (1953 & 88)].

A brick wall of 0.125m thickness in section 2.5 and three other brick walls of 0.5, 0.1 and 0.2m thickness in Chapter 9 are investigated. The limit of applicability of the thin plate theory to a 0.5m brick wall of longitudinal velocity equals to 2350Hz is shown in Figure 2.3 [Cremer (1953 & 88)]. The thin plate theory can only be applied below 2475Hz. For a brick wall of 0.1m, 0.125m and 0.2m thickness, the thin plate theory is only applicable below 1236Hz, 996Hz and 619Hz, respectively. As the frequency range of interest is 25Hz - 200Hz, thin plate theory can apply.

2.4.3 Modal behaviour

The vibration displacement w of the finite wall [Fahy (1985), Leissa (1993)] is expressed as;

$$B\left(\frac{\partial^2 w}{\partial y^2} + \frac{\partial^2 w}{\partial z^2}\right)^2 = -\rho_S\left(\frac{\partial^2 w}{\partial t^2}\right) \tag{2.14}$$

where t is the time.

A solution of this equation is

$$w(y,z,t) = \tilde{w}\,\exp\left[j\left(\omega t - k_y y - k_z z\right)\right] \tag{2.15}$$

where

$$k_y^2 + k_z^2 = k_b^2 = \left(\omega^2 \rho_S / B\right)^{1/2} \tag{2.16}$$

k_b is the free bending wavenumber and k_y, k_z are the wavenumber components in the y- and z-directions, respectively.

If a rectangular wall of sides L_y and L_z, is assumed simply supported i.e., no translational displacement at the edges, the normal vibration velocity distribution,

31

$v(y,z)$, takes the form

$$v(y,z) = v_{n_y n_z} \sin\left(\frac{\pi n_y y}{L_y}\right) \sin\left(\frac{\pi n_z z}{L_z}\right) \qquad (2.17)$$

for $0 \leq y \leq L_y$, $0 \leq z \leq L_z$, n_y, n_z are integers and $k_y = \dfrac{\pi n_y}{L_y}$, $k_z = \dfrac{\pi n_z}{L_z}$

Substituting k_y and k_z into Equation 2.16, the natural frequencies of a simply supported wall is given by [Warburton (1953), Leissa (1993)]

$$f_{n_y n_z} = \frac{1}{2}\left(\frac{B}{\rho_S}\right)^{1/2}\left[\left(\frac{n_y}{L_y}\right)^2 + \left(\frac{n_z}{L_z}\right)^2\right] \qquad (2.18)$$

$f_{n_y n_z}$ is also called the eigenfrequency of the structural mode, identified by the integers n_y and n_z. Those modes occur when the structural wave reflects to form a standing wave. Standing waves can be identified by the presence of points or lines of zero displacement, called nodes, and areas of maximum displacement, called anti-nodes. The modal pattern at an eigenfrequency is identified by the integers n_x and n_y.

Two types of mode shape can be identified. The first is when the flexural wave only propagates in one dimension e.g. $n_x = 1$. The second is when the structural wave propagates in two dimensions. Those structural modes are dependent on the frequency and the wall dimensions [Warburton (1953), Leissa (1993)]. Figure 2.4 shows one dimensional and two dimensional modes.

When the excitation frequency coincides with the natural frequency of the plate [Fahy (1985)], the panel is said to be resonant and can lead to a reduction in transmission loss. The excitation can be a single frequency, corresponding to the natural frequency and it can also be a broadband input, which contains the frequency component corresponding to the natural frequency of a system.

The number of modes and the mode shapes vary with the panel dimensions. The number of modes also differs between thin and heavyweight walls. Figure 2.5 shows the number of modes for a thin plate, while Figure 2.6 shows the number of modes for a heavyweight wall.

For the thin plate, the first structural mode is excited at low frequency. The mode density of a bending wave field, n(f), is independent of frequency and is given by [Beranek (1992)];

$$n(f) = \frac{\sqrt{12}\,S}{2\,c_L h} = \frac{\sqrt{12}\,S}{2\sqrt{\dfrac{E}{\rho_s(1-v^2)}}\,h} \qquad\qquad s \qquad\qquad (2.19)$$

where c_L is the longitudinal speed (m.s^{-1}).

For a thick wall, the first structural mode is excited higher in the frequency range and the modes are well spaced.

Modification of the dimensions changes the modal density and the mode shape, and therefore influences the sound transmission loss [Gargliadini (1991)]. However, those effects tend to be reduced when at least 3 modes per third octave bands are excited.

2.4.4 Forced Vibration

The response of the wall varies if the excitation is localised (e.g. a hammer) or extended (e.g. airborne sound). When excited by a localised force, the position of the excitation can be on a nodal line of zero displacement or at an anti-node of maximum displacements. If on the nodal line, the wall cannot be excited. Thus, the applied force should always be placed on an anti-node to get the best response.

When an acoustic wave strikes the surface of the wall, vibration occurs over the entire exposed surface of the plate. Free vibration occurs at frequencies corresponding to the eigenfrequencies of the wall. Forced vibration occurs when the acoustic wave forces the

33

wall surface to take the same mode shape as the acoustic mode.

2.4.5 Wall radiation

When the incident sound field drives the wall, free and forced vibrations take place. The air particle motion, normal to the vibrating surface, tends to cancel over a bending wavelength, in the middle of the wall surface. However, at boundaries, the cancellation is not total and radiation occurs. Therefore, radiation is strongly dependent on the ratio of the bending wavelength to that in air.

For a wall of dimensions greater than the acoustic wavelength, resonant modes can be classed as either acoustically fast (A.F.) modes or acoustically slow (A.S.) modes [Crocker (1982)]. The A.F. modes correspond to wavelengths greater than the acoustic wavelength. They always match the trace wavelength and the fluid cannot produce pressure waves which will move fast enough to cause any cancellation. The wall thus radiates from the whole surface area of the wall, giving a high radiation efficiency.

The A.S. modes correspond to wavelengths smaller than the acoustic wavelength. The fluid produces pressure waves which move fast enough to cause cancellation. The radiation efficiency is low. The radiation is first the result of A.S. modes at plate corners where cancellation is incomplete. At higher frequency, edge modes occur where the bending wave speed is subsonic only in a direction parallel to one pair of edges and supersonic in a direction parallel to the other pair. Cancellation can only occur in one edge direction.

When modes are not vibrating at their resonance frequencies, little sound is radiated and there is poor coupling between the wall and the fluid. The sound transmission is termed non resonant and gives rise to the mass law transmission.

For a finite wall of dimensions smaller that the acoustic wavelength, not many structural modes are present and their distribution is not even. Radiation varies with the excited structural mode [Schroter et al (1981), Lamancuza (1994)] and each mode has thus its

34

own radiation efficiency σ_{rad} defined as

$$\sigma_{rad} = \frac{W_{rad}}{<v_n^2> \rho_0 c_0 S} \qquad (2.20)$$

where $<v_n^2>$ is the normal of the space time average mean square vibration velocity of the radiating surface of area S and W_{rad} is the radiated sound power.

The odd-odd modes (e.g. modes (1,1), (5,3)) are found to radiate more than the even-odd modes (e.g. modes (2,1), (3,6)) and even more than the even-even modes (e.g. modes (2,2), (2,4)) [Schroter et al (1981), Fahy (1985)]. It can be explained by looking at the number of positive and negative cells seen in Figure 2.7. When cells situated on the opposite sides of the wall are of the same sign, the wall radiates more than that with cells of opposite sign. The radiation is also controlled by the surface of the cell. If there are many cells i.e. cells of small area, cancellation occurs reducing the amount of radiated energy.

The radiation efficiency of a mode can be altered with the force applied on the surface of the wall [Simmons (1989)]. Indeed, the wall surface can be forced to take the same shape as its eigenmode at any frequency. The radiation of the wall is then the sum of the radiation efficiencies of all the modes.

Radiation efficiency is dependent on the dimensions of the wall [Schroter et al (1981), Novak (1994)]. Low radiation efficiency is obtained for plates which are less than $16m^2$ and the critical frequency is not observed [Novak (1994)]. Radiation efficiency is dependent on the thickness of the wall [Schroter (1981), Lamancusa (1994)] and variable thickness can lead to minima in sound radiation [Lamancusa (1994)]. Radiation efficiency is dependent on the edge conditions as seen in Figure 2.8 [Maidanik (1962), Guyader at al (1994), Lamancusa (1994)]. The radiation efficiency is minimised when edges are clamped.

2.4.6 Damping

The damping may take the form of material damping, interface damping, or radiation into connected fluids. In most cases, damping does not significantly change the phase velocity and has not much effect in the sub-critical region of the party wall [Fahy (1985)], but is effective when the response of the panel is dominated by resonant modes. Resonant and coincidence regions are controlled by damping.

2.4.7 Edge Conditions

The two extreme wall edge conditions are simply supported and clamped. Simply supported allows no transverse displacement and produces shear force reaction, but rotational movement is not restrained. Clamped edge condition allows no transverse or rotational displacement. The change of edge conditions from simply supported to clamped condition results in a shift of the structural modes to higher frequencies [Warburton (1953), Cremer (1988)]. The modal pattern and thus the radiation of the wall is then modified [Warburton (1953), Maidanik (1970), Sewell (1970), Kihlman (1970), Nilsson (1972), Berry et al (1991), Guyader et al (1994), Lamancusa (1994)]. This in turn alters the transmission loss [Balike (1994), Berry et al (1994)].

When the wall is excited by an acoustic wavelength smaller than the panel dimensions, clamped conditions lead the thin plate to radiate twice the energy of the simply supported condition [Maidanik (1962), Sewell (1970), Kihlman (1970), Nilsson (1972)].

To summarise; edge conditions control the forced and free bending waves and thus the transmission loss.

2.5   MEASUREMENTS OF THE FREQUENCY RESPONSE OF MASONRY WALLS

At present, it was shown theoretically that masonry walls are characterised by a small

modal density, with a first eigenfrequency high in the frequency range. Also in section 2.4.7, it was highlighted that edge conditions control the modal density. It is therefore necessary to investigate experimentally the edge conditions of real walls as a prelude to investigating vibro-acoustic coupling in Chapter 9. It is not likely that the edge conditions of masonry walls are properly described as simply supported, clamped or any other classical condition. Therefore, the vibration response of typical brick walls was measured from which the installed edge conditions could be inferred.

2.5.1 Two Brick walls

Two brick walls of a transmission suite were chosen for this experiment as seen in Figure 2.9. The larger wall, A, was of dimensions 2.88 x 2.49m. The smaller wall, B, was 1.84 x 2.49m. Both walls were of 115mm brick, with one side painted and the other side covered with a plaster layer (internal face). Both were supported by a concrete slab with a concrete ceiling on the top (see Figure 2.10). The walls formed two junction types. The first was with the floor and the roof slab. The second formed a corner with the other brick walls.

2.5.2 Experiment set up

Figure 2.11 illustrates the experimental set up for measuring vibrational response. The measuring system comprised of an electro-dynamic shaker, a function generator, a power amplifier, two accelerometers, a charge amplifier and an oscilloscope.

The position of the shaker on each wall was chosen carefully to ensure that it was not at a structural node. According to Equation 2.18, modes (1,2), (2,1), (3,1), (1,3), (2,2), are likely to be excited below 200Hz. The corresponding nodal lines are along the centre of the walls or at a distance of one third dimensions from the edges. Therefore the shaker was located one quarter dimension from the edges. The shaker on wall A was placed at 1.15m from the bottom and 0.38m from the corner edge. The shaker was placed on the wall B at 0.61m from the bottom and 0.46m from the corner edge. The shaker was attached to a steel indenter of the same diameter as the drilled hole, by cementing and

bolting it in order to reduce the influence of local deformation.

2.5.3 Measurement procedure

The power amplifier and function generator were used to drive the electro-dynamic shaker with a slow swept sine signal over 0-200Hz. The signal sent to the shaker was shown on the oscilloscope and used as a reference. An accelerometer was used to record the acceleration amplitudes of the surface at points on a 0.300m x 0.355m grid for wall A and on a 0.300m x 0.250m grid for wall B. The signal from the accelerometer also was displayed on the screen of the oscilloscope and compared visually with the reference signal. The nodal lines were determined when the measured signal was a minimum or when the measured signal changed phase with respect to the reference signal. It was possible to identify several lower order modes as shown in Figures 2.12-13. Modes (1,1), (2,1), (3,1) and (1,3) of wall A (see Figure 2.12) and modes (1,1), (1,2), (2,1), (2,2) and (1,3) of wall B (see Figure 2.13) were obtained. The measurement of modes shapes was relatively easy at very low frequencies, but became more difficult as the frequency increased, particularly, the mode (1,3) of wall A.

2.5.4 Edge condition identification

In order to identify the likely corresponding edge conditions, the eigenfrequencies and their order were compared with theoretical prediction according to Warburton [1953] and Leissa [1993].

For a simply supported panel, the resonance frequencies are calculated from Equation 2.18. An approximate expression is given for a rectangular supported panel having one clamped edge [Leissa (1993)];

$$f_{n_y n_z} = \frac{\pi}{2} \sqrt{\frac{B}{\rho_s} \left(\left(\frac{n_y}{L_y} \right)^2 + \left(\frac{n_z + 0.25}{L_z} \right)^2 \right)} \qquad (2.21)$$

and for a rectangular supported panel having two clamped edges [Leissa (1993)];

$$f_{n_y n_z} = \frac{\pi}{2} \sqrt{\frac{B}{\rho_s}} \left(\left(\frac{n_y}{L_y}\right)^2 + \left(\frac{n_z + 0.5}{L_z}\right)^2 \right) \qquad (2.22)$$

As the wall properties were not known, the factor including bending stiffness and mass surface was defined using the wall dimensions and the measured eigenfrequency of the first mode. The other theoretical eigenfrequencies were then calculated. That means the clamped conditions cannot be calculated as the relationship not only depends on that factor but also depends on Poisson's ratio value. The clamped condition was therefore not calculated.

Figure 2.14 and Figure 2.15 show the frequency error ε, calculated between the theoretical and measured eigenfrequencies of the wall A and B, respectively, for simply supported, simply supported with one clamped edge, and simply supported with two clamped edges, according to the following relationship;

$$\varepsilon = \frac{\text{Predicted value} - \text{Measured value}}{\text{Predicted value}} \times 100 \qquad (2.23)$$

The smallest error for each mode was obtained for two simply supported and two clamped edges, whatever the wall.

In general, the edge conditions of a real party wall therefore lie between simply supported and clamped, a phenomenon already observed by Balike [1994]. However, the two walls have corner edges which often is not present in constructions of dwellings. Real party walls have T-edges, and they provide stiffer edge constraint than corner edges. The approach of this study therefore was to investigate the range of possible edge conditions likely, including simply supported, clamped and mixed edge conditions. The real conditions could be assumed to lie somewhere in this range.

2.6   CONCLUSION

Classical theory of sound insulation does not apply when the sound field is not diffuse and when the party wall has only a few structural modes in the frequency range of interest. The transmission loss is governed by the interaction of the acoustic and the structural modes. Thus any modification to the structural modal distribution will influence the transmission loss. The structural modal distribution is dependent on wall dimension and edge condition and in real buildings, those two factors are likely to vary significantly.

Measurements have shown that the real edge conditions of a brick wall are likely to lie between simply supported and clamped. Consequently, the sound transmission loss at low frequencies can only be predicted by taking account of the acoustical modal behaviour of the source and receiving rooms and of the structural modal behaviour of the party wall including the edge conditions. The acoustic field in rooms now will be investigated in Chapter 3.

2.7 REFERENCES

Balike, M. and Bhat, R.B., (1994): '*Noise transmission through a cavity backed flexible plate with elastic edge constraints*', 3rd International Congress on Air and Structure Borne Sound and Vibration, 335-343

Beranek, L.L. and Ver, I.L., (1992): '*Noise and Vibration Control Engineering: Principles and Applications*', Ed. J.Wiley and Sons

Bergassoli, A. and Brodut, M., (1970): '*Transparence des murs et des cloisons*', Acustica, Vol.23, 315-322

Berry, A. and Guyader, J.L., (1991): '*A general formulation for the sound radiation from rectangular baffled plates with arbitrary boundary conditions*', Journal of Acoustical Society of America, Vol.37 (5), 93-102

Berry, A. and Nicolas, J., (1994): '*Structural acoustics and vibration behaviour of complex panels*', Applied Acoustics, Vol.43, 185-215

Bhattacharya, M.C. and Guy, R.W., (1972): '*The influence of the measuring facility on the measured sound insulating property of a panel*', Acustica, Vol.26, 344-348

Bhattacharya, M.C., Guy, R.W. and Crocker, M.J., (1971): '*Coincidence effect with sound waves in a finite plate*', Journal of Sound and Vibration, Vol.18 (2), 157-169

Bies, D.A. and Hansen, C.H., (1996): '*Engineering noise control: Theory and practice*', 2nd Ed. E & FN SPON

Craik, R.J.M., (1981): '*Damping of building structures*', Applied Acoustics, C.81, 347-359

Cremer, L., (1953): '*Calculation of sound propagation in structures*', Acustica, Vol.3 (5), 317-335

Cremer, L., Heckl, M. and Ungar, E.E., (1988): '*Structure-Borne Sound*', Ed. Springer-Verlag

Crocker, M.J. and Kessler, F.M., (1982): '*Noise and Noise Control*', Vol.2, Ed. Crc Press

Fahy, F., (1985): '*Sound and structural vibration: radiation, transmission and response,*' Ed. Academic Press

Gargliadini, L. and Roland, J., (1991): '*The use of a functional basis to calculate*

acoustic transmission between rooms', Journal of Sound and Vibration, Vol.145 (3), 457-478

Gargliadini, L., (1990): '*Simulation numerique de la mesure en laboratoire de l'indice d'affaiblissement acoustique: Effets des sources et de la geometrie de la paroie*', Colloque de Physique, Colloque C2, Supplement n⁰ 2, Tome 51

Gibbs, B.M. and Gilford, C.L.S., (1976): '*The use of power flow methods for the assessment of sound transmission in building structures*', Journal of Sound and Vibration, Vol.49 (2), 267-286

Guyader, J.L. and Laulagnet, B., (1994): '*Structural acoustic radiation prediction: Expanding the vibratory response on a functional basis*', Applied Acoustics, Vol.43, 247-269

Halliwell, R.E. and Warnock, C.C., (1985), '*Sound transmission loss: Comparison of conventional techniques with sound intensity techniques*', Journal of Acoustical Society of America, Vol.77 (6), 2094-2103

Heckl, M. and Seifert, K., (1958): '*Investigations if the influence of eigen-resonances of rooms on the result of the sound insulation measurement*', Acustica, Vol.8 (4), 212-220

Heckl, M., (1981): '*The tenth Sir Richard Fayrey memorial lecture: sound transmission in buildings*', Journal of Sound and Vibration, Vol.77 (20), 165-189

Josse, R. and Lamure, C., (1964): '*Transmission du son par une paroie simple*', Acustica, Vol.14, 267-280

Kihlman, T., (1967): '*Sound radiation into a rectangular room. Application to airborne sound transmission in Buildings*', Acustica, Vol.18, 11-20

Kihlman, T., (1970): *Report on the influence of boundary conditions on the reduction index*, Report N0 ISO/TC43/SC2/WG2, Chalmers Tekniska Hogskila, Goteborg, Sweden

Kihlman, T and Nilsson, A.C., (1972): '*The effects of some laboratory designs and mounting conditions on reduction index measurements*', Applied Acoustics, Vol.5

Kropp, W., Pietrzyk, A. and Kihlman, T., (1994): '*On the meaning of the sound reduction index at low frequencies*', Acta-Acustica, Vol.2, 379-392

Lamancusa, J.S. and Eschenauer, H.A., (1994): '*Design optimisation method for rectangular panels with minimal radiation*', AIAA Journal, Vol.32 (3), 472-479

Leissa, A., (1993): '*Vibration of plates*', Ed. Acoustical Society of America

Ljunggren, S., (1991-a): '*Airborne sound insulation of thin walls*', Journal of Acoustical Society of America, Vol.89 (5), 2324-2337

Ljunggren, S., (1991-b): '*Airborne sound insulation of thick walls*', Journal of Acoustical Society of America, Vol.89 (5), 2338-2345

London, A., (1949): '*Transmission of reverberant sound through single walls*', Research Paper RP1998, Vol.42, 605-615

Maidanik, G., (1962): '*Response of a ribbed panels to reverberant acoustic fields*' Journal of Acoustical Society of America, Vol.34, 809-826

Maluski, S. and Bougdah, H., (1997): '*Predicted and measured low frequency response of small rooms*', Journal Building Acoustics, Vol.4 (2), 73-86

Maluski, S. and Gibbs, B.M., (1998): '*The influence of partitions boundary conditions on sound level difference between rooms at low frequencies*', Proceeding of Euro-Noise 98, Vol.2, 681-686

Muholland, K.A. and Lyon, R.H., (1973): '*Sound insulation at low frequencies*', Journal of Acoustical Society of America, Vol.54 (4), 867-878

Nilsson, A.C., (1972): '*Reduction index and boundary conditions for a wall between two rectangular rooms, Part I and II*', Acustica, Vol.26, 1-23

Novak, R. A., (1994): '*The radiation factor of finite plates at low frequencies*', Third International Congress on Air-and structure-borne sound and vibration, June 13-15, Montreal, 23-29

Novikov, I.I., (1998): '*Low-frequency sound insulation of thin plates*', Applied Acoustics, Vol.54 (1), 83-90

Osipov, A., Mees, P. and Vermeir, G., (1996): 'Low frequency airborne sound transmission in buildings: Single plane walls', Proceeding of Inter-Noise 96, 1791-1794

Osipov,A., Mees, P., and Vermeir, G., (1997): '*Low frequency airborne sound transmission through single partitions in Buildings*', Applied Acoustics, Vol.52 (3-4), 273-288

Pietrzyk, A. and Kihlman, T., (1997): '*The sensitivity of sound insulation to partition location -case of heavyweight partition*', Proceeding of Inter-Noise 97, 727-730

Rindel, J.H., (1988), '*Prediction of sound transmission through thick and stiff panels*', Proceeding of I.O.A., Vol.10 (8), 119-126

Schroter, V. and Fahy, F.J., (1981): *'Radiation from modes of rectangular panel into a coupled fluid layer'*, Journal of Sound and Vibration, Vol.74 (4), 575-587

Sewell, E.C., (1970): *'Transmission of reverberant sound through a single leaf partition surrounded by an infinite rigid baffle'*, Journal of Sound and Vibration, Vol.12 (1), 21-32

Sharp, B.H., (1978): *'Prediction methods for the sound transmission of building elements'*, Noise Control Engineering, September- October 1978, Vol.11 (2), 53-62.

Simmons, C. and Maxwell, R., (1989): *'Radiation index of baffled plates with stiffeners, using the finite element method and the fast fourier transform'*, Proceeding of Inter-Noise 89, 530-534

Utley, W.A., (1968*)*: *'Single leaf transmission loss at low frequencies'*, Journal of Sound and Vibration, Vol.8 (2), 256

Warburton, G.B. (1953): *'The vibration of rectangular plates'*, Proceeding of. Onst. Mechanical Engineering, Vol.168, 371-377
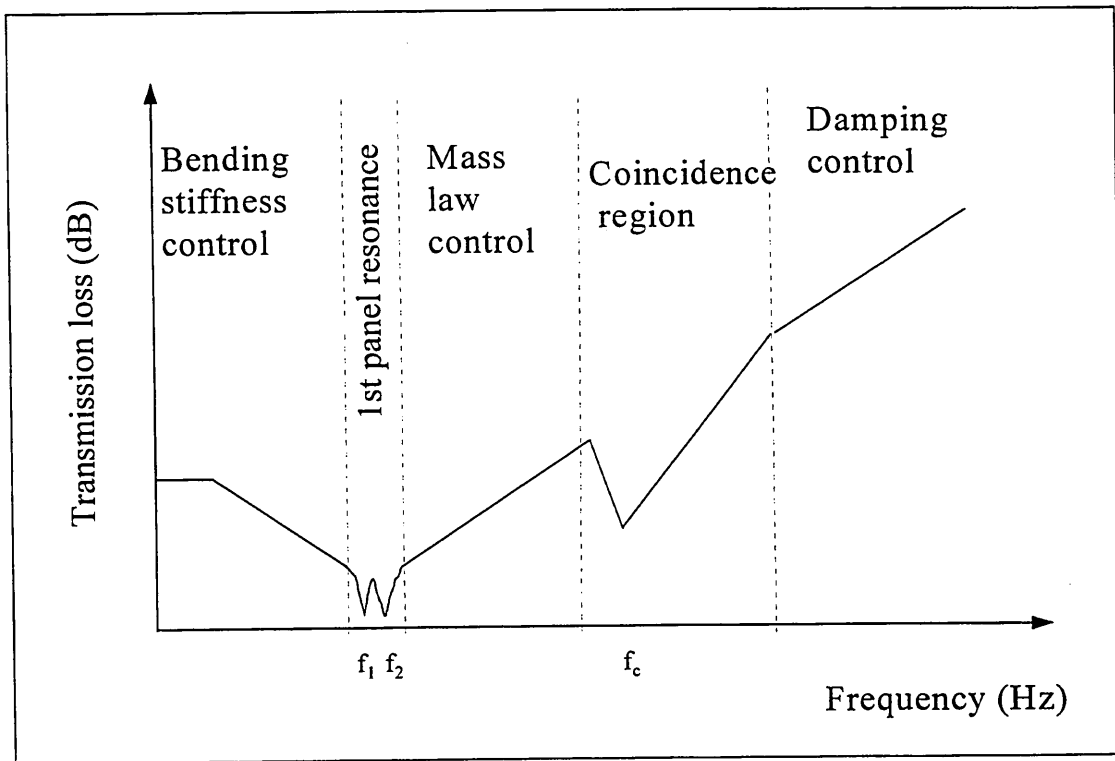
Figure 2.1. Transmission loss versus frequency
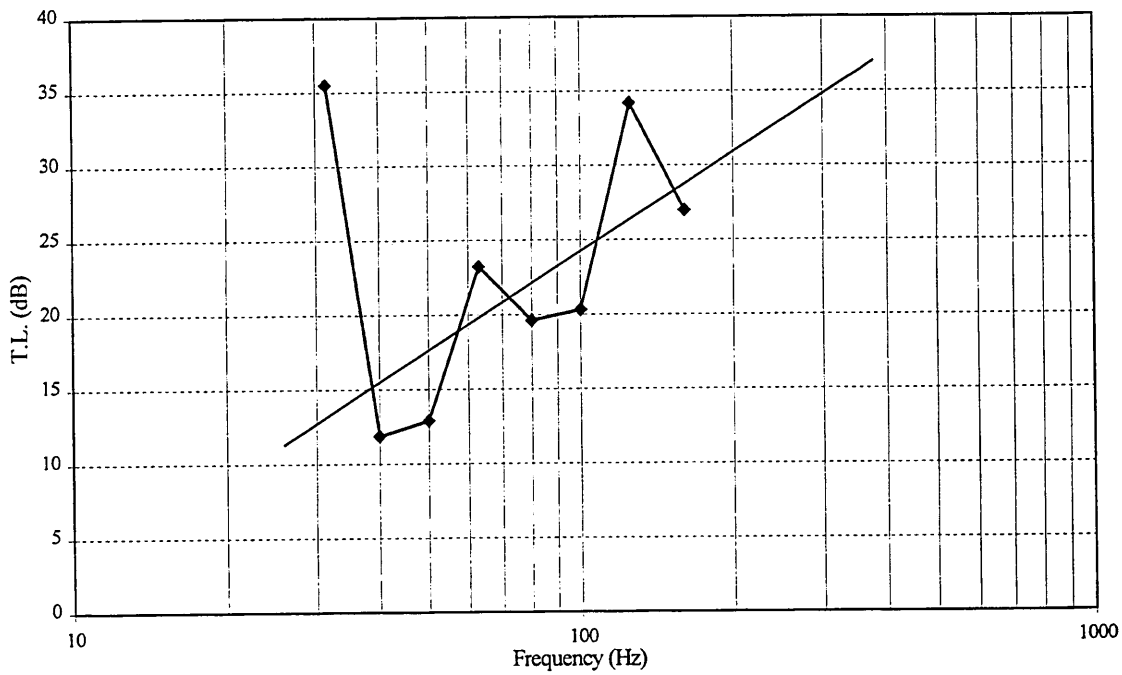
Figure 2.2 Transmission loss of a 0.05m brick wall [Maluski and Gibbs (1998)]

45
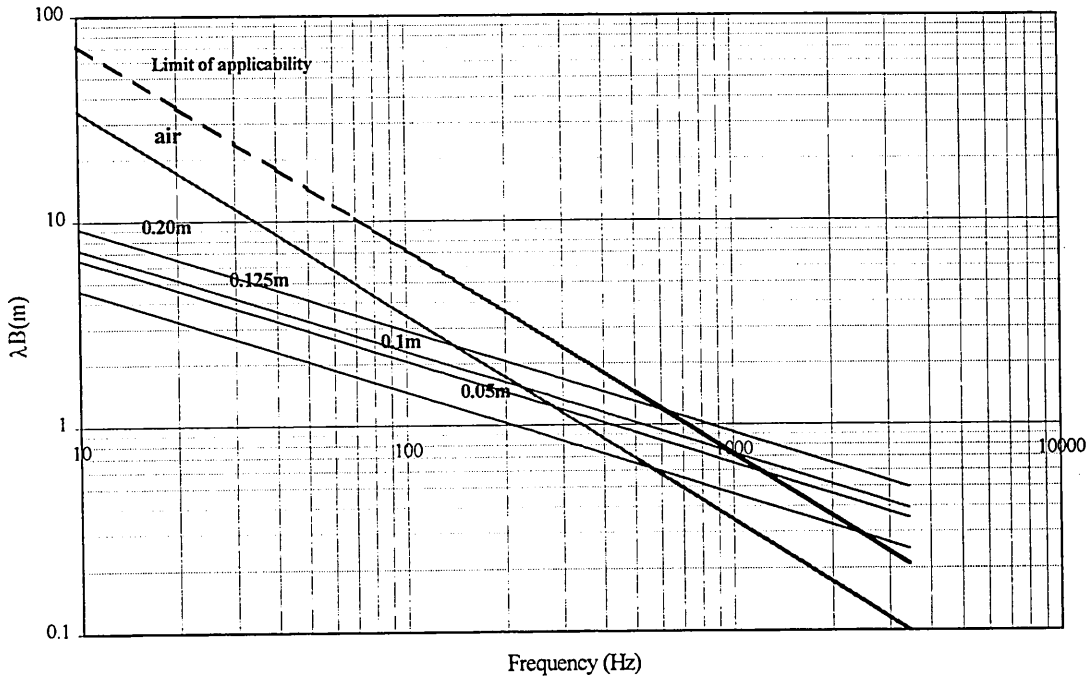
Figure 2.3. Limit of applicability of thin plate theory to a brick wall of different thickness
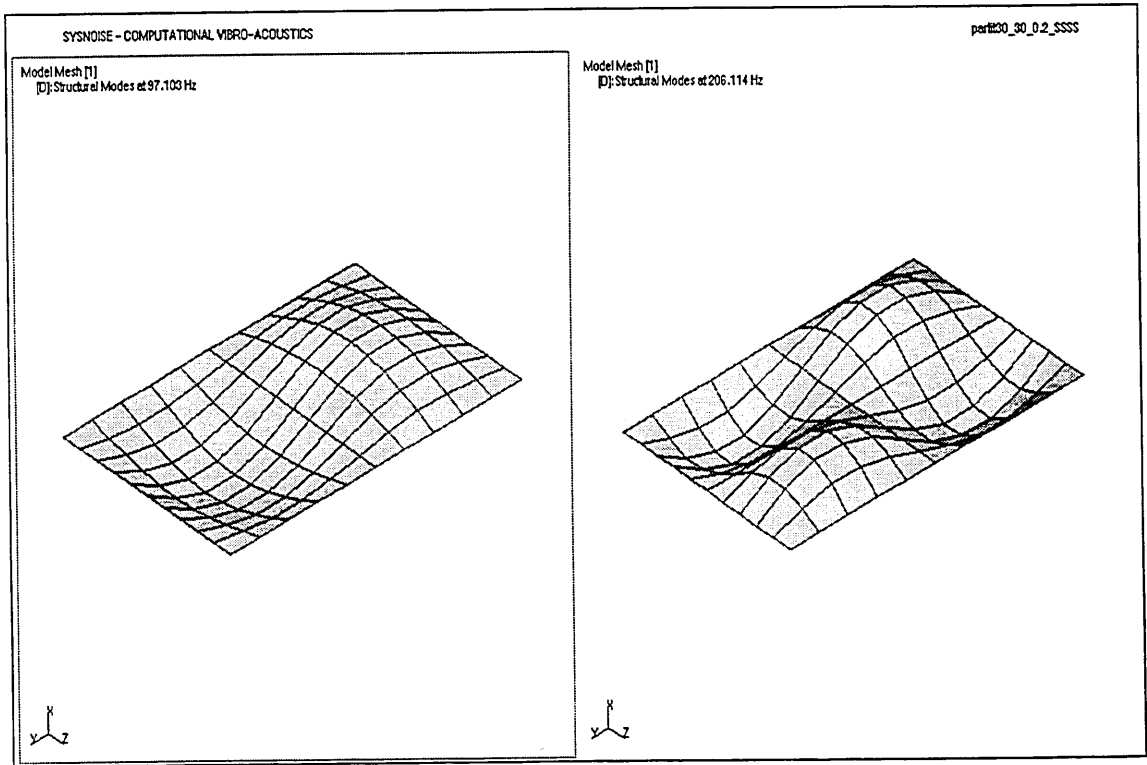
Figure 2.4. Mode (2,1) and Mode (2,2)
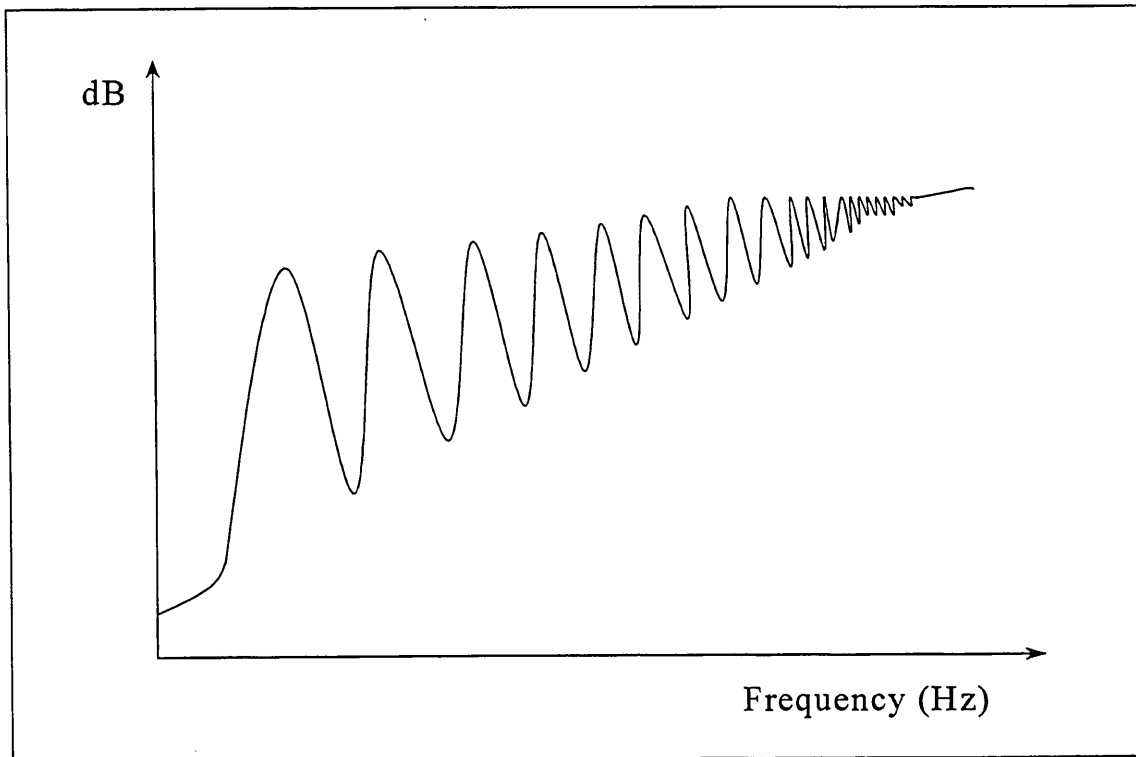
Figure 2.5. Frequency response of a thin wall
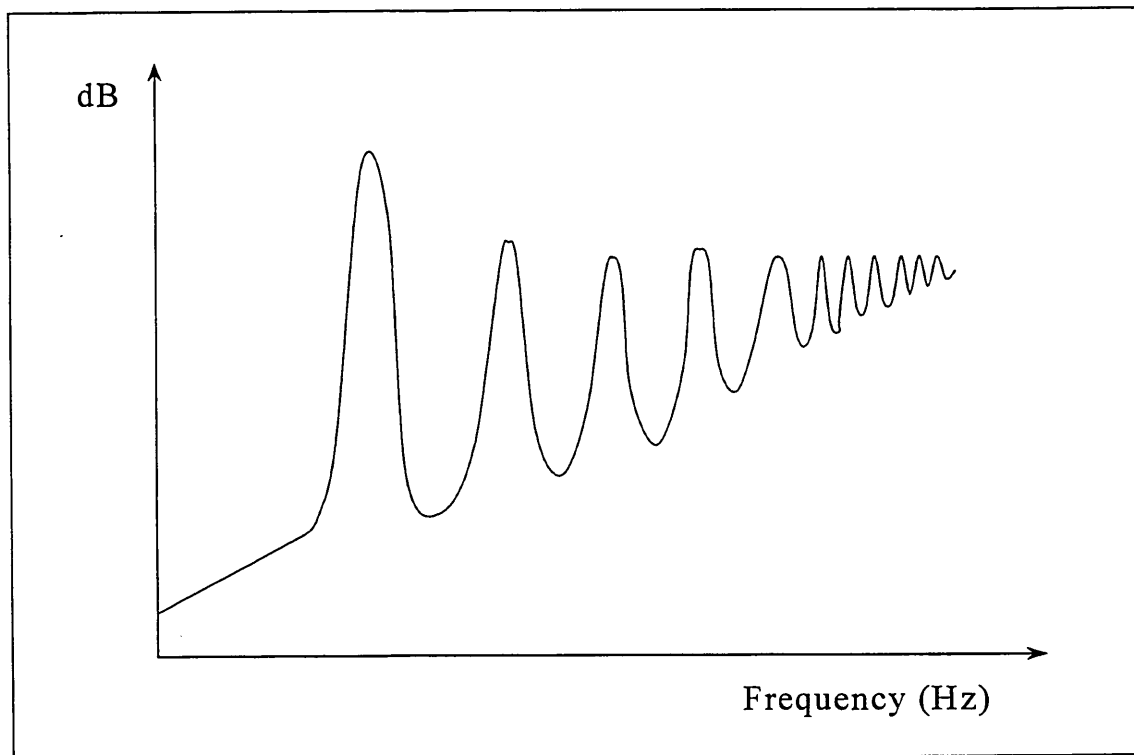
Figure 2.6. Frequency response of a thick wall
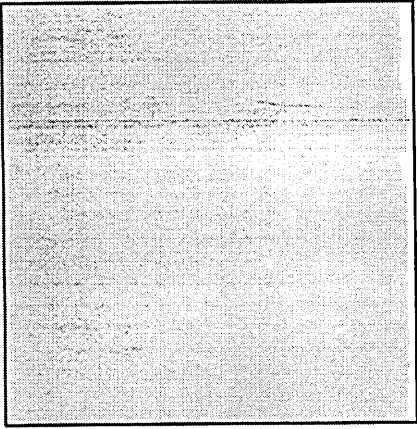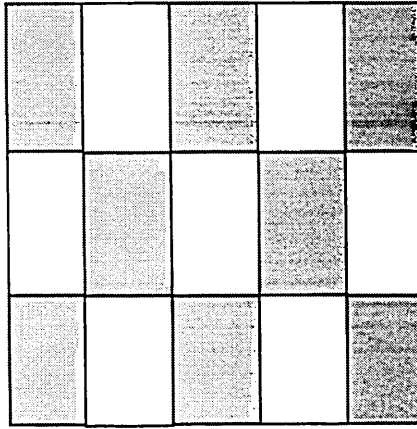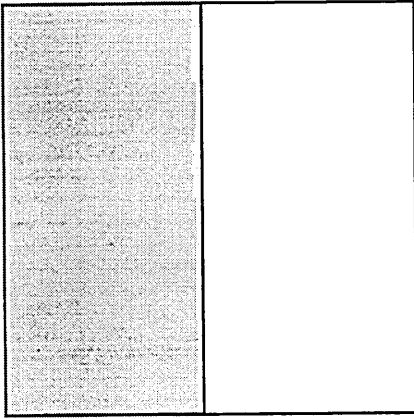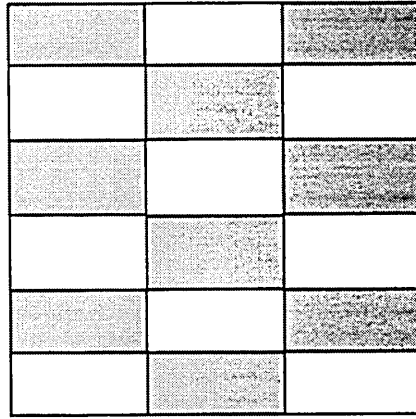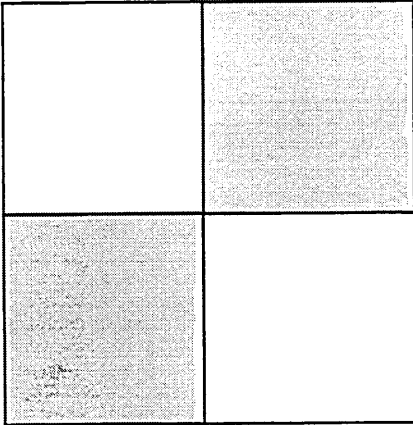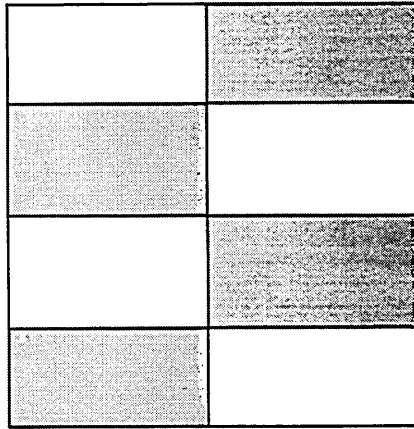
Figure 2.7. Modes (1,1), (5,3), (2,1), (3,6), (2,2), (2,4)
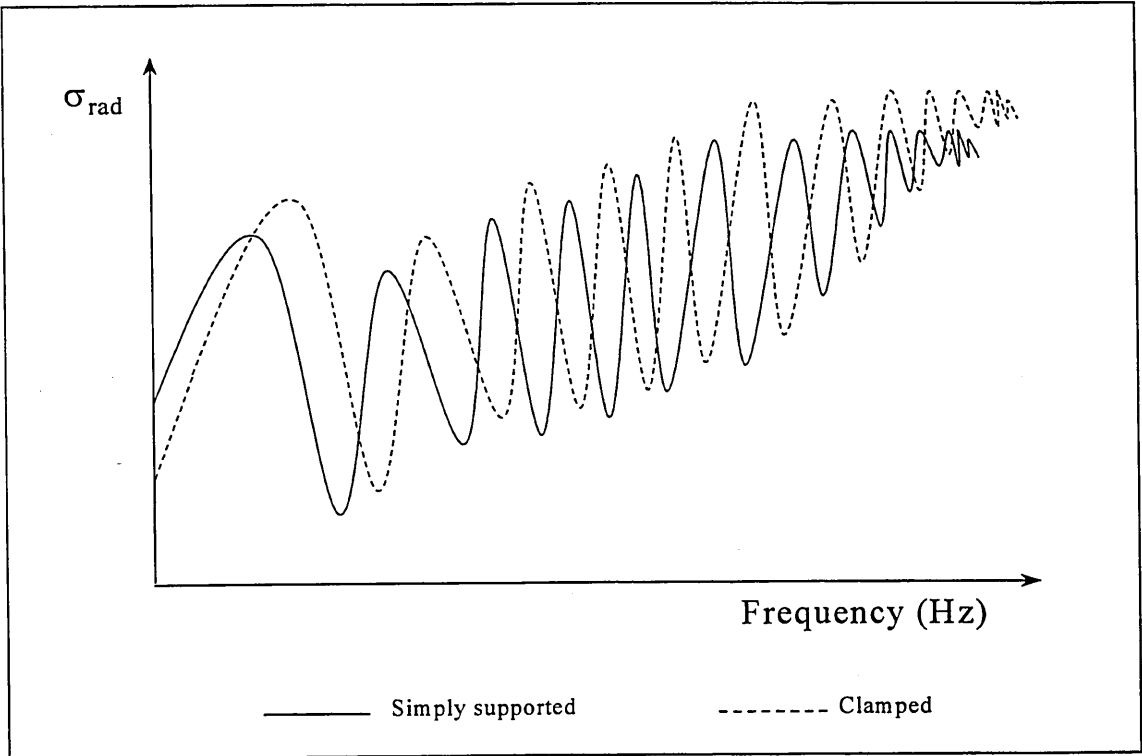
Figure 2.8. Radiation efficiency of the clamped and simply supported walls.

49
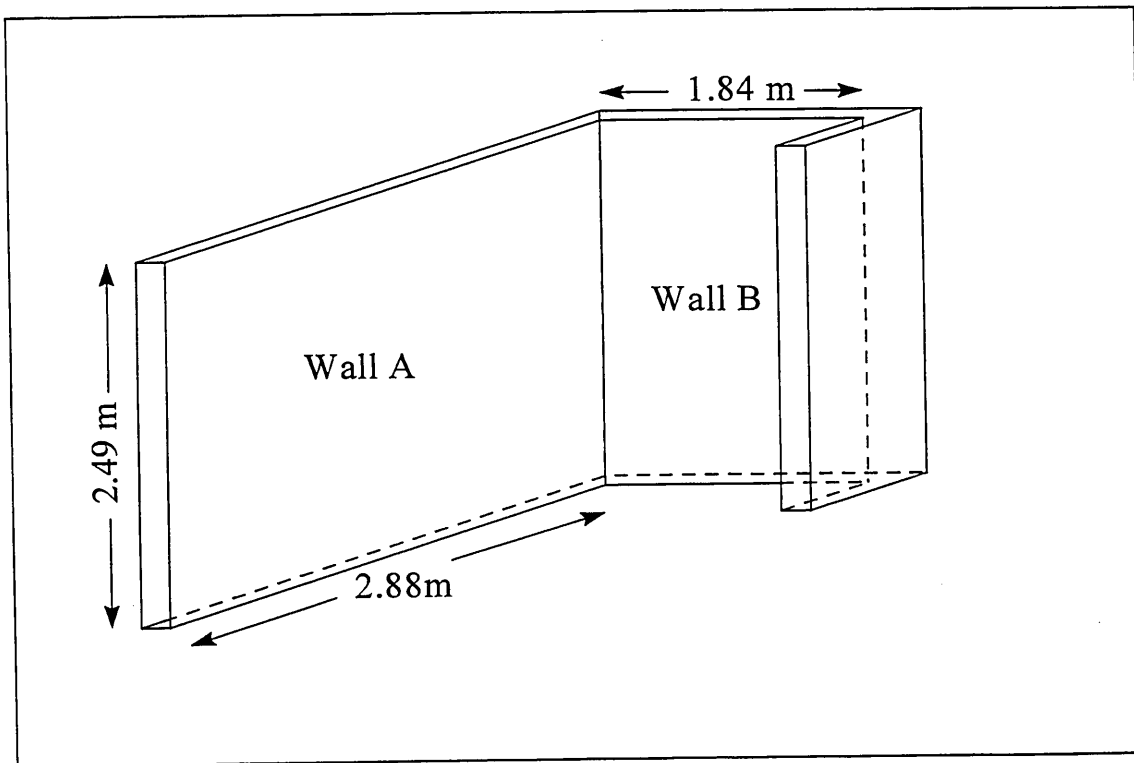
Figure 2.9. Walls A and B
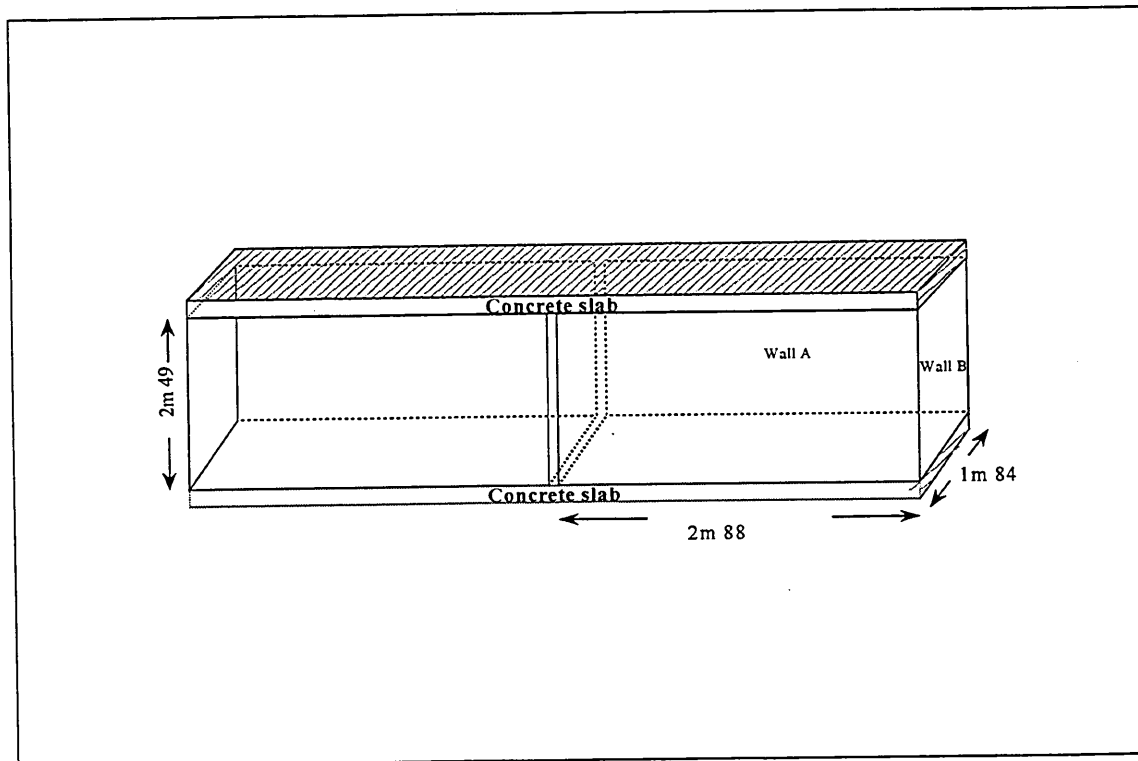
Figure 2.10. The transmission suite laboratory

50
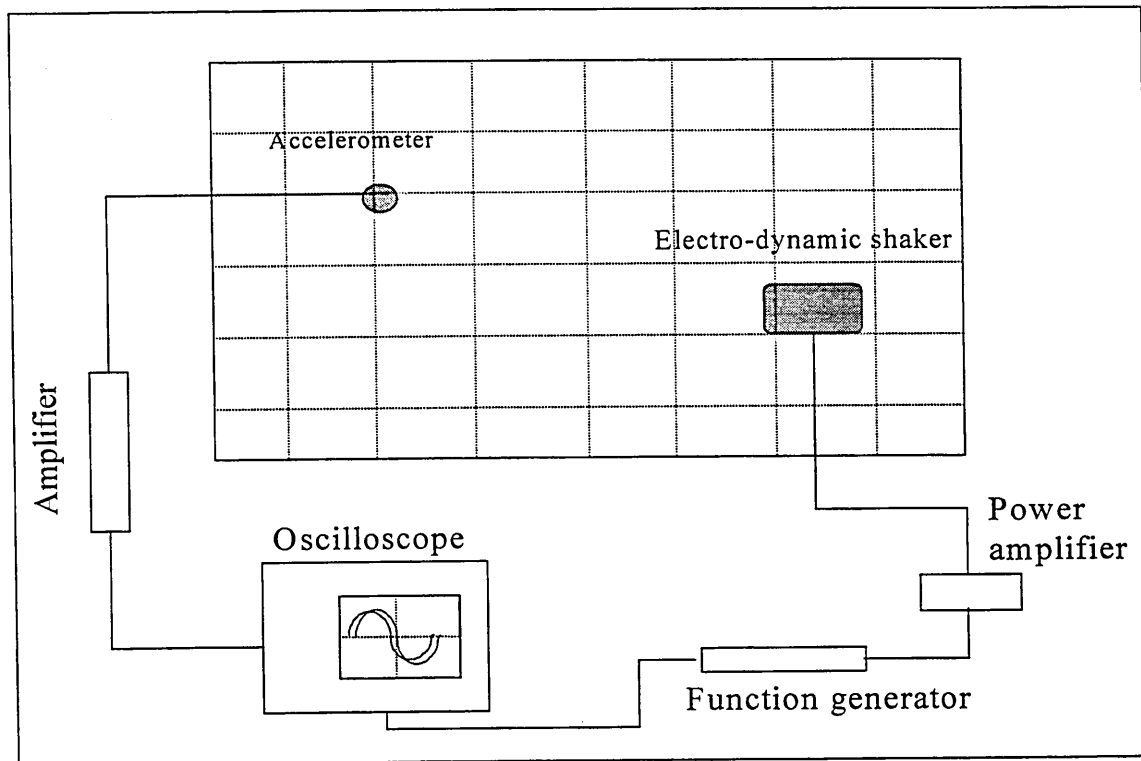
Figure 2.11. Experimental set up
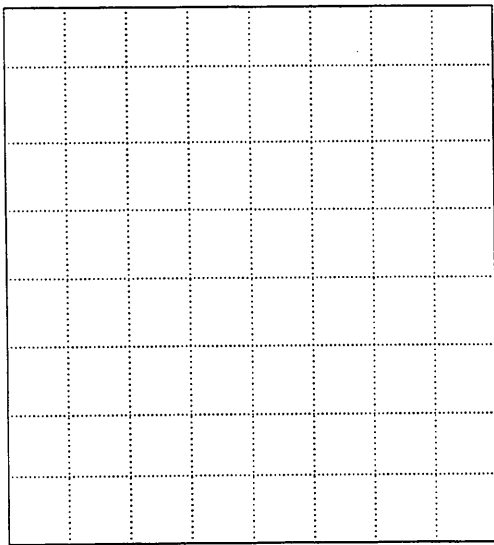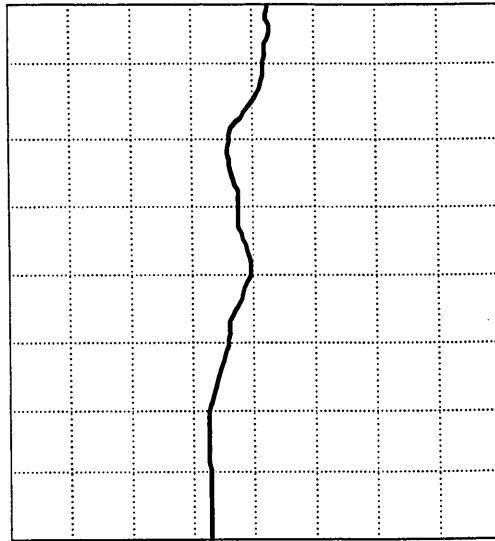
Mode (1,1): 43Hz   Mode (2,1): 86Hz
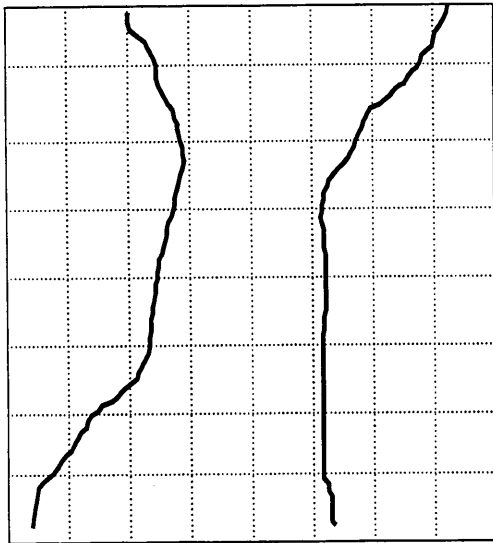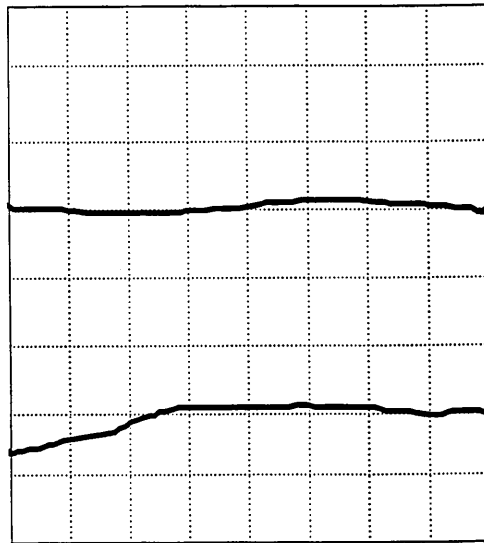
Mode (3,1): 134Hz   Mode (1,3): 185Hz

Figure 2.12. Identified modes on Wall A
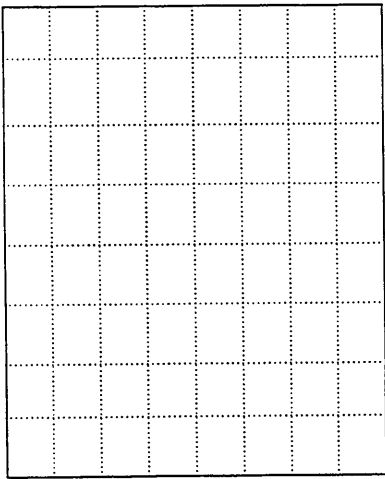
Mode (1,1): 56Hz
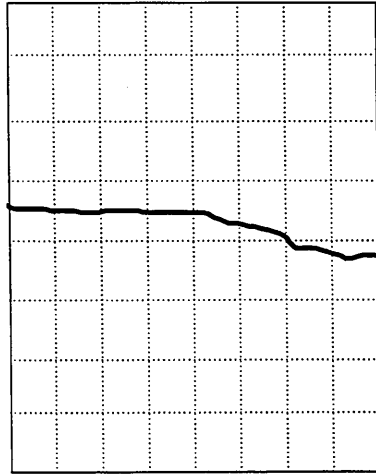
Mode (1,2): 110Hz

Mode (2,1): 129Hz
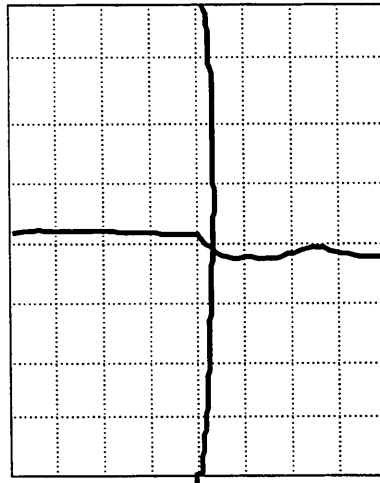
Mode (2,2): 172Hz
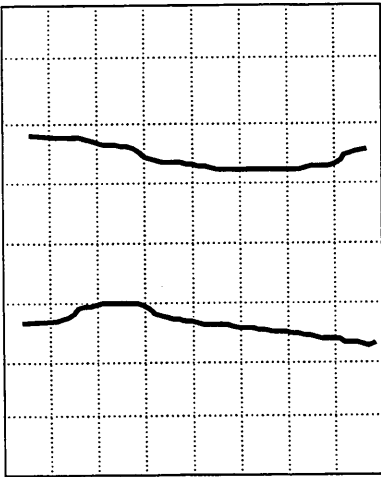
Mode (1,3): 179Hz

Figure 2.13. Identified modes on Wall B

53
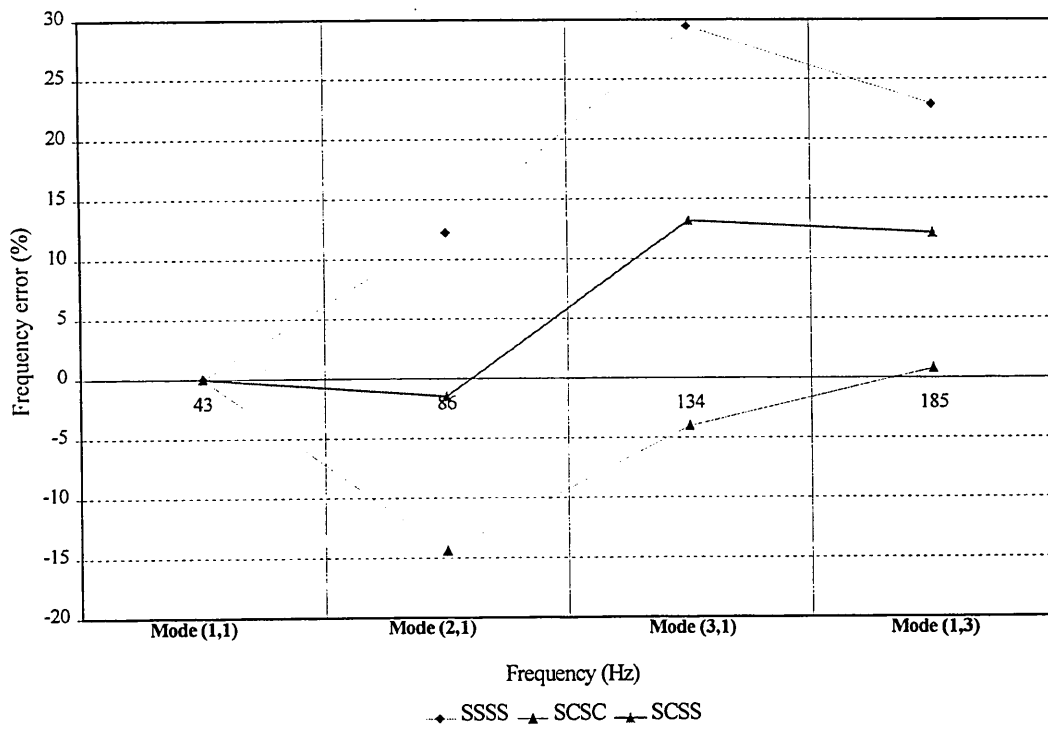
Figure 2.14. Frequency error of wall A
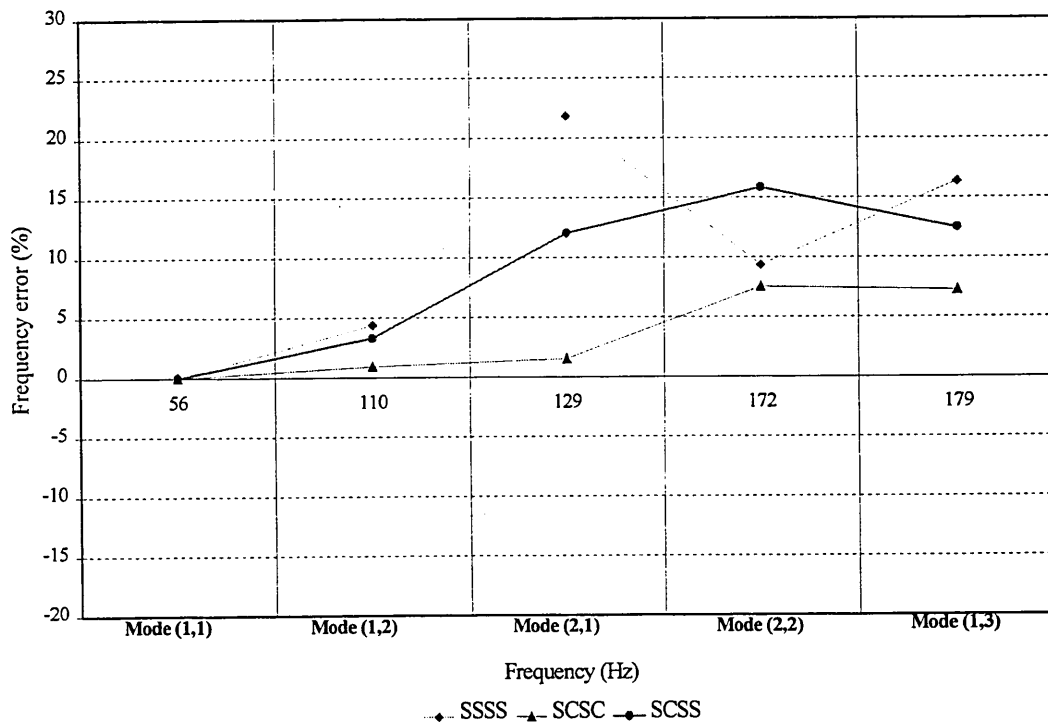
Figure 2.15. Frequency error of wall B

54

3   SOUND FIELD IN ROOMS AT LOW FREQUENCIES

3.1   INTRODUCTION

In Chapter 2, the transmission loss of party wall was shown to be dependent on the structural modal characteristic as well as the acoustic modal characteristic. The objective of this chapter is to look at the behaviour of sound fields at low frequencies. It will be shown that the sound field is dependent on room shape, dimensions and position of sources; factors which are not taken account in the classical room acoustics theory.

3.2   SOUND FIELD AT LOW FREQUENCIES

Large fluctuations in the sound pressure level inside an enclosure are obtained at low frequencies [Morse (1948), Bolt (1950)]. This is explained by the eigenmode spacing, which is large, usually greater than half an octave at low frequencies. The phenomenon also is observed in small rooms [Knudsen (1932)]. The room volume of the enclosure controls the density of room modes (see Section 3.3) [Bonello (1981), Walker (1992)] and accurate measurement of frequency response at low frequencies can be difficult [Knudsen (1932), Walker (1992)]. Introduction of damping e.g. by placing absorption on the floor or on the walls has been observed to reduce the large fluctuations of the sound level [Craggs et al (1989), Pedersen (1997), Fuchs (1998)]. The damping affects the decay of each room mode and also can alter the frequency response of the room [Craggs et al (1989), Walker (1992)]. Cavity-wall coupling also can play a part in the response of the room in the low frequency range [Pretlove (1965), Bhattacharya (1969), Pretlove et al (1970), Nefske et al (1990), Pan et al (1990)], affecting the steady state sound field levels and the room reverberation time. The source and receiver positions also must be considered.

3.2.1 Standing waves

The sound pressure throughout the volume of a rectangular enclosure with the dimensions L_x, L_y and L_z (see Figure 3.1) is governed by the wave equation [Morse (1948)];

$$\frac{\partial^2 p}{\partial x^2} + \frac{\partial^2 p}{\partial y^2} + \frac{\partial^2 p}{\partial z^2} = \frac{1}{c_0^2} \frac{\partial^2 p}{\partial t^2} \qquad (3.1)$$

where t is the time and c_0 is the speed of sound in air.

Equation 3.1 can be rewritten as an Helmholtz Equation ;

$$\nabla^2 p + k^2 p = 0 \qquad (3.2)$$

where $k = 2\pi f/c$

The sound field is strongly dependent on the room boundaries [Bies (1996)]. If the six surfaces are considered hard i.e. the air particle velocity is equal to zero and the variation of the pressure normal to the surface of the walls is also equal to zero, then;

$$\frac{\partial p}{\partial n} = 0 \qquad (3.3)$$

where ∂n is the normal to the surface of the wall

Using separable functions, the boundary condition is satisfied by the form;

$$p = p_0 \cos\left[\frac{\pi n_x x}{L_x}\right] \cos\left[\frac{\pi n_y x}{L_y}\right] \cos\left[\frac{\pi n_z x}{L_z}\right] \qquad (3.4)$$

for $0 \le x \le L_x$, $0 \le y \le L_y$, $0 \le z \le L_z$ where n_x, n_y, n_z are integers and p_0 is the maximum pressure amplitude.

The corresponding wavenumber components are

$$k_x = \frac{\pi n_x}{L_x}, \quad k_y = \frac{\pi n_y}{L_y}, \quad k_z = \frac{\pi n_z}{L_z} \qquad (3.5)$$

with
$$k^2 = k_x^2 + k_y^2 + k_z^2 = \left(\frac{\omega}{c_0}\right)^2 \qquad (3.6)$$

The eigenfrequencies f_{n_x,n_y,n_z} are then calculated from Equation 3.6, where

$$f_{n_x,n_y,n_z} = \left(\frac{c_0}{2}\right)\sqrt{\left(\frac{n_x}{L_x}\right)^2 + \left(\frac{n_y}{L_y}\right)^2 + \left(\frac{n_z}{L_z}\right)^2} \qquad (3.7)$$

The eigenfrequencies identify normal modes of vibration which have nodes, positions of minimum pressure, and anti-nodes, positions of maximum pressure. Those modes of vibrations are called standing waves.

Equation 3.7 applies to standing waves inside rectangular rooms. It can be observed, that the eigenfrequencies are shifted upward when the room dimensions decrease. If the room width and the length have the same dimensions, then standing waves will be created with different integers n, but with the same frequency. If the room volume is kept constant but the dimensions are altered, the number of eigenfrequencies within a set frequency range remains approximately the same but the particular values of (n_x, n_y, n_z) and their order on the frequency scale will differ. A more random distribution of eigenfrequencies can be created by a room with irregular walls and thereby create a more uniform room response [Bolt (1939), Morse (1948)]. Equations have been derived for non rectangular rooms but it is a very difficult task to calculate the eigenfrequencies.

3.2.2 Axial, tangential and oblique modes

Three categories of normal modes can be identified, described as axial, tangential and oblique modes.

Axial waves travel parallel to the axes of the room with nodal planes normal to the x-

axis and parallel to the end walls (see Figure 3.2). In this case, two of the three integers n_x, n_y, n_z in Equation 3.7 are zero, where;

x-axial waves, parallel to the x axis (n_y, n_z = 0),

y-axial waves, parallel to the y axis (n_x, n_z = 0),

z-axial waves, parallel to the z axis (n_x, n_y = 0).

Tangential waves travel parallel to two opposite walls (see Figure 3.3) of the enclosure while reflecting from the other four walls and have one integer zero, where;

y,z-axial waves, parallel to the y,z plane (n_x = 0),

x,z-axial waves, parallel to the x,z plane (n_y = 0),

x,y-axial waves, parallel to the x,y plane (n_z = 0).

Oblique waves travel in paths non parallel with all room surfaces and all integers are non zero (see Figure 3.4).

3.2.3 Modal density

For modes with frequency less than f, Equation 3.7 is rewritten as

$$f_{n_x, n_y, n_z} > \left(\frac{c_0}{2}\right) \sqrt{\left(\frac{n_x}{L_x}\right)^2 + \left(\frac{n_y}{L_y}\right)^2 + \left(\frac{n_z}{L_z}\right)^2} \qquad (3.8)$$

The total number of eigenfrequencies below a frequency, f, is given by the number of points in the positive octant of the ellipsoid represented by Equation 3.8. The number of points equals the volume of this octant and thus the number N of eigenmodes having frequencies less than f is given by

$$N = \frac{1}{8} \frac{4\pi}{3} \left(\frac{2L_x f}{c_0}\right) \left(\frac{2L_y f}{c_0}\right) \left(\frac{2L_z f}{c_0}\right) = \frac{4\pi}{3} V \frac{f^3}{c_0^3} \qquad (3.9)$$

where V is air volume in the room.

This expression is for the case where the acoustic wavelength is small compared with the room dimensions and therefore becomes inaccurate at low frequencies. Maa [1939] therefore introduced a correction term to Equation 3.9. Points lying on the co-ordinate planes are shared between two octants and those on the axes by four octants. Therefore Equation 3.9 is corrected by the addition of half the number of points on the co-ordinate planes and half the number on the axes. A new relationship is given;

$$N \approx \left(\frac{4 \pi f^3 V}{3c_0^3} \right) + \left(\frac{\pi f^2 S_{encl}}{4c_0^2} \right) + \left(\frac{f L_{encl}}{8c_0} \right) \tag{3.10}$$

where S_{encl} is the total area of the enclosure and L_{encl} is the length of all the edges of the enclosure.

The modal density is obtained from Equation 3.10 by differentiating N with respect to frequency f;

$$\frac{dN}{df} \approx \left(\frac{4 \pi f^2 V}{c_0^3} \right) + \left(\frac{\pi f A_{encl}}{2c_0^2} \right) + \left(\frac{L_{encl}}{8c_0} \right) \tag{3.11}$$

The following example illustrates the application of the theory. Different room configurations were selected, varying from 25m³ to 65m³, where width and height of each room are the same (L_y = 4m and L_z = 2.5m). The number of eigenmodes calculated by Equations 3.9 and 3.10 are presented in Table 3.1. It shows that the predicted number of modes below 200 Hz for room volume smaller than 60m³ is greater when using Maa's Equation 3.10 than with the classical theory (see Equation 3.9).

Room Volume (m³)	Number of eigenmodes below 200 Hz	
	Equation 3.9	Equation 3.10
25	21	38
30	25	44
35	30	50
40	34	56
45	38	62
50	42	69
55	46	75
60	51	81
65	55	87

Table 3.1. Number of modes using the classical and Maa's Equation

The eigenfrequencies for the 25m³ room also are calculated according to Equation 3.7. The first eigenfrequency is 45.6Hz corresponding to the mode (0,1,0) and the 38th mode, the last mode below 200 Hz, is the mode (2,3,1). The total number of modes below 200Hz corresponds then to the number calculated according to Equation 3.10. Maa's Equation must therefore be used for rooms smaller than 60m³.

Equations 3.9 & 10, apply to rectangular rooms only. Non rectangular rooms e.g. a L shaped room, which are found in some dwellings, thus, are problematical. However, they are not developed or described here as rectangular rooms remain the most popular configuration.

The determination of the sound pressure level in a frequency band, not only includes the modes with maxima inside that band, but also modes with residuals, here called 'tails', inside the band. In Figure 3.5, a window is selected in order to calculate the sound level. Three modes are present in the band, but also the 'tails' of the modes excited in the neighbourhood of the windows. The tails must therefore be taken into account as they contribute to the total sound level.

3.2.4 Resonant sound fields

At low frequencies, mainly axial and tangential waves are excited and the modal density is low. The sound field is characterised by a large spatial and spectral variation in pressure as seen in Figure 3.6. When the frequency of the sound source equals one of the eigenfrequencies, resonance occurs, generating a strong room response. This phenomenon is emphasised when the room dimensions are equal and the frequency response of the enclosure is strongly distorted.

At higher frequencies, the number of axial modes and tangential modes are small compared with the oblique modes excited. The modes have small frequency spacing and are difficult to identify separately, producing weak resonances. The modes in a band need only be considered and 'tails' can be neglected. In this case, there is approximately the same mean energy flow in all directions at any point in the field and the pressure is the same at any position (see Figure 3.7). The steady state sound field depends only on the power and frequency characteristics of the sound source, its position in the room and an average room absorption. The sound field is said to be diffuse.

The sound field is said to be diffuse above a specific frequency, called the cut-off frequency, f_c, defined by the following equation [Schroeder (1969), Crocker (1975 & 97)]

$$f_c = \left(\frac{3\,M\,c_0 T}{8.8\,\pi V} \right)^{1/2} \tag{3.12}$$

where M is the modal overlap, T is the reverberation time.

The modal overlap is a measure of the spacing between modes and overlap of the sound field [Schroeder (1969)]. As seen in Figure 3.8, the modal overlap is calculated from the bandwidth Δf of each mode, called here i, which is the width in Hertz if the response curve of the mode measured 3dB down from the peak response in the measurement frequency band, B_d. It is defined as follows;

61

$$M = \frac{\sum_{i=1}^{i} \Delta f_i}{B_d}$$

(3.13)

According to Schroeder, a modal overlap equal or greater than 3, means that the sound field is 'sufficiently diffuse' [Schroeder (1969)]. The frequency where this occurs will be referred to as the high frequency range [Crocker (1997)]. Crocker and Price [1975], however, have shown that M= 1/3 provides a sufficiently diffuse field. Lyons [1993] preferred an intermediate value M =1. All three criteria will be considered in section 3.4.

3.3 DAMPING

The presence of damping inside rooms affects the room modes, by reducing the amplitude of the standing waves. The presence and the position of absorption is less effective on the axial modes than the tangential and oblique modes. The axial modes have the longest mean free path and undergo the smallest number of reflections per second. The oblique modes are more affected than the tangential modes, because they have the shortest mean free path and undergo the greater number of reflections. Moreover, the surfaces are less absorbing for grazing than oblique incidence sound.

The absorption in the enclosure can be quantified by measuring the reverberation time of the room [Kuttruff (1979), Beranek (1992)] which is one of the fundamental quantities in architectural acoustics. It is the time taken for the sound energy to decay by 60dB. The decay can be described as a multitude of mode decays close to each other in frequency (See Figure 3.9). The initial decay is controlled by the oblique waves which decrease more rapidly than the tangential and axial modes. The final decay curve is controlled by the axial modes, which are less damped than those of the oblique and tangential modes. When the mode density is small, such as in rooms smaller than 50m^3 or at low frequencies, the logarithmic decay will not be linear due to the difference in the damping constant of the modes [Hirata (1982)] (see Figure 3.10). This leads to large variations in measured decay rate and to poor repeatability and reproducibility at low

frequencies [Bartel (1978), Halliwell (1983), Davy (1988), Yegnaranayana (1974)].

The reverberation time measurements also depend upon the position of the measurements point, the room volume, shape and contents [Knudsen (1932), Davy (1988)]. Therefore, the accuracy of the reverberation time can be improved by placing the microphones close to the wall [Waterhouse (1955)] in order to measure more oblique modes or by having an irregular room where nodal lines are distributed randomly [Sato et al (1959)].

Consequently, the measurement of damping inside enclosures is difficult at low frequencies and in small rooms, due to the low modal density. In general, the classical theory of reverberation time is inadequate for low frequencies, because the theory assumes a large modal density [Davy (1988), Knudsen (1932)].

3.4   NUMBER OF MODES REQUIRED FOR SOUND FIELD SIMULATION

In Chapter 9, a description is given of an investigation of the effects of room configurations on the sound level difference in the frequency range of 25-160Hz using a Finite Element Method. A question arises on how many modes, including the tails of the modes in the neighbourhood of the bandwidth, are required to properly estimate room response. The modal approach is assumed unnecessary when diffuse sound field conditions were reached, as identified by the cut off frequency. The cut-off frequency was calculated for the room volumes: 20m³, 30m³, 35m³, 40m³ and 50m³ according to Equation 3.12. Each cut off frequency therefore set a limit where any individual modes calculated above it, will not affect the room response.

The cut off frequency depends on absorption, and thus the reverberation time, values of which were obtained from the literature. Jackson et al [1972] show that the reverberation time in typical living rooms is close to 0.5s in the mid and high frequency,

but is higher at lower frequencies. They measured an average value of 0.69s at 100Hz, which is close to the value obtained by Johansson and Shi [1996]. They found that the averaged reverberation time in a room of 66m^3 is 0.76s in the third octave band from 31.5Hz to 100Hz. However, specific materials used for example in studios and placed at carefully chosen positions [Walker (1992)] can damped the low frequency modes and reduce the reverberation time to 0.4s. Such conditions were not considered as those materials are seldom, if ever used in dwellings.

Assuming the reverberation time is 0.8s in any room, the cut off frequency and the corresponding wavelength are presented in Table 3.2.

	Modal overlap, M					
	1/3		1		3[1]	
Room volumes (m^3)	f_c (Hz)	λ_c (m)	f_c (Hz)	λ_c (m)	f_c (Hz)	λ_c (m)
20	138.3	2.5	239.5	1.4	415	0.8
30	113	3	195.5	1.7	339	1
35	104.5	3.3	181	1.9	313.6	1.1
40	98	3.5	169.3	2	293.3	1.2

Table 3.2: Cut off frequency calculated with T = 0.8s [Johansson and Shi (1996)]:

[1]: Value given by Schroeder [1969]

For the cases considered, when the modal overlap is equal to 1/3, the wavelength remains larger than the smallest room dimension and therefore this criterion was rejected. When M= 1, the cut-off frequencies for the smallest room volume, 20m^3, was above the frequency range of interest 31.5Hz-200Hz. Values for the larger room volumes considered were in the frequency range of interest. Therefore, the modes of natural frequencies above the critical frequency would need to be processed in order to have a predicted frequency response from 25Hz-200Hz.

Consequently a modal overlap of 1 was assumed to provide acceptable simulation of the room modes for each room configuration as seen in Chapters 7 to 9.

3.5 INFLUENCE OF SOURCE POSITION

When the sound field is diffuse, the sound field is not influenced by the source position [Beranek (1992)]. Knudsen [1932] and others [Davy (1989), Gargliadini (1991)], however, show experimentally that the sound field at low frequencies or in small rooms is dependent on the loudspeaker position. This phenomenon is described numerically by Gargliadini [1991]. An axial mode is best excited when the loudspeaker is placed at the end wall i.e. at a pressure anti-node. The corner position is the best position to excite the largest number of room modes [Knudsen (1932), Gargliadini (1991), Beranek (1992)] because every room mode has a pressure anti-node. It has been suggested that two loudspeakers should be placed in opposite corners when measurements are carried out below 300Hz in order to ensure that all room modes are properly excited and thus have small sound level fluctuations [Benello (1981), Craggs (1989)]. The excitation of the sound field in large rooms is better when three loudspeakers are used with one of them in a corner [Walker (1992)]. A better low frequency performance is obtained by placing the loudspeakers near the longest side of the room and without any contact with the floor. The type of loudspeaker can influence the excitation of the sound field. A spherical sound source excites the sound field better than a plane sound source. Two 'octospeakers', not placed in a corner [Seller (1998)], will provide a good excitation due to the different directivities.

3.6 CONCLUSION

The sound field at low frequencies in small rooms, has been shown not to be statistical. The frequency response and the reverberation time measurements, two parameters which characterise the sound field properties, are thus inaccurate or unrepresentative. Classical theory is not applicable to the low frequencies since the sound field is strongly dependent on the modal density and thus on the room shape and dimension, and on the source and microphone positions.

The investigation of sound transmission between rooms at low frequencies must involve a study of modal behaviour of the two rooms as well as of the structural modal

behaviour of the party wall.

In the next chapter, a description is given of the implementation of classical and other theories in the development of standard and non standard test methods of sound insulation between dwellings.

3.7 REFERENCES

Bartel, T. W. and Magrab, E.B., (1978): *'Studies on the spatial variation of decaying sound fields'*, Journal of Acoustical Society of America, Vol.63 (6), 1841-1850

Beranek, L.L. and Ver, I.L., (1992): *'Noise and Vibration Control Engineering: Principles and Applications'*, Ed. J.Wiley and Sons

Bhattacharya, M.C. and Crocker, M.J., (1969): *'Forced vibration of a panel and radiation of sound into a room''*, Reports BS/A/69/1, University of Liverpool.

Bies, D.A. and Hansen, C.H., (1996): *'Engineering Noise Control theory and practice'*, 2nd Ed. E & FN SPON

Bolt, R.H., (1939): *'Normal modes of vibration in room acoustics: Experimental investigations in Non rectangular enclosures'*, Journal of Acoustical Society of America, Vol.11, 184-197

Bolt, R.H., (1950): *'Frequency response fluctuations in rooms'*, Journal of the Acoustical Society of America, Vol.22 (2), 280-289

Bonello, J., (1981): *'A new criterion for the distribution of normal room modes'*, Journal of Audio Engineering Society, Vol.29 (9), 597-606

Craggs, A. and Buma, C.J., (1989): *'The Effect of an absorbent lining on the natural frequencies and modal damping factors of a small rooms'*, Applied Acoustics, Vol.28, 229-239

Crocker and Price, (1975): *'Noise and Noise Control'*, Vol.1, CRC, Press 1975, 189.

Crocker, M.J., (1997): *'Encyclopedia of Acoustics'*, Vol.3 (9), Ed. Wiley-Interscience

Davy, J.L., (1988): *'The variance of decay rate at low frequencies'*, Applied Acoustics, Vol.23, 63-79

Davy, J.L., (1989): *'The variance of reverberation time measurements due to loudspeaker position variation'*, Journal of Sound and Vibration, Vol.132 (3), 403-409

Fuchs, H.V., Zha, X., Spah, M. and Pommerer, M., (1998): *'Qualifications of small freefield and reverberation rooms for low frequencies'*, Proceeding of Euro-Noise 98, Vol.2, 657-662

Gargliadini, L. and Roland, J., (1991): *'The use of a functional basis to calculate acoustics transmission between two rooms'*, Journal of Sound and Vibration,

Vol.145 (3), 457-478

Halliwell, (1983): *'Inter laboratory variability of sound absorption measurements'*, Journal of Acoustical Society of America, Vol.73 (3), 880-886

Hirata, Y., (1982): *'Dependence of the curvature of sound decay curves and absorption distribution on room shapes'*, Journal of Sound and Vibration, Vol.41, 195-198

Jackson, G M and Leventhall, H G., (1972): *'The Acoustics of Domestic Rooms'*, Applied Acoustics, Vol.5, 265-277

Johansson, C. and Shi, W., (1996): *'Experimental Determination of Reverberation Time for Low Frequencies in an Impact Sound Laboratory'*, Proceeding of Inter-Noise 96, 1779-1782

Knudsen, V.O., (1932): *'Resonance in small rooms'*, Journal of the Acoustical Society, July 1932, 21-37

Kuttruff, H., (1979), *'Room acoustics'*, 2nd Ed. :Applied Science

Lyons, R., (1993): *'Building elements of low sound insertion loss'*, Ph.D. Thesis, University of Liverpool

Maa, D.Y, (1939): *'Distribution of eigentones in a rectangular chamber at low frequency range'*, Journal of Acoustical Society of America, Vol.10, 235

Morse, P. M., (1948): *'Vibration and Sound'*, 2nd Ed. McGraw-Hill

Pan, J. and Bies, D.A., (1990): *'The effect of fluid structural coupling on sound wave in an enclosure'*, Journal of the Acoustical Society of America, Vol.87 (2), 691-707

Pedersen, D.B., (1997): *'Laboratory measurement of the low frequency sound insulation'*, DAGA 97, Kiel, 105-106

Pretlove, A.J. and Craggs, A., (1970): *' A simple approach to coupled panel-cavity vibrations'*, Journal of Sound and Vibration, Vol.11 (2), 207-215

Pretlove, A.J., (1965): *'Free vibration of a rectangular panel backed by a closed rectangular cavity'*, Journal of Sound and Vibration, Vol.2 (3), 197-209

Sato, K. and Koyaso, M., (1959): *'The effect of the room shape on the sound field in rooms (studies of the measurement of absorption coefficient by the reverberation chamber Method'*, Journal of the Physical Society of Japan, Vol.14 (3), 365-373

Schroeder, M.R., (1969): *'Effects of frequency and space averaging on the transmission response of multimedia'*, Journal of Acoustical Society of America, Vol.46 (2)

Seller, J., Private communication in April 1998

Walker, R., (1992): *'Low frequency room responses'*, BBC Report RD 1992/8

Waterhouse, R.V., (1955): '*Interference patterns in reverberant sound fields*', Journal of the Acoustical Society of America, Vol.27, 247-258

Yegnaranayana, B., (1974): '*Wave analysis of sound decay in rectangular rooms*', Journal of Acoustical Society of America, Vol.56 (2), 534-541
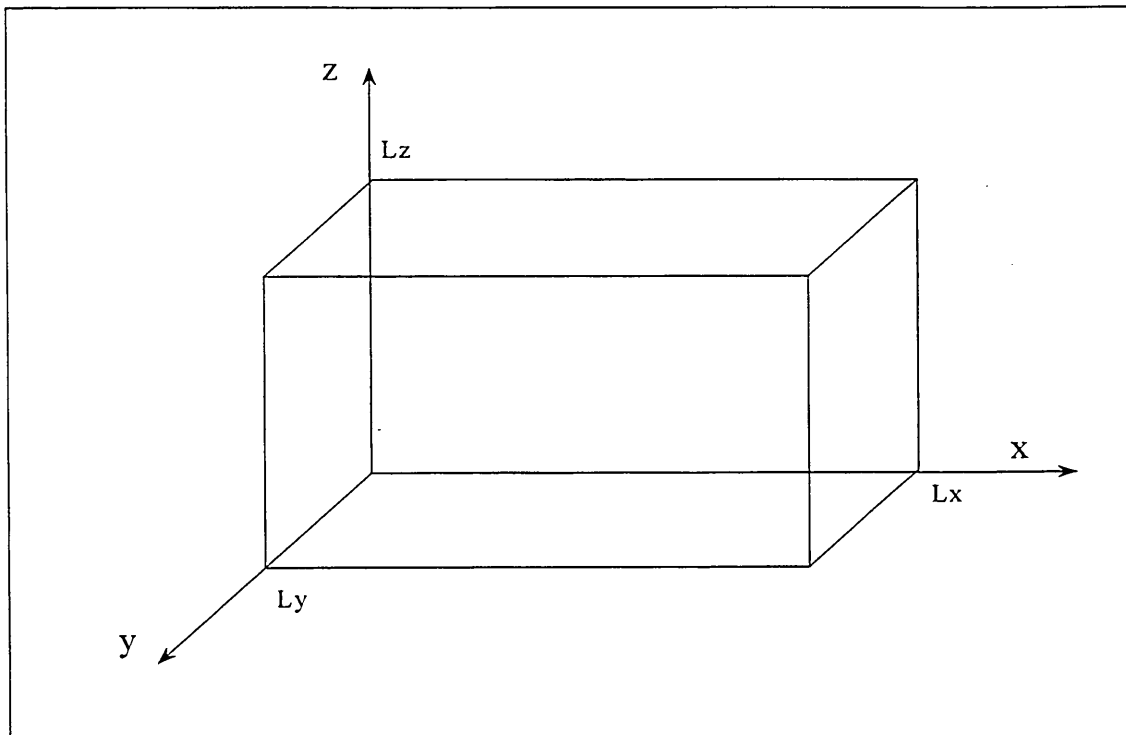
Figure 3.1. Room with co-ordinate system
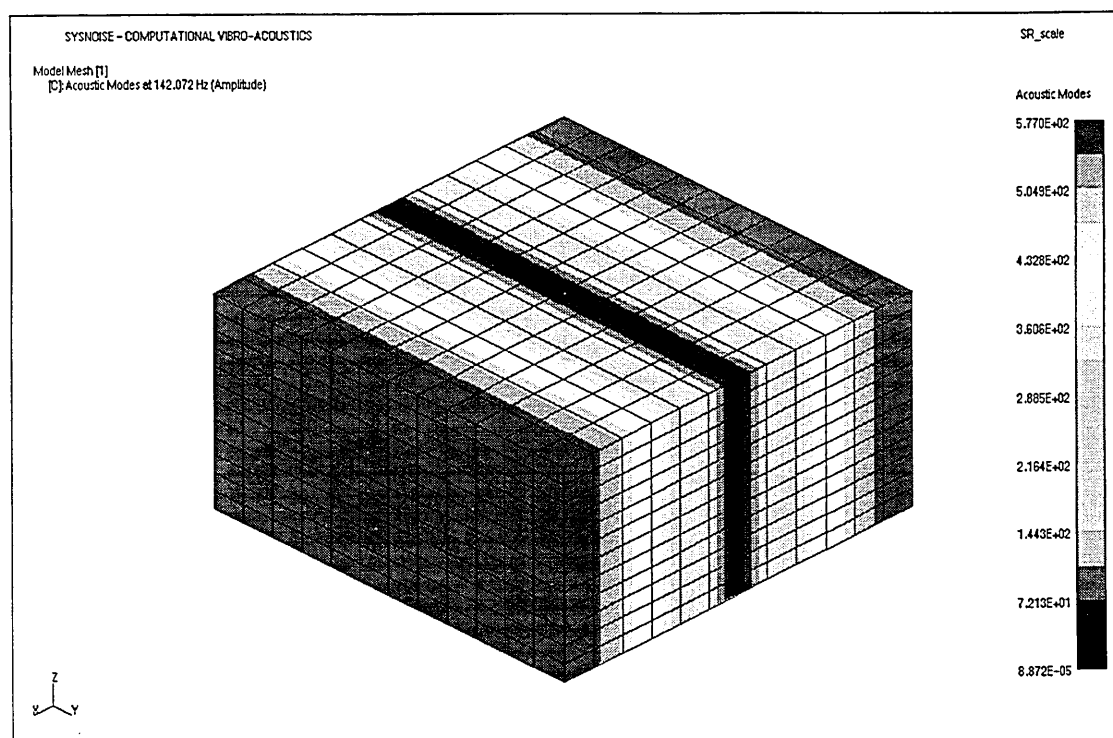
Figure 3.2. Axial mode (1,0,0)
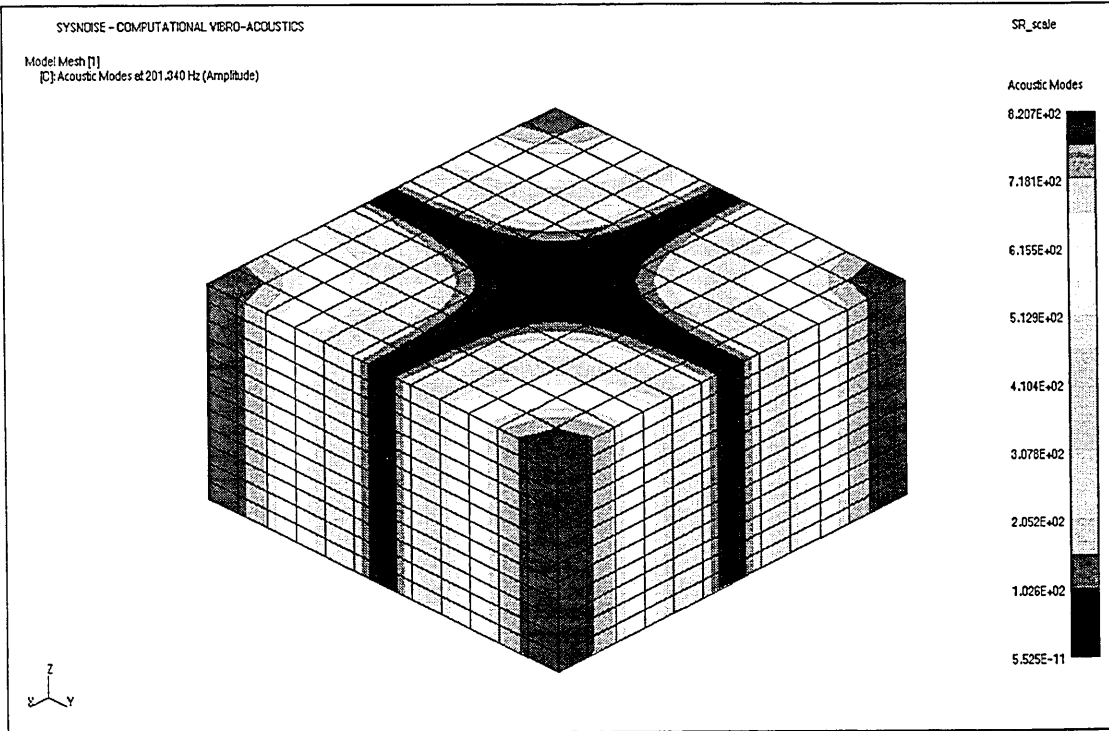
Figure 3.3. Tangential mode (1,1,0)
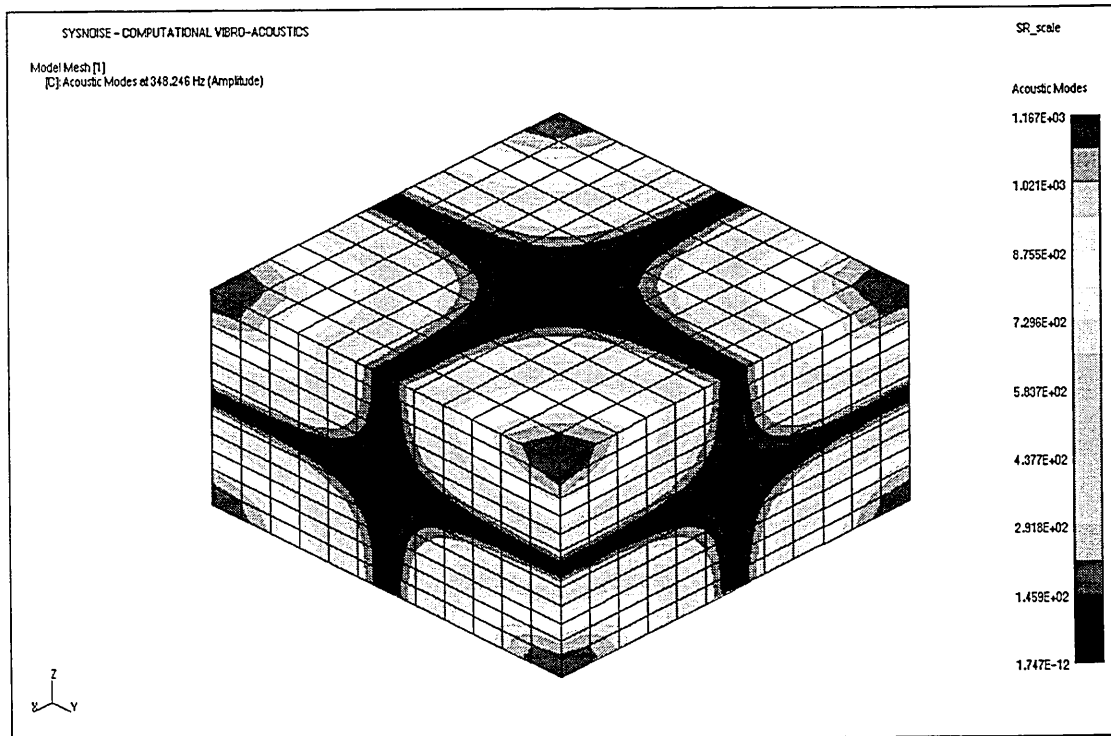
Figure 3.4. Oblique mode (1,1,1)
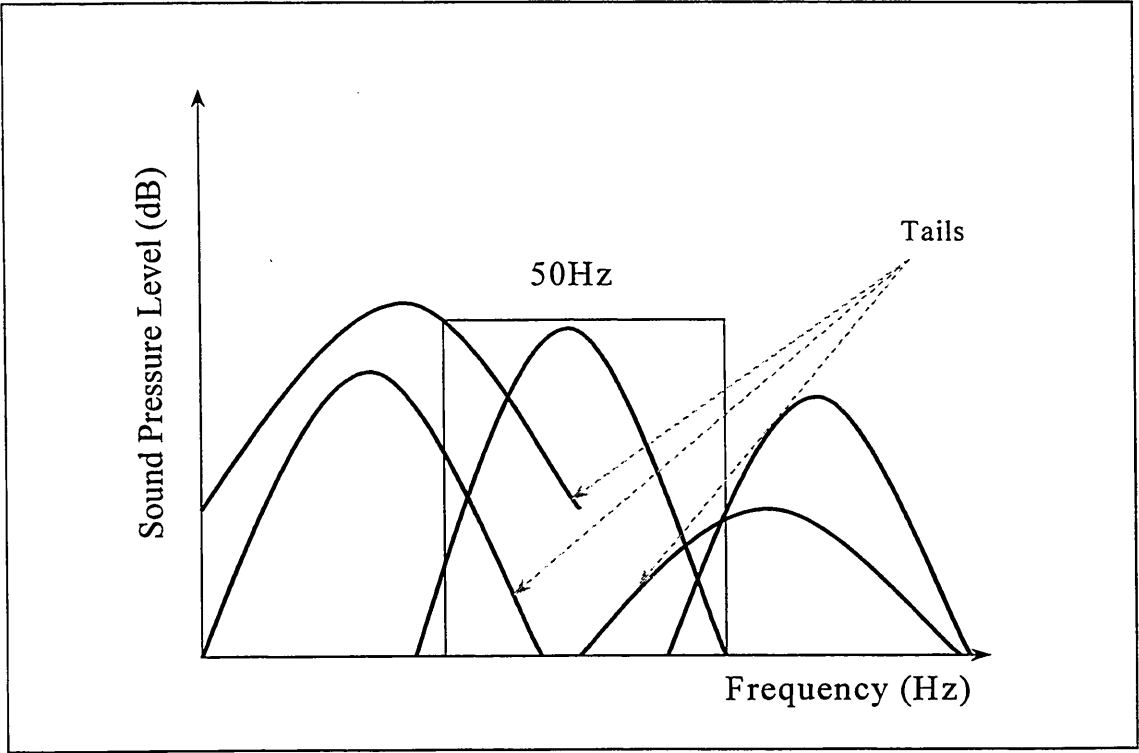
Figure 3.5. Modes with 'tails' inside the band
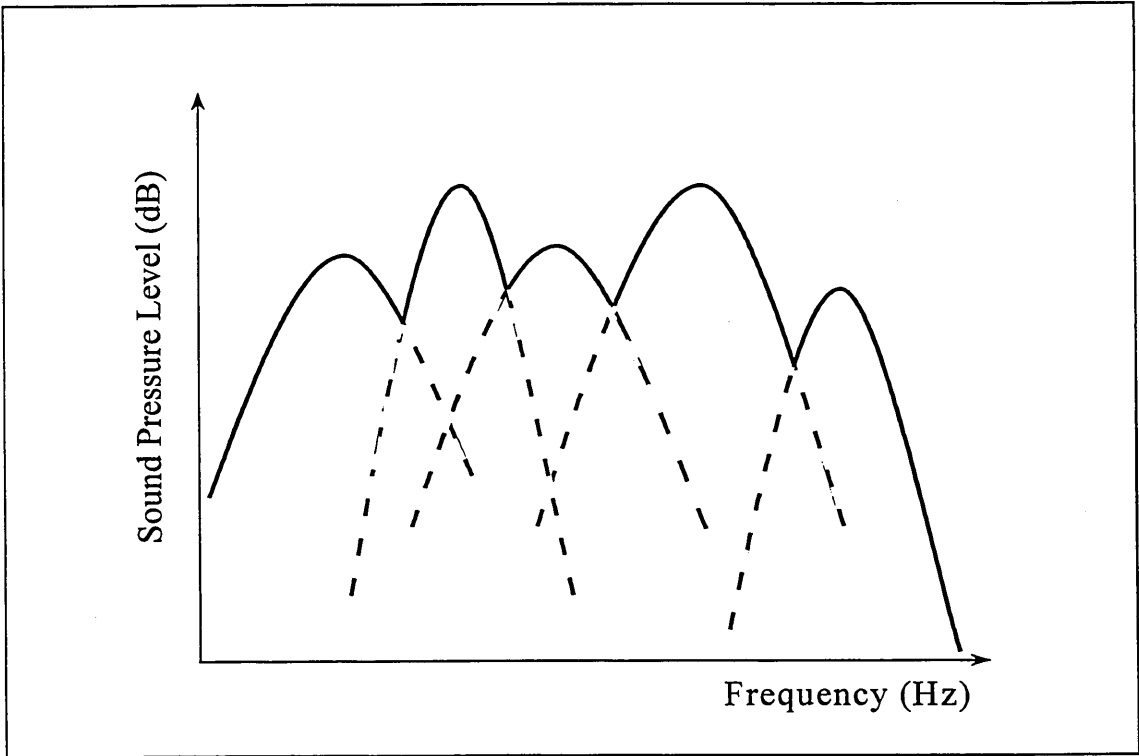
Figure 3.6. Frequency response at low frequencies

72
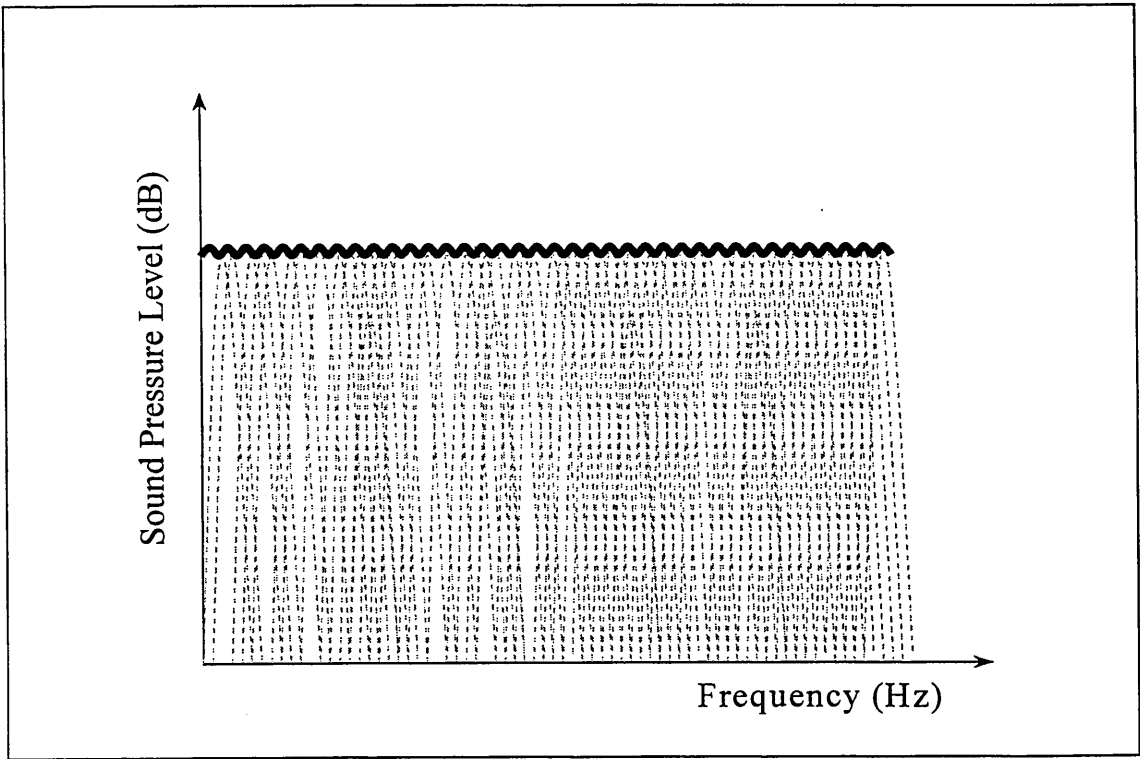
Figure 3.7. Frequency response at higher frequencies
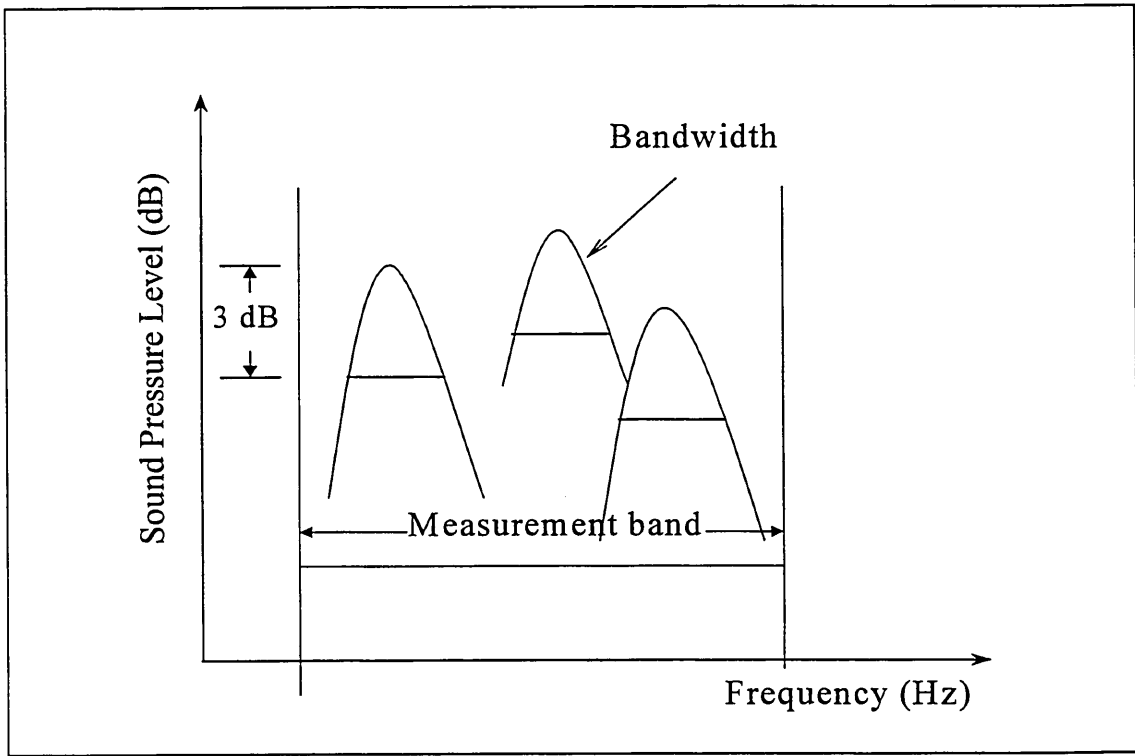
Figure 3.8. Modal overlap
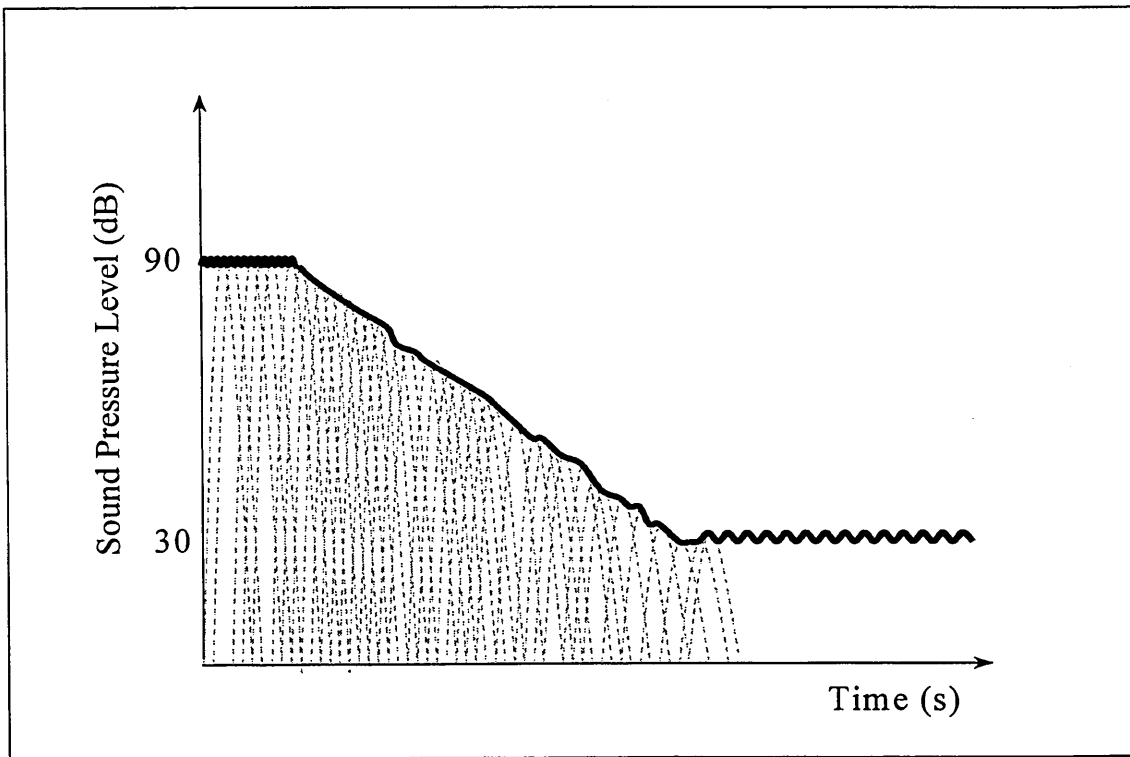
Figure 3.9. The reverberation time
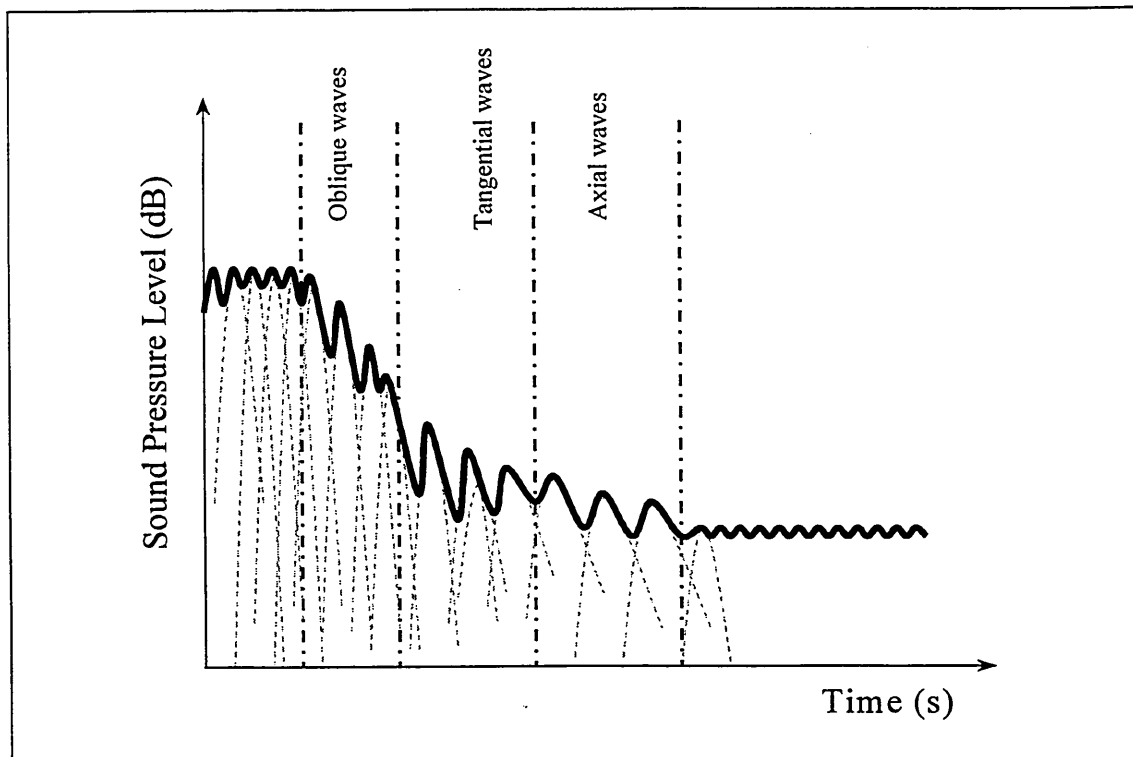
Figure 3.10. The reverberation time at low frequencies or in small rooms

74

4   SOUND INSULATION MEASUREMENT

4.1   INTRODUCTION

Field measurements of sound transmission between rooms does not distinguish between the paths of sound transmitted directly (airborne) and that by indirect (flanking) transmissions. Different methods of measurement are available, but only the method found in ISO140, part3 [1995] and part4 [1978], is recognised internationally. The objective of this chapter is to investigate the present methods of measurement of sound insulation and to show that all were developed from assumptions derived from the classical theory described in Chapters 2 and 3. It will be demonstrated that the methods are generally not appropriate for rooms smaller than $50m^3$ and for frequencies below 100Hz, which are the conditions of special study in this thesis.

4.2   STANDARD METHOD

The conventional two-room method is the most widely used for sound insulation measurements. It is defined in the International Standards ISO 140 part 3 [1995] and 4 [1978], which correspond to the measurement of sound insulation in laboratories and in the field, respectively. Part 4 was written in 1978. Part 3 was reviewed recently, in 1995, including an annex for sound insulation measurements at low frequencies. The method is also found in the British Standard, BS 2750 [1980]. The method applies when the party wall is between two adjacent rooms. The sound energy passing from one room to the other can then be estimated by calculating the sound pressure level difference. Two formulae, one for laboratory measurements and one for the field measurements are defined.

Assuming that the sound field is diffuse inside the source room and the receiving room, and that flanking transmission effects are negligible, the sound insulation is obtained by measuring the difference between the spatial-averaged sound pressure levels in the source and receiving rooms. The difference is normalised by adding a correction factor

to take into account the sound absorption inside the receiving room. The sound reduction index, R, is then obtained from Equations 2.1 and 2.2, assuming that all the energy transmitted from the source room to the receiving room comes through the wall, to give

$$R = L_1 - L_2 + 10 \log\left(\frac{S}{A}\right) \qquad \text{dB} \qquad (4.1)$$

where L_1 and L_2 are the space-averaged sound pressure levels in the source room and in the receiving room, S is the surface area of the party wall, A is the absorption in the receiving room.

That relationship is based on the definition given for an infinite panel, with dimensions greater than the acoustic wavelength (see Chapter 2) and for diffuse sound [Beranek (1992)]. The laboratory design must therefore be constructed under specific conditions to justify those assumptions. They are:

1. Room volumes are greater than 50m^3 with at least a 10% difference between volumes.

2. The sound field must be steady and have a continuous spectrum in the frequency range considered. It has to be diffuse in each room. Diffusing panels can be installed to ensure this.

3. The area of the party wall must be 10m^2 with the shorter edge being not less than 2.3m. A smaller size will be allowed if the wavelength of free flexural waves at the lowest frequency considered is smaller than half the minimum dimension.

4. Edge conditions of the panel must be specified.

5. Flanking transmission is minimised.

Six microphone positions outside the direct field of the sound source, are required to measure the sound field. They must be well spaced from each other and 1/4 wavelength from the loudspeaker and from room boundaries. An averaging time of 6s is required for frequencies below 400Hz. The loudspeaker must produce a sound level 10-15dB above

the background noise and the radiation must be uniform and omnidirectional.

Assuming that the sound fields in the source room and in the receiving room are diffuse, the measurements in the field are comparable to the laboratory measurements by using the following relationship

$$R' = L_1 - L_2 + 10 \log\left(\frac{T}{T_0}\right) \qquad\qquad dB \qquad (4.2)$$

where R' is called the apparent sound reduction index or standardised level difference, T is the reverberation time measured in the receiving room, and T_0 is the reference reverberation time equals to 0.5s. The term $10 \log\left(\frac{T}{0.5}\right)$ is introduced to normalise the sound insulation of the party wall whatever the furniture and thus the absorption in the receiving room where the measurements are performed.

The methods for the laboratory and field require measurements from 100Hz to 3150Hz/ 5000Hz. It is only recently, in the ISO 140 Part 3 [1995], that an informative annex considers measurements from 50Hz to 100Hz with a 1/3 octave band resolution. Guidelines are given for microphones, loudspeakers and for measurements. The minimum distance between microphones and between microphone and the room boundaries is 1.2m. The number of microphones must be double that for 100Hz to 3150Hz, and distributed homogeneously inside the enclosure. Their positions have to be selected carefully in order to measure the low and high pressure levels inside the room at resonances. The averaging time should be greater than 15s in the 50Hz third octave band. Guidelines recommend the use of three loudspeaker positions, but the positions are not defined. It is also recommended that damping material is installed inside the enclosures to improve the modal overlap but, again, little detail is given.

The accuracy of measurement of sound insulation using the conventional two room method depends on the measurements of the steady state sound field and of the reverberation time. The sound field at low frequencies depends strongly on loudspeaker position and number, microphone number and position, and on the averaging time

[Fothergill (1982)]. The method for field measurements is derived from the formulae given for laboratory measurement and the two relationships are said to be equivalent when the sound fields are diffuse and when flanking transmission is negligible. The former is not likely to be the case, particularly at low frequencies, where wavelength is greater than room and wall dimensions [Halliwell et al (1985)]. The number of microphones is too small to provide a meaningful average. In a furnished room, the number of microphones cannot be increased if the 0.5m distance from the boundary requirement is to be respected. The guidelines given in Annex F of ISO 140, part 3 [1995] are therefore generally not applicable to small rooms.

Reverberation time measurements at low frequencies also produce decays which are not linear at low frequencies (see Section 3.3) [Davy (1988)]. The interrupted source (gun) method gives unacceptable repeatability. The sound source does not provide sufficient energy and thus the decaying signal is quickly masked by the background noise.

There have been several attempts to improve reverberation time measurements at low frequencies. The interrupted method can be improved when used with a time reversed analysis to give smooth sound pressure level decays [Rasmussen et al (1991)]. However, the decay range may be insufficient due to the short impulse which does not excite the sound field significantly [Milosović et al (1998)]. Repeatability is improved when the source and the microphone positions are close to the wall since the relative contribution of oblique modes is increased [Jacobsen (1982)]. This explains the use of the Waterhouse correction factor (see Section 4.3). Another proposal is to average a large number of initial decay rate measurements [Brüel (1978), Larsen (1978), Jacobsen (1982)]. The methods, however, are not considered in ISO 140, part 3 [1995] and 4 [1980] and moreover are time consuming.

The agreement between successive measurements of sound reduction index data of the same party wall under the same condition is poor at low frequencies [Kropp (1994), Farina (1996)]. The differences in room dimensions and the non statistical behaviour of the two sound fields explain such discrepancies. However, recently, the use of bass absorbers placed in the four corners of each room with a sufficient coverage (20% average by Compound Baffle Absorber (CBA) coverage modules according to Fuchs

[1998]) to damp the acoustic modes, were found to improve the repeatability of measurements from 50Hz to 300Hz [Fothergill (1982), Walker (1992), Pedersen (1997), Fuchs (1998)].

The measurement of sound insulation, using the conventional method, also gives rise to differences between the sound reduction index measured in different laboratories and between the sound reduction index measured in laboratories and in the field [Lang [1972], Fothergill (1980)]. The differences between laboratories are thought to be the results of differences in edge conditions of the test wall [Kihlman (1970), Kihlman et al (1972), Guy et al (1985)] and in the type of laboratories used [Utley (1968), Bhattacharya (1972), Halliwell et al (1985), Guy et al (1985), Craik (1992), Roland (1995)]. The apparent sound reduction index includes the sound power transmitted by flanking elements, which are present in dwellings, while practically non existent in laboratories. Moreover, the room dimensions in dwellings are appreciably smaller than standard test chambers. Special diffusors, used in test chambers, do not exist in dwellings. Mounting conditions of party walls in dwellings are also different from those in laboratories [Goydke (1998)]. It can also be added that rooms in dwellings have doors and windows, with resonances which can alter the sound fields. It is therefore not surprising that poor reproducibility is obtained between the field and laboratory data.

To summarise; the most common method for sound insulation measurements is recommended in ISO140, part3 and 4. The method, however, is inaccurate at low frequencies, due to large variations of the sound field. It also does not take into account the effect of room volume and shape, which assume importance when the wavelength is of the same order as room dimensions. Microphones and loudspeaker position recommendations are not applicable to rooms smaller than $50m^3$. It remains to describe more recent proposals for field measurements of sound insulation, with particular references to the low frequency problem.

4.3   WATERHOUSE CORRECTION FACTOR

The Waterhouse correction factor was first introduced for measurements carried out in the middle of reverberant rooms to calculate the total sound energy in the enclosure, but it is also used to increase the accuracy of sound insulation measurements at low frequencies where the energy density inside an enclosure is actually not uniformly distributed [Larsen (1980), Halliwell et al (1985)].

The use of the Waterhouse correction factor takes account of the increase of pressure near room boundaries by considering the room volume and the total surface area of the enclosure and wavelength [Waterhouse (1955)]. It is defined as;

$$W_H = 1 + \frac{\lambda_i \, S_{encl}}{8 \, V} \qquad (4.3)$$

In decibel form, the correction factor is expressed as

$$\begin{aligned} C_w &= 10 \log W_H \\ &= 10 \log \left(1 + \frac{\lambda_i \, S_{encl}}{8 \, V} \right) \end{aligned} \qquad (4.4)$$

Larsen [1980] used it for sound power measurements and showed that the insertion of the correction factor reduces the standard deviation. The correction is shown in Figure 4.1 for the room sizes typical in this study. Its introduction reduces the discrepancy between the transmission loss data measured by the standard method and that by the intensity method (see section 4.4)at low frequencies.

The Waterhouse correction factor, however, assumes a diffuse sound field in the room centre and takes no account of the modal behaviour of the sound field. Uosukainen [1995] defined a new correction factor, taking into account the modal density of the room. The number of axial and tangential modes, which are greater than the number of oblique modes in small rooms, are therefore considered. The modified Waterhouse correction factor, again, has an obvious effect on the standard method. However, the discrepancy between the standard method and the intensity method remains large

[Halliwell et al (1985), Jonasson (1991 & 93), Uosukainen (1995)]. The use of the Waterhouse correction factor remains under investigation.

4.4 INTENSITY METHOD

The intensity method is not new [Schultz (1956)], but was only commercialised at the end of 1970 when digital signal processing and FFT analysers improved speed and reliability of the method. The method is mainly used for the determination of sound power of complex sources, radiation of highly reactive sound fields near panel surfaces or energy flow in ducts. It is also used for the measurements of acoustic absorption and sound transmission loss in laboratories and in situ [Halliwell et al (1985), Hopkins (1996), Nightingale (1996), Jonasson (1991 & 93)].

The method for sound insulation is not yet standardised, but a draft proposal is in circulation [Hopkins et al (1996), Jacobsen (1997)]. To measure transmission loss, one reverberant room only is necessary, the other space can be any size and can be free field or partially reverberant. The transmitted power, p_t, is determined from the surface averaged sound intensity as

$$p_t = I_t . S \qquad (4.5)$$

where the transmitted intensity, I_t, is measured directly on the receiving side of the party wall surface. The transmission loss is obtained by combining Equations 4.5 and 2.2 to give the following relationship:

$$T.L. = 10 \ \log\left(\frac{\left(p_i^2 / 4\rho_0 c_0\right)S}{I_t S}\right) \qquad (4.6)$$

$$T.L. = L_p - L_I - 6 \ dB \qquad (4.7)$$

where L_p is the averaged sound pressure level inside the source room and L_I is the normal sound intensity in the receiving room. L_p is measured as in the draft standard i.e. as a spatial average from different microphone positions and L_I is measured by scanning the wall surface with an intensity probe or by placing it at fixed positions on the

receiving side of the wall.

The method is shown to be accurate, when compared with the conventional method, when the Waterhouse correction factor is included [Haliwell et al (1986)]. The method is not affected by flanking transmission [Jonasson (1991 & 93)] or high background noise. The fixing conditions of the party wall, the different parts of a composite party wall, or areas of leakage can be identified [Cops et al (1984)]. The sound reduction index of small area walls can be measured and components which gives large sound transmission can be identified [Brüel & Kjær (1980)].

The incident sound field, however, must be diffuse. If not, the standard deviation calculated from measurements between laboratories will be high at low frequencies [Roland (1995)]. On the other hand, Pedersen [1997] showed that the reproducibility is improved by placing a large number of microphones inside the source room, all close to the party wall, or by placing an absorbent material on the wall opposite to the party wall in the receiving room and then performing a large number of intensity measurements close to the party wall surface. It can be argued that such method is only applicable to source rooms of volumes greater than 50m^3. The procedure is time consuming and the presence of an operator is required for the scanning of the surface of the party wall. Errors result due to movement of operator or probe and if the surface is not sampled uniformly. Even if uniformly sampled, errors arise when the wall radiates at resonances. Some parts of the wall may radiate more than others and the sampling will not correctly represent their contribution [Brüel & Kjær (1988)]. Flanking transmission, when included in the measurement, gives an overestimated sound power level [Nightingale (1996)]. Measurements of panels with high absorption result in overestimation of the transmission loss [Cops et al (1984), Halliwell et al (1985), Jacobsen et al (1996)]. In fact, the partition provides a significant part of the absorption of the receiving room. The error depends on the ratio between the absorption of the wall and the total absorption of the room.

To summarise; the sound intensity method is reliable for sound insulation measurements for frequencies greater than 100Hz and does not require a measurement of reverberation time. However, the sound field inside the source room must be diffuse and this seldom will be the case in dwellings. Measurements therefore are not accurate at low

frequencies, as described in Section 4.2.

4.5 POWER METHOD

Reverberation time is an indirect indication of the sound power inside the receiving room, but cannot be measured accurately at low frequencies [Brüel (1978), Larsen (1980)]. Sound reduction index can instead be measured by determining the sound power emitted by the wall into the receiving room by comparing it with a reference sound source.

Transmission loss is expressed under the assumption that the sound field is diffuse in the source room and in the receiving room:

$$R = L_1 + 10 \log\left(1 + \frac{\lambda_i S_{encl_1}}{8 V_1}\right) + 10 \log\left(\frac{S}{S_o}\right) - 6 - (L_2 + L_{WR} - L_{2R}) \quad dB \quad (4.8)$$

where L_1 and L_2 are the spatial averaged sound pressure levels in the source and in the receiving rooms, respectively, S_{encl_1} is the surface area of the source room , V_1 is the volume of the source room, S is the area of the party wall, $S_0 = 1m^2$ is a reference value, L_{2R} is the spatial averaged sound pressure level inside the receiving room when the reference sound source is switched on, and L_{WR}, the power level, is defined as

$$L_{WR} = 10 \log\left(\frac{W_R}{W_0}\right) \quad dB \quad (4.9)$$

with $W_0 = 10^{-12}$ Watts and W_R is the sound power emitted by the reference sound source. It can be seen that the term $(L_2 + L_{WR} - L_{2R})$ is equal to the sound power level emitted into the receiving room by the party wall.

The method consists of measuring the sound pressure level difference between two rooms and the power level in the receiving room, in terms of the averaged pressure with a reference sound source switched on. A reference sound source is placed 1.5m from the

walls and the microphone is placed far from the speaker. The power method is quick since only measurements of sound pressure levels are required. The errors relate only to sound level difference. The instrumentation required to measure the sound insulation is simple. There are no observed effects of room configuration in the frequency range 100-3150Hz.

Large discrepancies, however, are obtained at low frequencies, when the Waterhouse correction factor is not included as described in section 4.3. The power level inside a small receiving room volume is difficult to measure as the microphone cannot be placed far from the speaker and the speaker cannot be placed far from the walls. The averaged pressure level depends on the averaging time, microphone and loudspeaker positions. The sound field also depends on the directivity of the reference sound source. It is also difficult to drive loudspeakers much above the background noise. The method, therefore, does not offer significant advantages for the measurements of the sound insulation at low frequencies.

4.6   SHORT TEST METHODS

Sound insulation measurements are time consuming and costly when applying ISO 140. Within the last 20 years, there have been several proposals for a simple method of measurement, in particular in a CEN draft [Vorländer (1995), Cocchi (1989), Schmitz (1997)]. The CEN method involves a visual estimate of the room dimensions and the furniture in order to estimate the acoustic properties of the room, and a measurement of the sound pressure level difference [Vorländer (1995)]. The method is defined according to the following;

$$D_{nT} = L_1 - L_2 + \Psi \qquad\qquad dB \qquad\qquad (4.10)$$

where D_{nT} is the standardised sound pressure level difference, L_1 and L_2 are the averaged sound pressure levels in the source room and in the receiving room, Ψ is the

reverberation term, equal to $10\log\left(\dfrac{T_1}{T_0}\right)$, with T_1 the reverberation time of the source room and $T_0 = 0.5$s, the reference reverberation time.

D_{nT} is measured, by performing the measurements with an operator who moves the sound level meter or microphone [Vorländer (1995)], or by measuring the sound level difference in dB(A) according to ISO/TC43/SC2/WG10 [Cocchi et al (1989)]. Ψ is given in Tables contained in the standard. The domestic rooms are classed in four categories: volumes smaller than 15m^3, between 15m^3 and 35m^3, between 35m^3 and 60m^3 and greater than 60m^3. The state of the room, furniture and surface absorption are considered separately in each category.

The advantages of this method are that only one operator is required and reverberation time measurements are not required. Again, the method, however, was only developed for sound insulation measurements above 100Hz or from the 63Hz octave band. Also, when A-weighted sound pressure level difference are considered, only frequencies above 100Hz are considered.

4.7   CONCLUSION

There are many available methods for measurement of sound insulation. The methods are seen to be strongly dependent on the accuracy of the measurements of the sound fields and of the reverberation time. In general, they show poor repeatability and poor reproducibility at low frequencies. This is because all methods were defined primarily with the assumption that the sound fields are diffuse. Consequently, the present methods of measurements are not accurate enough for sound insulation measurements at low frequencies.

The problem of accuracy of sound insulation measurements at low frequencies still needs to be investigated further. It remains to investigate it by computer simulation, where different methods are available.

4.8 REFERENCES

Beranek, L.L and Ver, I.L., (1992): 'Noise and Vibration Control Engineering: Principles and Applications', Ed. J.Wiley and Sons

Bhattacharya, M.C. and Guy, R.W., (1972): 'The influence of the measuring facility on the measured sound insulating property of a panel', Acustica, Vol.26, 344-348

Brüel and Kjær, (1988): 'Sound Intensity', B&K booklet

Brüel, P.V., (1978), 'The enigma of the sound power measurements at low frequencies', Brüel&Kjær, N° 3, 3-40,

BS 2750, (ISO 140/III: 1978), (1980): 'Measurements of sound insulation in buildings and of building elements. Part 3. Laboratory measurements of airborne sound insulation of building elements'

BS 2750, (ISO 140/IV: 1978), (1980): 'Measurements of sound insulation in buildings and of building elements. Part 4. Field measurements of airborne sound insulation of building elements'

Cocchi, A. and Garai, M., (1989): 'Experimental Verification of a short method for the determination of the acoustical insulation index of party walls', Applied Acoustics, Vol.28, 83-94

Cops, A., and Minten, M., (1984), 'Comparative study between the sound intensity method and the conventional two room method to calculate the sound transmission loss of wall construction', Noise Control Engineering Journal, May-June 1984, 104-111

Craik, J.M., (1992): 'The influence of the laboratory measurements of walls performance', Applied Acoustics, Vol.35, 25-46

Davy, J. L., (1988): 'The variance of decay rate at low frequencies', Applied Acoustics, Vol.23, 63-79

Farina, A, Fausti, P., Pompoli, R. and Scamoni, F., (1996): 'Inter-comparison of laboratory measurements of airborne sound insulation of partitions pompoli', Proceeding of Inter-Noise 96, 881-886

Fothergill, L.C., (1980): 'Recommendations for the measurements of sound insulation between dwellings', Applied Acoustics, Vol.13, 171-187

Fothergill, L.C., (1982): 'Simple methods for assessing reverberation time', Applied

Acoustics, Vol.15, 11-29

Fuchs, H.V., Zha, X., Spah, M. and Pommerer, M., (1998): *'Qualifications of small freefield and reverberation rooms for low frequencies'*, Proceeding of Euro-Noise 98, Vol.2, 657-662

Goydke, H., (1998): *'Investigations on the precision of laboratory measurements of sound insulation of building elements according to the revised Standard ISO 140'*, Proceeding of Inter-Noise 98, 480

Guy, R.W., De Mey, A., and Sauer, P., (1985), *'The effect of some physical parameters upon the laboratory of sound transmission loss'*, Applied Acoustics, Vol.18, 81-98

Halliwell, R.E. and Warnock, C.C., (1985), *'Sound transmission loss: Comparison of conventional techniques with sound intensity techniques'*, Journal of Acoustical Society of America, Vol.77 (6), 2094-2103

Hopkins, C. and Emmanuel, (1996): *'Intensity measurements for building acoustics'*, Proceeding of I.O.A., Vol.18 (3), 21-30

ISO 140, (1978): *'Measurements of sound insulation in buildings and of building elements. Part 4. Field measurements of airborne sound insulation of building elements'*

ISO 140, (1995): *'Measurements of sound insulation in buildings and of building elements. Part 3. Laboratory measurements of airborne sound insulation of building elements'*

Jacobsen, F. and Ding, H., (1996), *'Observations of the systematic deviations between the results of the conventional method and the sound intensity method of measuring transmission loss'*, Proceeding of Inter-Noise 96, 2719-2724

Jacobsen, F., (1982): *'Decay rate and wall absorption at low frequencies'*, Journal of Sound and Vibration, Vol.81 (3), 405-412

Jacobsen, F., (1997): *'Sound intensity and its measurements'*, Fifth International Congress on Sound and Vibration, December 15-18, Adelaide

Jonasson, H.G., (1991): *'Measurements of the sound reduction index with intensity technique'*, Nordtest Project 746-788, SP report 1991:23, Swedish National testing and research institute, Borås

Jonasson, H.G., (1993), *'Sound intensity and sound reduction index'*, Applied Acoustics, Vol.?, 281-293

Kihlman, T and Nilsson, A.C., (1972): *'The effects of some laboratory designs and mounting conditions on reduction index measurements'*, Applied Acoustics, Vol.5

Kihlman, T., (1970): *'Report on the influence of boundary conditions on the reduction index'*, Report N0 ISO/TC43/SC2/WG2, Chalmers Tekniska Hogskila, Goteborg, Sweden

Kropp, W., Pietrzyk, A., Kihlman, T., (1994): *'On the meaning of the sound reduction index at low frequencies'*, Acta Acustica, Vol.2, 379-392

Lang, J., (1972): *'Differences between acoustical insulation properties measured in the laboratory and results of measurements in situ'*, Applied Acoustics, Vol.5, p21-37

Larsen, H., (1978): *'Reverberation Process at low frequencies'*, Brüel and Kjær Technical Review, N°4, 3-42

Larsen, H., (1980): *'Power based measurements of sound insulation'*, Brüel and Kjær Technical Review: Transmission loss, N°3, 3 -22

Milosovic, M.A. and Ćiric, D.G., (1998): *'Short reverberation time measurement using integrated impulse method'*, Proceeding of Euro-Noise 98, Vol. 2, 711-716

Nefske, D.J. and Sung, S.H., (1990): *'Sound in small enclosures'*, Engineering Mechanics Department, General motor Research Laboratories Research Publication GMR-7069

Nightingale, T.R.T., (1996): *'Acoustic intensity as a tool for assessing sound isolation and flanking transmission in lightweight buildings'*, Proceeding of Inter-Noise 96, 2685-2690

Pedersen, D.B., (1997), *Laboratory measurement of the low frequency sound insulation*, DAGA 97, Kiel, 105-106

Rasmussen, B., Rindel, J. H. and Heinriksen, H., (1991): *'Design and measurements of short reverberation times at low frequencies in talk studios'*, Journal of Audio Engineering Society, Vol.39 (1/2), 47-57

Roland, J., (1995): *'Adaptation of existing test facilities to low frequencies measurements'*, Proceeding of Inter-Noise 95, 113-1115

Schmitz, A. and Raabe, G., (1997): *'Testing of the CEN survey method for building acoustic measurements in Germany'*, Proceeding of Inter-Noise 97, Vol.3, 1453-1456

Schultz, T.J., (1956), *'Acoustic Wattmeter'*, Journal of Acoustical Society of America,

Vol.28, 693-699

Uosukainen, (1995): '*On the use of the Waterhouse correction*', Journal of Sound and Vibration, Vol.186 (2), 223-230,

Utley, W.A., (1968): '*Single leaf transmission at low frequencies*', Journal of Sound and Vibration, Vol.8 (2), 256-261

Vorländer, M., (1995): '*Survey test methods for acoustic measurements in buildings*', Building Acoustics, Vol.2 (1), 377-389

Walker, R., (1992): '*Low frequency room responses. Part 1: Backgroung and qualitative considerations*', BBC Report RD 1992/8

Waterhouse, R.V., (1955): '*Interference patterns in reverberant sound fields*', Journal of the Acoustical Society of America, Vol.27, 247-258
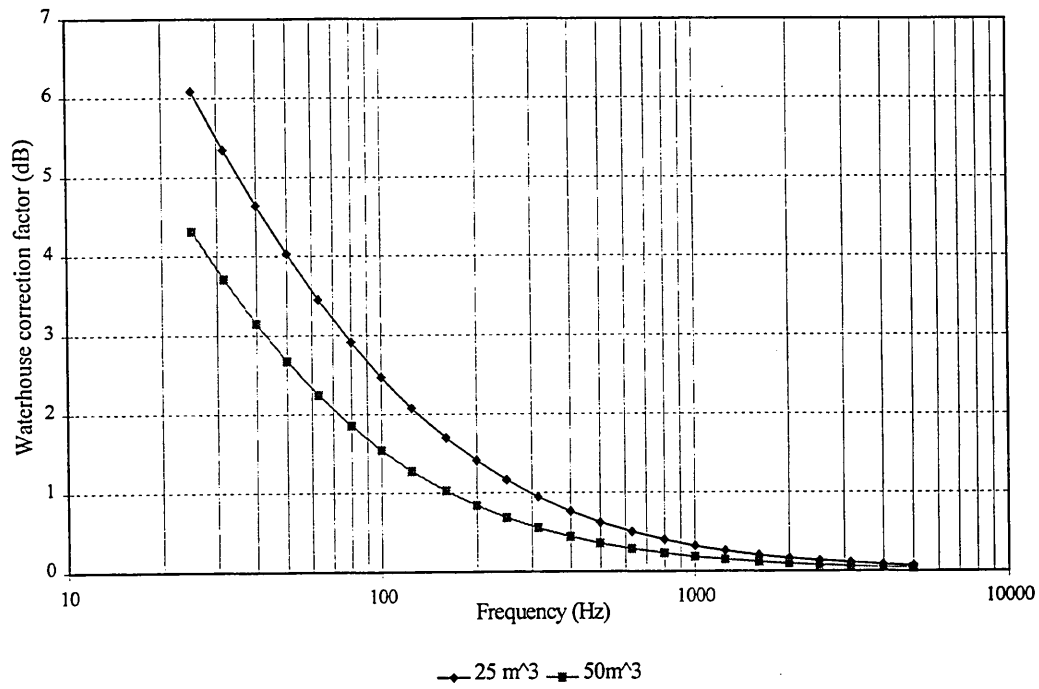
Figure 4.1. Calculated Waterhouse correction factor for the 25m^3 and 50m^3 rooms

5   CHOICE OF INVESTIGATIVE METHOD

5.1   INTRODUCTION

Sound insulation measurements at low frequencies between domestic rooms are shown in chapter 4 to be not controllable when using full scale measurements. The classical diffuse sound field theory has limited application in this frequency range. Other predictive methods are thus required. Their application to sound insulation at low frequencies is investigated in this present chapter. It will be demonstrated that analytical modal decomposition methods can only be used for the simplest room geometry and for the simplest wall edge conditions. Geometrical acoustics, using ray tracing or image source methods, does not take account of the wave phenomenon and the fluid-structural interaction. It is most commonly used in large room acoustics where the ratio of wavelength to room dimensions is small.

What is required, is a robust, flexible prediction method, which will highlight the dominant resonant characteristics of rooms and walls and which will allow consideration of irregular room shapes and edge conditions of the party wall. Hence, numerical modal modelling will be shown to be an appropriate tool to predict sound transmission at low frequencies and for small rooms.

5.2   ANALYTICAL MODEL METHOD

The method has been considered in studies of panel response to acoustic fields and the resultant insulation [Maidanik (1962), Sewell (1970), Gurovich (1978)]. The modal approach initially was developed to model the panel response when backed by a closed cavity [Pretlove (1965), Bhattacharya (1969), Pretlove et al (1970), Guy (1973 & 79)]. Here the modal characteristics of the panel were taken account, but also the modal characteristics of the sound field. Theoretical studies of sound transmission have been undertaken by Heckl [1958], Josse and Lamure [1964], Kihlman [1967], Nilsson [1972], Mulholland [1973], who considered the room - partition - room system. The lack of

computational power at the time of their studies, limited the work although the phenomenon of room coupling was highlighted. More recently, Gargliadini et al [1991], Kropp et al [1994] and Osipov [1997-a] have been able to develop the approach for low and medium frequency sound transmission between two rectangular rooms of different volumes.

The principles of the analytical model are to describe the room – party wall – room system by a set of equations expressing the coupling between the sound fields and the panel displacements. The room pressure amplitudes and wall displacements are obtained from the plate equation of motion and from the continuity conditions between the sound fields and the plate surfaces [Osipov (1997-a)]. This method results in a large set of equations and requires computers for solutions.

The analytical model has become more accessible in the last 10 years due to the availability of much greater computing power than previously. It can be used to calculate the frequency response of the two rooms, the party wall and the coupling between those sub-systems. It works for rectangular shapes and for the study of asymmetric and symmetric room configurations [Gargliadini (1991)]. It also was preferred to other methods for the short computation times required [Kropp et al (1994)]. Different analytical models can be defined to predict the sound transmission, but Osipov [1997-a] shows that the analytical model of the room-partition-room system is the best method when compared with the baffled plate and infinite plate models; the last being the worst model.

The method has limitations in that rectangular and cubic shapes only are considered to facilitate the modal decomposition of the panel displacement and the sound field of the enclosure [Gargliadini (1991)]. It does not take account of wall position, i.e. where the partition is placed within the test opening [Kihlman et al (1994)] and it cannot handle non-uniform distributions of surface treatment.

The party wall is assumed simply supported since other boundary conditions are too difficult to model [Gargliadini (1991), Atalla & al (1994), Osipov (1997-a)]. Modelling the party wall as a baffled or infinite plate, ignores the coupling between structural

92

modes and acoustic modes [Osipov (1997-a)]. The analytical model is not as accurate as is required; there are large discrepancies between prediction and measurement due to the selected energetic equations, and due to the effect of edge conditions on the party wall at low frequencies [Gargliadini (1991)]. It is also time consuming to truncate all energetic equations inside a computer program.

To summarise; the analytical method could be used for the study of sound transmission at low frequencies between two finite sound fields, but modelling the room-panel-room system and developing a computational program to resolve the set of equations would be excessively time consuming. Changing the boundary conditions at the wall edges would be intractable. The use of an analytical method for modelling the sound transmission at low frequencies will not be pursued any further.

5.3   GEOMETRIC MODELS

Ray tracing and image source methods were proposed 30 years ago [Krokstad (1983)] and continue to be developed as useful predictive tools in room acoustics [Ondet (1988&89), Raynoise (1993), Dance (1995), Christensen et al (1998)] although each method has its advantages and disadvantages [Hammad (1988)].

5.3.1 Ray tracing method

Ray tracing [Schroeder (1970)] was originally developed for the study of auditoria, where it was used to understand the relationship between the shape of an enclosure and the sound decay characteristics [Schroeder (1970)]. The method then has found application for other large enclosures [Dance (1995)].

To simulate a sound field, an enclosure is modelled using room dimension co-ordinates and material characteristics. The source is modelled as a point [Ondet (1988 & 89)], or a surface [Raynoise (1993)], in three dimensional space. Energy particles leave the source at the same speed of sound along a ray coming from the centre of the source [Kuttruff

(1991)]. Rays are randomly and regularly distributed inside the room and build up a sound field by reflecting along the plane surface according to Snell's law of specular reflection; the reflected angle equals the incident angle as shown in Figure 5.1.

Each ray is traced until its energy content decreases below a set value. The receiver sums the energy of the direct and reflected rays passing through it in order to predict the sound energy inside the enclosure. The sound energy propagation takes account of the effects of air absorption and surface absorption, the latter by a factor $(1-\alpha)$, where α is the absorption coefficient of the surface. Obstacles inside the enclosure diffract the rays and rough surfaces scatter the rays according to Lambert's law [Vorländer (1998)]. The sound field can be presented in two ways. The first is to add the energy of each ray to achieve a steady state behaviour. Contour plots can then be displayed showing the sound pressure level distribution in the enclosure. The second is the impulse response, displayed in the form of an histogram; vertical lines are displayed against time, each one representing a reflected ray separated by the travel time delay, and the decreasing amplitude represents the reflection order. Acoustical parameters like reverberation time, Early Decay Time, speech intelligibility, sound transmission and others thus are derived. Computation time is reduced because the calculation is reciprocal i.e. if the source and receiver are interchanged, the result will be the same.

Ray tracing is mainly used for the study of the acoustics of large rooms e.g. auditoria [Kleiner (1993), Madalik (1996), Raynoise (1993), industrial buildings [Raynoise (1993), Dance (1995)], environmental problems [Raynoise (1993)], train stations, airports and stadia [McCulloch (1998)]. The main application was and still is for auditoria as ray tracing can be used for any enclosure shape with different absorption coefficients assigned to any surfaces of the room [Hammad (1988)], with or without obstacles [Benedetto et al (1984), Dance (1995)]. The method also is used for the prediction of non diffuse fields such as the interior of factories, reviewed by Dance [1995]. It is recognised to be the most accurate geometrical method for predicting the factory noise level [Beranek (1992)] and the effect of barrier insertion loss [Benedetto (1984)]. Ray tracing also is used for the study of sound field inside car enclosures at mid and high frequencies due to noise transmission of the engine [McCulloch (1997)]. The

method is cheaper, faster and more flexible when compared with measurements carried out on physical scale models.

The method has limitations in that vibrating surfaces are not taken into account and again, the coupling effects between sound field and vibrating panels are neglected. The method is applicable to a statistical sound field above the cut off Schroeder frequency, when the ratio wavelength/room dimensions is small. Time is consumed in the design of the database representing the wall characteristics of the model and in defining the position of source and receiver [Vorländer (1998)]. It requires powerful computer processing when the defined model is large and therefore does not lend itself to large-scale parametric surveys.

5.3.2 Image source method

The image source method was first developed for the study of the steady-state sound field and the distribution of absorption in rectangular rooms [Gibbs et al (1972)] and since, has been developed for many other applications, as described by Dance [1995].

The principle of the image source method is to consider a room as a combination of acoustic 'mirrors' at the room surfaces. The sound source gives rise to a large (theoretically, infinite) number of image sources which contribute to the sound field. This is the same as the sound source sending a ray of a given intensity in the room, which is then mirrored by the first surface impinged. According to the optical geometry law, an image source is built up symmetrical to the main source through the wall and creates a reflected ray forming an angle with the surface equal to the incident angle. Another image source is then formed from the first image source, when the reflected ray impinges upon another wall and so on, shown by Figure 5.2.

A large number of image sources is then processed, created as a regular lattice in three-dimensional space around the room. The steady state energy density at one point in the room is then calculated by adding the energy radiated by the sound source and the image sources through the different walls of the room [Allen et al (1979)]. The transient response, is processed as a histogram in the same way as in ray tracing. Such prediction

of the energy density of the field is dependent on the directivity of the sources, the reflection coefficients of the surfaces and the distance travelled by the sound. The energy intensity of each ray varies with the introduction of absorption inside the room by attributing properly reduced acoustic power to the image sources. Other methods can be used for scattering effects [Akil (1995)], but are not discussed here. The method also has been used for the prediction of reverberation time in small rooms [Allen et al (1979)].

The model mainly has been developed for noise prediction and control inside factories [Shield (1980), Dance et al (1994 & 97-a&b), Dance (1995)]. It is also used for the study of the room acoustics in auditoria [Kirszenstein (1984), Kleiner et al (1993)], predicting the decay time, clarity, speech transmission index in a similar manner as ray tracing.

The method is generally limited to prediction of sound pressure level in rectangular rooms and where the ratio wavelength/room dimensions is large. Large computational time and memory size are required to process and test the validity of the lattice of virtual sources needed for the prediction [Kuttruff (1991)]. Interference effects are normally not included, but Dance and Shield [1997-a] showed that such effects can be considered if intensity is replaced by sound pressure including phase difference between the incident ray and the first reflected ray.

Recently, hybrid models have been developed, using the ray tracing method to process image sources [Ondet et al (1989), DeGeets (1996), Dance et al (1995 & 97-b), McCulloch (1997)]. Such models can predict the sound field where the wavelength is still long with respect to room dimensions i.e. by modelling the eigenmodes. They are modelled using coherent image sources i.e. by including the phase between the direct and the first order reflected ray or between two reflected rays. The sound fields at low frequencies in large rooms [Dance and Shield (1997-b)] or the sound fields in smaller rooms at medium frequencies [DeGeets (1996)] can be predicted. Good agreement was obtained with Boundary Element Methods (see Section 5.4.1) for rectangular rooms. Prediction at very low frequencies, however, is still poor [DeGeets (1996)].

According to McCulloch [1998], the sound transmission between two rooms could be predicted using geometric methods. The sound field in the sending room is calculated and reused to calculate the sound field in the receiving room by considering the frequency dependent transmission properties of the wall. However, the wave phenomena created by the coupling between the two or three subsystems still will not be represented and the sound insulation will depend on material properties measured in laboratories which often are not accessible below 100Hz. Ray tracing and image source methods are therefore not suitable for the modelling of the sound transmission between two rooms at low frequencies.

5.4   NUMERICAL MODEL METHODS

5.4.1 Boundary Element Method

The Boundary Element Method (BEM), was developed after the Finite Element Method (FEM) to model the system at its boundaries and to predict radiation and scattering phenomena in infinite domains [Cops (1994), Atalla et al (1994), Crocker (1997)]. The principle of BEM is to discretize any systems into surface elements to which surface potentials are allocated. A matrix equation is created, linking the normal velocity distribution and the surface pressure distributions. Such variables are used to predict the radiation and the resultant sound fields in semi- infinite and infinite media.

Two boundary element methods are commonly used; the direct boundary element method and the indirect method. The first allows the normal velocities and surface pressure to be processed to predict interior or exterior fields. The second yields the pressure and normal velocity discontinuity through the surface, predicting mixed regions i.e. involving interior and exterior spaces simultaneously [Sysnoise (1993), Crocker (1997)]. When the system is divided into surface elements at the boundaries, the fluid density and speed of sound, or material properties, are assigned to the system. The sound pressure distribution on the surface of the body and at other points in the field, the sound intensity and the sound power then are processed.

BEM is very popular for the study of radiation phenomena and the insertion loss of barriers in the field [McCulloch (1997)]. Complex surfaces with junctions also can be modelled. BEM is used for the prediction of muffler and silencer performance of sound barriers and for the control of noisy machines [Augusztinovicz (1998)] and it is recognised to be the most suitable method for radiation prediction and scattering problems. It describes accurately the geometry of the model i.e. corners, edges, curvatures and a relatively short time is necessary to model a three dimensional system. The modelling requires only the discretization of the surfaces and not of the adjacent or surrounding medium, for which general properties such as density and sound velocity are assigned. The dimension is therefore reduced by one and leads to a more effective computational process. Reflecting surfaces can be assigned with an arbitrary reflection coefficient and a range of boundary conditions, including the impedance boundary conditions, are available. Point sources can be included.

BEM requires meshes fine enough to represent the vibration or sound pressure distribution on surfaces of the system. The size of the surface element has to be carefully defined with respect to the upper frequency range of interest. Coarser meshes can be used for finite acoustic fields, but the surface meshes require a large computational effort, hence, a long processing time [Pietrzyk (1996)]. BEM is limited in the prediction of acoustics modes in enclosures and prediction of acoustic modes is less accurate than by the Finite Element Method.

To summarise, the Boundary Element Method is appropriate for predicting interior and exterior sound fields and takes into account the fluid and structural interaction. However, the main application is for exterior problems as acoustic mode prediction is relatively poor. The method therefore was not selected for the prediction of the sound transmission at low frequencies.

5.4.2 Finite Element Method

Finite Element Methods (FEM) were first developed for structural problems in the

1960s [Gladwell (1965), Gladwell et al (1965 & 71), Zienkiewicz (1971)] and more recently as reviewed by Crocker [1997] and Astley [1998]. Important contributions have been made by Craggs [1973, 1994], Petyt et al [1976], Nefske et al [1990], Easwaran et al [1995 a&b, 1996] and Astley [1998] by predicting the sound field inside complex enclosures, including the effect of damping and boundary flexibility. An important break-through was in the application to coupled systems where mutually interdependent structural and acoustical subsystems are solved simultaneously [Augusztinovicz (1998)].

The principle of FEM is to solve a system described by a set of governing differential equations, by discretizing it into elements [Zienkiewicz (1971), Pietrzyk (1996), Tetambe (1996), McCulloch (1997), Crocker (1997), Astley (1998)]. The elements can have different geometry, straight or curved, and each is described by a motion equation. They are characterised by a number of nodes, which fulfil continuity conditions between elements. The choice of the number of elements is determined by the upper frequency of the range of interest [Astley (1998)]. FEM is used to model structural and acoustic systems and can be used to model the coupling between radiating walls and the enclosed sound fields [Craggs (1973)]. The structural model describes the wall vibration in terms of a mass matrix, stiffness matrix, with or without a damping matrix. The nodal variable is displacement. The acoustic model describes the enclosed field in terms of pressure variable, mass matrix, stiffness matrix, and with or without a damping matrix, and the nodal variable is pressure. To model the sound transmission between two rooms, the structural modes are linked to the acoustic modes by adding the acoustical mass matrices and structural matrices [Atalla et al (1994)].

The numerical method is renowned for solving interior problems and is recognised to be the best method for the modelling of sound fields and associated wall vibrations [Wright (1996), Pietrzyk (1996 & 97)]. It allows simulations of acoustic fields as functions of frequency and space, where the wavelength is comparable to the dimensions of the room. It also includes wall radiation onto finite spaces, and therefore predicts acoustic-structural coupling. There is no need to redefine the matrices of elements when processing the frequency response of the system resulting in relatively small computer processing time. The matrices are symmetric, allowing data reduction and reduced

99

memory size. The computational process can be also reduced using modal superposition. The sound field can be predicted within rectangular or complex room shapes, with or without surface absorption [Easwaran et al (1996)]. Point sources and vibrating surfaces can be assigned to the model. The eigenfrequencies of the two and three-dimensional models are easy to obtain. Sound pressure level, including phase, displacement and other acoustical parameters can be extracted from the simulation. The method is applicable to simulation at low and mid frequencies.

There are limitations to the method in that the time necessary for the discretization of the three-dimensional model is greater than for a BEM model. The element size has to be small enough, at least a 1/6 of the wavelength for reliable prediction [Atalla et al (1994)]. The process of data acquisition also is slow, depending on the size of the defined system, on the number of elements and on the processing power of the computer. FEM can only be used to study the system at low and mid frequencies, as more elements are required to model higher frequencies. Also, the more complicated the model geometry, the more elements are necessary, leading to a longer computation time. When coupling an acoustic model with a structural model, the meshes must match [Sysnoise (1993), Pietrzyk (1996)], which often leads to an underestimation of the panel radiation. A large number of elements is needed to approximate an infinite or semi-infinite sound field and the method is not appropriate for such problems.

To summarise; FEM is a numerical method which models finite sound and vibrational fields and the structural-acoustic interactions. It gives accurate prediction of acoustic modes which can be linked to the structural model to predict the effect of the incident sound field on a wall and the effect of a radiating wall on a sound field. Although long processing times and powerful computers are required, FEM is the best method to investigate the effect of edge conditions of the separating wall and of the sound fields inside complex room shapes. It also can include the effect of absorption inside the room [Geddes et al (1988)]. The method therefore was selected to predict sound transmission between two rooms at low frequencies. Although FEM has yet to be used extensively in building acoustics, recent works by Pietrzyk et al [1996 & 97] and Osipov [1997-b] support the decision to use this approach in the present investigation.

100

5.4.3 SYSNOISE

Sysnoise Vol.5.3 is a numerical system for acoustic and structural acoustic modelling [1996]. It is designed to model fluid-structure interaction by combining an acoustic with a structural finite element model. Sysnoise is used to assign a numerical method to imported discretized models. The structural and acoustical models are simulated after the material and air properties have been assigned. Solutions are expressed in different ways: sound pressure level contours, acoustic and structural eigenfrequencies, panel displacements, etc.

Sysnoise was seen as a software package which could address the following components of the proposed investigation;

1. effect of a finite acoustic field on a structural field,

2. effect of finite acoustic field and structural field coupling on a finite acoustic field,

3. effect of varying room dimensions and wall boundary conditions on sound level difference between rooms.

5.5   CONCLUSION

In laboratories and the field, the methods of measuring sound insulation give poor repeatability and reproducibility at low frequencies. The relationship between sound level difference between rooms and the sound reduction index of the intervening wall has yet to be established at low frequencies. To this end, analytical methods have been considered but are shown to be time consuming, expensive, and inflexible. A comparison of other numerical methods shows that the FEM is the most appropriate approach for this study. It provides a description of room-wall combinations, including edge effects. It was foreseen that there would need to be a compromise between prediction accuracy and computational power and time and therefore, the full study would have to be preceded by a methodical selection of element number supported by a comparison between prediction and measurements in order to validate the numerical

5.6 REFERENCES

Akil, H.A., (1995): *The scattering of sound by fittings in industrial buildings'*, PhD thesis, University of Liverpool

Allen, J.B., Berkley, D.A., (1979): *'Image method for efficiently simulating small room acoustics'*, Journal of acoustical society of America, Vol.65, 934-950

Astley, R.J., (1998): *'Finite elements in acoustics'*, Proceeding of Inter-Noise 98, 538

Atalla, N. and Bernhard, R.J., (1994): *'Review of Numerical Solutions for Low Frequency Structural-Acoustic Problems'*, Applied Acoustics, Vol.43, (3), 271-294

Augusztinovicz, F., (1998): *'State of the art of practical applications of numerical methods in vibro-acoustics'*, FIA, 18e Encontro da Sobrac, Congresso Iberoamericano de Acustica, 154-168

Benedetto, G. and Spagnolo, R., (1984): *'A study of barrier in enclosures by ray tracing computer model'*, Applied Acoustics, Vol.17, 183-199

Beranek, L.L. and Ver, I.L., (1992): *'Noise and Vibration Control Engineering: Principles and Applications'*, Ed. J.Wiley and Sons

Bhattacharya, M.C. and Crocker, M.J., (1969): *'Forced vibration of a panel and radiation of sound into a room''*, Reports BS/A/69/1, University of Liverpool.

Christensen, C.L. and Foged, H.T., (1994): *' A room acoustical computer model for industrial environments-the model and its verification'*, Proceeding of Euro-Noise 98, Vol.2, 671-676

Cops, A., *'Progress in building acoustics'*, Proceeding of Inter-Noise 94, August 29-31, Yokoham-Japan, 23-42

Craggs, A., (1973): *'An Acoustic Finite Element Approach for studying boundary flexibility and sound transmission between irregular room'*, Journal of Sound and Vibration, Vol.30 (3), 343-357

Craggs, J., (1994): *'A finite element method for free vibration of air in ducts and rooms with absorbing walls'*, Journal of Sound and Vibration, Vol.173, 568-576

Crocker, M., (1997): *'Recent developments in acoustics and vibrations'*, 5th international Congress on Sound and Vibration, (choice of FEM and BEM),

Dance, S.M. and Shield, B.M., (1994): *'Noise control modelling in non-diffuse*

enclosed space using an image –source model', Proceeding of I.O.A, Vol.16 (2), 515-523

Dance, S.M. and Shield, B.M., (1997-a): *'Computer prediction of sound propagation in enclosed spaces using a pressure based model'*, Fifth International Congress on Sound and Vibration, December 15-18, Adelaide, South Australia

Dance, S.M. and Shield, B.M., (1997-b): *'The complete image –source method for the prediction of sound distribution in non-diffuse enclosed spaces'*, Journal of Sound and Vibration, Vol.201 (4), 473-489

Dance, S.M., (1995): *'The development of computer models for the prediction of factory noise'*, Building Acoustics, Vol.2 (2), 437-454

De Geets, F. and Patzold, H., (1996): *'Comparison between room transmission functions calculated with a boundary element method and a ray tracing method including phase'*, Proceeding of Inter-Noise 96, 3177-3180

Easwaran, V. and Craggs, A., (1995-a): *'On Further Validation and Use of the Finite Element Method to Room Acoustics'*, Journal of Sound and Vibration, Vol.187 (2), 195-212

Easwaran, V. and Craggs, A., (1995-b): *'Transient response of lightly damped rooms: A finite element approach'*, Journal of the Acoustical Society of America, Vol.99 (1), 108-113

Easwaran, V. and Craggs, A., (1996): *'An application of acoustic finite element models to finding the reverberation times of irregular rooms'*, Acta Acustica, Vol.82, 54-64

Gargliadini, L., Roland, J., and Guyader, J.L., (1991): *'The used of functional basis to calculate acoustic transmission between two rooms'*, Journal of Sound and Vibration, Vol.145 (3), 457-478

Geddes, E.R., and Porter, J.C.C., (1988): *'Finite element approximation for low frequency sound in a room with absorption'*, Journal of Acoustical Society of America, Vol.83 (4), 1431-1435

Gibbs, B.M. and Jones, D. K., (1972): *'A simple image method for calculating the distribution of sound pressure levels within an enclosure'*, Acustica, Vol.26, 2432

Gladwell, G.M.L. and Zimmermann, G., (1965): *'On energy and complementary*

energy formulations of acoustical and structural vibration problems', Journal of Sound and Vibration, Vol.3 (3), 233-241

Gladwell, G.M.L., (1965): *'A finite Element Method for acoustics'*, Proceeding Fifth Int. Con. Acoustics Liege, L33

Gladwell, G.M.L., and Mason, V., (1971): *'Variational finite element calculation of the acoustic response of a rectangular panel'*, Journal of Sound and Vibration, Vol.14 (1), 115-135

Gurovich, Yu.A., (1978): *'Low frequency acoustic reduction of a rectangular panel'*, Journal of Soviet Physical of Acoustics, Vol.24 (4), 289-292

Guy, R., (1979): *'The steady state transmission of sound at normal and oblique incidence through a thin panel backed by a rectangular room -a Multi-Modal Analysis.'*, Acustica, Vol.43 (5), 295-304

Guy, R.W. and Bhattacharya, M.C., (1973): *'The transmission of sound through a cavity-backed finite plate*, Journal of Sound and Vibration, Vol.27 (2), 207-223

Hammad, R. N. S., (1988): *'Simulation of noise Distribution in rectangular rooms by means of computer modelling techniques'*, Applied Acoustics, Vol.24, 211-228

Heckl, M. and Seifert, K., (1958): *'Investigations if the influence of eigen-resonances of rooms on the result of the sound insulation measurement'*, Acustica, Vol.8 (4), 212-220

Josse, R. and Lamure, C., (1964): *'Transmission du son par une paroie simple'*, Acustica, Vol.14, 266-280

Kihlman, T., (1967): *'Sound radiation into a rectangular room. Applications to airborne sound transmission in buildings'*, Acustica, Vol.18, 11-20

Kihlman, T., Kropp, W. and Pietrzyk, (1994): *'Concept of reduction index at low frequencies'*, Proceeding of Inter-Noise 94, August 29-31, Yokohama-Japan, 1463-1468

Kirszenstein, J., (1984): *'An image source computer model for room acoustics. Analysis and electroacoustic Simulation'*, Applied Acoustics, Vol.17 (4), 275-290

Kleiner, M., Orlowski, R., and Kirszensstein, J., (1993): *'A comparison between the results from a physical scale model and a computer image source model for architectural acoustics'*, Applied Acoustics, Vol.38, 245-265

Krokstad, A., Strom, S. and Sorsdal, S., (1983): '*Fifty years experience with computerised ray tracing*', Applied Acoustics, Vol.16, 29-31

Kropp, W., Pietrzyk, A. and Kihlman, T., (1994): '*On the meaning of the sound reduction index at low frequencies*', Acta-Acustica, Vol.2, 379-392

Kulowski, A., (1985): '*Algorithmic representation of the ray tracing technique*', Applied Acoustics, Vol.18, 449-469

Kuttruff, H., (1991): '*Review article*', Bulletin of I.O.A., September/October, 5-8

Madalik, L., (1996): '*Used of the Odeon room acoustic modelling program in design*', Nordic Acoustical Meeting, 12-14 June 1996, Helsinki, A7, 59-64

Maidanik, G., (1962): '*Response of a ribbed panels to reverberant acoustic fields*' Journal of Acoustical Society of America, Vol.34, 809-826

McCulloch, C., (1997): '*Acoustic modelling - A personal view*', Bulletin of I.O.A., August 1997

McCulloch, C., (1998): Private Communication

Mulholland, K.A. and Lyon, R.H., (1973): '*Sound insulation at low frequencies*', Journal of Acoustical Society of America, Vol.54 (4), 867-878

Nefske, D.J. and Sung, S.H., (1990): '*Sound in small enclosures*', Engineering Mechanics Department, General motor Research Laboratories Research Publication GMR-7069

Nilsson, A.C., (1972): '*Reduction index and boundary conditions for a wall between two rectangular rooms*', *Part I and II*, Acustica, Vol.26, 1-23

Ondet, A.M. and Barbry, J.L., (1988): '*Sound propagation in fitted rooms-Comparison of different models*', Journal of Sound and Vibration, Vol.125 (1), 137-149

Ondet, A.M. and Barbry, J.L., (1989): '*Modelling the sound propagation in fitted workshops using ray tracing method*', Journal of Acoustical Society of America, Vol.47 (2), 424-430

Osipov, A, Mees, P. and Vermeir, G., (1997-b): ' *'Numerical simulation of airborne sound transmission at low frequencies: the influence of the room and the partition parameters*', Proceeding of Inter-Noise 97, Vol.52 (3/4), 273-288

Osipov, A., Mees, P. and Vermeir, G., (1997-a): '*Low frequency airborne sound transmission through single partitions in Buildings*', Applied Acoustics, Vol.52

(3-4), 273-288

Petyt, M., Lea, J. and Koopman, H., (1976): '*A finite element method for determining the acoustic modes of irregular shapes cavities*', Journal of Sound and Vibration, Vol.45 (4), 495-502

Pietrzyk, A. and Pedersen, D.B., (1996): '*Numerical simulation of laboratory sound insulation determination experiments*', Proceeding of Inter-Noise 96, Vol.4, 1773-1778

Pretlove, A.J. and Craggs, A., (1970): '*A simple approach to coupled panel-cavity vibrations*', Journal of Sound and Vibration, Vol.11 (2), 207-215

Pretlove, A.J., (1965): '*Free vibration of a rectangular panel backed by a closed rectangular cavity*', Journal of Sound and Vibration, Vol.2 (3), 197-209

Raggs, A., (1972): '*The use of simple three dimensional acoustic finite Elements for determining the natural modes and frequencies of complex shaped enclosure*', Journal of Sound and Vibration, Vol.23 (3), 331-339

Raynoise Vol.2.0A, Manual, (1993)

Schroeder, M.R., (1970): '*Digital simulation of sound transmission in reverberant space*', Journal of Acoustical Society of America, Vol.47 (2), 424-430

Sewell, E.C., (1970): '*Transmission of reverberant sound through a single-leaf partition surrounded by an infinite rigid baffle*', Journal of Sound and Vibration, Vol.12 (1), 21-31

Shield, B.M., (1980): '*A computer model for the prediction of factory Noise*', Applied Acoustics, Vol.13, 471-486

Sysnoise, (1996), Software V.5.3, Numerical Integration Technologies

Sysnoise, V5.3, (1993): "Manuals", Vol.1-4

Tetambe, R.P. and Rakajumar, C., (1996): '*Computers & Structure, Estimation of error in finite element acoustic finite analysis*', Computers and Structures, Vol.61 (1), 13-19

Vorländer, M., (1998): '*Recent progress in room acoustical computer simulations*', FIA, 43-52

Wright, J R., (1996): '*Acoustic modelling of enclosed spaces*', Bulletin of Institute of

Acoustics, Sept./Oct., 10 -12

Zienkiewicz, O.C., (1971): '*The Finite Element Methods in Engineering Sciences*', McGraw-Hill, London
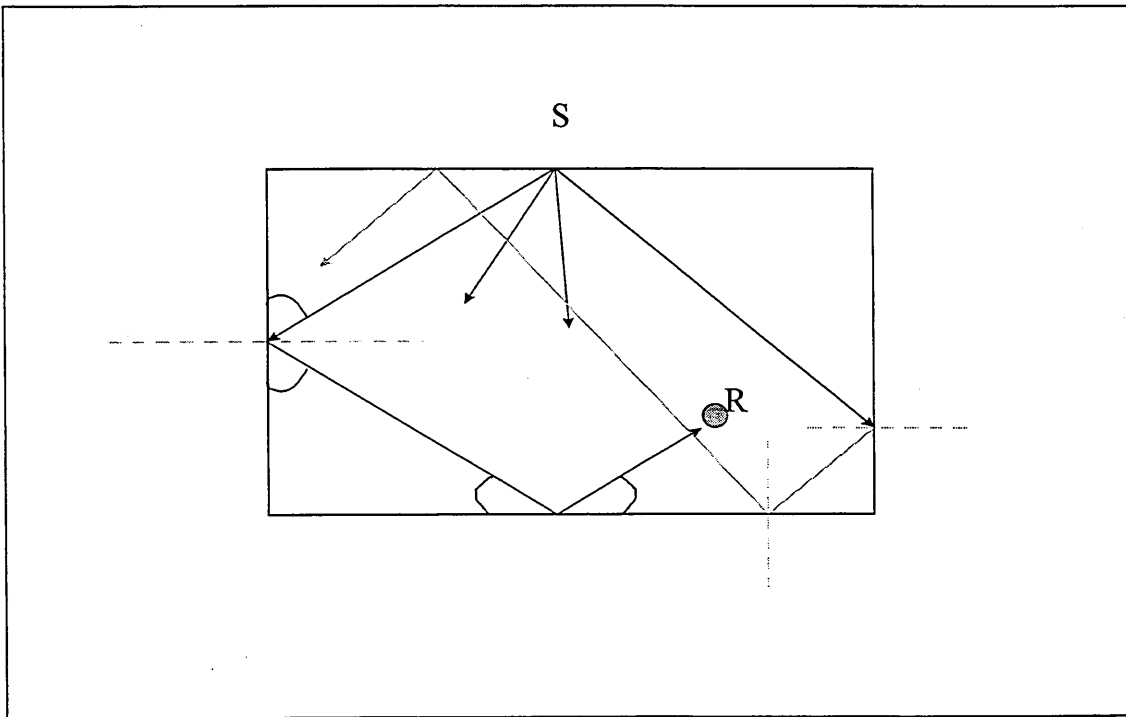
Figure 5.1. Construction of the first rays reaching the receiver position
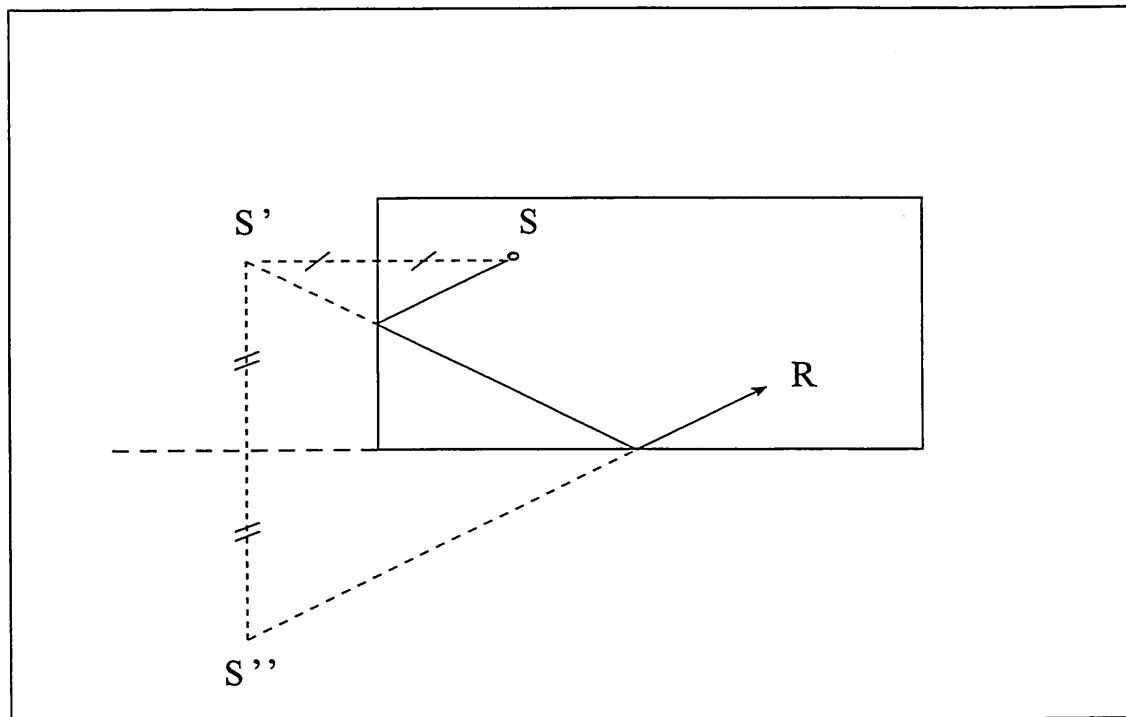
Figure 5.2. Construction of the first and second order image sources

6   IMPLEMENTATION OF TRANSMISSION ROOMS MODEL

6.1   INTRODUCTION

No method of measurements is found to be reliable enough to measure sound insulation at low frequencies as seen in Chapter 4. In Chapter 5, a Finite Element Method (FEM), was selected as the most appropriate approach to model sound transmission between two rooms at low frequencies. Despite requiring long computer processing times to simulate a large model and a large frequency range of interest, it is a method easy to use.

The sound transmission between two rooms is estimated by knowing the pressure field in each room and the vibrational velocity of the party wall [Fahy (1985)]. This requires the determination of the effect of the sound source on the source room acoustic volume, the effect of the pressure field on the vibration of the separating wall and response of the receiving room acoustic volume to the vibration of the party wall. Each system was modelled using a software package, Sysnoise V5.3 [1996]. It was, however, important to ensure numerical stability because previous investigations had shown that such an analysis suffered from numerical errors due to the mesh size [Tetambe et al (1996)]. That means the acoustic field models and the structural model need to be discretized with a finite number of elements sufficient to accurately reproduce the pressure and displacement variation.

The objectives of this chapter are therefore to find the number of elements to correctly model the sound pressure level variation inside the enclosures and the surface displacement of the party wall. A compromise had to be found between the number of elements and the CPU time in order to simulate the sound transmission between two rooms within an acceptable accuracy.

6.2   ROOM MODEL

6.2.1 Introduction

As seen in Chapter 3, the sound field at low frequencies is not statistical, but is characterised by distinguishable room modes. Also, as seen in Chapter 4, the measurement of reverberation time at low frequencies is problematical, leading to a poor repeatability and poor reproducibility. Previous works by Craggs [1994], Geddes [1988], Easwaran et al [1995-a&b, 1996], using FEM, investigated the effect of introducing damping inside an enclosure [Astley (1998)]. The absorbing surfaces were assumed to be locally reacting, for which sound propagation parallel to the absorber surface is prohibited. So, the absorber areas were considered large compared with the wavelength and the sound field is dominated by oblique modes. That explains why room volumes greater than 100m³ were chosen. However, other works have shown that modelling an enclosure with 6 hard walls (of infinite impedance) gives values which agree with measurements [Walker (1992)]. Therefore, for the purposes of this study, it was decided to adopt a 'worse case' where all the surfaces are non absorbing and where the effects of furnishing is not included. It was expected that fluctuations in predicted sound level would be large as well as the variance of spatial and spectral averages. However, whilst the measurements and characterisation of low frequency room absorption remains problematical, this approach would appear logical.

6.2.2 Discretization

The sound field is discretized into a number of contiguous elements. An element, as seen in Figure 6.1 can have different shapes, such as rectangular, or hexahedron [Zienkiewvich (1971)]. The corners of each element are called nodes. The use of straight-edged elements depends on the shape of the sound field. The sound field under investigation as seen in Figure 6.2 is rectangular, allowing the use of straight-edged elements such as cubes. In order to model the sound field, each element possesses a mathematical formula, which is associated with a simple geometrical description, irrespective of the overall geometry of the sound field. The mathematical formula is expressed as a function of the nodal values, which are values of the field variable i.e. the unknowns called degrees of freedom. The unknowns correspond to the sound pressures and their spatial derivatives. Consequently, the element forms a polynomial function

with a number of coefficients corresponding to the number of degrees of freedom. The co-ordinates of the nodes are substituted in this polynomial function in order to define the sound pressure and the pressure gradient in the directions given by the element (i.e. three directions if the element is cubic, or two directions if the element is square). The polynomial function can then be written as

$${p} = [N] {p}_e \qquad\qquad (6.1)$$

where ${p}$ is the pressure function in each element, ${p}_e$ are the nodal values of the pressure function associated with the element and [N] is a listing of shape functions of the co-ordinates only. The shape functions are therefore used to express both the co-ordinates and pressure of an internal point in term of values at the nodes.

When the function of each element is defined, an algebraic equation for the overall finite element system is required, which corresponds to Equation 6.15 and Equation 6.17. To do so, continuity conditions must exist between elements i.e. no discontinuities, overlaps or openings must take place between elements when adjacent elements deform.

The discretization has to be done accurately otherwise numerical errors occur. Indeed, the discretization of the sound field at one specific frequency will not necessarily be applicable for higher frequencies [Tetambe et al (1996)]. The number of required elements is therefore dependent upon the upper frequency of interest with the initial assumption that 6 elements are required to properly represent the pressure/displacement over the governing wavelength [Astley (1998)]. As seen above, the sound field can be discretized with cubic elements, which, however, can have different numbers of nodes. For example, a Hex8 element is a cubic element with 8 nodes; a Hex 16 is a cubic element with 16 nodes; a Hex 20 is a cubic element with 20 nodes and so on. The more nodes are present to describe the sound field, the less number of elements are required to process the sound field. A large number of nodes, however, involves the manipulation of a large matrix ${p}_e$ and therefore a large overall matrix. Thus the CPU time necessary to process that overall matrix will be greater than that defined with Hex8 to the detriment of the accuracy. Indeed, it has been shown [Crocker (1997)] that the prediction of eigenfrequencies is more accurate with a Hex20. The next two chapters,

however, will show that the selection of Hex 8 provides a good agreement between prediction and measurement.

The discretization of the acoustic field, begins by first considering the dimensions of the transmission room. As seen in Chapter 1, the size of typical domestic rooms is not generally represented in the acoustic laboratories. In this study, the transmission rooms represented typical rooms in adjacent dwellings, 4m x 4m x 2.5m and 3.5m x 4m x 2.5m. The size of the mesh depends upon the maximum frequency of interest, which, in this study, was 200 Hz, corresponding to a wavelength of 1.7m. Compared with the longest room dimension, 4m, 14 elements ideally are required to represent the pressure variation over a wavelength along the y-axis (See Figure 6.2). The same number of elements was selected to discretize the sound pressure level variation along the x- and z-axes, x being the largest dimension. The number of elements required for the $\lambda/6$ criterion is as follows; 12.35 along the x- axis (equal to 3.5m) and 9 elements along the z-axis (equal to 2.5m). A model discretized with 14^3 elements, was known as 14 mesh model, while a model discretized with different number of elements was known as l x m x n mesh model.

6.2.3 Acoustic field

The sound pressure level inside an enclosure can be written as an Helmholtz equation;

$$\nabla^2 p + k^2 p = 0 \tag{6.2}$$

The 6 walls of the enclosures were considered as hard surfaces i.e. the air particle velocity is equal to zero and the variation of the pressure normal to the surface of the walls is also equal to zero:

$$\frac{\partial p}{\partial n} = 0 \tag{6.3}$$

where δ n is the normal to the surface of the wall.

It is impossible to determine an exact solution to the differential equation of the sound field i.e. an explicit expression for p in terms of known functions, which exactly satisfy

the governing equation and boundary conditions. However, the use of a variational method allows an approximate solution with an element wise Rayleigh -Ritz treatment and shape function discretization. The acoustic field is therefore discretized into finite elements [Petyt et al (1976)], using Equation 6.1.

The total acoustic sound energy, E, is the sum of the acoustic potential energy P and the acoustic kinetic energy C [Zienkiewicz (1971)] where;

$$P = \frac{1}{2} \int p.\varepsilon_v dV \qquad (6.4)$$

where p is the pressure, V is the volume of the enclosure and ε_v, is the volumetric strain related to the pressure by the bulk modulus:

$$\varepsilon_V = \frac{p}{\rho_0 c_0^2} \qquad (6.5)$$

Equation 6.4 can therefore be rewritten by using Equation 6.5

$$P = \frac{1}{2} \int_V \frac{p^2}{\rho_0 c_0^2} dV \qquad (6.6)$$

The kinetic energy of the sound field is defined as

$$C = \frac{1}{2} \int_V \rho_0 \chi^2 \, dV \qquad (6.7)$$

where χ is the pressure velocity defined as

$$\chi = -\frac{\delta p}{j\rho_0 \omega} \qquad (6.8)$$

where δ means a small variation.

Equation 6.7 can be rewritten as

$$C = -\frac{1}{2} \int_V \frac{\delta p^2}{\rho_0 \omega^2} dV \qquad (6.9)$$

Equations 6.6 and 6.9 are discretized using Equation 6.1, where

$$P = \frac{1}{2}\{p\}^T \left(\int_V \frac{[N]^T [N]}{\rho_0 c_0^2} dV \right) \{p\} \qquad (6.10)$$

$$P = \frac{1}{2\rho_0}\{p\}^T [M]\{p\}$$

where [M] is the acoustic mass matrix $[M] = \int_V \frac{[N]^T [N]}{c_0^2} dV$

$$K = -\frac{1}{2\rho_0 \omega^2}\{p\}^T \left(\int_V [B]^T [B] dV \right) \{p\} \qquad (6.11)$$

$$K = -\frac{1}{2\rho_0 \omega^2}\{p\}^T [K]\{p\}$$

where [K] is the acoustic stiffness matrix $[K] = \int_V [B]^T [B] dV$

The total energy, E, of the sound field is the sum of the potential and kinetic energy, according to the Hamilton's principle;

115

$$E = P + K$$

$$E = \frac{1}{2\rho_0}\{p\}^T[M]\{p\} - \frac{1}{2\rho_0\omega^2}\{p\}^T[K]\{p\} \qquad (6.12)$$

The solution of this equation is obtained by minimising the total energy E

$$\frac{\partial E}{\partial p} = 0$$

$$[M]\{p\} - \frac{1}{\omega^2}[K]\{p\} = 0 \qquad (6.13)$$

$$([K] - \omega^2[M])\{p\} = 0 \qquad (6.14)$$

In the presence of an acoustic force resulting from a loudspeaker or/ and an oscillating fluid-structure interface at the boundary of the acoustic domain, Equation 6.14 is rewritten as

$$([K] - \omega^2[M])\{p\} = -i\rho_0\omega\{Q\} \qquad (6.15)$$

where {p} and {Q} are the amplitudes of nodal pressures and flows, respectively. The two matrices are only calculated once and are independent of the frequency.

The resonance frequencies of the enclosure are obtained when there are no acoustic force {Q}=0 and the frequency response of the enclosure is calculated according to Equation 6.15. The method is called the Acoustic Finite Element (AFE) method [Sysnoise (1993)].

It is however time consuming to process the pressure distribution when using Equation 6.15, as it requires to resolve that equation for each frequency. A quicker way to solve this equation is by using modal superposition [Sysnoise (1993)], which reduces the system of equations. The modes have to be processed first and then the pressure is calculated in the form of a linear combination of a limited number of modal eigenvectors;

116

$$\{p\} = \sum_{i=1}^{m} 1_i \{\Theta_i\} = [\Theta]\{1\} \qquad (6.17)$$

where $\{1\}$ contains the modal participation factors and $[\Theta]$ is a matrix whose columns are the m retained modal eigenvectors. The unknown of the problems become the modal participation factors and they are the solution of the following m x m system of equations:

$$\left([\Theta]^T [K - \omega^2 M] [\Theta]\right)\{1\} = [\Theta]^T \{Q\} \qquad (6.18)$$

6.2.4 Modelling

The acoustic field was defined using software, P3/Patran [1993]. The acoustic field was designed from a reference point of co-ordinates (0, 0, 0) again, (see Figure 6.2). The Sysnoise software cannot link two acoustic models with one structural model to simulate the sound transmission between two rooms, but can link one acoustic model with the structural model. Consequently, a solid of dimensions representing the two rooms combined (7.5m x 4m x 2.5m) was defined. The solid was then discretized by defining firstly the number of nodes on each edge of the box, incorporating elements of type Hex8. Once the dimensions and elements were defined, the mesh model was generated and imported into the software package Sysnoise V5.3 (see Chapter 5) to apply the Acoustic Finite Element method. The matrix bandwidth depends on the largest difference between internal numbers of nodes connected to the same elements [Sysnoise (1993)]. Consequently, before defining the properties of the sound field, i.e. the stiffness and mass matrices, it is normal to renumber the nodes of the imported mesh model in order to have the smallest possible matrix bandwidth. This reduces storage memory and CPU time. The smallest bandwidth is therefore obtained by renumbering the internal nodes while the external number remains the same. In the present case, the number of nodes is quite small when compared with large models or high frequencies, but the renumbering option was used each time an AFE model was defined, as a check. The

stiffness matrix and the mass matrix were defined from values given for mass density and sound velocity. Here, no air absorption was considered giving a sound velocity, $c_0 = 340$ m.s^{-1} and mass density $\rho_0 = 1.225$kg.m^{-3}. In order to obtain the room modes of the source and receiving rooms, a 'hard' wall of zero thickness [Sysnoise (1993)] had to be created at the position of the party wall (x = 4m) to distinguish the source room from the receiving room. The nodes situated at x = 4m and the elements connected to them were selected. The nodes were then duplicated by creating a new set of nodes connected to the selected set of elements having the same co-ordinates as their parent nodes [Sysnoise (1993)]. Two volumes are now created, defining the source room and the receiving room. The room modes can be calculated for the whole system by superimposing the modes of the source room and of the receiving room.

As the frequency range of interest is 25Hz to 200Hz, the eigenfrequencies were computed from the 1st acoustic mode to a mode having an eigenfrequency greater than 200Hz (See section 3.4).

6.2.5 Accuracy versus Mesh Size

The CPU time can be large, depending upon the number of finite elements and on the processing power of the computer [Zienkiewicz (1971), Astley (1998)]. It was found that two days of processing were required for the simulation of the room modes for 12 mesh and greater models. The simulation run was much longer than CPU time, since the network system was shared with other users. It was also foreseen that the CPU time for simulating the transmission, obtained by coupling the Acoustic Finite Element (AFE) and the Structural Finite Element (SFE) would be also large. Consequently, an optimum between accuracy of simulation and required CPU power had to be determined.

It was necessary to reject the 6 elements per wavelength condition, at least in one direction. Consequently, a range of seven acoustic models were constructed from 5 to 11 meshes in order to select a mesh model for which the CPU time is acceptable, and eigenfrequencies would be processed within an acceptable error. Also, two acoustical

models were defined with a 7x8x5 mesh (i.e. 7 elements in the x direction, 8 elements in the y direction and 5 elements in the z direction) and a 8x9x6 mesh. To evaluate the error due to the finite element discretization, an error ratio ε_0 was calculated by comparing the theoretical eigenfrequencies given by Equation 3.7 with the finite element eigenfrequencies processed for each mesh model, where

$$\varepsilon_0 = \frac{\text{numerical eigenfrequency - theoretical eigenfrequency}}{\text{theoretical eigenfrequency}} \times 100 \qquad (6.19)$$

Figure 6.3 shows the error for the 7, 8, 9 and 7x8x5 and 8x9x6 mesh models plotted against the number of modes. The prediction for the 7x8x5 and 8x9x6 mesh models had a greater error than the 8 and 9 mesh models, as the number of defined elements along x and z directions are greater than for the 7x8x5 and 8x9x6 mesh models. The pressure variation is therefore better described by selecting mesh models with equal number of elements in each direction. Figure 6.4 shows the error from a 5 mesh to a 11 mesh model plotted against the number of modes, which corresponds to a frequency range of 0 to 220Hz. The room mode calculation for a 5 mesh model has a maximum error of 17%, which occurs in the upper part of the frequency range of interest, whereas the calculated modes for a 11 mesh model are within an error of 6%. This was expected as the number of elements must be increased to describe accurately the variation of sound pressure level along a standing wave at mid and high frequencies. That explains the similar trend observed for all curves.

The calculated errors are positive, which means that the numerical modes are too stiff, due to the discretization [McCulloch (1998)]. The observed peaks are not only due to the mesh size, but also due to the calculation procedure when the room modes of the transmission suite are processed. By duplicating the nodes along the position of the party wall, the calculation procedure gives an increased error when identical modes in the source room and in the receiving room are processed. If an error of 10% is considered as the maximum allowed error, the 10, 9 and 8 mesh models are seen to be acceptable.

6.2.6 Estimation of the Frequency Response

Another way to select the correct mesh model is to look at the frequency response obtained at one position (3, 3.5, 1.75m) in each mesh model using Field point (see Chapter 7). The level difference is calculated between the sound pressure level of the 11mesh model with those obtained with the other mesh models from 31.5Hz to 160Hz 1/3 octave bands. The data are presented in Figure 6.5.

As expected, the greatest level differences are obtained for the 5 and 6 mesh model. It varies between −7 to 13dB. When the number of elements is increased, the discrepancy becomes smaller, making the 9, the 10 and the 11 mesh models the most appropriate AFE models to study the frequency response of the room.

6.3   PANEL MODEL

6.3.1 Introduction

The proposed use of the method was to model the domestic rooms with typical party walls found in dwellings. Here, the wall separating the two rooms was to be of brick. It was modelled as a finite isotropic panel of dimensions L_y and L_z (see Figure 6.6).

In order to model the surface displacement, it was necessary to distinguish between thin plate and thick plate assumptions. In this study, the wall was of 100mm brick, with a surface area of $10m^2$ (4m x 2.5m). Such a wall has a critical frequency of approximately 152Hz. As seen in Chapter 2, the wall can be considered as a thin plate when $\lambda_b \geq 6$ [Cremer (1957 & 88)], where λ_b is the governing bending wavelength and t is the wall thickness. Thus, the wall can be assumed to be a thin plate below 1100Hz. This assumption is also confirmed by Llungren [1991]. Therefore thin plate theory was assumed to apply in the frequency range of interest 25-200Hz.

6.3.2 Discretization

120

The surface displacement was discretized into a number of contiguous elements, which describe the governing differential equations described in Chapter 2. The requirement that the wavelength should be described with 6 elements, also applied to the surface displacement. The bending wavelength of a 0.1m thick brick wall is obtained from Equation 2.11 and is equal to 1.5m at the highest frequency of interest, 200Hz. In the same manner as in Section 6.2.2, the wavelength was divided into 6 elements to define the length of the element. That was then compared with 4m the longest dimensions of the party wall to define the number of elements. The panel vibration was therefore modelled with 16 elements using elements with 4 nodes, known as QUAD 4. The elements were chosen for the same reasons given for the selection of HEX8 elements in Section 6.2.3. It was foreseen that the simulation of the structural model would be faster than for the acoustic modes as the amount of time required for the solution is proportional to n_{el}^3 where n_{el} is the number of elements along one axis [Zienkiewicz (1971), Maluski et al (1997), Maluski et al (1998)]. The polynomial function of the element has the same expression as Equation 6.1, but now the variables are displacements and their derivatives.

6.3.3 Structural field

As with the acoustic damping (see Section 6.2.1), the structural damping is also difficult to measure at low frequencies [Craggs(1994)]. The party wall was therefore modelled with zero damping in order to reduce the number of errors introduced during the modelling and the simulation. As in Section 6.2.3, the wall surface displacement was discretized into finite elements using a variational method [Zienkiewicz (1971)], giving an equation of a form;

$$([K_s] - \omega^2 [M_s])\{w\} = -j\rho_0\omega\{F\} \qquad (6.20)$$

where $[K_s]$ and $[M_s]$ are the stiffness and the mass matrices, $\{w\}$ is the displacement vector and $\{F\}$ is the force applied on the surface of the panel. .

As for the acoustic modes, the structural eigenfrequencies of the party wall are obtained when $-j\rho_0\omega\{F\}=0$

$$([K_s] - \omega^2 [M_s]) \{w\} = 0 \qquad (6.21)$$

Like for the Acoustical Finite Element model, the two matrices are only calculated once and are independent of the frequency. The numerical method used to define the structural modes and the displacements is called the Structural Finite Element (SFE) method [Sysnoise (1993)].

6.3.4 Modelling

The process was practically the same as for the acoustic field except that the party wall is modelled as a structural finite element (SFE) model. Using P3/Patran [1993] the mesh model of the party wall was defined in the plan (y-z) at the reference point (4, 0, 0) corresponding to the position of the party wall from the reference point (0,0,0) (See Figure 6.6) defined in Section 6.2.4. The panel was discretized by defining all the elements of type Quad 4 on the surface of the wall. The mesh model is now ready to be transferred to Sysnoise.

SFE was selected before importing the mesh model, then the nodes were renumbered in order to reduce the matrix bandwidth (see Section 6.2.2). Before assigning the properties of the brick wall, the mesh model could be defined as a panel or a shell. As seen in Chapter 2, the edge conditions of a brick wall could be assumed to lie between simply supported and clamped conditions meaning that rotational and translational displacements were moving in three dimensional space. A plate model allows three degrees of freedom per node: one normal translation and two of rotation. The plate element can be modelled in the XY-plane only. A shell model allows curved bodies, with 6 degrees of freedom per node giving three displacements (U_x, U_y, U_z) and three rotations (R_x, R_y, R_z), to be modelled. A shell can be modelled in any direction. Consequently, the mesh model was modelled as a shell with the material properties corresponding to a brick wall [Gibbs (1973)]:

Young's Modulus, **E**: 1.1 E^{10} N.m^{-2}

Mass density, ρ: 1860 kg.m^{-3}

Poisson's ratio, ν: 0.4

For the study of the accuracy of mode process and assuming that the software processes linearly, only one thickness was defined

Thickness: 0.1m

As it is only a matter of finding the correct number of elements to model the surface displacement of the panel, the calculation of eigenfrequencies is easier for the simply supported condition with no translational displacement;

$$U_x = 0, U_y = 0 \text{ and } U_z = 0. \tag{6.22}$$

The structural model was now defined and the eigenfrequencies processed according to Equation 6.21.

6.3.5 Accuracy versus mesh size

12 modes were processed for the 5 to 14 mesh models, the last structural eigenfrequency being well above the upper frequency range of interest. Mesh models greater than 14 were not considered as the elements of the structural model must geometrically be identical to the corresponding faces of the AFE model. Also, mesh models defined with a number of elements along the y-axis different from the z-axis were not selected as such modelling was not chosen for the acoustic modes (see Section 6.2.5).

The error of the estimate was expressed as in Equation 6.19 with respect to theoretical eigenfrequencies calculated from Equation 2.21 . Results are shown in Figure 6.7. The structural mode calculation for a 5 mesh model give a maximum error of 91%, which occurred in the low and upper part of the frequency range of interest, whereas the calculated modes for a 9 to 14 mesh model are within an error of 20%. Only the 14 mesh model gives errors within an initial target of 10%. Instead of displaying error versus mode number, the results can be displayed as error versus mesh model. Figure 6.8 shows that panel modes 7, 8, 9, 11 and 12 of the 9 mesh model and modes 7, 11 and 12 of the 10 mesh model have an error equal or greater than 10%, but the eigenfrequencies of the modes 11 and 12 are outside the frequency range of interest. Also, the error tends to be negative for the first and second modes. This is the result of

having too many elements to describe the surface displacement. [McCulloch (1998)]. It was observed that the time necessary to process the eigenfrequencies was much less than that for the acoustic eigenfrequencies, as expected. Consequently, the structural eigenfrequencies were predicted with an error of 8% when the model was discretized with 11^3 elements or more.

6.4 MESH SELECTION

The aim of this study was to model the sound transmission between two rooms i.e. to predict the fluid-structural interaction effects for which prediction, accuracy and computer processing time are acceptable. In order to do so, different acoustic and structural mesh models were investigated individually. The eigenfrequencies of the Acoustic models of 5^3, 6^3, 7^3, 8^3, 9^3, 10^3 and 11^3 elements were compared with the theoretical ones. The 8, 9 10 and 11 mesh models were found to have their eigenfrequencies processed with an error less than 8%. The predicted structural eigenfrequencies of the 5 to 14 mesh models were compared with the theoretical ones. The 10, 11, 12, 13 and 14 mesh models were found to have their eigenfrequencies processed with an error less or equal to 10%. The transmission room is modelled by linking the Acoustic Finite Element Model with the Structural Finite Element model. The structural mesh size needs to be the same as the acoustical mesh size [Sysnoise (1993)]. By selecting the 11 AFE mesh model, the simulation ran within an error of 6%. The panel simulation ran within an error of 7%. By selecting the 10 AFE mesh model, the simulation ran within an error of 7%. When the panel was modelled with 10^3 elements, the simulation ran within an error of 8% except at 144Hz where the error was 10%. By selecting the 9 AFE mesh model, the simulation ran within an error of 8.5%. When the panel was modelled with 9^3 elements, the simulation ran within an error of 11% except at 144Hz where the error was 16%. The error for the 9 SFE mesh model is therefore too high and therefore was not selected. The 11 mesh transmission room model also was not selected because it takes more time to process the acoustic eigenfrequencies than the 10 mesh model does. Consequently, the coupled system was modelled using a 10 mesh model for room and party wall and can be seen in Figure 6.9.

6.5   CONCLUDING REMARKS

Before processing the simulation of the sound transmission between two rooms, the number of elements had to be chosen carefully when discretizing the sound field of the source room, of the receiving room and of the panel displacement. Many AFE models and many SFE models were considered in order to find the right number of elements for which the eigenfrequencies are processed accurately, but a compromise is required with the computational power and time. The predicted eigenfrequencies were compared with the theoretical eigenfrequencies. It was found that the simulation of each sound field discretized with 10^3 cubic elements and the party wall discretized with 10^2 surface elements had their eigenfrequencies processed with an error of 8%, except at 144Hz where the simulation of the party wall had an error of 10%. Such selection needs now to be validated by comparing the predicted and measured frequency response of a single room in Chapter 7, and by comparing the predicted and measured sound pressure level difference of a transmission room in Chapter 8.

6.6 REFERENCES

Astley, R.J., (1998): 'Finite elements in acoustics', Proceeding of Inter-Noise 98, 538

Craggs, J., (1994): 'A finite element method for free vibration of air in ducts and rooms with absorbing walls', Journal of Sound and Vibration, Vol.173, 568-576

Cremer, L., (1953): 'Calculation of sound propagation in structures', Acustica, Vol.3 (5), 317-335

Cremer, L., Heckl, M., Ungar, E.E., (1988): 'Structure-Borne Sound', Ed. Springer-Verlag

Crocker, M.J., (1997): 'Encyclopedia of Acoustics', Ed. Wiley Interscience

Easwaran, V. and Craggs, A., (1995-a): 'On Further Validation and Use of the Finite Element Method to Room Acoustics', Journal of Sound and Vibration, Vol.187 (2), 195-212

Easwaran, V. and Craggs, A., (1995-b): 'Transient response of lightly damped rooms: A finite element approach', Journal of the Acoustical Society of America, Vol.99 (1), 108-113

Easwaran, V. and Craggs, A., (1996): 'Application of acoustic finite element method models for finding the reverberation time of irregular rooms', Acta Acustica, Vol.82, 54-64

Fahy, F., (1985): 'Sound and structural vibration: radiation, transmission and response', Ed. Academic Press

Geddes, E R and Porter, J C, (1988): 'Finite Element Approximation for Low Frequency Sound in A Room with Absorption', Journal of Acoustical Society of America, Vol.83 (4), 1431-1485

Gibbs, B.M., (1974): 'The direct and indirect transmission of vibrational energy in building structures', Ph.D. thesis at University of Birmingham

Llungren, S., (1991): 'Airborne Sound Insulation of Thick Walls', Journal of Acoustical Society of America, Vol.89 (5), 2338-2345

Maluski, S. and Bougdah, H., (1997): 'Predicted and measured low frequency response of small rooms', Journal Building Acoustics, Vol.4 (2), 73-86

Maluski, S., Gibbs, B., and Bougdah, H., (1998): 'Predicted and measured low frequency response of small rooms', I.O.A. Proceeding, Cranfield, Vol.20 (1),

87-92

McCulloch, C., (1998): Private conversation in April

P3/Patran (1993): *'User Manual'*, PDA Engineering

Petyt, M, Lea, J. and Koopman, G.H., (1976): *'A finite element method for determining the acoustic modes of irregular shaped cavities'*, Journal of sound and vibration, Vol.45 (4), 495-502

Sysnoise, (1993): *User Manual*

Sysnoise, (1996): Software Package V5.3, NIT

Tetambe, R.P. and Rakajumar, C., (1996): *'Computers & Structure, Estimation of error in finite element acoustic finite analysis'*, Computers and Structures, Vol.61 (1), 13-19

Zienkiewicz, O.C., (1971): *'The Finite Element Method in Engineering Science'*, Ed. McGraw Hill
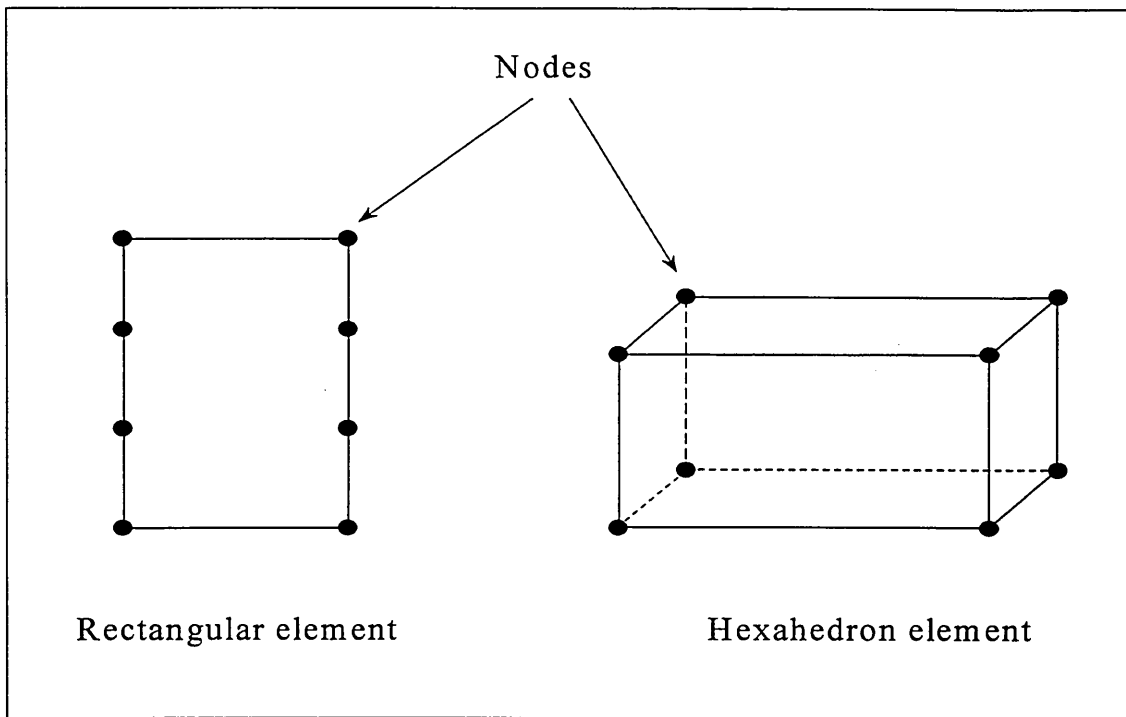
Figure 6.1. Rectangular or hexahedron elements
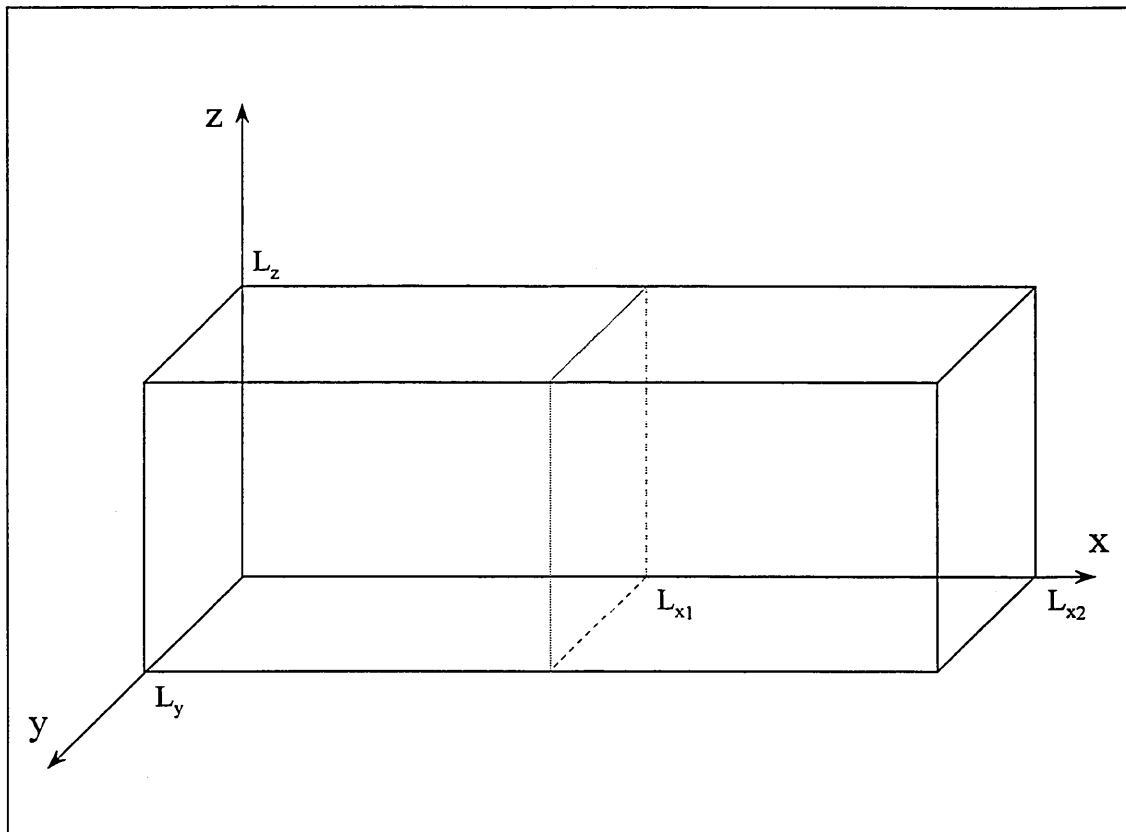
Figure 6.2. Model of the two rooms of the transmission room with co-ordinate system

128
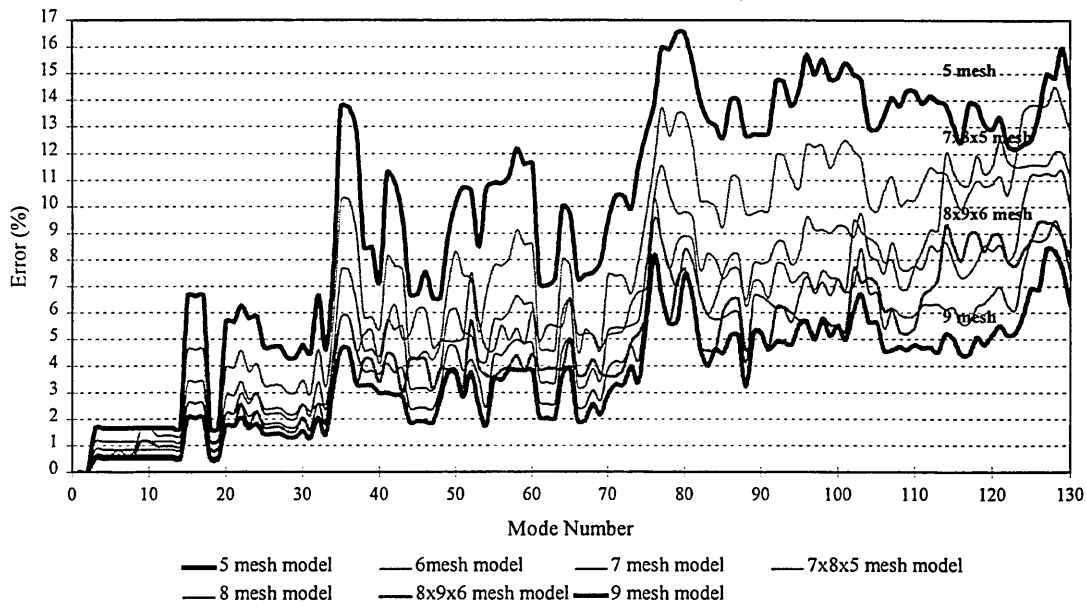
Figure 6.3: Acoustic model: Error versus Mode number
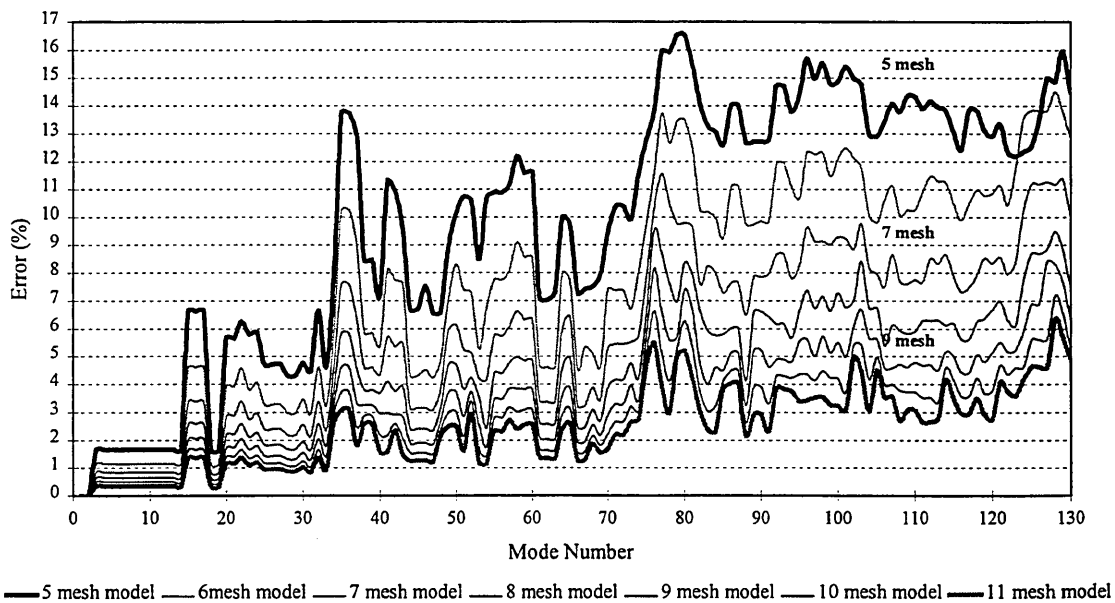
Figure 6.4. Acoustic model: Error versus Mode number
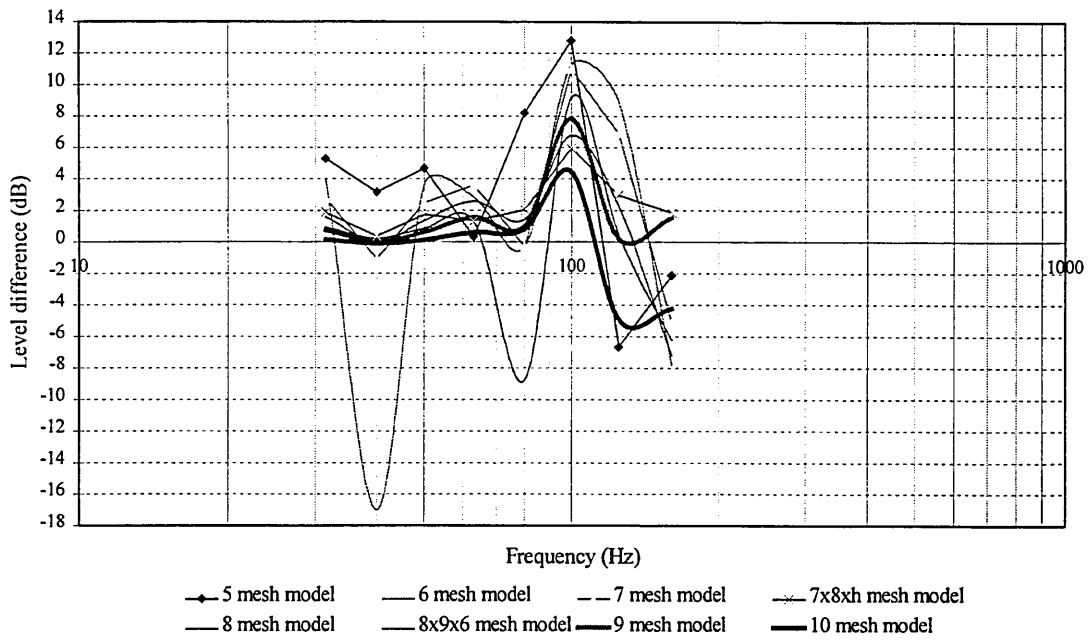
Figure 6.5. Frequency responses of different mesh models compared with the 11 mesh model
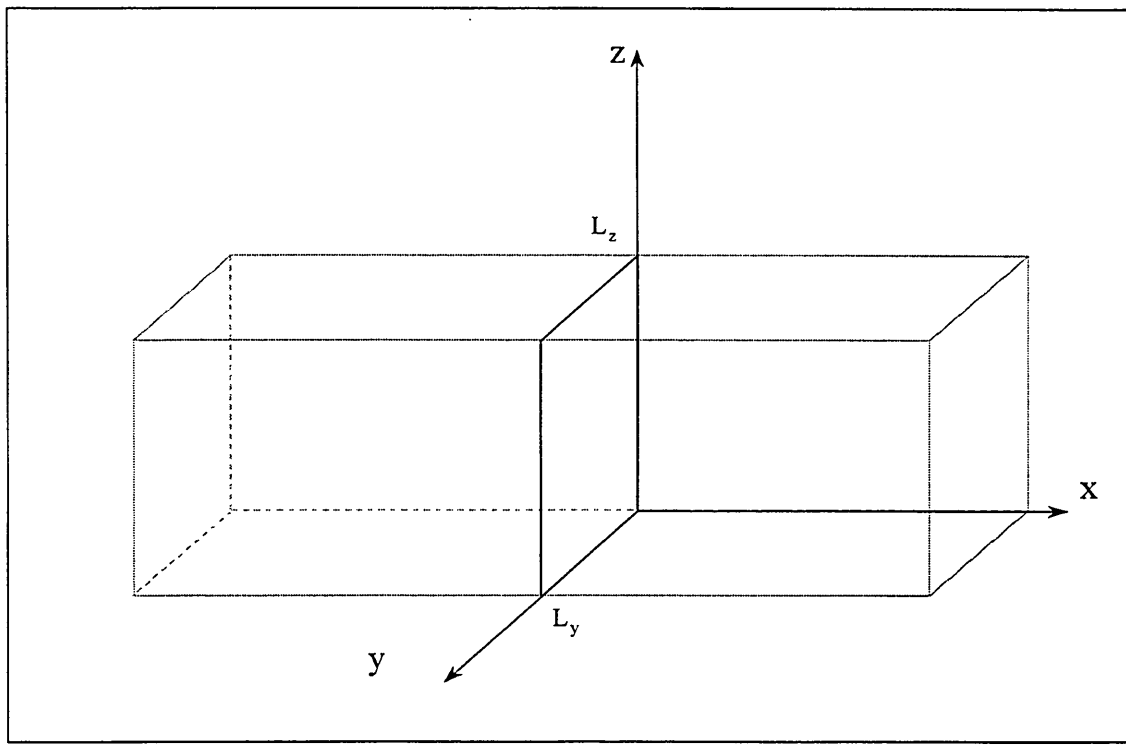
Figure 6.6. Party wall
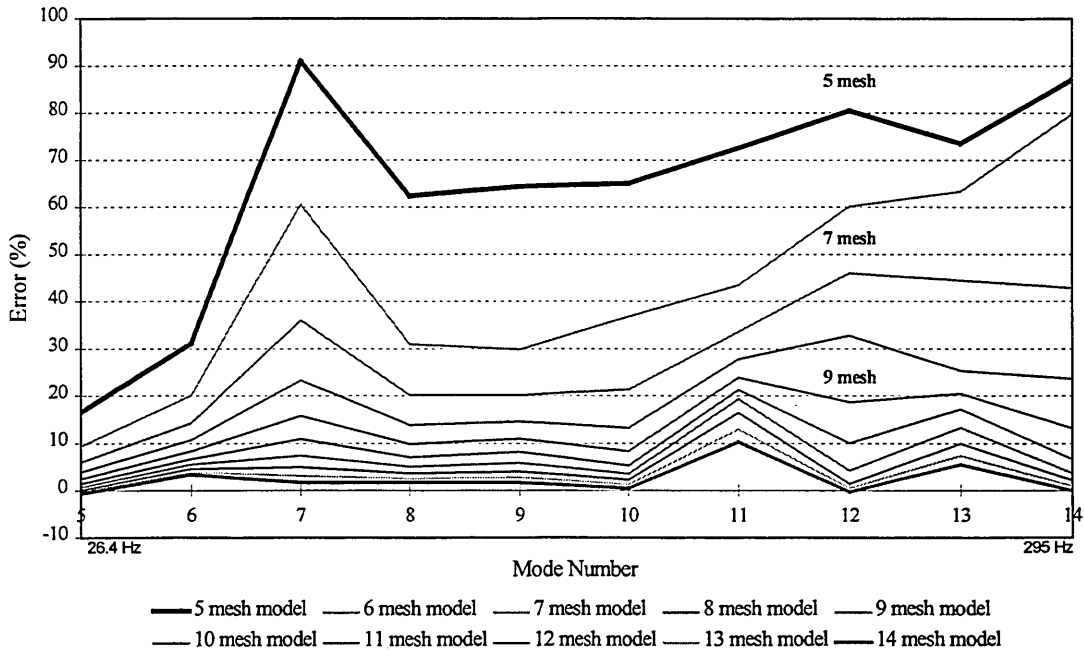
Figure 6.7. Structural model : Error versus Mode

131

Mode 1 (1,1) = 26.77Hz
Mode 2 (2,1) = 49.33Hz
Mode 3 (1,2) = 84.52Hz
Mode 4 (3,1) = 86.93Hz
Mode 5 (2,2) = 107.08Hz
Mode 6 (4,1) = 139.57Hz
Mode 7 (3,2) = 144.68Hz
Mode 8 (1,3) = 180.78Hz
Mode 9 (4,5) = 197.32Hz
Mode 10 (2,3) = 203.34Hz
Mode 11 (5,1) = 207.25Hz
Mode 12 (3,3) = 240.94Hz
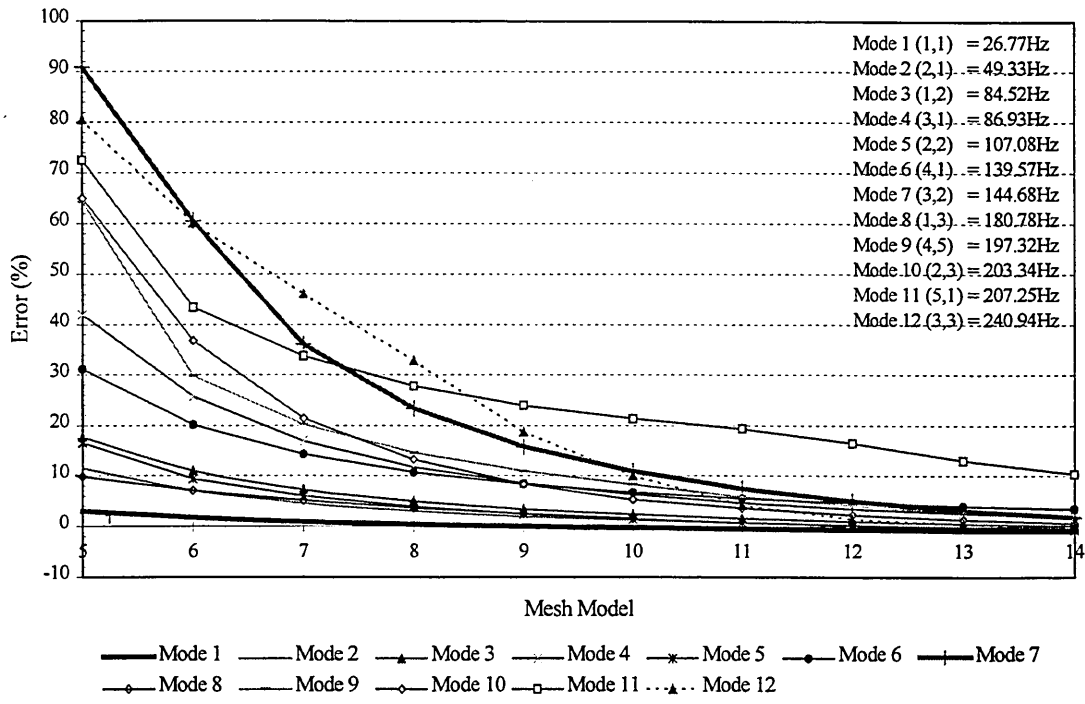
Figure 6.8. Structural model: Error versus Mesh Model
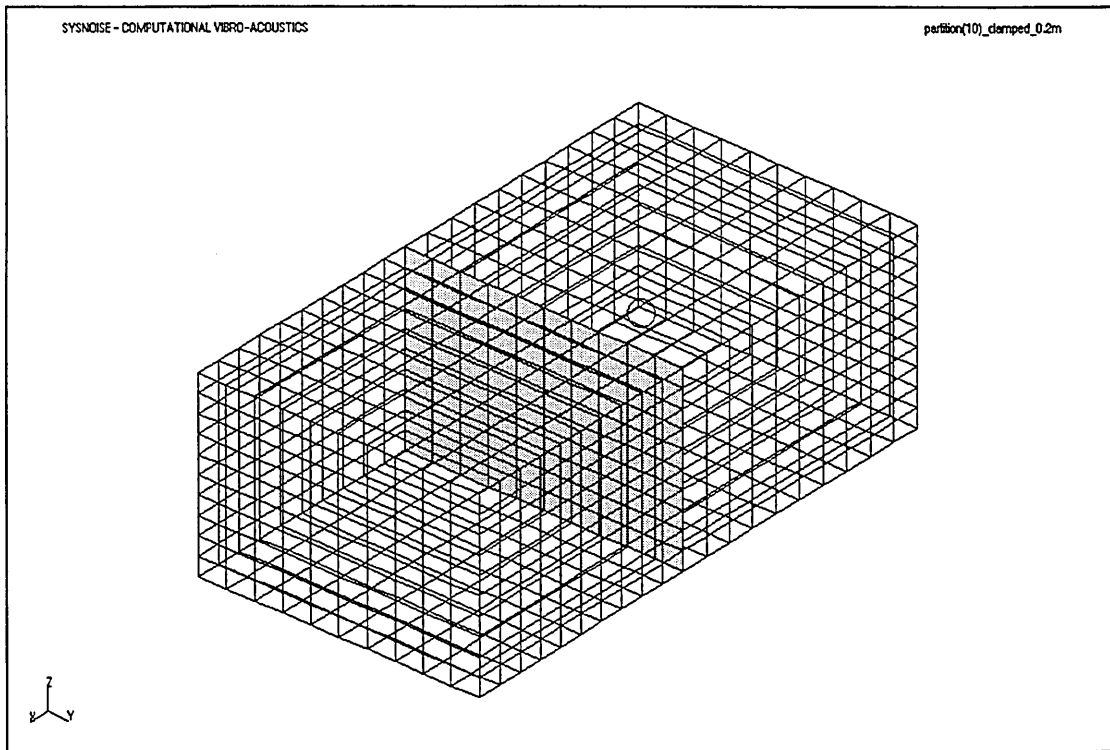
Figure 6.9. The transmission room model

132

7   EXPERIMENTAL VALIDATION FOR ONE ROOM

7.1   INTRODUCTION

In Chapter 6, 10^3 elements were selected to model enclosures of volumes smaller than $50m^3$ and 10^2 elements for the party wall in order to have an acceptable time process for simulation. The acoustic and structural modes were estimated within an error of 10%. The objective of this chapter is therefore to validate this mesh selection by comparing the predicted frequency response of a single room with that of a 1:4 scale room model in order to use a FEM model for subsequent studies.

7.2   REVIEW

Although the frequency response of enclosures is difficult to measure accurately at low frequencies, as seen in Chapters 3 and 4, it is possible to obtain a representative response signature and the number of peaks corresponding to the room modes. Chapter 4 shows that the measured frequency response is strongly influenced by the background noise level, the loudspeaker and microphone positions, and the construction of the enclosure. The background noise level at low frequencies is often high and a correction factor is required when the difference between the signal and the background level is less than 10 dB [ISO140, part 3 (1995)]. If the difference is less than 3dB, the response measurements will not be accurate and normally are ignored. Some methods circumvent the problem by driving the loudspeaker to a maximum power within the limitations of the loudspeaker technology, or by providing a conditioned input [Chu (1984), Zuomin et al (1993), Vorländer et al (1997-a)]. Using a pseudo-random signal, the signal can be pre-averaged yielding a greater signal/noise ratio [Chu (1984), Vorländer et al (1997-a)].

The loudspeaker position influences the frequency response (see Section 3.5). If the loudspeaker is placed at the node of a mode, the sound level in the room will be a minimum and this particular mode will not be observed on the frequency response.

When the loudspeaker is placed at an anti-node, the sound level will be maximum and will dominate other modes [Beranek (1992)]. By placing the loudspeaker in one of the corners of the room, it is found that a maximum of room modes is excited (see Chapter 3) [Knudsen (1932), Bolt (1950)]. In addition, the best excitation is when the loudspeaker radiates uniformly in all directions with a flat frequency response. It then can be considered as a point source in the computer simulation.

Similarly, the position of microphones should be such that all room modes are registered. As seen in Chapter 3, the sound pressure is maximum in the corner of the rectangular room, while it is a minimum at the centre of the room when one of the integers n_x, n_y, or n_z is odd. Sound level differences of 30dB can occur between positions in corners and middle of a room [Fuchs (1998)]. Also, the pressure will be a minimum at the centre of one of the walls when two of the three integers are odd. Those different positions must be avoided to get a correct frequency response.

The frequency response of a room is strongly affected by vibration of the enclosing walls [Pan et al (1990)]. A panel can act as a secondary sound source when excited into vibration by a loudspeaker nearby and becomes a non-zero boundary impedance [Craggs (1973), Nefske (1990)]. Additional peaks, corresponding to acoustical-structural couplings can then be observed in the room frequency response [Pan (1992)]. Panel vibration must therefore be avoided in order to obtain the true frequency response of the enclosure.

The frequency response at low frequencies is therefore difficult to measure accurately since it is strongly influenced by background noise including that due to wall vibration, and the low power of the loudspeaker. A physical scale model must be designed to overcome all the difficulties.

Physical scale models are a design aid or a research tool [Hegvold (1971), Burd (1975), Barron (1983)]. They are mostly used to study the room acoustics of large projects such as auditoria, theatres [Jordan (1970 & 80), Barron (1983))], but also for sound transmission [Gibbs (1974), Osipov (1997)]. A physical scale model is similar to a full scale system at least geometrically, but often little attention is paid to the detailed

134

acoustic characteristics of the surfaces of the walls.

7.3 FREQUENCY RESPONSE MEASUREMENTS

7.3.1 Physical scale model

A 1:4 physical scale model of dimensions 1.2 m x 1.2 m x 0.6m as seen in Figure 7.1 was used to measure the frequency response of a single enclosure. Five walls of the enclosure were made of 18mm blockwood. They were glued and screwed to form rigid corners, which then were sealed with mastic to avoid acoustic leaks. The sixth wall was to be the party wall in future measurements of level difference between rooms. At present, a 10mm perspex sheet of dimensions 1.2 x 0.6m was sealed and screwed at 100mm centres. An additional 115mm of perspex formed a perimeter to the party wall to reduce future flanking transmission between the connected rooms.

The model was placed in a small sound transmission suite where the background noise level was low and was positioned on 400mm resilient foam to reduce vibration to and from the floor. To approximate a point source, a hole of 100mm diameter was drilled in one of the corner of the enclosure, opposite to the future party wall, allowing a loudspeaker to radiate into the enclosure. Microphones were inserted through two holes in the top of the enclosure. The positions of the microphones were carefully chosen to avoid room nodes. Position 1 was at (0.5, 0.4, 0.4m) and position 2 was at (0.8, 0.8, 0.2m) (see Figure 7.2). Another microphone was located in front of the loudspeaker to measure the direct field. A photograph of the model is shown in Figure 7.3.

7.3.2 Maximum Length Sequence measurements

The frequency range of interest, in the full scale, is 25-200Hz, which converts to 100-800Hz in the quarter-scale model. Different methods can be used to measure the frequency response of an enclosure. A well established method involves the use of a slow swept sine [Chu (1984 & 85)]. A pure tone excitation is used and a specific number of frequencies are selected. The slow swept sine starts then from the lowest frequency of the selected frequency range and is incremented till the upper frequency.

The sweep has to be very slow in order to pick up all peaks and dips and repeated several times. That makes the method time consuming [Chu (1984 & 85)]. White noise can be used, with the microphone response being swept filtered. The spectral energy of white noise is distributed continuously over the frequency band, causing the room modes of interest to be excited. Being a random signal, however, the rms values and hence the power are not the same when changing the bandwidth. In order to increase the signal noise ratio, the measurements are repeated several times, creating stochastic deviations. Those deviations tend to disappear when using a deterministic signal such as a Maximum Length Sequence (MLS) [Bjor (1994), Chu (1984 & 85)].

MLS is a recent innovation in building acoustics [Zuomin et al (1993): Chu (1994), Bjor (1994), Vorländer (1997-a,b), Bietz (1997)], environmental measurements [Vorländer (1997-b), Heutschi (1997)], loudspeaker characteristics measurements [MLSSA (1992), MLSSA (1987 et al)], and also in medicine [Schneider et al (1995)]. It is a pseudo-random sequence which approximates a series of Dirac impulses. The spectrum of the MLS is flat. The length period of the M-sequence is equal to

$$J = 2^m - 1 \tag{7.1}$$

where m is the order of the sequence and J is the largest possible number of pulses in a repeated pattern at the output of the system.

The input and output of the system, therefore, are deterministic, giving an enhanced signal/ noise ratio (SNR) according to;

$$SNR = 10 \, Log \, \Upsilon \tag{7.2}$$

where Υ is the period of the Maximum Length Sequence.

For example, if the signal is pre-averaged 10 times, the SNR is increased 10dB. The method has been shown to be as accurate as the sweep frequency technique and is much faster [Chu (1984)]. MLS was therefore selected for the measurement of the frequency response of the sound field and later in Chapter 8 for the sound pressure level

136

difference.

A MLS analyser card for PC [MLSSA (1987 & 94)] was used in this investigation. A burst MLS stimulus of length $J = 2^{16}-1$ was used as a source of excitation. MLSSA, like a digital scope, acquired and displayed 2^{16} points sampled at 4000Hz. The result is a response as a time history. To get a fine resolution of the power spectrum, a FFT rectangular window of 8192 points was selected, giving a spectral resolution of 0.49Hz from 0 to 1000Hz. A Blackman-Harris window is then applied to obtain the power spectrum from 100Hz to 800Hz with the same resolution.

7.3.3 Set up of the experiment

A loudspeaker of 50mm cone diameter was used. It had a stated flat frequency response from 180Hz to 800Hz, which was confirmed by measurements in the free field as seen in Figure 7.4. An increase of 4dB is observed from 100Hz to 180Hz and the response then is flat till 800Hz. The loudspeaker was positioned outside the model enclosure in front of the 10cm diameter hole.

The input signal was amplified by a Quad 4 to the loudspeaker. The sound pressure level was measured by one of three B&K ½ inch microphones (B&K type of 4165), amplified and then processed by MLSSA. The sound pressure level was amplified using a dual microphone supply (B&K type 5935). The gain for each microphone was adjusted until they were matched i.e. when microphone 1 registered the same sound pressure level as microphone 2 when each was at the same position. The experimental arrangement is shown in Figure 7.5.

7.4   MODELLING ONE ROOM

7.4.1 Mesh selection

As seen in Chapter 6, the eigenfrequencies of a 10 mesh model for a transmssion room

and a vibrating party wall could be estimated within an error of 8%. To validate the selection of the mesh model, the frequency response of a single room was investigated as a prelude to the study of the two room model, described in the next chapter. In the previous chapter, it was shown that the eigenfrequencies of a 35m³ and 40m³ rooms are processed within an error of 8% when each room is discretized by 10^3 elements, whereas the modes are processed with very little error when the models are discretised by 14^3 elements, each. In order to define the number of elements to discretise the enclosure for which the eigenfrequencies are processed within 8%, a ratio ι was defined as following;

$$\iota = \frac{\text{Mesh model having an error of 8\%}}{\text{Mesh model having very little error}} = \frac{10}{14} = 7.14 \ 10^{-1} \qquad (7.3)$$

The model of the quarter scale enclosure, for which the eigenfrequencies can be processed with very little error, as defined in Chapter 6, is given by a 17 mesh. It follows then that the model of the ¼ scale enclosure which will give an error of 8% is defined by a 12 mesh model.

The quarter-scale model was therefore modelled with 12^3 elements which will give eigenfrequencies within an error less than 8%.

7.4.2 Sound field simulation

As seen in Chapter 6, the sound field in the enclosure was modelled using the software package P3/Patran. The model is imported into Sysnoise V5.3 after having selected the acoustical finite element method. The AFE model was defined with 6 hard walls in order to have no structural - acoustical interactions. The mass density and the sound velocity were assigned and 90 room modes were then processed, 30 of which had eigenfrequencies above the frequency range of interest. A point source was defined in one of the corners of the room at a position as close as possible to the selected position in the experimental set up. This selection was carefully chosen as the modal behaviour of the sound field is strongly dependent on the loudspeaker position (see Section 3.5).

138

The best position for the loudspeaker was (0.05, 0,0.05). A sound power was assigned to the point source, which initially did not correspond to the power obtained in the experimental set up. This was not critical, since the measurement was a prelude to an investigation of sound level difference between rooms (see Chapter 8). Indeed, the source sound power in the source room and receiving room is cancelled out when calculating the sound pressure level difference. The frequency response was processed with a resolution of 1Hz from 100Hz to 800Hz using modal superposition. The pressure was then evaluated at the field points, which is calculated by using the shape function to perform an interpolation between the known nodal values (see Appendix 1). The field points behave as microphones and have no influence on the sound field. Two field points were defined called microphone 1 (0.5, 0.4, 0.4) and microphone 2 (0.8,0.8,0.2). The data was then compared with the measured data to validate the simulation. The acoustic model can be seen in Figure 7.6.

7.5   FREQUENCY RESPONSE

The sound pressure level measurements at microphone positions 1-3 are shown in Figure 7.7. The sound pressure level displays maxima and minima corresponding to the room modes of the enclosure. The peak at 150Hz corresponds to the mode (1,0,0), the peak at 210Hz corresponds to the mode (0,1,0), etc. The sound field is therefore modal at low frequencies, as expected. The peaks corresponding to all room modes are identified by the three microphones. As expected, the sound level at microphone position 3 is greater than the sound level measured at microphones 1 and 2, which display overall the same level. From 650Hz, the fluctuations measured at microphones 1 and 2 tend to reduce. Although the frequency response measured at microphone 1 is similar to that of the microphone 2, the dips are less pronounced. The frequency response, therefore, depends strongly on the microphone position.

The predicted sound pressure levels at positions 1 and 2 are shown in Figure 7.8. As with the measured frequency responses, the sound pressure level fluctuates as a series of maxima and minima due to the room modes. The sound pressure level measured at

positions 1 and 2 display the same maximum level; only the magnitudes of the dips differ between the two curves.

Figures 7.9 and 7.10 show the predicted and measured sound pressure levels at positions 1 and 2, respectively. Predicted and measured frequency responses show common peaks and dips, but a shift between the first two measured and predicted modes are observed at position 1 and 2. Such differences could be explained by vibrations of the walls of the enclosure. It was also observed in the upper part of the frequency range, that many peaks were not measured at microphone position 1 and 2. It was thought that the number of elements is too low to provide an accurate frequency response. Microphone 3, however, displayed more peaks in the same upper part of the frequency range. That means the number of elements is still sufficient enough to predict the sound field. Those differences observed at microphones 1 and 2 are probably due to the effect of damping which increases as the frequency increases and when the microphone is far from the loudspeaker.

The magnitude of the measured peaks and dips are not as great as predicted. This was expected since the computer model did not include absorption. At high frequencies, the agreement between prediction and measurement is less good because of the limited number of mesh elements used to describe the frequency response.

Different frequency resolutions were used for prediction and measurements and therefore sound levels were re-calculated with a 1/12 octave band resolution in order to compare data. Results are presented as a level difference (simulation-measurements) in Figure 7.11. The large differences are the result of the often quite small frequency shifts observed with respect to expected peaks. Again, the numerical model does not include surface or air absorption and therefore the simulation may over emphasise peaks and dips.

The sound levels were then calculated with a 1/6 octave bands resolution in Figure 7.12. Both curves display nearly the same trend except from 180Hz to 400Hz. The maximum discrepancy between simulation and measurements is 25dB at 141Hz and 18dB at 315Hz. The discrepancy is less for the microphone position 1 than for position 2. This

can be explained by the fact that the former was closer to the loudspeaker than the latter, and was therefore less affected by the absorption of the room. Also microphone 2 is placed closer to the perspex panel, which may vibrate more than the other surfaces. Both curves show that the sound field is overestimated by the prediction.

In real measurements, the data are commonly presented in 1/3 octave bands (see Figure 7.13). Figures 7.11 and 7.12, compared with Figure 7.13, show that the discrepancy between simulation and measurement decreases when calculated within a larger bandwidth. The peak at 141Hz, which corresponds to the 1st room mode, is again evident in all curves. The maximum discrepancy between simulation and measurements is 15dB. The discrepancy is less for the microphone position 1 than for position 2. The simulation overestimates the overall sound level by approximately 5-10dB in third octave bands. This could be explained by the sound power of the point source, which may have been incorrectly assigned. Viscous and thermal losses in air and at boundaries were not included in the FEM model as it is difficult to quantify at low frequencies [Davern (1987), Swenson (1993)]. A frequency response of high levels with sharp peaks is created. However, it will be shown in Chapter 8 that if two rooms are modelled in the same manner, these effects will cancel each other when calculating the sound pressure level difference.

The comparison between calculated and measured frequency response using 1/12, 1/6 and 1/3 octave bands show that the band resolution can induce errors due to the non statistical behaviour of the sound field. The position and the levels of peaks and dips can alter the calculated level in each band. Although the presentation in 1/12, 1/6 or 1/3 octave bands is acceptable in order to compare the experiment and the simulation, such presentation, and particularly the 1/3 octave band presentation, tends to cancel the non statistical behaviour of the sound field.

To summarise, the AFE model was validated by comparing the predicted with the measured frequency response of a 1:4 scale model enclosure. Three microphone positions were selected in the 1:4 scale model, but only two (positions 1 and 2) were chosen in the predicted model. The narrow band presentation shows that the predicted and measured frequency response at positions 1 and 2, show common peaks and dips.

141

However, some shifts were observed as well as some missing peaks in the upper part of the frequency range of interest and the predicted dip and peak amplitudes are greater than the measured ones. Those differences [Maluski et al (1997), Maluski et al (1998)]were explained as follows;

1. The eigenfrequencies are processed within an error of 10%

2. Error in assigning the source position and source power

3. No acoustic damping was assigned in the predicted model

The presentation of the frequency response with different band resolutions (1/12, 1/6 and 1/3 octave bands) emphasised these differences. This explains why the discrepancy obtained for position 1 is smaller than for position 2. However, both positions show that the simulation emphasises the frequency response. This is due to the non-introduction of acoustic damping and also of stiffer elements at the upper part of the frequency range of interest.

7.6   CONCLUDING REMARKS

Measured and predicted frequency responses of an enclosure at low frequencies show that the sound field is not statistical. The effects of room resonances are stronger when measured far from the loudspeaker. The comparison between measured and predicted data show that the predicted frequency response is an overestimate due to errors in assigning source power and in the positioning of the point source, and no absorption. The effects of those errors need now to be investigated further when FEM is used for modelling sound transmission between two rooms.

7.7   REFERENCES

Barron, M., (1983): '*Auditorium acoustic modelling now*', Applied Acoustics, Vol.16. 2769-290

Beranek, L.L. and Ver, I.L., (1992): '*Noise and Vibration Control Engineering: Principles and Applications*', Ed. J.Wiley and Sons

Bietz, H., Bethke, G. and Schmitz, A., (1997): '*Effects of time variances using MLS technique in building acoustics for measuring sound insulation and reverberation time*', Proceeding of Inter-Noise 97, 1429-1432

Bjor, O. and Winsvold B., (1994): '*Deterministic excitation signals reduces statistical spread and extraneous noise contamination in sound transmission measurements*', Proceeding of Inter-Noise 94, 1469-1474

Bolt, R.H., (1950): '*Frequency response fluctuations in rooms*', Journal of the Acoustical Society of America, Vol.22 (2), 280-289

Burd, A.N., (1975): '*Acoustic modelling –Design tool or research project?*', Auditorium Acoustics, Ed. Applied Science Publisher Ltd

Chu, W.T., (1984): '*Architectural acoustic measurements using periodic pseudorandom sequences and FFT*', Journal of Acoustical Society of America, Vol.76 (2), 475-478

Chu, W.T., (1985): '*Room response measurements in a reverberation chamber containing a rotating diffuser*', Journal of Acoustical Society of America, Vol.77 (3), 1252-1256

Chu, W.T., (1994): '*Application of the M-sequence correlation technique for sound transmission measurements*', Proceeding of Inter-Noise 94, 1479-1484

Craggs, A., (1993): '*An acoustic finite element approach for studying boundary flexibility and sound transmission between irregular enclosures*", Journal of Sound and Vibration, Vol.30 (3), 343-357

Davern, W.A., (1987): '*Measurements of low frequency absorption*', Applied Acoustics, Vol.21 (1), 1-11

Fuchs, H.V., (1998): '*Qualification of small freefield and reverberation rooms for low frequencies*', Proceeding of Euro-Noise 98, Vol.2, 657-666

Gibbs, B.M., (1974): '*The direct and indirect transmission of vibrational energy in*

building structures', Ph.D. thesis at University of Birmingham,

Hegvold, L.W., (1971): '*A 1:8 scale model auditor*', Applied Acoustics, Vol.4, 237-256

Heutschi, K. and A. Rosenheck, (1997): '*Outdoor sound propagation measurements using an MLS technique*', Applied Acoustics, Vol.51 (1), 13-32

ISO 140, (1995): '*Measurements of sound insulation in buildings and of building elements. Part 3. Laboratory measurements of airborne sound insulation of building elements*'

Jordan, V.L., (1970), '*Acoustical criteria for auditoriums and their relation to model techniques*', Journal of the Acoustical Society of America, Vol.47, 408-412

Jordan, V.L., (1980), '*Acoustical design of concert halls and theatres*', Ed. Applied Science Publishers, London

Knudsen, V.O., (1932): '*Resonance in small rooms*', Journal of the Acoustical Society, July 1932, 21-37

Maluski, S. and Bougdah, H., (1997): '*Predicted and measured low frequency response of small rooms*', Journal Building Acoustics, Vol.4 (2), 73-86

Maluski, S., Gibbs, B., and Bougdah, H., (1998): '*Predicted and measured low frequency response of small rooms*', I.O.A. Proceeding, Cranfield, Vol. 20 (1), 87-92

MLSSA, (1987-94): Reference Manual, version 9.0, DRA Laboratories, Copyright 1987-1994

MLSSA, (1992): '*Brings speaker design in from the cold*', Electronics World + Wireless World, January 1992, 26-29

Nefske, D.J. and Sung, S,.H., (1990): '*Sound in small enclosures*', Research Publication GMR-7069

Osipov, A., Mees, P., and Vermeir, G., (1997): '*Low frequency airborne sound transmission through single partitions in Buildings*', Applied Acoustics, Vol.52 (3-4), 273-288

P3/Patran (1993): '*User Manual*', PDA Engineering

Pan , J. and Bies, D.A., (1990): '*The effect of fluid-structural coupling on sound waves in an enclosure-Theoretical part*', Journal of Acoustical Society of America, Vol.87 (2), 691-707

Pan, J., (1992): *'The forced response of an acoustic-structural coupled system'*, Journal of Acoustical Society of America, Vol. 91 (2), 949-956

Schneider, T. and Jamieson, G., (1995): *'Using Maximum Length Sequence coherence for broadband distortion measurements on hearing aids'*, Journal of the Acoustical Society of America, 2282-2292

Swenson, G.Jr., (1993): *'A standing wave facility for low frequency impedance/absorption measurements'*, Applied Acoustics, Vol.40, 355-363

Sysnoise, (1996): Software V.5.3

Vorländer, M. and Kob, M., (1997-a): *'Practical Aspects of MLS measurements in Building acoustics'*, Applied Acoustics, Vol.52 (3/4), 239-258

Vorländer, M. and Mommertz E., (1997-b): *'Guidelines for the application of the MLS technique in building acoustics and in outdoor measurements'*, Proceeding of Inter-Noise 97, 1423-1428

Zuomin, W. and Chu, W.T., (1993): *'Ensemble average requirement for acoustical measurements in noisy environment using the m-sequence correlation technique'*, Journal of Acoustical Society of America, Vol.94 (3), Pt.1, 1409-1414
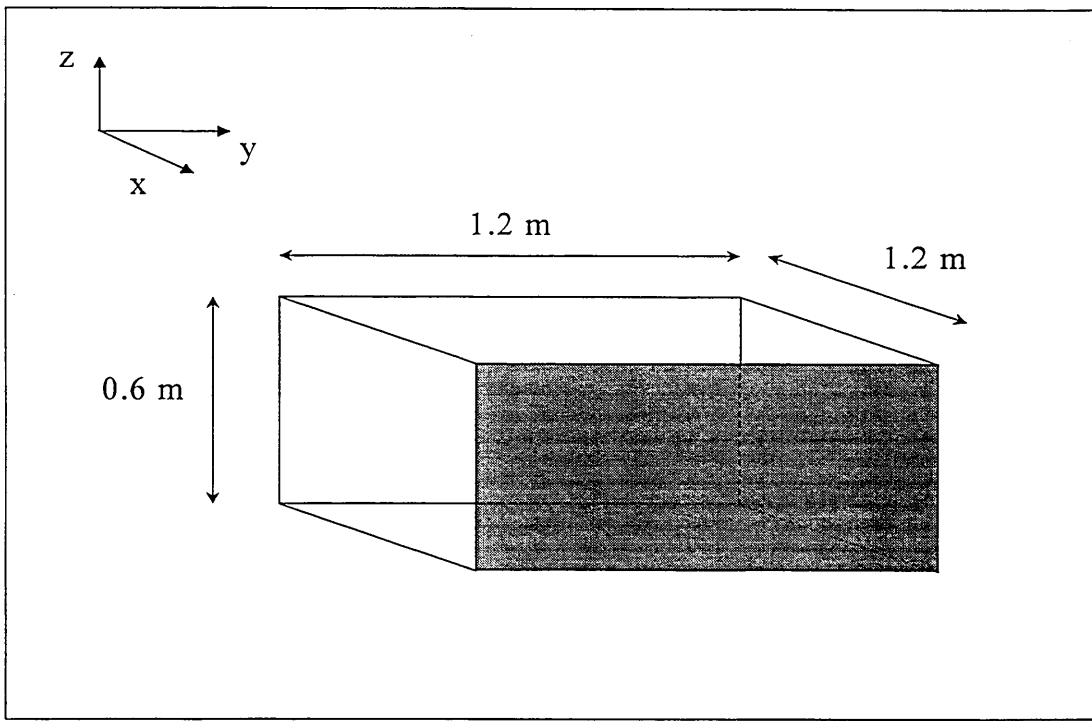
Figure 7.1. Dimensions of the 1:4 scale enclosure
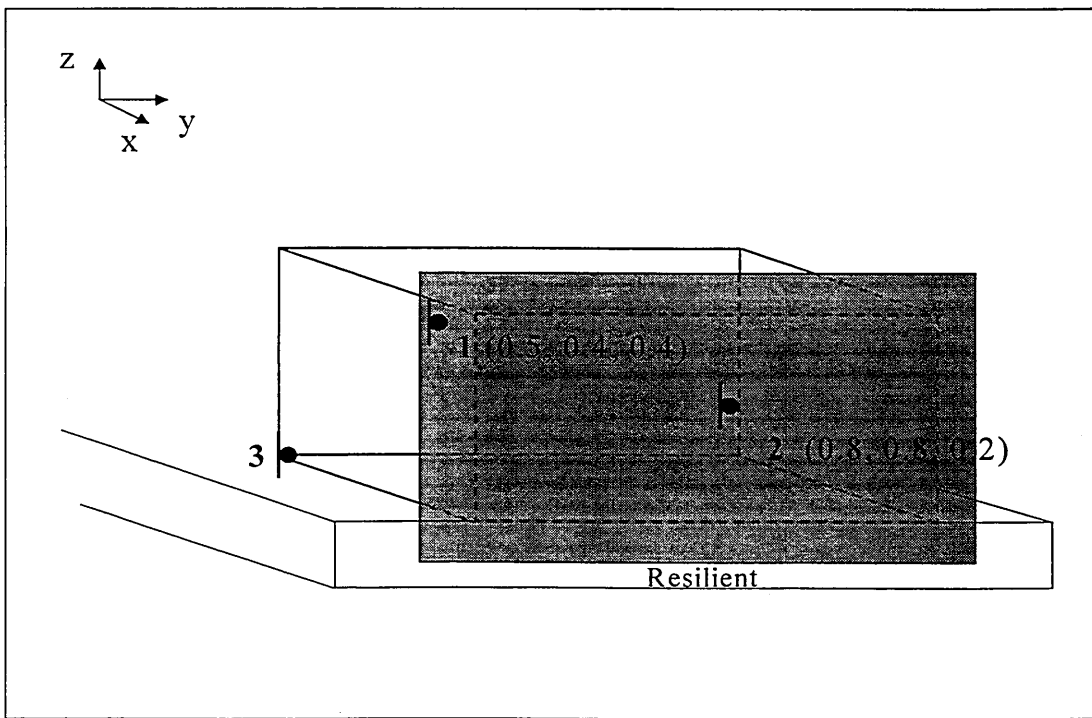
Figure 7.2. Microphone positions

146
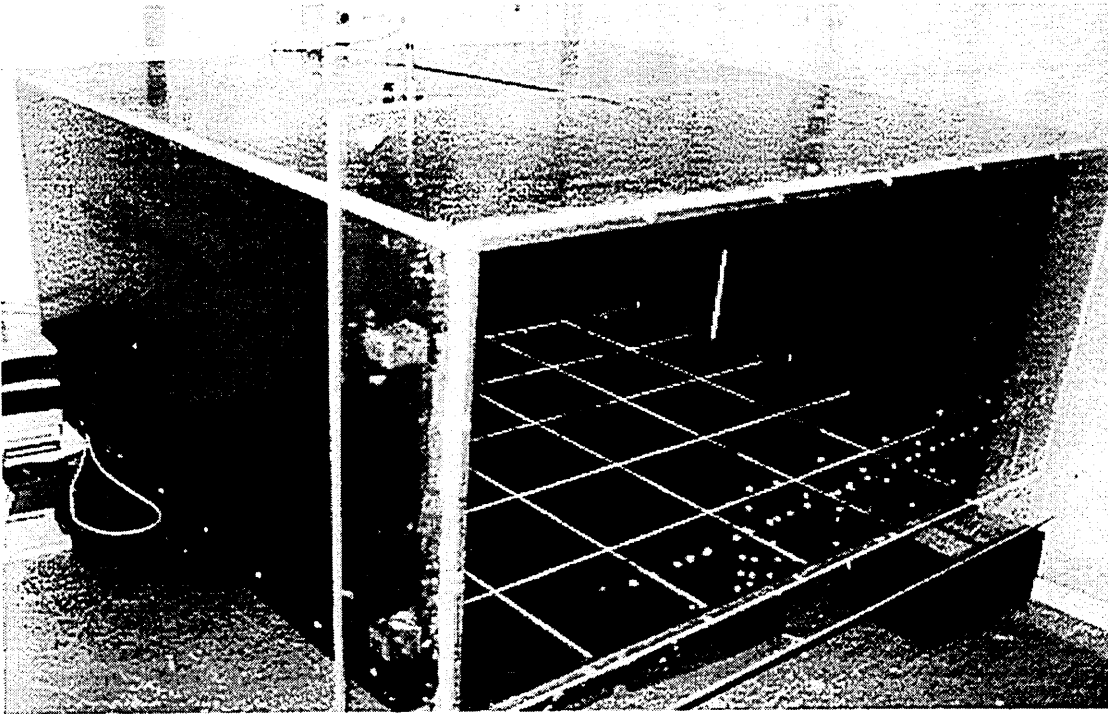
Figure 7.3. Physical scale model
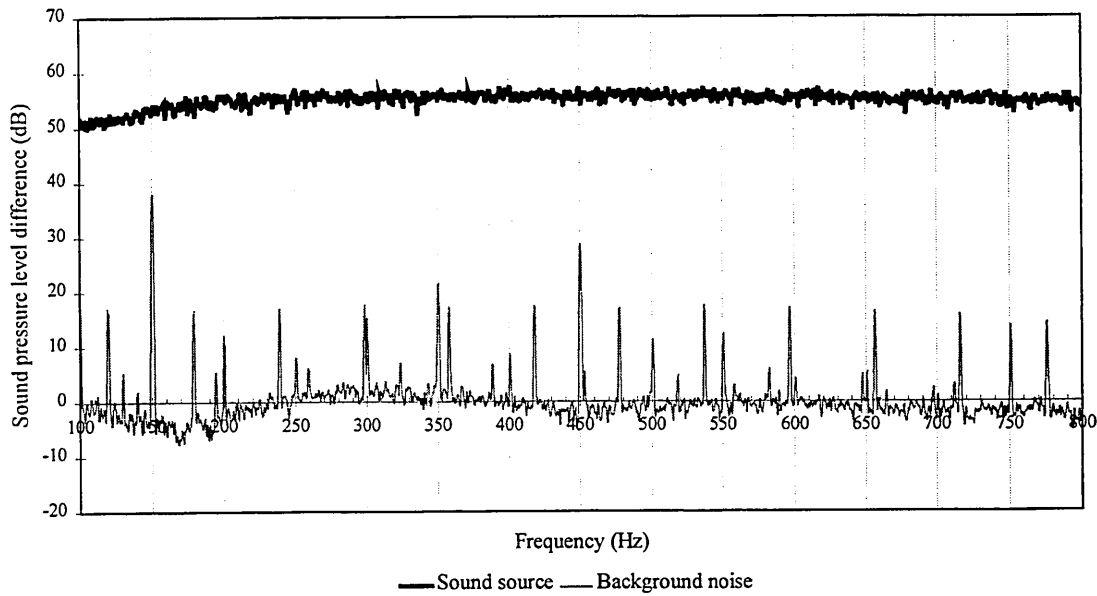
Figure 7.4. Spectrum of the sound source measured in an anechoic chamber

147
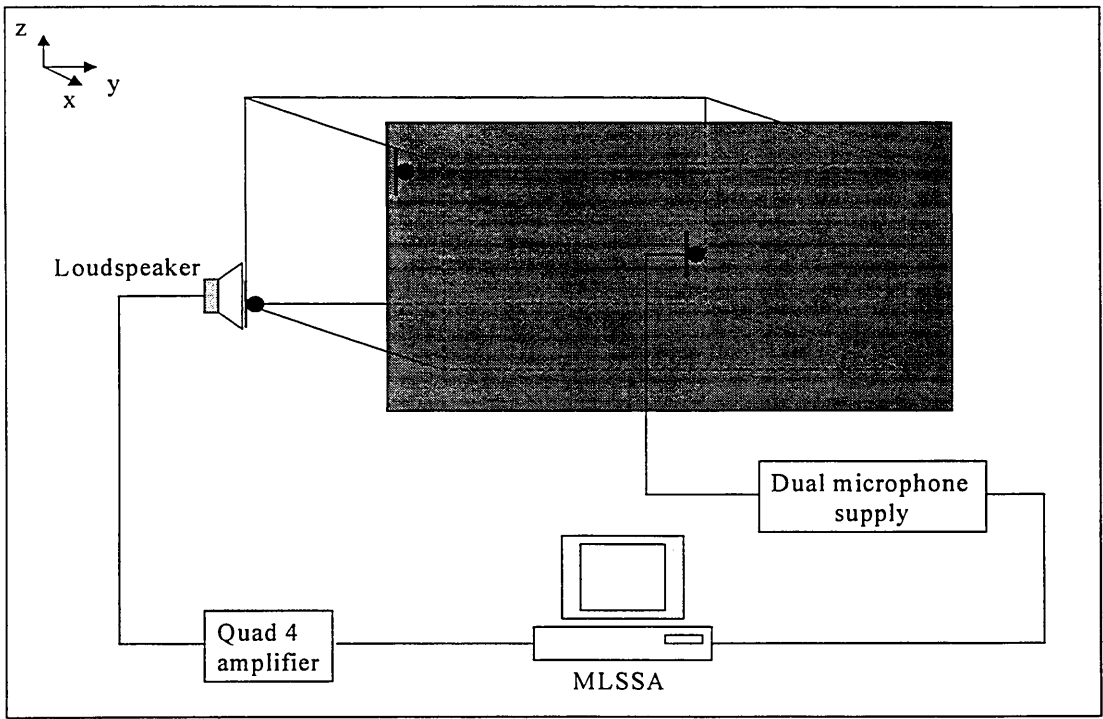
Figure 7.5. Experimental set up for frequency response measurements
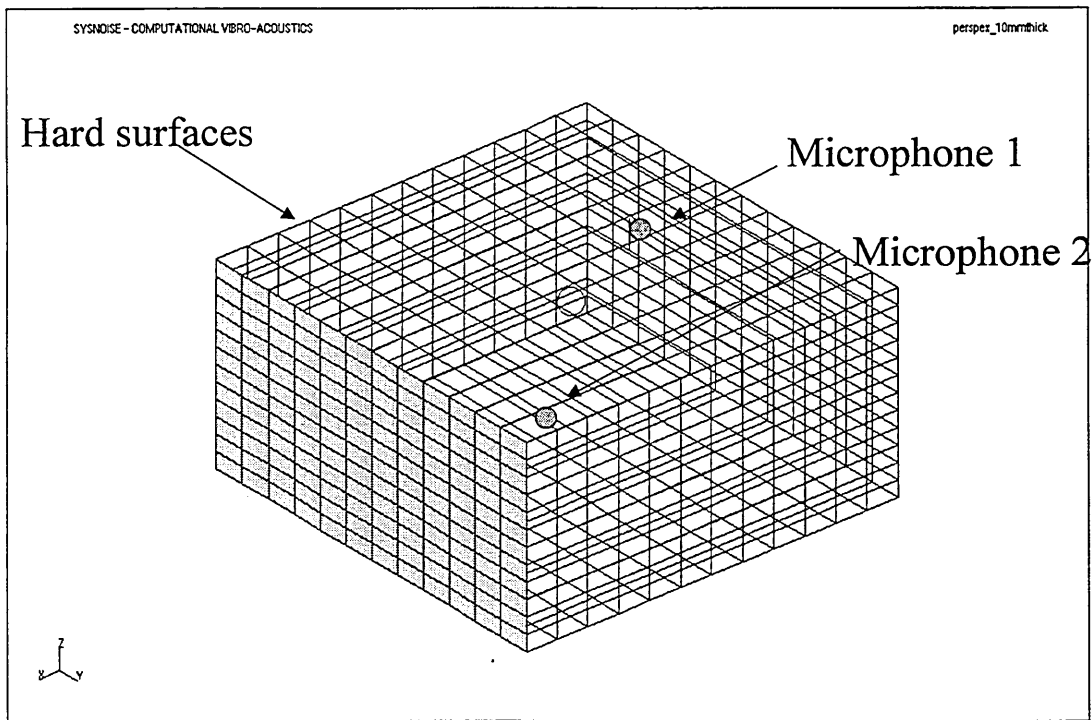
Figure 7.6. Acoustic Finite Element Model of the enclosure

148
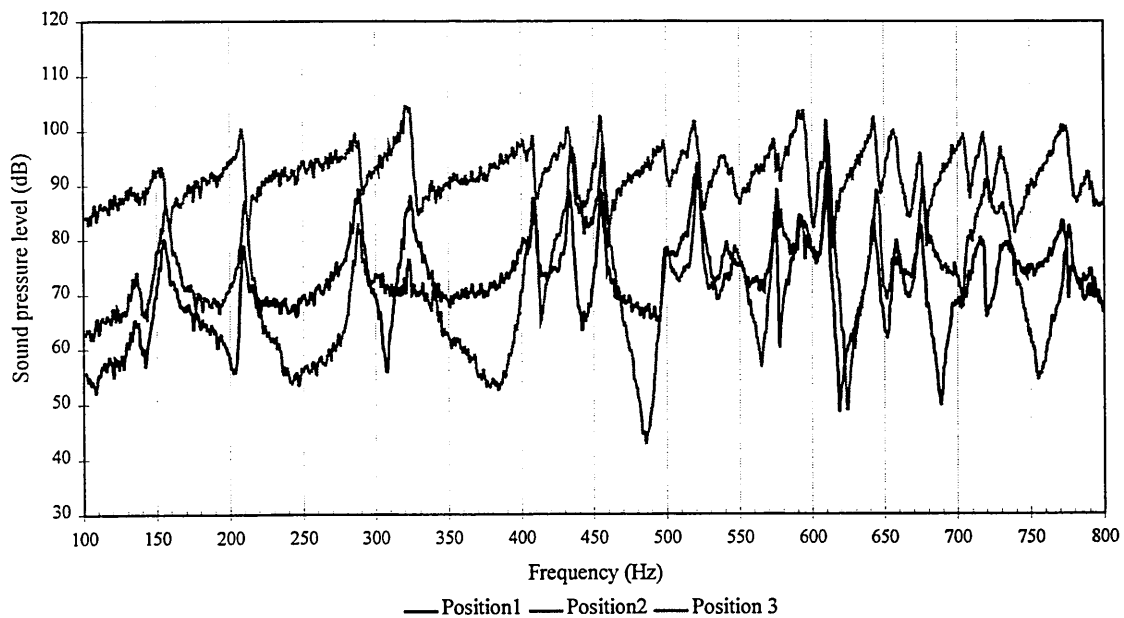
Figure 7.7. Frequency response measured at three microphone positions
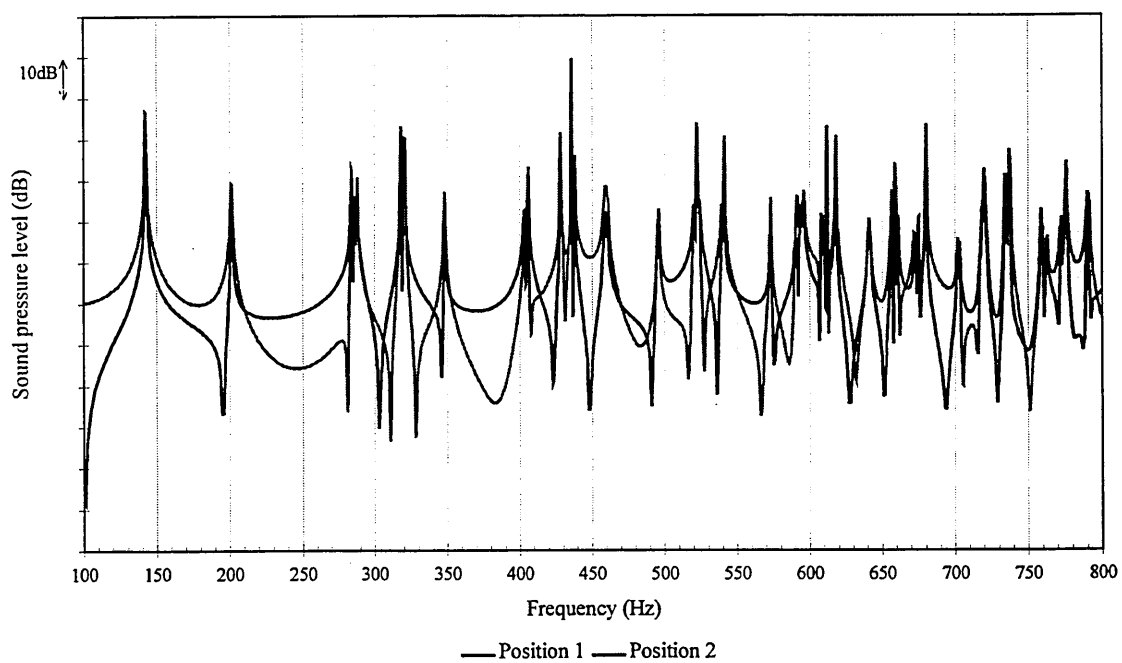
Figure 7.8. Frequency response predicted at positions 1 and 2

149
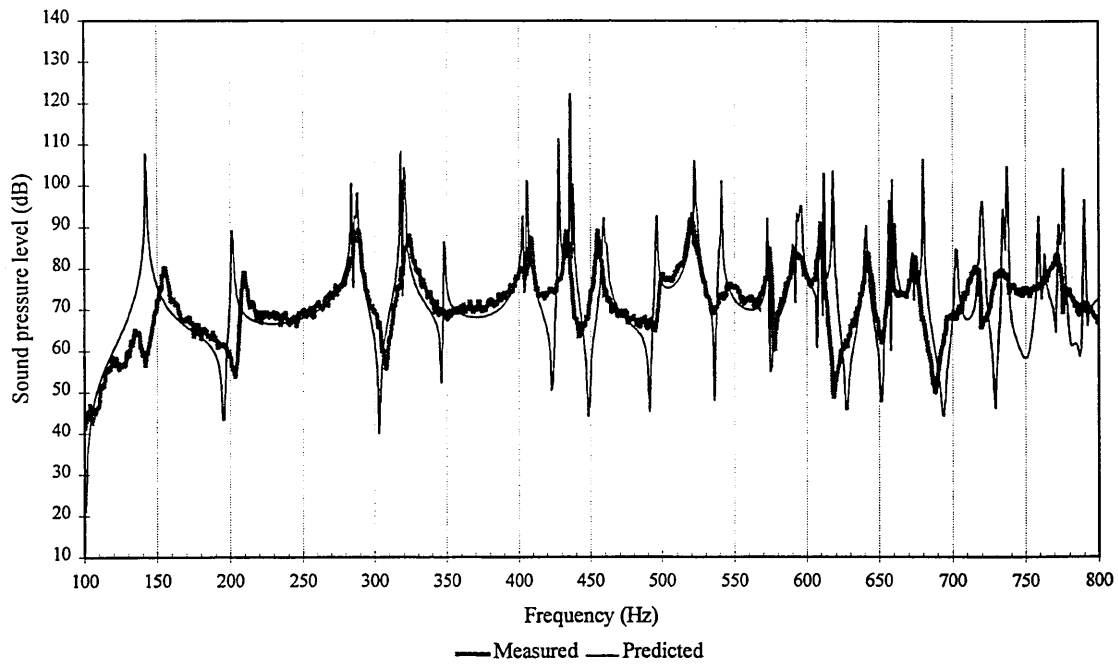
Figure 7.9. Frequency response at microphone position 1
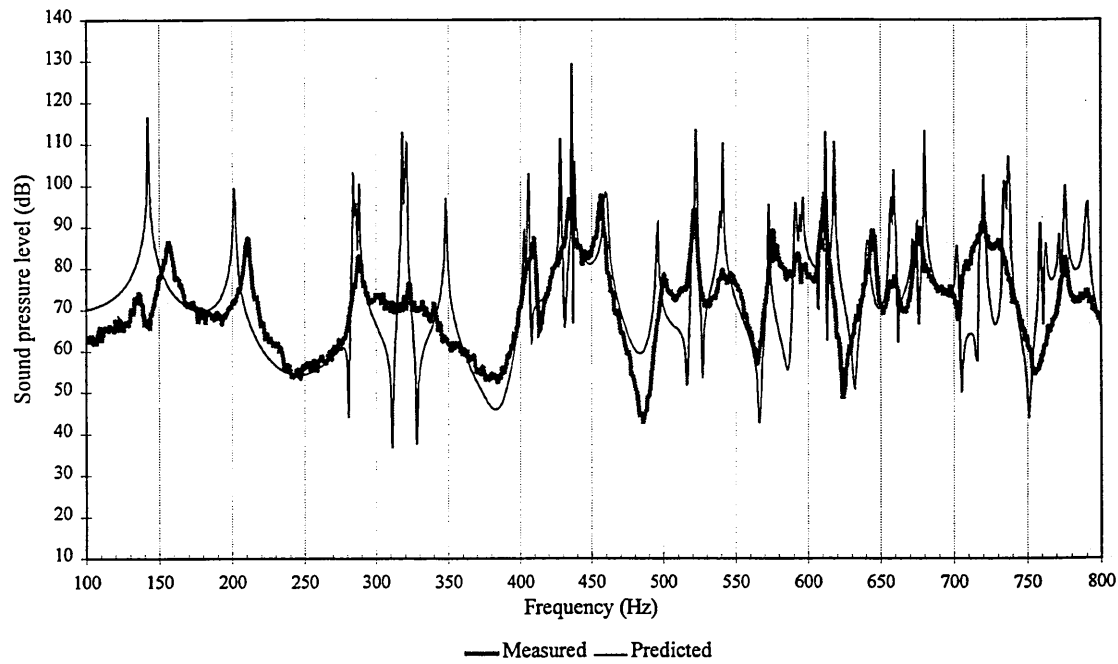
Figure 7.10. Frequency response at microphone position 2
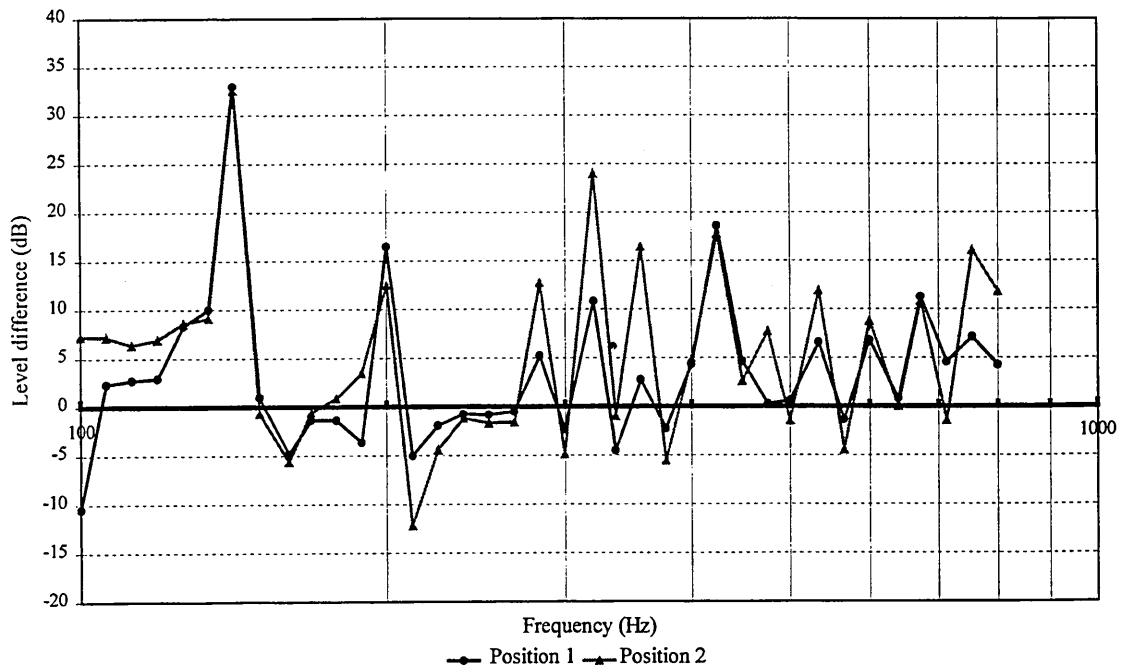
Figure 7.11. Simulation compared with measurements in a 1/12 octave band.
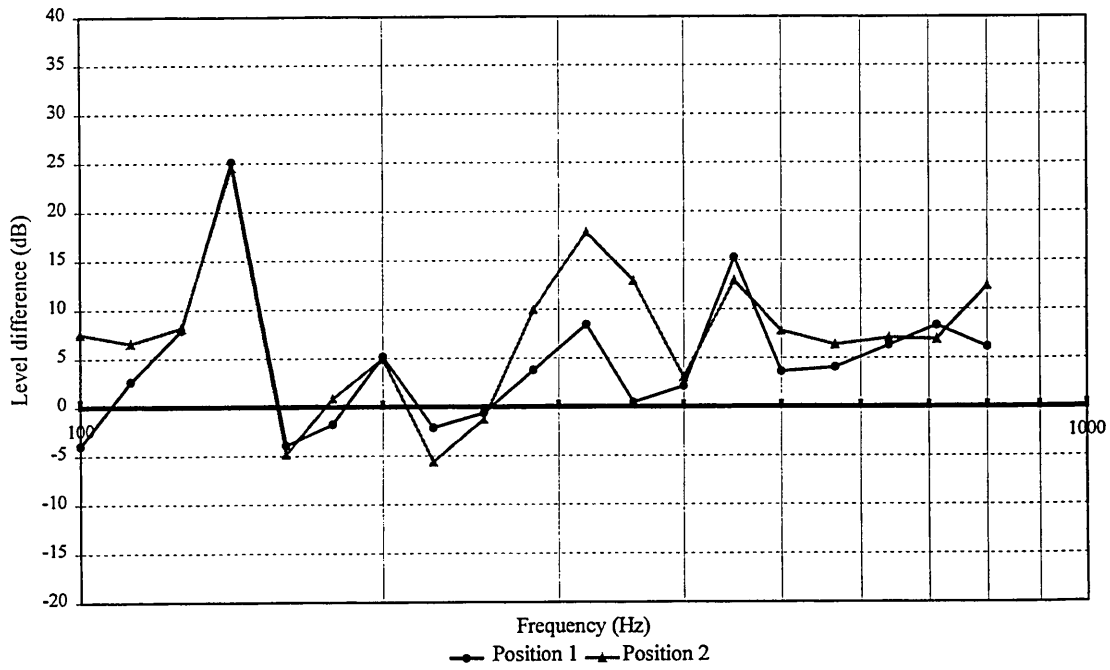
Figure 7.12. Simulation compared with measurements in a 1/6 octave band.

151
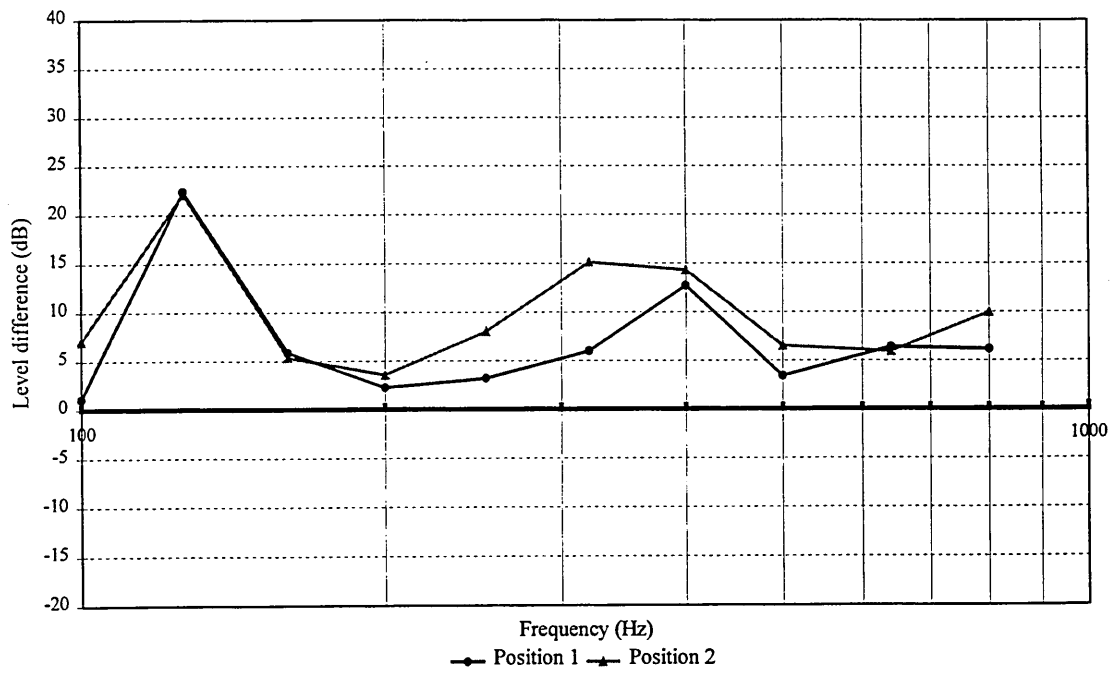
Figure 7.13. Simulation compared with measurements in a 1/3 octave band.

8 EXPERIMENTAL VALIDATION FOR TWO ROOMS

8.1 INTRODUCTION

In chapter 7, it was argued that incorrect assignment of sound power to the source and non-inclusion of absorption in the FEM model explained the discrepancies between the predicted and measured frequency response of one enclosure. It was suggested that the effects of the two causes would cancel when calculating sound level difference between rooms. A transmission room model was therefore created by linking an acoustic FE model with a structural FE model as described in Chapter 6, and a physical scale model was built to validate the computer model.

The objectives of this chapter are to validate the transmission room model by comparing the predicted and measured frequency response of the receiving room. Then, by comparing the predicted and measured sound pressure level differences.

8.2 THEORY OF SOUND TRANSMISSION BETWEEN RECTANGULAR ROOMS

8.2.1 Analytical approach

Various analyses are available for the sound transmission between rooms at low frequencies [Josse and Lamure (1964), Utley (1968), Nilsson (1972), Mulholland (1973), Fahy (1985), Gargliadini (1991)]. A transmission room is considered of dimensions as shown in Figure 8.1. The two rooms are built with hard wall surfaces, the sixth wall being the party wall at position (0,0,0). The sound field in the source room, Γ_1, is the results of two sources. The primary source is the sound source Ω_1, and the secondary source is the vibrating panel Ω_2 [Fahy (1985), Nilsson (1972)]. The sound field in the receiving room, Γ_2, is due only to the panel radiation [Nilsson (1972)]. The sound transmission is defined by calculating the two steady state sound fields, which

have the same time dependence as the source function Q. N_1 represents the modes of the source room of integers n_{x_1} n_y, n_z. N_2 represents the modes of the receiving room of integers n_{x_2}, n_y, n_z. and N represents the modes of integers n_y n_z of the panel.

The sound field in the source room is described by

$$\Gamma_1 = \Omega_1 + \Omega_2 \tag{8.1}$$

where Ω_1 is the sound field created by the sound source only

$$\nabla^2\Omega_1 - \frac{1}{c_o^2}\frac{\partial^2\Omega_1}{\partial t^2} = 0 \tag{8.2}$$

for which the boundary conditions are

$$\frac{\partial\Omega_1}{\partial n} = 0 \tag{8.3}$$

and Ω_2 is the sound field created by the wall vibration only. The initial source strength is doubled because of the reflections

$$\nabla^2\Omega_2 - \frac{1}{c_o^2}\frac{\partial^2\Omega_2}{\partial t^2} = 2\,\delta(x)\zeta \tag{8.4}$$

for $-L_{x_1} \le x \le L_{x_1}$; $0 \le y \le L_y$; $0 \le z \le L_z$; where $\delta(x)$ is the Dirac function and ζ is the party wall velocity and for which the boundary conditions are

$$\lim_{x \to -0}\left[\frac{\partial\Omega_2}{\partial x}\right] = -\zeta \tag{8.5}$$

$$\frac{\partial\Omega_2}{\partial n} = 0 \text{ everywhere except for the party wall} \tag{8.6}$$

154

The secondary sound field only is considered. Equation 8.4 is solved by considering the boundary conditions, defined by Equation 8.6, which are satisfied by the normalised and orthogonal eigenvectors. Also the functions of Γ_1, Γ_2 and ζ, for the steady state solution, have the same time dependence as the source function Q, which is given by $e^{i\omega t}$. The details of the derivations are not included but can be found in the work of Nilsson [1972] to give;

$$\Omega_2 = \sum_{N_1=0}^{\infty} \alpha_{n_{x1}} \frac{2}{\sqrt{L_{x1}}} \frac{\zeta_N \, g_{N_1}}{k^2 - k_{N_1}^2} e^{j\omega t} \qquad (8.7)$$

where $\alpha_{n_{x1}}$ are the normalising factors, ζ_N are the expansion coefficients for the panel velocity, g_{N_1} are the orthogonal eigenvectors in 3 dimensions, $k_{N_1}^2$ are the eigenvalues corresponding to g_{N_1} and $k^2 = \dfrac{\omega^2}{c_0}$ is the complex wavenumber.

The primary sound field is given by Equation 8.2. This equation is solved in the same manner as for Equation 8.4 for the secondary sound field, where ;

$$\Omega_1 = \sum_{N_1=0}^{\infty} 2 \frac{Q_N}{k_{N_1}^2 - k^2} g_{N_1} e^{j\omega t} \qquad (8.8)$$

Q_N is the expansion coefficient for the sound source. The equation expresses the dependence of the excitation of the room modes on loudspeaker position.

The sound field in the source room is then the sum of Equations 8.7 and 8.8;

$$\Gamma_1 = \sum_{N_1=0}^{\infty} g_{N_1} \left[K_{N_1} + \frac{2\alpha_{n_{x1}}}{\sqrt{L_{x1}}} \frac{\zeta_N}{k^2 - k_{N_1}^2} \right] e^{j\omega t} \qquad (8.9)$$

where $k_{N_1}^2$ is the square of the eigenvalue corresponding to the orthogonal eigenvector in y-z plane and K_{N_1} is the expansion coefficient.

The sound field in the receiving room is defined as follows

$$\nabla^2 \Gamma_2 - \frac{1}{c_o^2}\frac{\partial^2 \Gamma_2}{\partial t^2} = -2\,\delta(x)\zeta \qquad (8.10)$$

for $-L_{x_2} \leq x \leq L_{x_2}$; $0 \leq y \leq L_y$; $0 \leq z \leq L_z$; and for which the boundary conditions are;

$$\frac{\partial \Gamma_2}{\partial n} = 0 \text{ except the party wall}$$

$$\lim_{x \to +0}\left[\frac{\partial \Gamma_2}{\partial x}\right] = -\zeta \text{ at the party wall} \qquad (8.11)$$

The steady state sound field is given [Nilsson (1972)];

$$\Gamma_2 = -\sum_{N_2=0}^{\infty} \frac{2\alpha_{n_{x2}}}{\sqrt{L_{x2}}}\frac{\zeta_N\, g_{N_2}}{\left[k^2 - k_{N_2}^2\right]}e^{j\omega t} \qquad (8.12)$$

where $\alpha_{n_{x2}}$ is the normalising factor, ζ_N is the expansion for the panel velocity, g_{N_2} is the orthogonal eigenvector in three dimensions, $k_{N_2}^2$ is the eigenvalues corresponding to g_{N_2}.

The wall velocity ζ is then derived from the equations obtained for the sound field in the source room and in the receiving room, by calculating the sound pressure level difference at $x = 0$. The panel velocity is then described by the sound source term. When the equation of the panel velocity is inserted in Equations 8.9 and 8.12, the two unknown equations are then only dependent on the sound source.

Consequently, the expressions given for the sound field of the source room and receiving room are different from the equations given by the classical theory [Fahy

156

(1985), Beranek (1992)]. The sound transmission is dependent on the closeness of the eigenfrequencies of the acoustic modes and on the degree of spatial matching between the acoustic mode pressure distribution over the panel and the distributions of panel mode displacements.

8.2.2 Numerical approach

Sound transmission between two rooms is simulated by taking into account the two sound fields of the source room and of the receiving room, the structural behaviour of the panel and the coupling.

The frequency response of the acoustic field is given by an equation of form

$$\left[K - \omega^2 M\right]\{p\} = \{Q\} \tag{8.13}$$

The frequency response of the structural field is of form;

$$\left[K_s - \omega^2 M_s\right]\{w\} = \{q'\} \tag{8.14}$$

A link, described in Appendix 2, is formed between the structural and acoustical models to create the model of the sound transmission between rooms. Equations 8.13 and 8.14 are grouped into a global coupled system of equations;

$$\begin{bmatrix} K_s - \omega^2 M_s & C^t \\ C & K - \omega^2 M \end{bmatrix} \begin{Bmatrix} w \\ p \end{Bmatrix} = \begin{bmatrix} Q \\ q' \end{bmatrix} \tag{8.15}$$

where C is the geometrical coupling matrix

8.3   SCALE MODEL MEASUREMENT

8.3.1 Transmission rooms

157

Two enclosures of the same dimensions, (1.2 x 1.2 x 0.6m), and construction as the enclosure described in section 7.3.1 formed the quarter scale transmission room system. The model was placed in a transmission suite, where the background noise was low. Thick resilient foam was placed under the model to reduce vibration from the floor. A photograph of the model is shown in Figure 8.2.

Four microphone positions were selected. Microphone 1 (0.5,0.4,0.4) and 2 (0.8, 0.8, 0.2) were the same as in Chapter 7. The two microphone positions (4 and 5) in the receiving room had co-ordinates (1.6, 0.5, 0.4) and (1.9, 0.75, 0.2), respectively. The set up is shown in Figure 8.3. The frequency response was measured at the four calibrated microphones using the same set up as described in Chapter 7. The sound level difference was then calculated between position 1 and 4, positions 1 and 5, positions 2 and 4 and positions 2 and 5.

8.3.2 Party wall

Two perspex sheets of dimensions 1.430 x 0.830m and thickness 10mm and 5mm formed the party wall. Their material properties, were [Gibbs (1974)];

Young's Modulus. E: 5.610^9 N.m^{-2}

Material density, ρ: $1.2 \; 10^3$ kg.m^{-3}

Poisson's ratio: 0.4

Thickness, h: 5mm and 10mm

The plate was attached to the source room using wood screws distributed at 100mm centres along the perimeter. The two sides of the perspex panel were sealed with flexible mastic to prevent acoustic leaks.

As described in Chapter 2, party wall edge conditions affect the structural eigenfrequencies and the wall radiation. Measurements on a full-scale masonry wall showed that the edge conditions could be assumed to lie between simply supported and clamped. Simply supported is described by a rotational stiffness equal to zero, while the

clamped condition is defined by an infinite rotational stiffness. In both conditions, translational stiffness is infinite.

It is by no means straightforward to physically model the two conditions. Clamped conditions can be approximated by clamping the panel between two metallic strips using screws on each side [Balike (1994)] or by placing the panel between two demountable steel frames with screws [Gibbs et al (1987), Sung et al (1997)]. Whatever the method used for clamping the plate, the clamped condition was not fully provided, causing plastic deformation when too firmly clamped or allowing small displacements when not tight enough. Clamped design also has a higher chance of increasing the flanking transmission between the two rooms. The clamped conditions thus are not possible to simulate exactly [Balike (1994)].

Simply supported edges can be created by cutting a notch parallel to the edges and the plate beyond the notch is clamped [Gibbs (1987)]. The rotational stiffness, Λ, of the plate is defined as

$$\Lambda = \left(\frac{h_b}{h}\right)^3 \left(\frac{B}{\Delta l}\right) \tag{8.16}$$

where B is the bending stiffness of the plate at the notch, h_b and h are the thickness of the notch and of the plate respectively and Δl is the width of the notch (see Figure 8.4).

The rotational stiffness can also be expressed in terms of the unnotched plate stiffness, Λ', as

$$\Lambda' = \frac{\left(\frac{h_b}{h}\right)^3}{\Delta l} \tag{8.17}$$

The simply supported condition is approximated but with a finite rotational stiffness which can be determined. Moreover, simply supported condition design will not increase the flanking transmission. Due to the small thickness, the perspex panel was

notched on one side to a width of 200mm at the perimeter, and the two notches were of different depths. The first was 2mm deep for the 5mm perspex panel giving a rotational stiffness of 2.22×10^3 N and the second was 3mm deep for the 10mm sheet, giving a rotational stiffness of 7.50×10^3 N. The 10mm perspex can be seen in Figure 8.5, when the panel is fixed to the source room.

50 modes were calculated for the 5mm panel, with the first eigenfrequency at 19Hz and the highest eigenfrequency at 901Hz. 28 modes were processed for the 10mm panel. The first eigenfrequency was at 37Hz and the highest calculated at 921Hz. The first eigenfrequencies are therefore excited well below the frequency range of interest.

8.4 NUMERICAL MODEL

According to Section 7.4.1, each room was discretized into 12^3 elements. The party wall could only be linked to the rooms, when the structural mesh model matched the acoustical mesh model. Hence, the party wall was discretized into 12^2 elements.

Both the acoustic and the structural models were first defined using P3/Patran, and then exported into Sysnoise V5.3 [1996]. 180 acoustical modes i.e. 90 room modes in each enclosure were processed after having defined an infinite hard wall at position x = 1.2m, which is the position of the party wall (see Chapter 6). The frequency response was then obtained with a resolution of 1Hz from 100Hz to 800Hz after a point source was defined in the corner opposite to the party wall as seen in Chapter 7.

The structural FE model was defined in Sysnoise V5.3 at position x = 1.2m. 5mm and 10mm perspex sheets were defined, giving two structural models. Two different sets of eigenfrequencies were processed: 50 structural modes for the 5mm panel and 28 structural modes for the 10mm panel.

Once the acoustical and structural models were defined, the sound transmission between two rooms was modelled (see Figure 8.6). The faces at position x = 1.2m of the acoustic model was selected and linked to all elements of the structural model (See Appendix 2)

and a fluid-structural behaviour was created. The sound level was calculated at two field points in the source room and at two field points in the receiving room. The sound level difference was then calculated between the four field points to compare with that obtained from measurements on the scale model. A schematic diagram in Figure 8.7 presents a summary of the simulation of the transmission room.

8.5   VALIDATION

8.5.1 Frequency response of the receiving room

Figures 8.8 and 8.9 show the frequency response of the receiving room at position 4 for the 5mm panel and the 10mm panel, respectively. Both show alternating maxima and minima. The measured peaks correspond to the room modes, but the predicted peaks are emphasised more for the 10mm panel. The sound field behaves like in an enclosure of six hard surfaces. The sound field in the receiving room, like in the source room (see Chapter 7), is clearly non-statistical. The predicted frequency response displays more peaks and dips than the measured frequency response due to the structural modes. The simulation emphasises the effects of the structural modal characteristics on the sound field.

The measured and predicted frequency responses at positions 4 and 5 are compared by calculating the level difference (predicted - measured) in 1/12 octave band. The results are shown in Figure 8.10. As for the source room, the large differences are the results of small shifts in observed resonant frequency with respect to expected ones. The assigning sound power is not correct as well as the loudspeaker position. The acoustic absorption was not modelled. Some differences are also due to the presence of peaks corresponding to the structural modes, which are emphasised as no structural damping was modelled.

Overall, the measured and predicted frequency responses display a good agreement. The degree of agreement between predictions and measurements, is practically the same for the 5mm and 10mm panels. However, the simulation tends to overestimate the

frequency response for the same reasons given in Chapter 7 and overemphasises the contribution of the structural modes to the sound field of the receiving room.

8.5.2 Sound level difference

Measured and predicted sound level difference for a 5mm panel are shown in Figures 8.11-14. Each figure shows frequencies where the sound pressure level difference is negative, for example at 280Hz, 420Hz, 630Hz. These frequencies correspond to a strong acoustic-structural coupling creating a sound level greater in the receiving room than in the source room. This phenomenon is observed more often when sound pressure level difference is predicted. Thus, the effect of acoustic-structural coupling tends to be emphasised by the simulation, but the predicted and measured curves still show similar trends.

The sound level difference of the 10mm panel are shown in Figures 8.15-18. As with the 5mm panel, the predicted and measured sound level difference curves display similar trends. Doubling the thickness of the panel increases the measured sound pressure level difference and reduces the number of negative dips, except at 320Hz and 410Hz as seen on Figures 8.17 and 8.18. Those two frequencies correspond to two room modes excited in the source room and receiving room, giving rise to strong acoustic couplings.

The representation of the measured and predicted sound pressure level difference in narrow band shows good agreement, although the simulation emphasises the different couplings which take place between the acoustic fields and acoustic-structural fields. Increasing the thickness of the party wall reduces the number of couplings and the occurrence of negative sound pressure levels differences.

The sound level differences for the two panels were calculated for microphone positions 2 and 5 with a 1/12 octave band resolution, shown in Figures 8.19-20. The presentation of sound level difference in a 1/12 octave band is the sum of many sound level difference data in each band which results in better agreement between the simulation

and the measurements than the narrow band resolution shows. Figures 8.21-22 show the sound level difference between the averaged sound level of microphones 1 and 2 and the averaged sound level of microphone positions 4 and 5 to decrease the effects of sound level fluctuations taking place in the two enclosures. Again, large discrepancies are the result of often quite small shifts in observed with respect to expected resonant frequencies, but the differences between measurements and prediction of the 10mm panel tend to be smaller than that of the 5mm panel. This is the result of the prediction which emphasises the structural resonances.

As in real measurements, the data are commonly presented in 1/3 octave bands. The sound level difference was calculated with a 1/3 octave band resolution, for all the microphone positions in combination, for the 5mm and 10mm panels. The results are shown in Figures 8.23-30. It is observed that for both panels, the signature of the sound level difference curves change with the microphone combinations. This observation again highlights the non-diffusitivity of the sound field inside the source room and of the receiving room. Alternating maxima and minima are cancelled because there are averaged in each third octave band. The predicted and measured sound level difference displays similar trends for any microphone combination, whatever the thickness of the panel.

Figures 8.31-32 present the sound level difference between the averaged sound levels of microphones 1 and 2 and the averaged sound levels of microphones 4 and 5 for the 5mm and 10mm panels. Again, the measurements overestimate the sound level difference. The overall discrepancy between the predicted and measured sound level differences of the 10mm panel is about 4dB. However, the discrepancy obtained for the 5mm panel is 6dB. That difference is explained by emphasised predicted couplings when the party wall is 5mm and by the edge conditions of the perspex which are more rigid than the predicted. Despite such differences, there is generally good agreement.

The discrepancies obtained for the 5mm and 10mm panels are compared by presenting the discrepancy of the 5mm and 10mm panels obtained between positions 1 and 4 (see Figure 33); between positions 2 and 5 (see Figure 8.34); and between the averaged positions 1 & 2 and 4 & 5 (see Figure 8.35). Figure 8.33 displays the same trend with a

discrepancy of 2-3dB, between the 5mm and 10mm panels. However, the discrepancy increases to 4-5dB (see Figure 8.34) due to emphasised acoustic and acoustic-structural couplings. Figure 8.35 shows that when positions are averaged, the discrepancy between the two curves is about 3-4dB. The effect of emphasised peaks and dips recorded in the narrow band frequency response tends to average out. The tendency of the prediction, also, is to underestimate the sound level difference by less than 5dB except at 640Hz, where its increases to 14dB due to an insufficient number of elements in the numerical model.

The presentation of the sound level difference in 1/12 and 1/3 octave bands shows that peaks and dips are less obvious than for the narrow bands. Similarly for average sound level difference calculated for two microphone positions in each room. That explains why many authors [Utley (1968), Osipov (1997)] show that the presentation of the sound insulation at low frequencies in octave bands improves the repeatability of the measurements.

To summarise; the numerical model was validated by comparing the predicted and measured frequency response of the receiving room at two positions. The predicted response was found to overestimate the frequency response as expected. That is caused by the same reasons given for the numerical enclosure model. However, extra peaks and dips due to panel resonances are emphasised causing also an overestimation of the frequency response. The predicted sound pressure level difference was then compared with the measured one. Good agreement was obtained between measurement and simulation irrespective of the party wall thickness. Better agreement is obtained when the measured or predicted frequency responses at the two microphones in the source room or in the receiving room are averaged. Averaging indeed tends to make less obvious the peaks and dips.

The good agreement between the predicted and measured sound pressure level difference means that the errors responsible for the overestimation of the sound field, identified in Chapter 7 are found to cancel each other when the sound pressure level difference is calculated. However, the tendency of the simulation is to underestimate the sound pressure level difference by 4-8dB. As seen in Section 8.3.2, a simply supported

edge condition was difficult to model physically. However, the rotational stiffness of the 5mm panel is closer to zero than that of the 10mm panel. When the structural model was defined into Sysnoise, the rotational stiffness was assumed zero. Consequently, the real edge conditions are stiffer, giving a measured sound level difference greater than the predicted sound level difference.

8.6 CONCLUDING REMARKS

The Finite Element Method simulation was validated by comparing the predicted and measured frequency response of a single room. The simulation was found to overestimate the sound field because no surface or air absorption was included. Moreover, the simulation emphasises the structural resonances. The FEM model was then validated by comparing predicted and measured sound level difference between two rooms. The effects of the incorrectly assigned power to the point source and the assumed zero acoustic damping cancel each other by calculating the sound level difference. However, the predicted sound level difference was found to be underestimated compared to the measured sound level difference by 4-8dB, except at 640Hz where it is 14dB. That was caused by the edge conditions of the panel, which are stiffer that those defined in the numerical model. Despite that, the choice of Finite Element model for the coupled room model was validated. The effect of room configuration on the sound level difference of masonry walls can now be investigated.

8.7 REFERENCES

Balike, M., Bhat, R.B. and Rakheja, S., (1994): *'Noise transmission through a cavity backed flexible plate with elastic edge constraints'*, Third international Congress on Air-and Structure-Borne sound and vibration, June 13-15, Canada, 335-343

Beranek, L.L. and Ver, I.L., (1992): *'Noise and Vibration Control Engineering: Principles and Applications'*, Ed. J.Wiley and Sons

Fahy, F., (1985): *'Sound and Structural Vibration: Radiation, Transmission and Response'*, Ed.Academyc Press

Gargliadini, L., Roland, J. and Guyader, J. L., (1991): *'The used of functional basis to calculate acoustic transmission between two rooms'*, Journal of Sound and Vibration, Vol.145 (3), 457-478

Gibbs, B.M., (1974): *'The direct and indirect transmission of vibrational energy in building structures'*, PhD thesis at University of Birmingham

Gibbs, B.M. and Shen, Y., (1987): *'The predicted and measured bending vibration of an L-combination of rectangular thin plates'*, Journal of Sound and Vibration, Vol.112 (3), 469-485

Johansson, C. and Shi, W., (1996): *'Experimental determination of reverberation time for low frequencies in an impact sound laboratory'*, Proceeding of Inter-Noise 96, 1779-1782

Josse, R. and Lamure, C., (1964): *'Transmission du son par une paroie simple'*, Acustica, Vol.14, 266-280

Mulholland, K.A. and Lyon, R.H., (1973): *'Sound insulation at low frequencies'*, Journal of Acoustical Society of America, Vol.54 (4), 867-878

Nilsson, A.C., (1972): *'Reduction index and boundary condition for a wall between two rectangular rooms; Part I: Theoretical Results'*, Acustica, Vol.26, 1-18

Osipov,A., Mees, P., and Vermeir, G., (1997-a): *'Low frequency airborne sound transmission through single partitions in Buildings'*, Applied Acoustics, Vol.52 (3-4), 273-288

Sung, C.C. and Jan, J.T., (1997): *'The response of sound power radiated by a clamped rectangular plate'*, Journal of Sound and Vibration, Vol.207 (3), 301-317

Sysnoise, (1996): Software Package V5.3, NIT

Utley, W.A., (1968): '*Single leaf transmission loss at low frequencies*', Journal of Sound and Vibration, Vol.8, 256
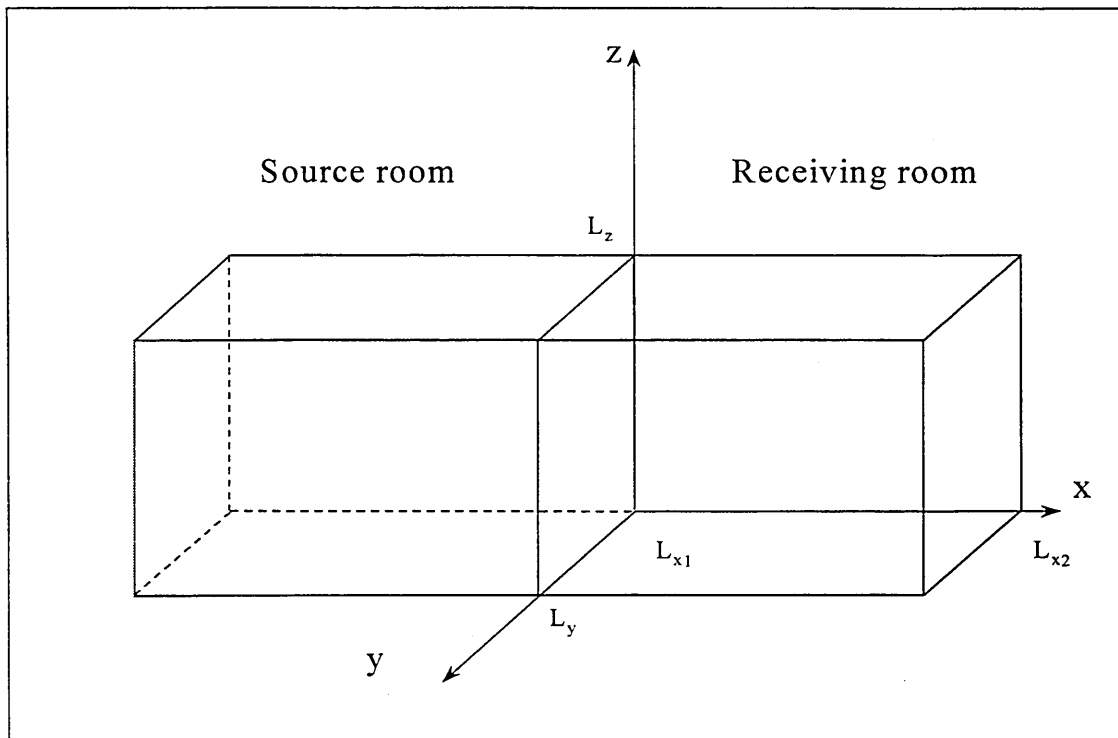
Figure 8.1. The sound transmission room
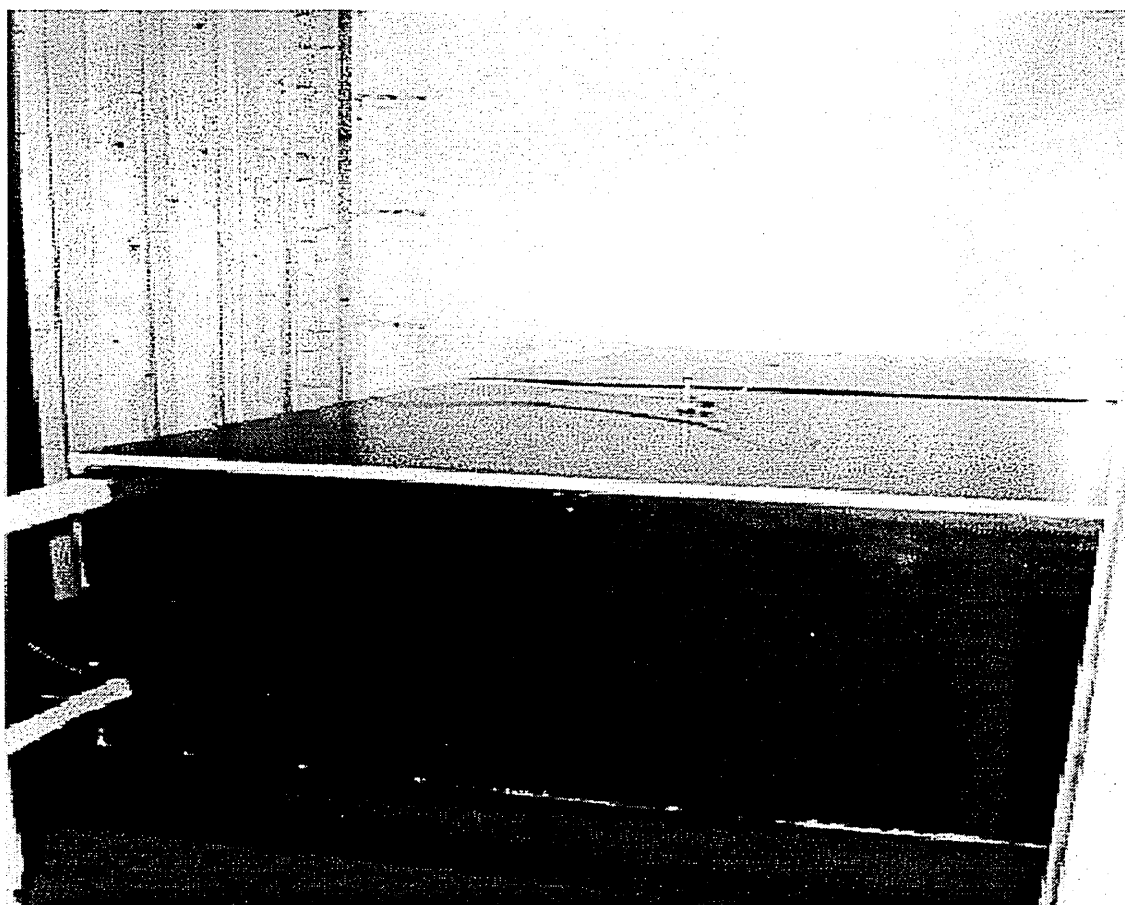
Figure 8.2. The 1:4 scale transmission room model
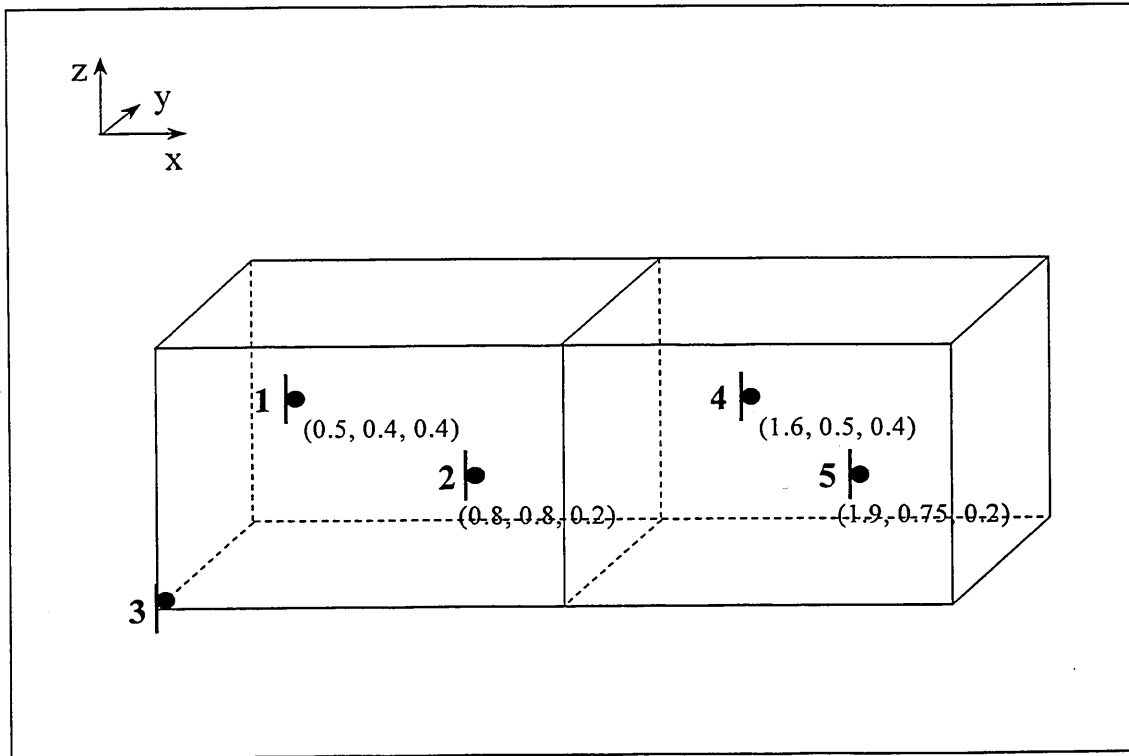
Figure 8.3. Microphone positions in the transmission rooms
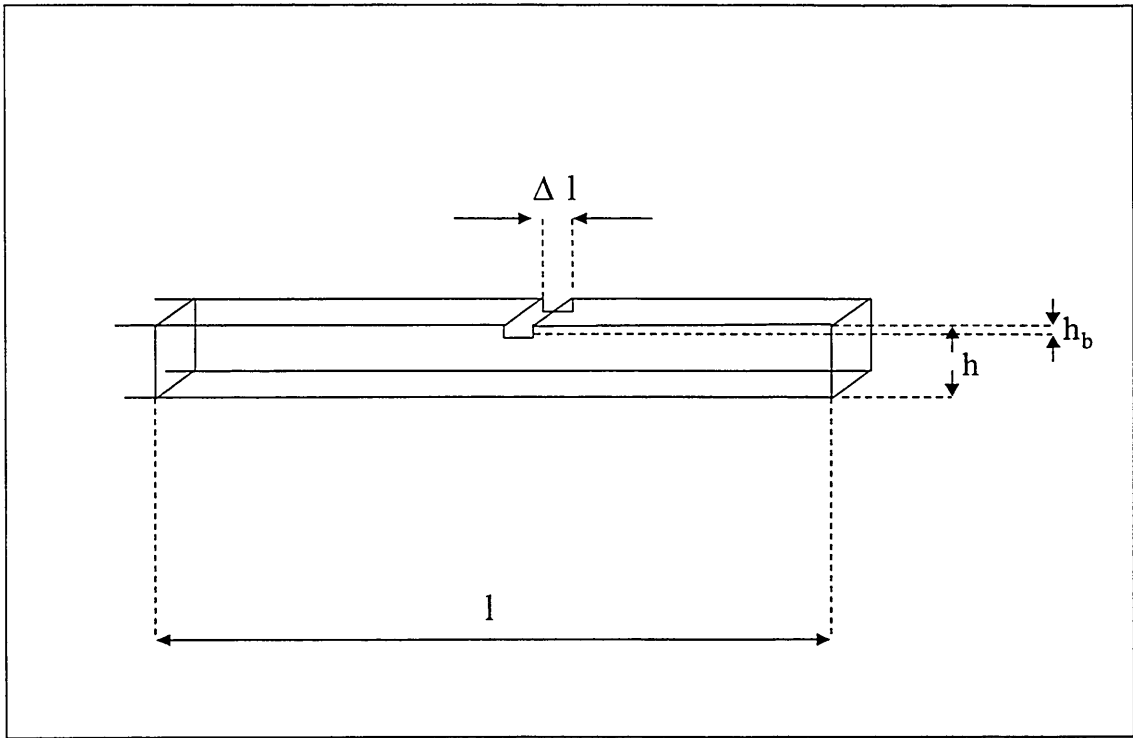
Figure 8.4. Edge notched

Figure 8.5. Picture of the edge notched

170
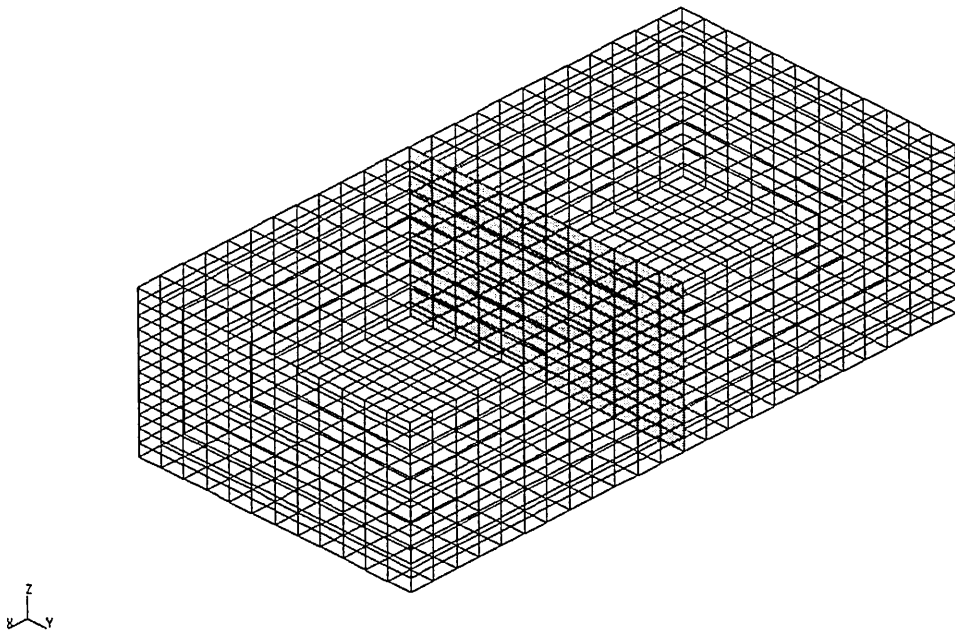
Figure 8.6. Model of the transmission rooms
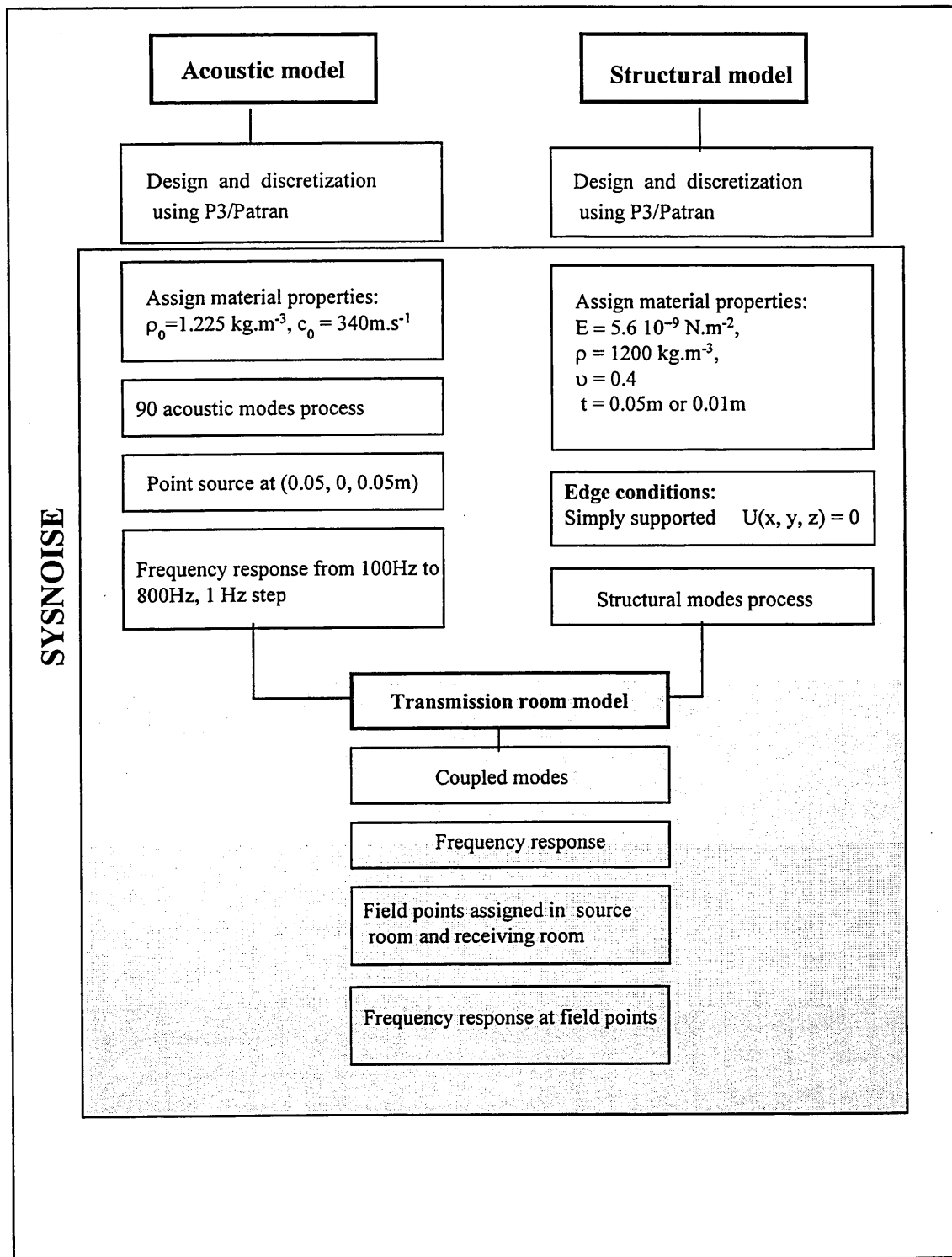
Figure 8.7. Schematic of the simulation
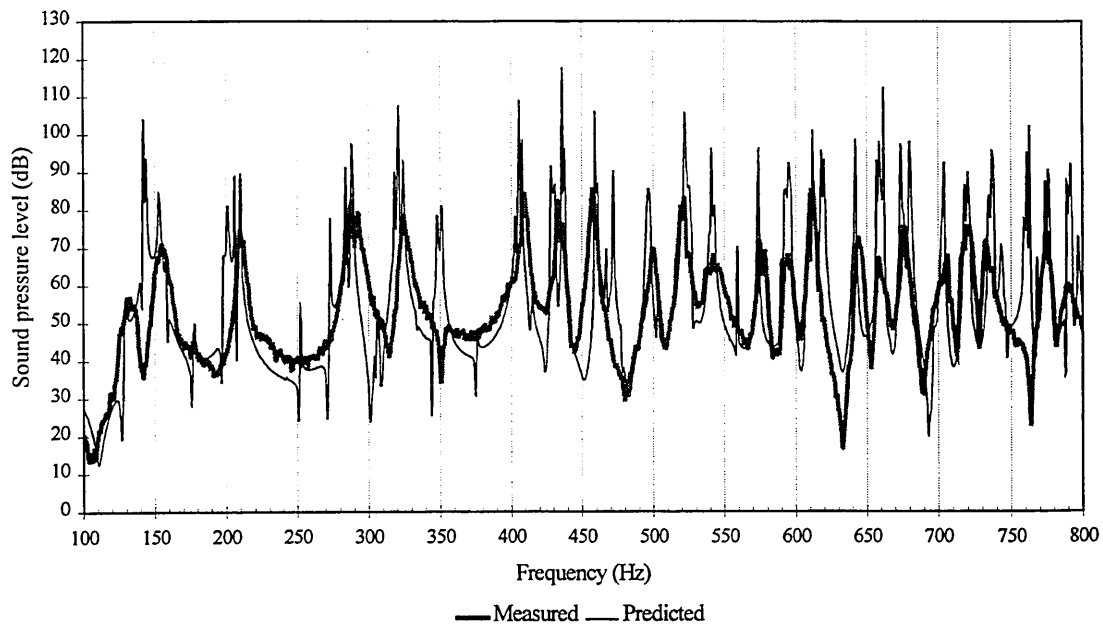
Figure 8.8. Measured and predicted frequency response of the 5mm panel at position 4
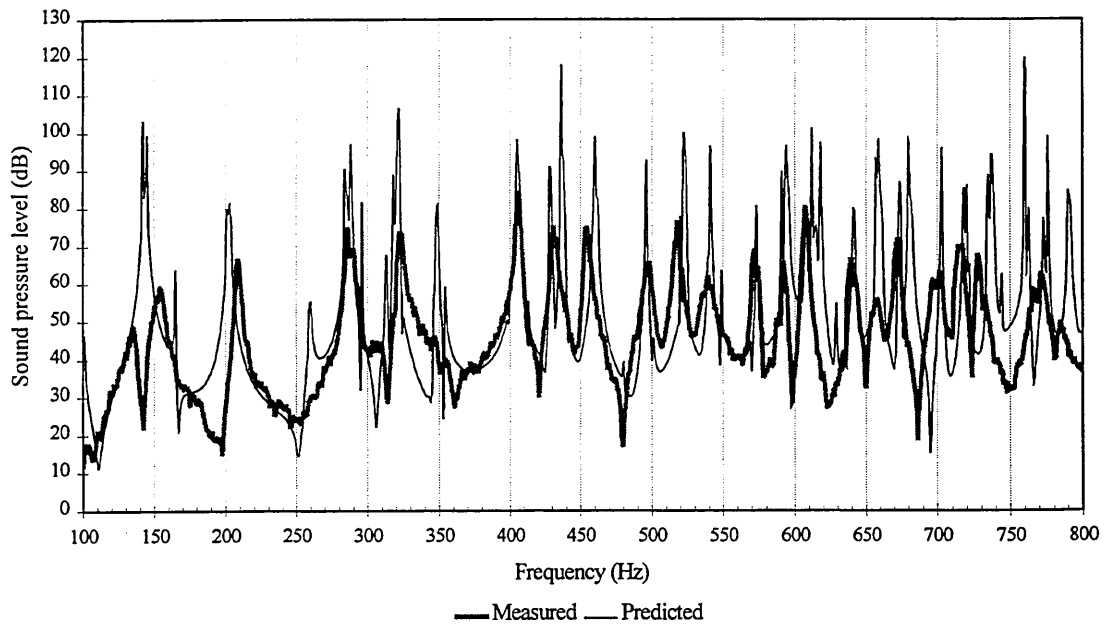
Figure 8.9. Measured and predicted frequency response of the 10mm panel at position 4

173
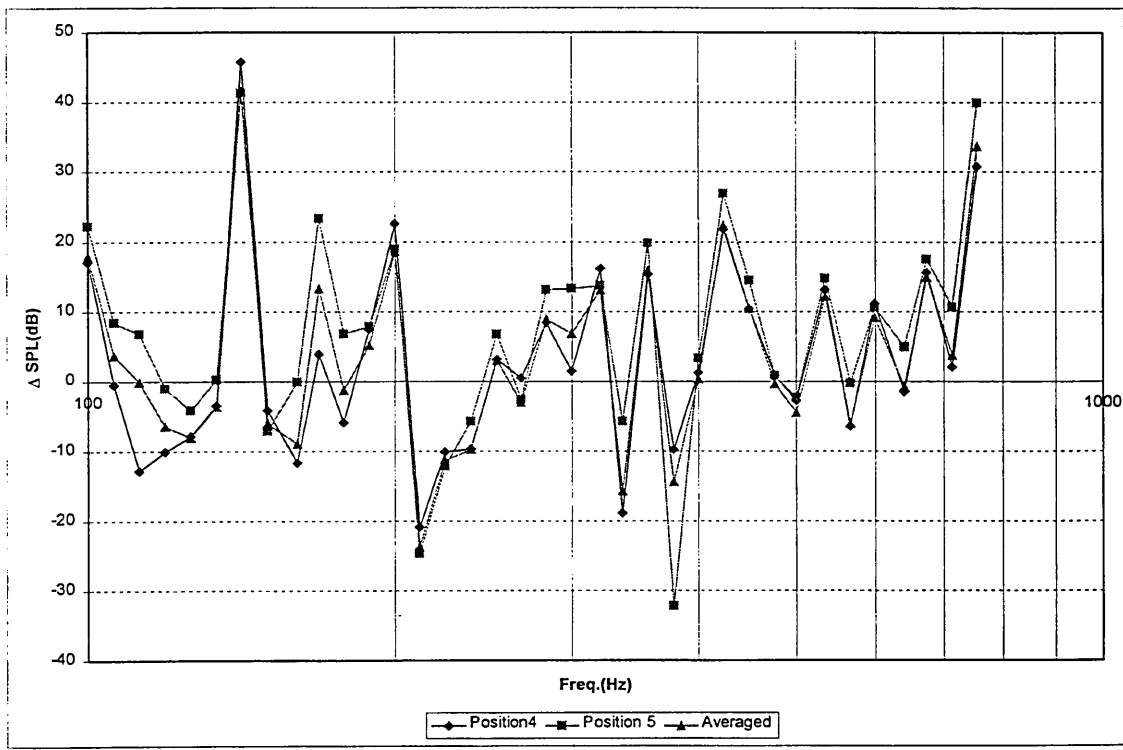
Figure 8.10. Comparison of predicted and measured sound level difference in 1/12 octave bands
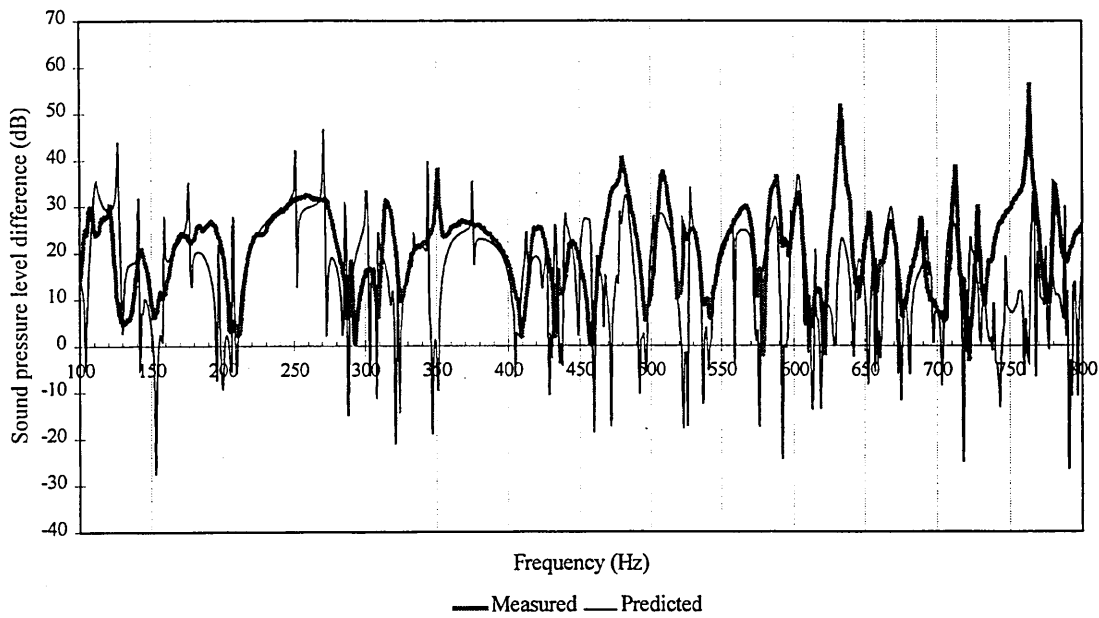
Figure 8.11. Sound pressure level difference between positions 1 and 4 of the 5mm panel
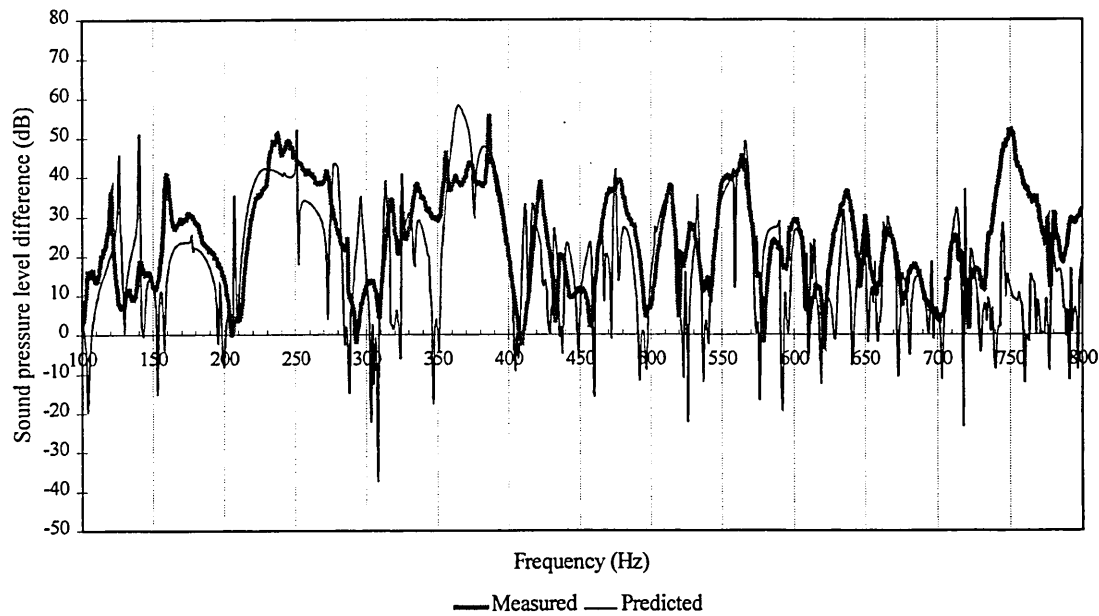
Figure 8.12. Sound pressure level difference between positions 1 and 5 of the 5mm panel
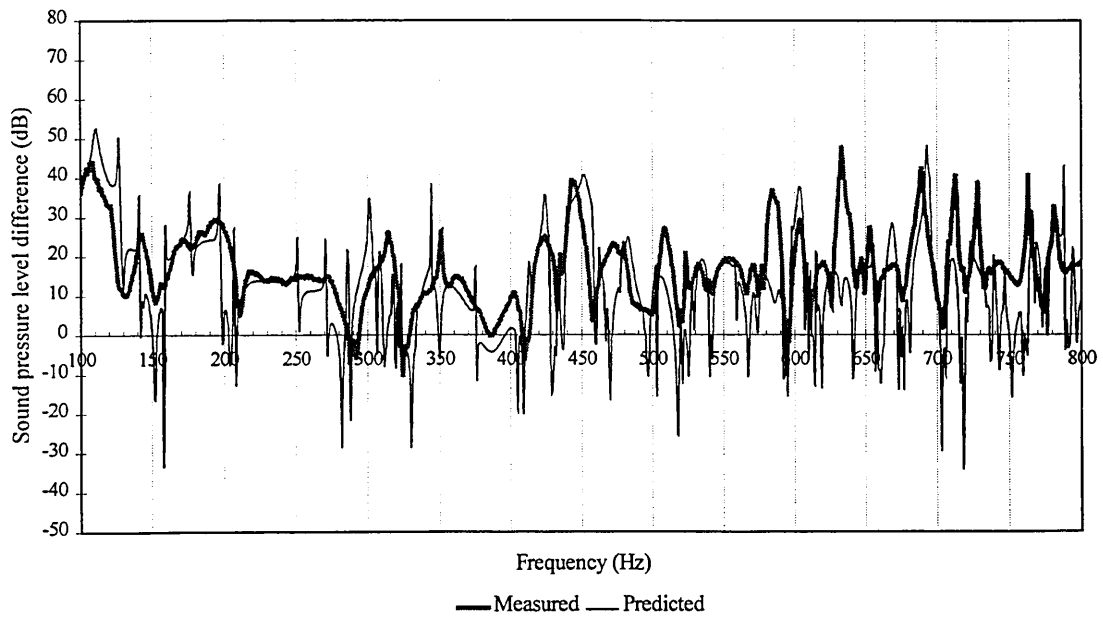
Figure 8.13. Sound pressure level difference between positions 2 and 4 of the 5mm panel
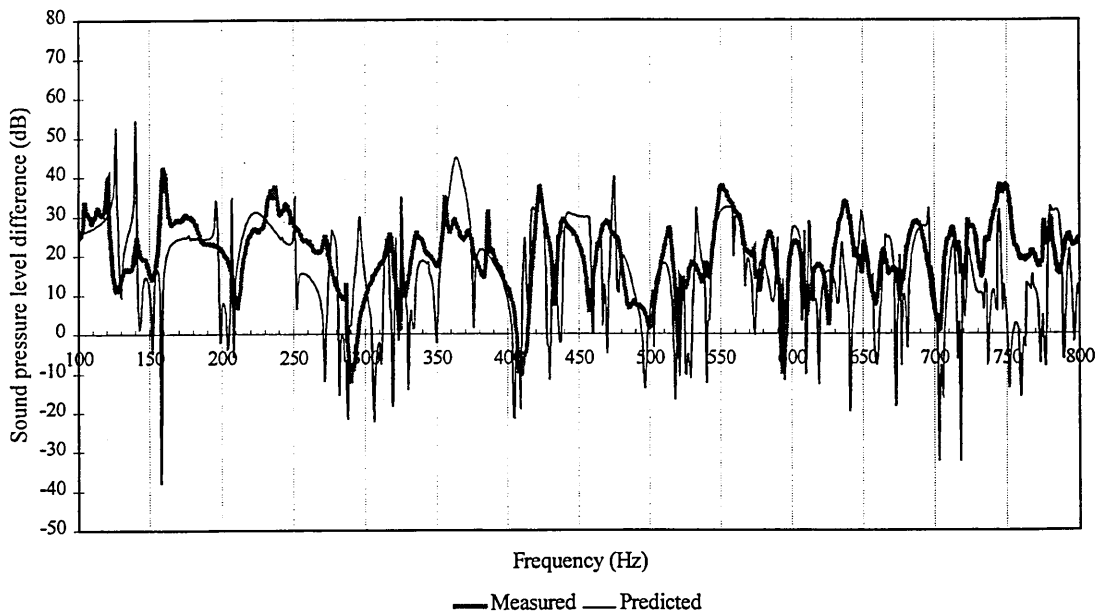
Figure 8.14. Sound pressure level difference between positions 2 and 5 of the 5mm panel

176
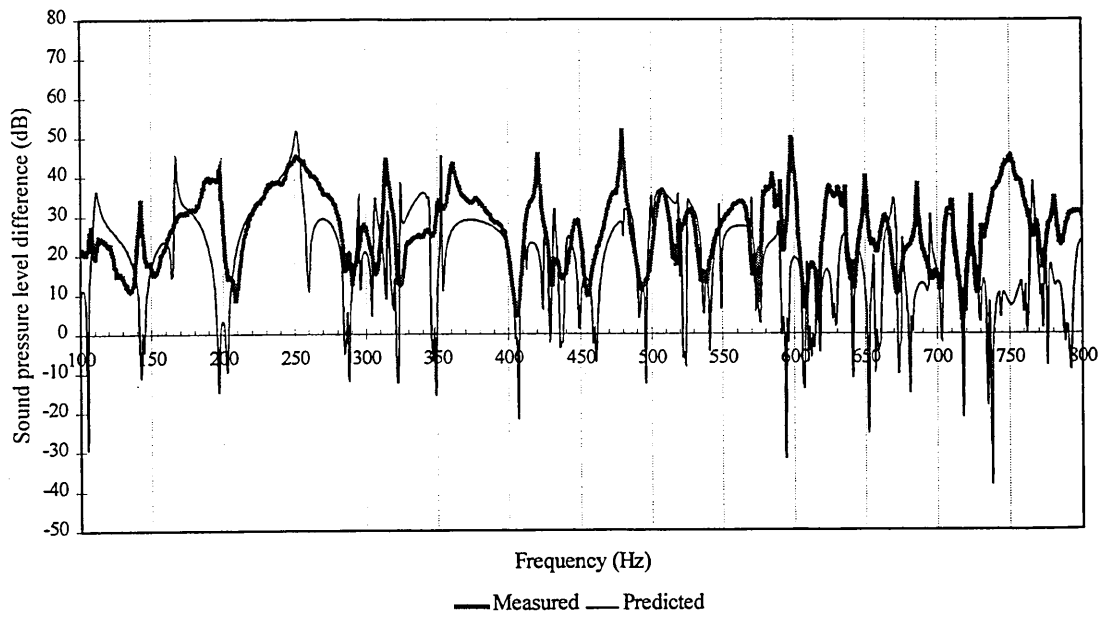
Figure 8.15. Sound pressure level difference between positions 1 and 4 of the 10mm panel
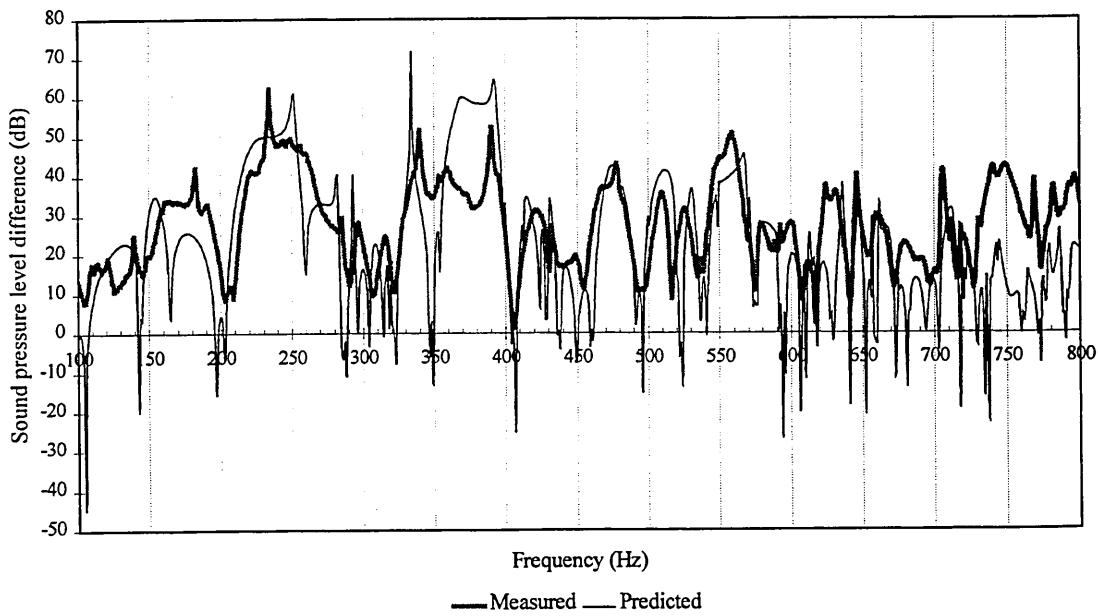
Figure 8.16. Sound pressure level difference between positions 1 and 5 of the 10 mm panel
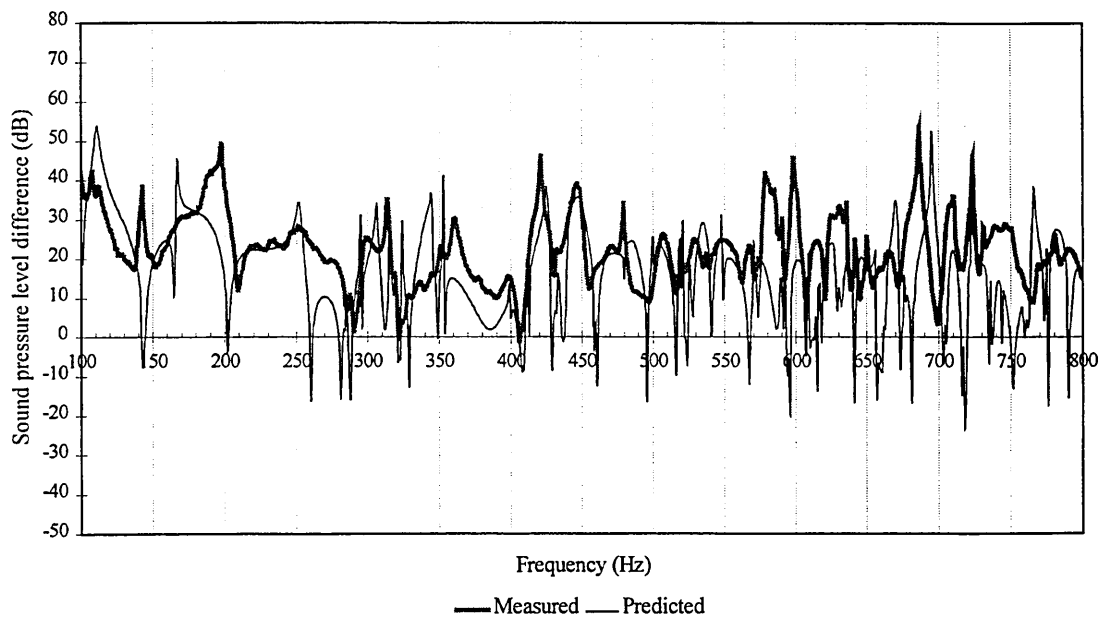
Figure 8.17. Sound pressure level difference between positions 2 and 4 of the 10mm panel
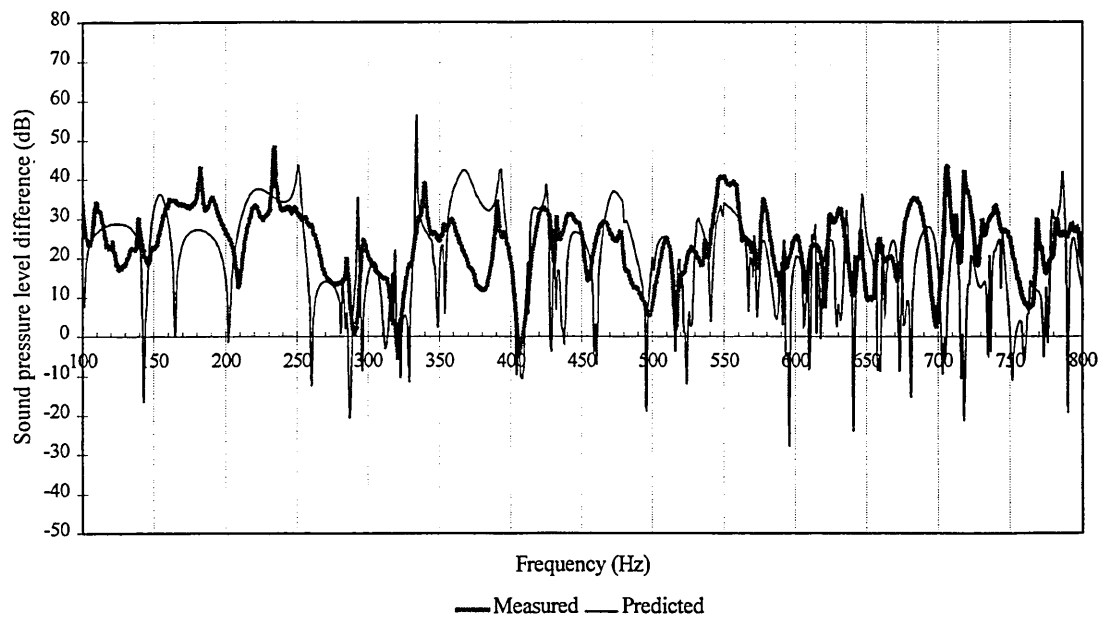
Figure 8.18. Sound pressure level difference between position 2 and 5 of the 10 mm panel

178
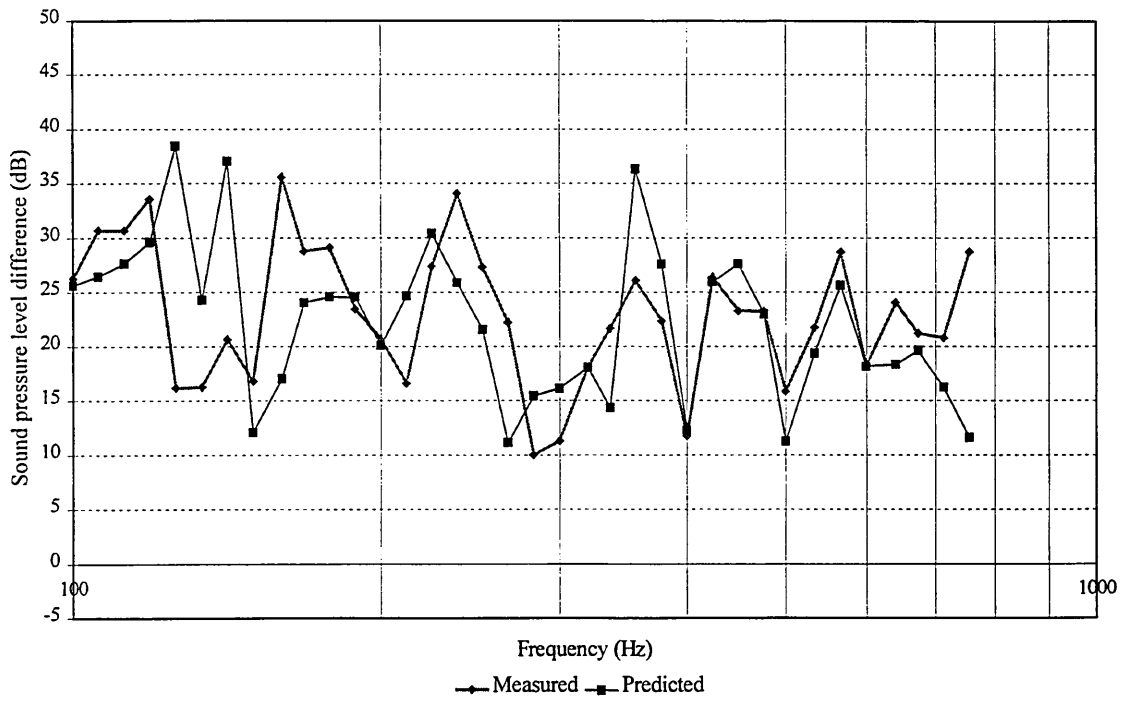
Figure 8.19. Sound level difference between positions 2 and 5 of a 5mm perspex panel in a 1/12 octave band
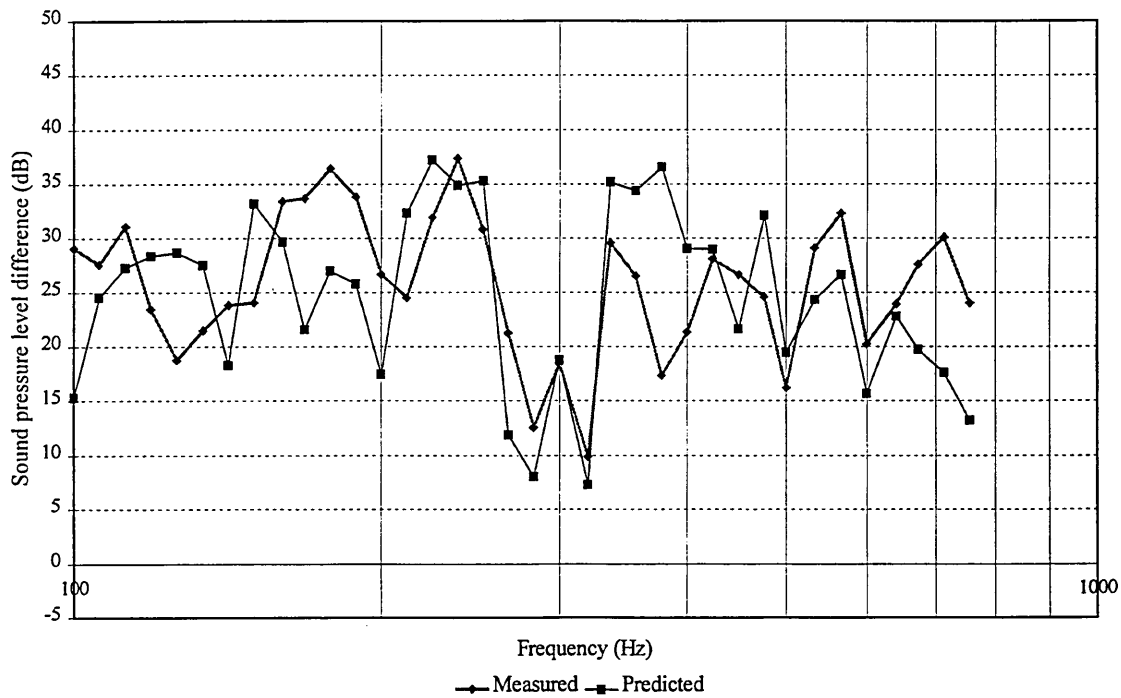
Figure 8.20. Sound level difference between positions 2 and 5 of a 10mm perspex panel in a 1/12 octave band

179
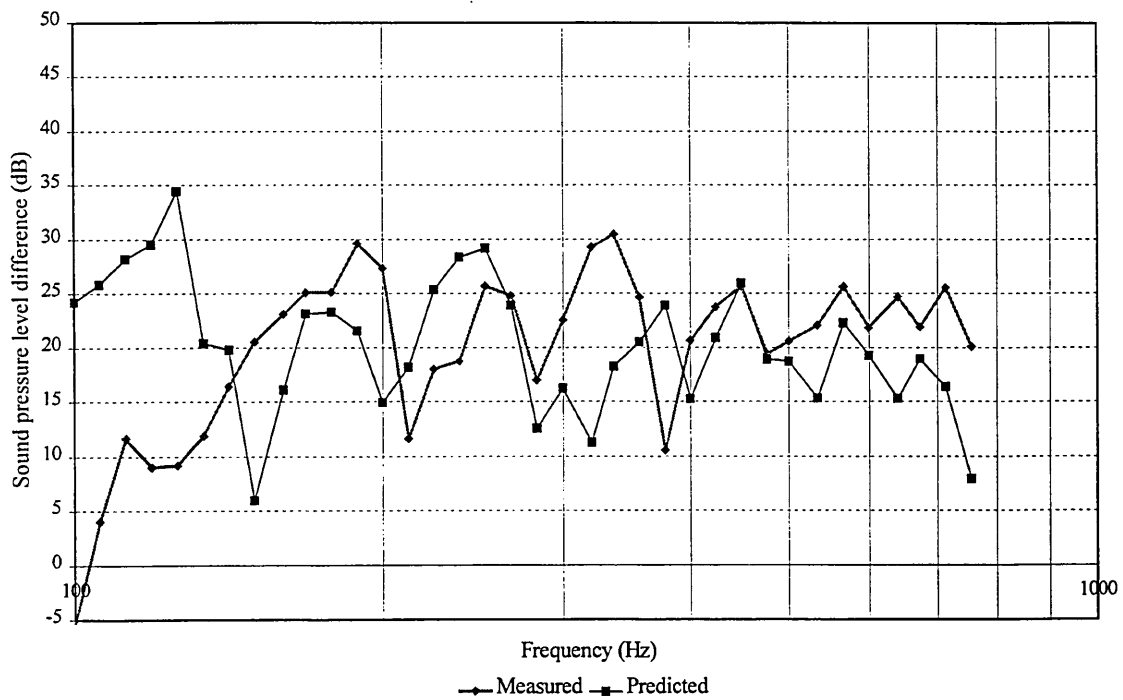
Figure 8.21. Sound level difference between averaged positions of a 5mm panel in a 1/12 octave band
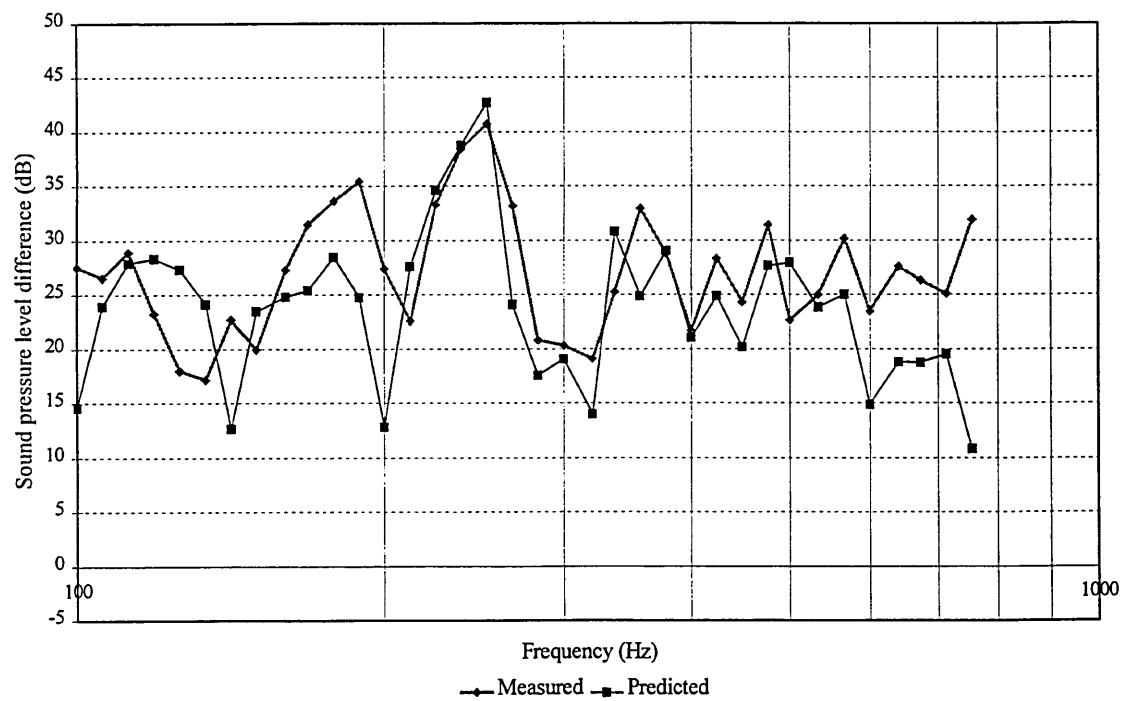
Figure 8.22. Sound level difference between averaged positions of a 10mm panel in a 1/12 octave band
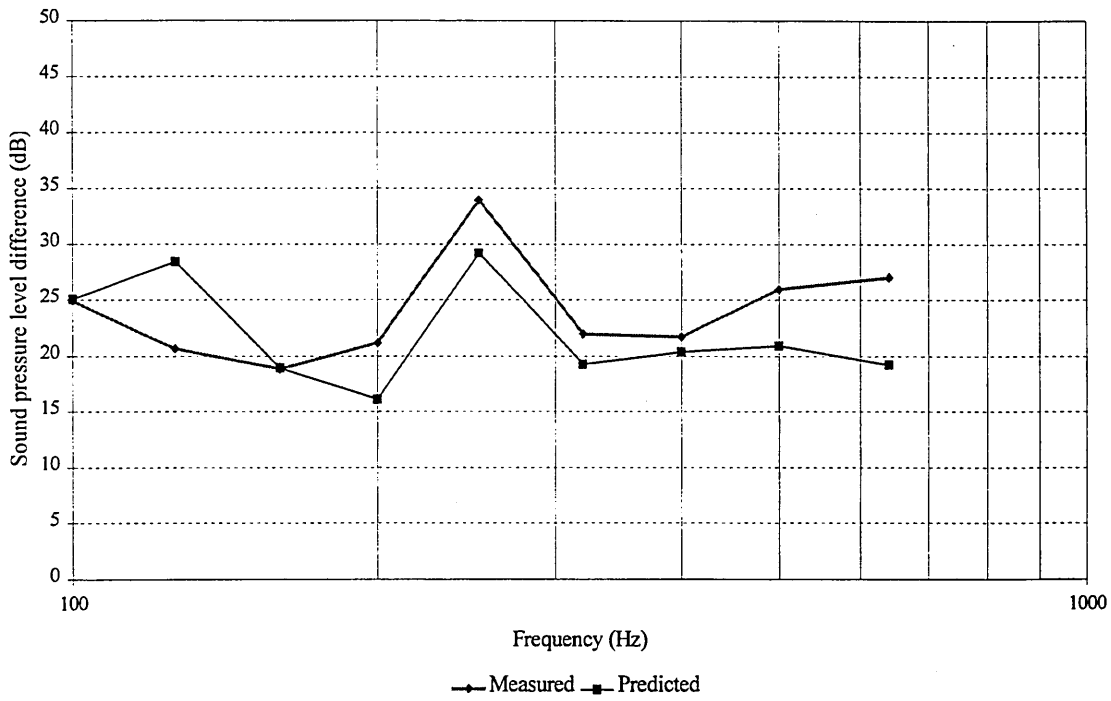
Figure 8.23. Sound pressure level difference between positions 1 and 4 of a 5mm panel in 1/3 octave bands
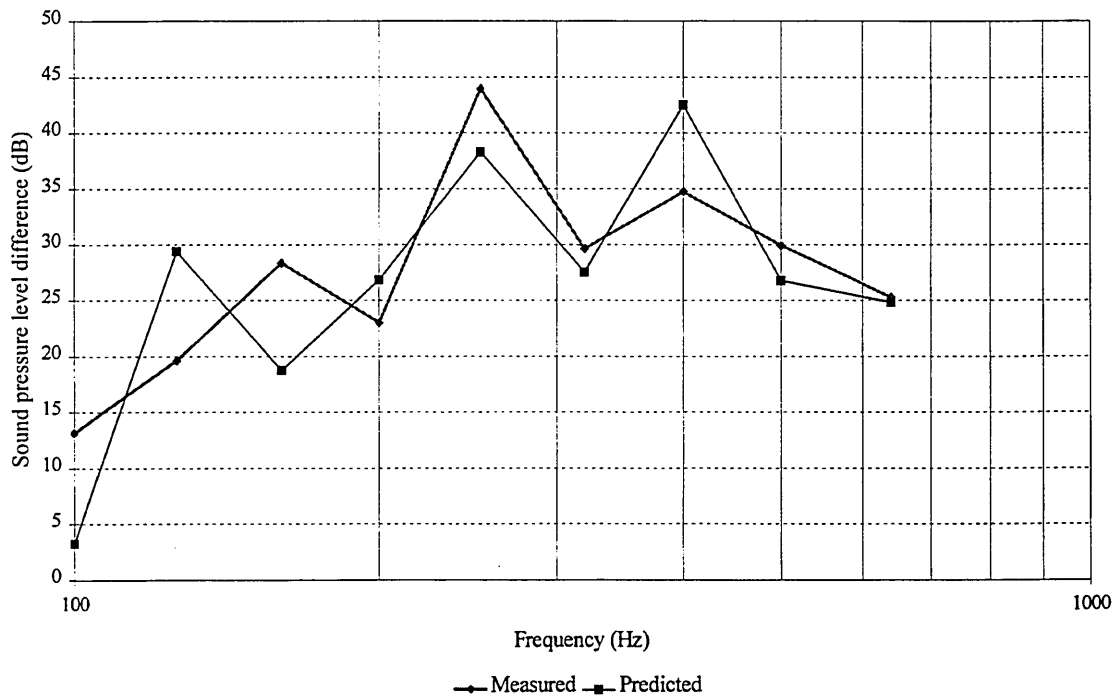
Figure 8.24. Sound pressure level difference between positions 1 and 5 of a 5mm panel in 1/3 octave bands
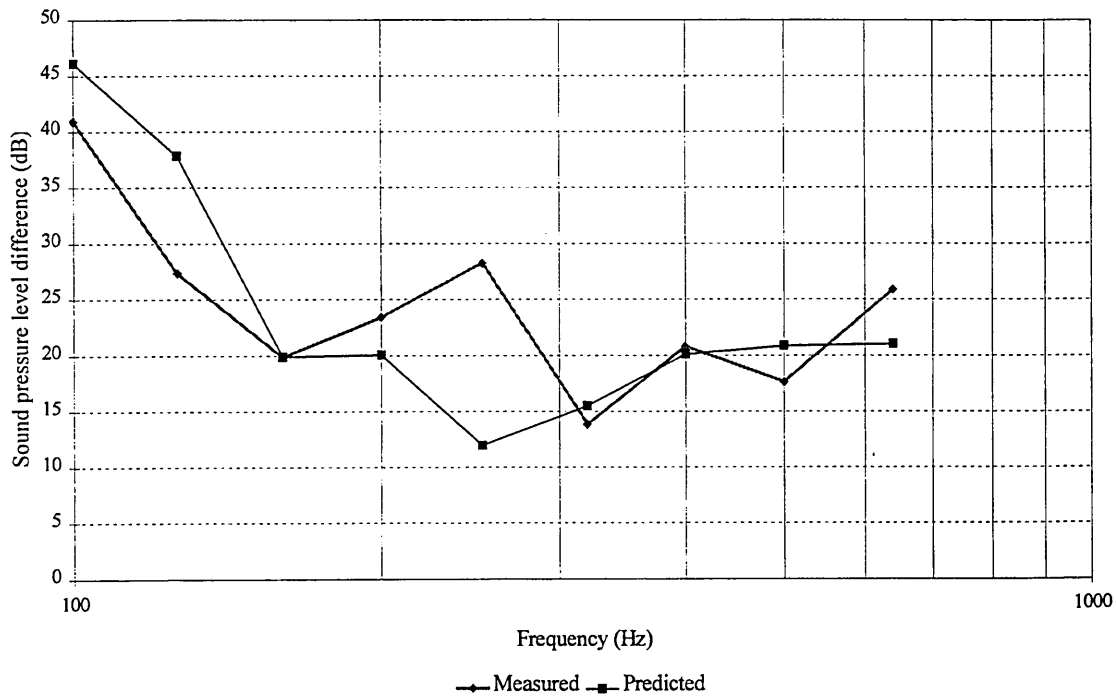
Figure 8.25. Sound pressure level difference between positions 2 and 4 of a 5mm panel in 1/3 octave bands
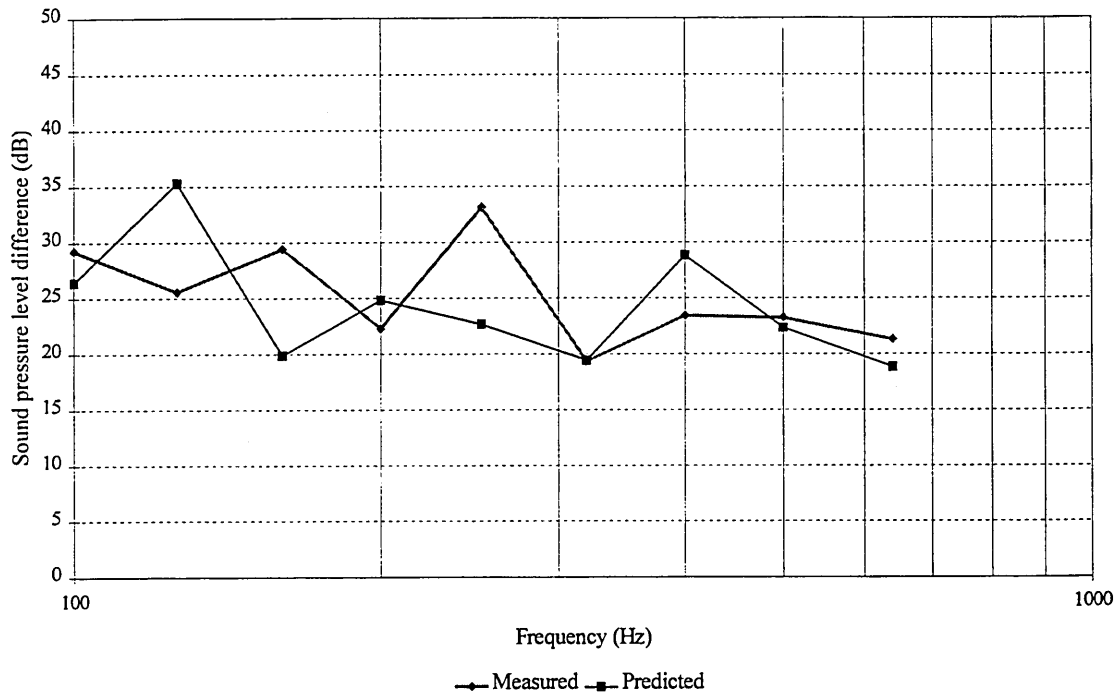
Figure 8.26. Sound pressure level difference between positions 2 and 5 of a 5mm panel in 1/3 octave bands
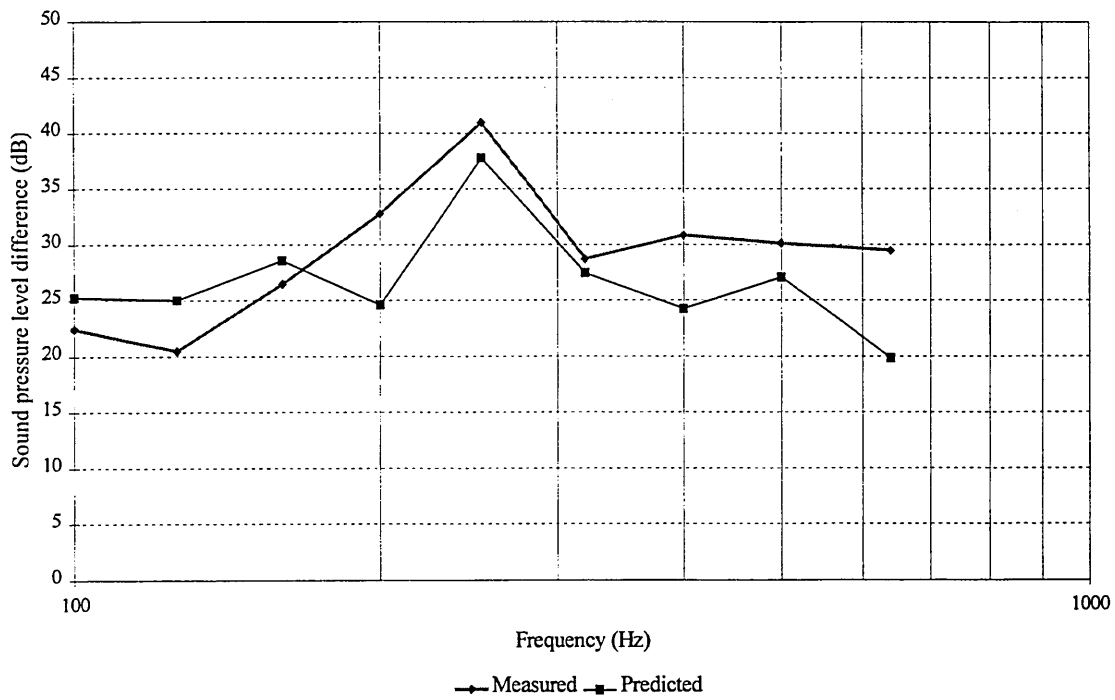
Figure 8.27. Sound pressure level difference between positions 1 and 4 of a 10mm panel in 1/3 octave bands
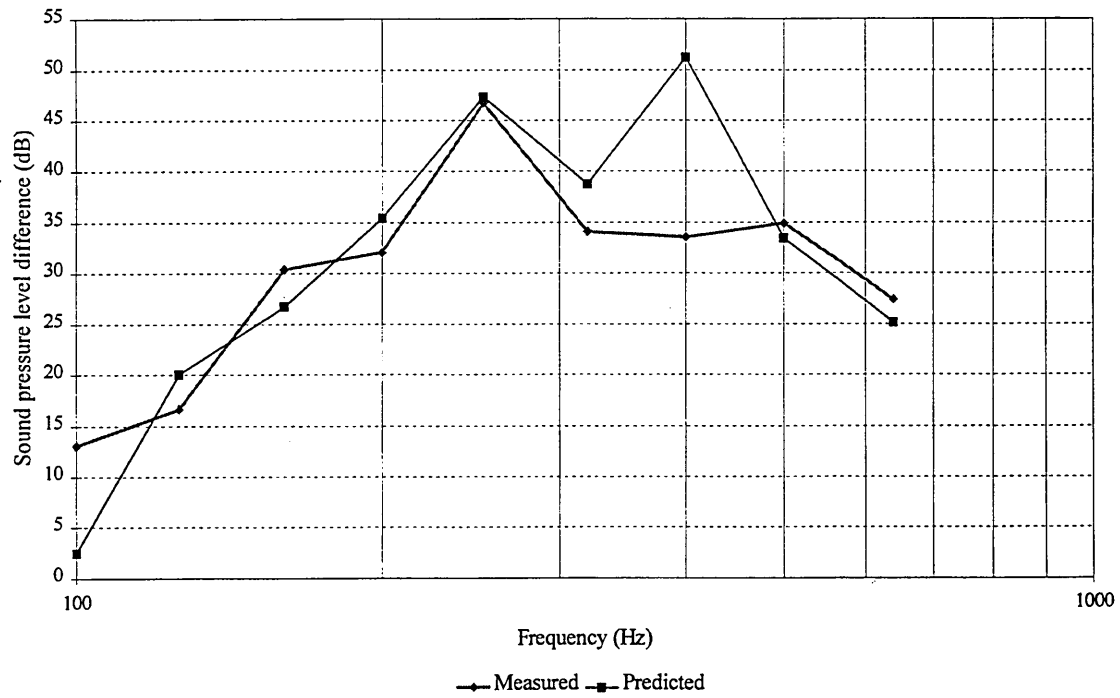
Figure 8.28. Sound pressure level difference between positions 1 and 5 of a 10mm panel in 1/3 octave bands

183
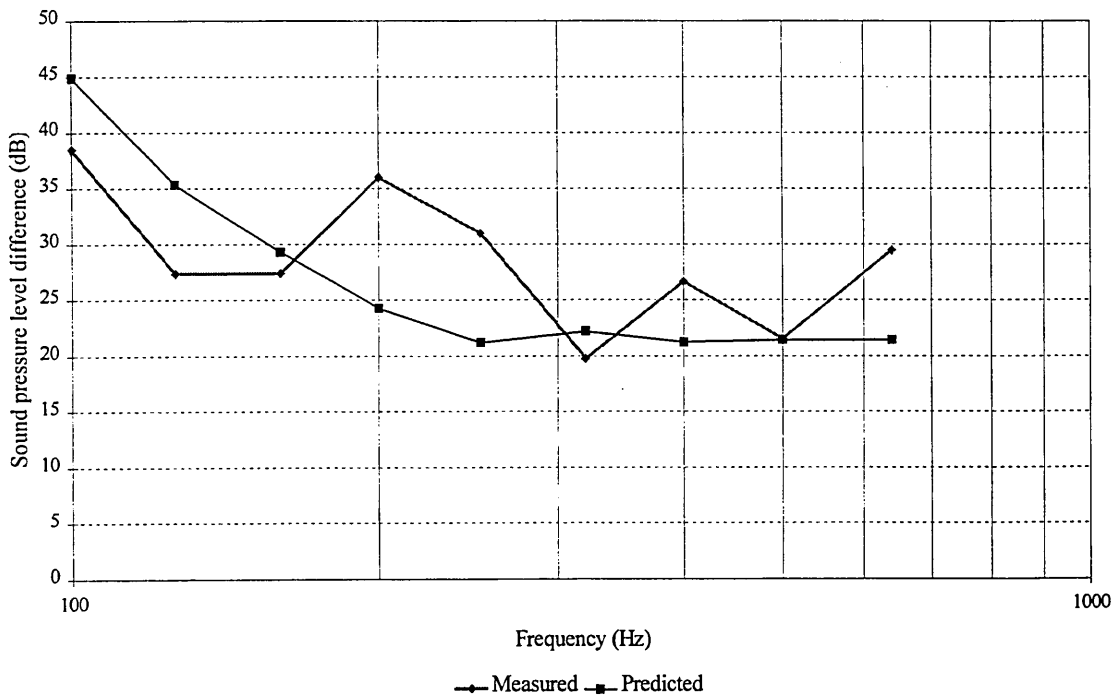
Figure 8.29. Sound pressure level difference between positions 2 and 4 of a 10mm panel in 1/3 octave bands
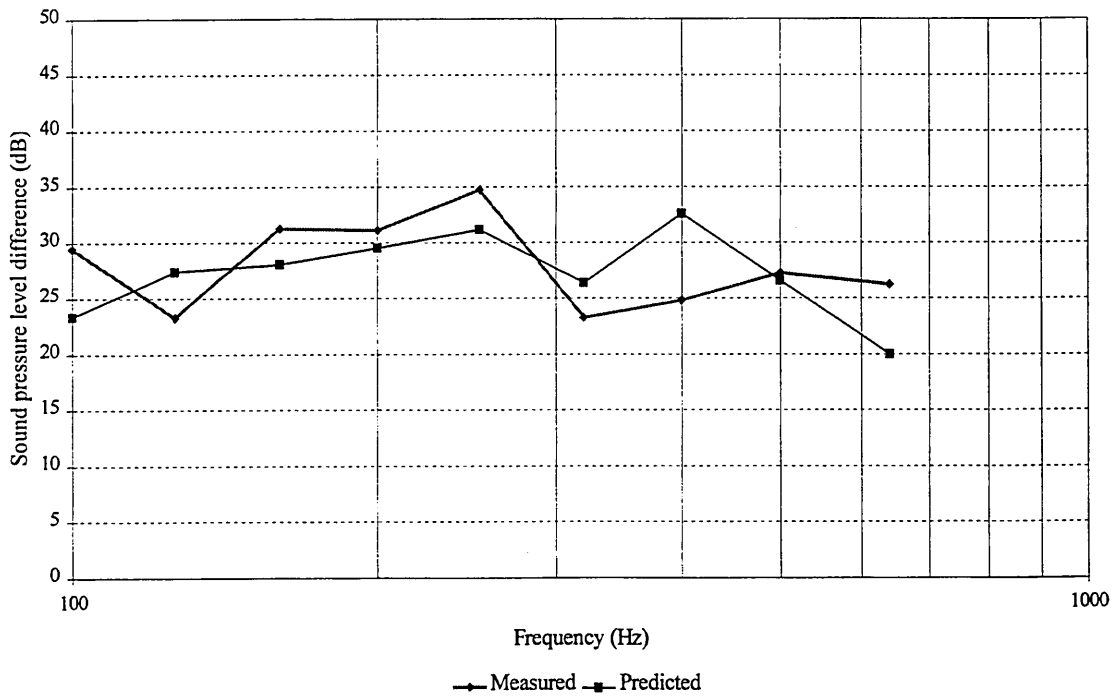
Figure 8.30. Sound pressure level difference between positions 2 and 5 of a 10mm panel in 1/3 octave bands
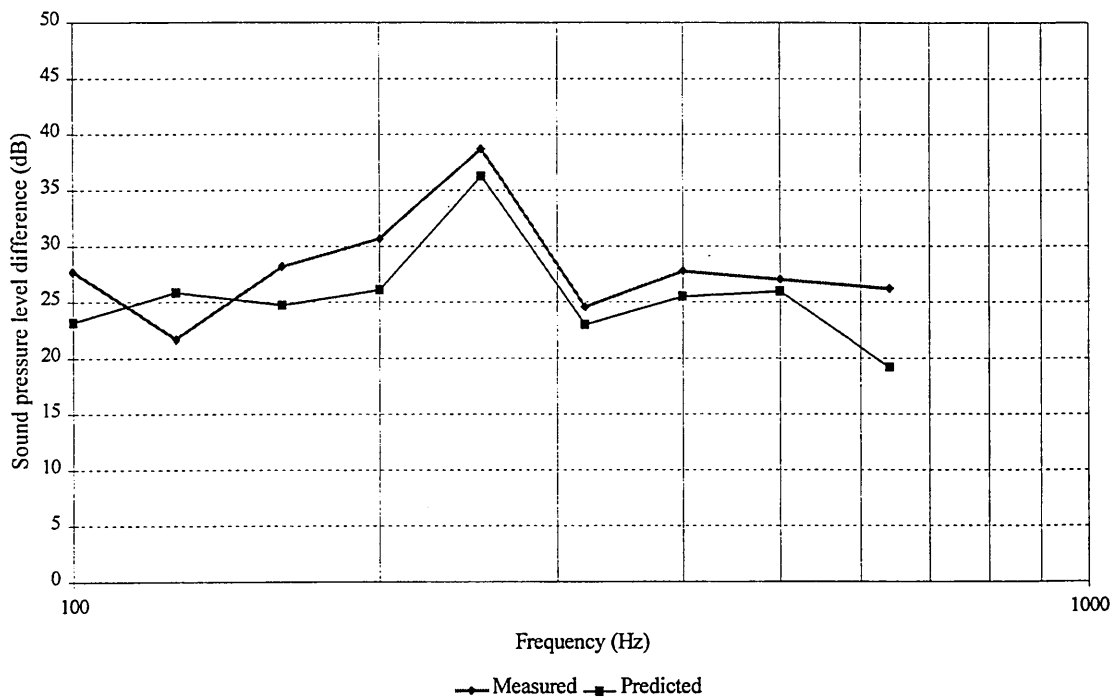
Figure 8.31. Sound pressure level difference between averaged positions of a 10mm panel in 1/3 octave bands
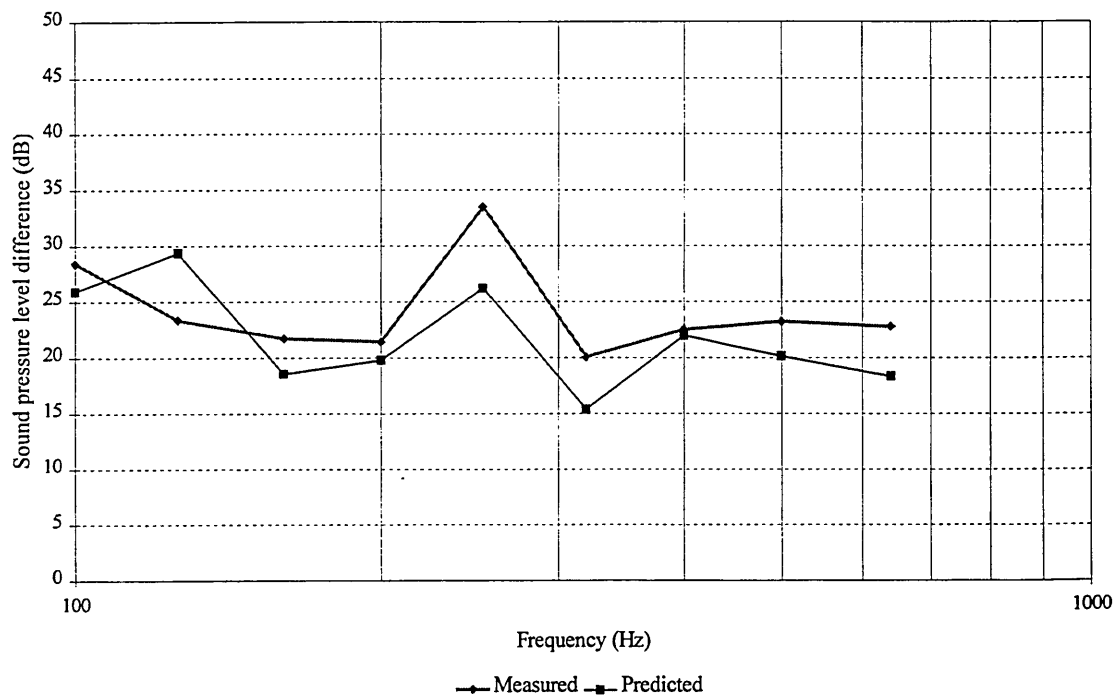
Figure 8.32. Sound pressure level difference between averaged positions of a 5mm panel in 1/3 octave bands

185
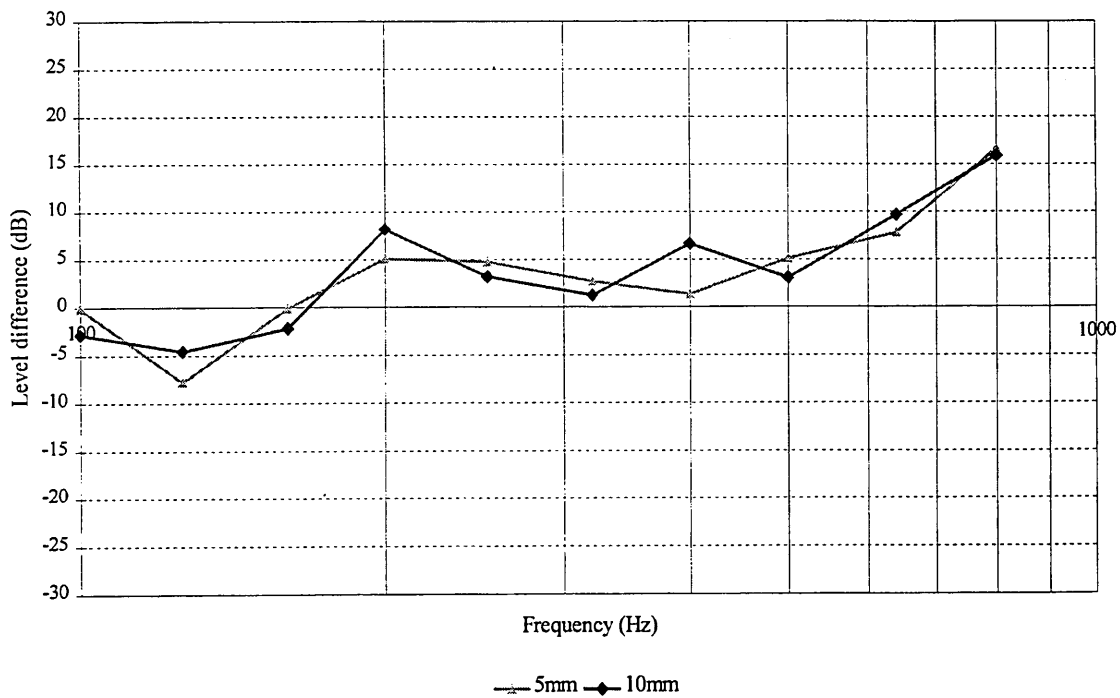
Figure 8.33. Positions 1 and 4: Measured sound pressure level difference compared with predicted level difference in a 1/3 octave band
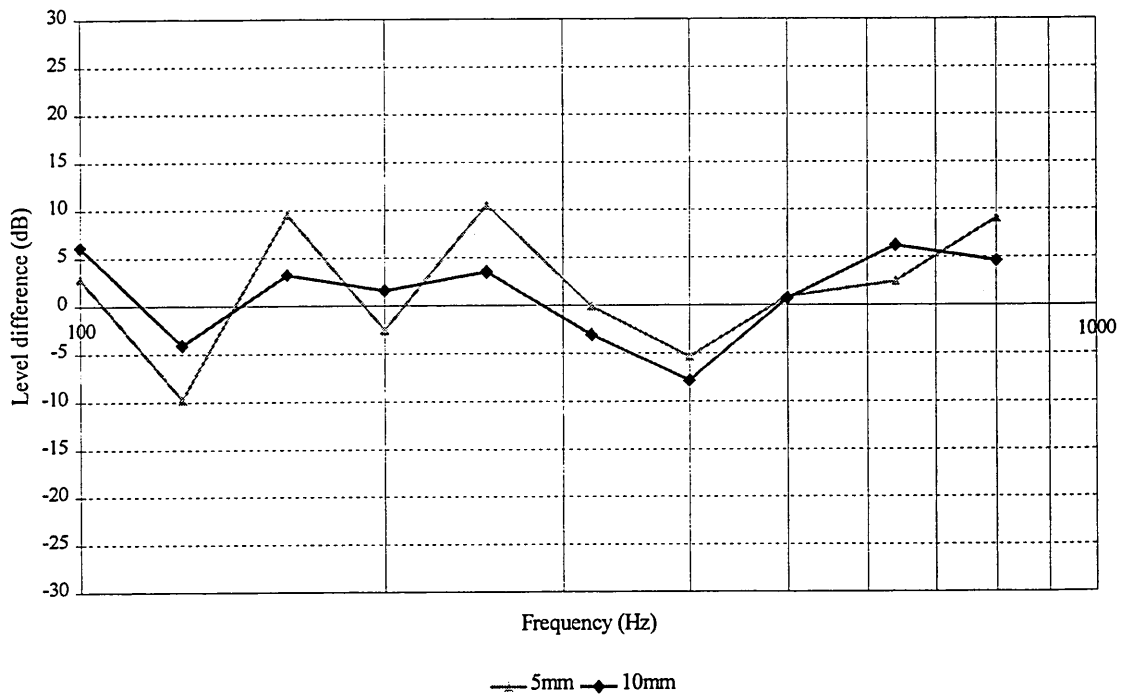
Figure 8.34. Positions 2 and 5: Measured sound pressure level difference compared with predicted level difference in a 1/3 octave band
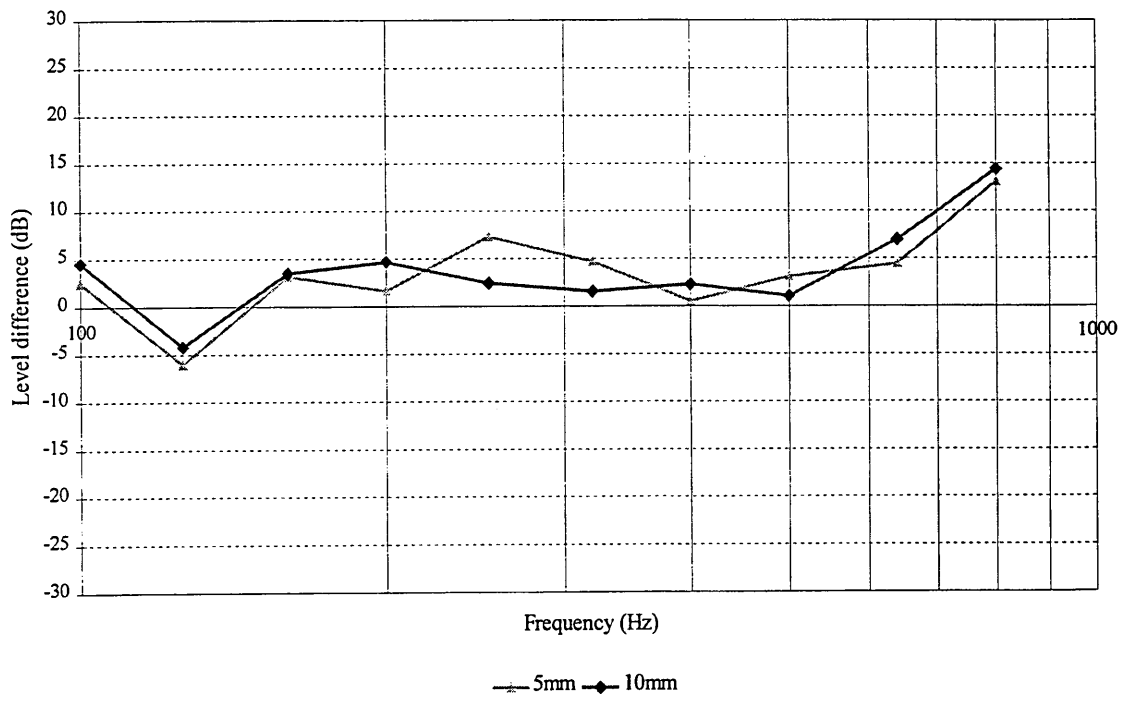
Figure 8.35. Measured mean sound pressure level difference compared with predicted mean sound pressure level difference in a 1/3 octave band

9 EFFECTS OF EDGE CONDITION ON THE SOUND INSULATION OF A SINGLE WALL

9.1 INTRODUCTION

Many investigations [Josse and Lamure (1964), Kihlman (1967,1970), Nilsson (1972), Kihlman and Nilsson (1972), Gargliadini (1991), Kropp et al (1994), Osipov (1997-a), Pietrzyk (1996 & 97)] have examined the sound transmission at low frequencies for simply supported single walls. Measurements of the structural modal shapes on the surface of a brick wall as seen in Chapter 2, showed, however, that the edge conditions lie between simply supported and clamped conditions. Moreover, a change in boundary condition at the edges of a party wall affects the wall displacement field and thus its radiation, which might have a strong influence on the sound transmission. Problems of repeatability and reproducibility of sound insulation measurements at low frequencies have been highlighted and are explained by the non statistical behaviour of the sound field (see Chapter 3), as well as the differences in room volume and test wall boundary conditions between laboratories (see Chapter 4). The use of FEM allows the investigation of a range of edge conditions and the simulation of the sound field in any transmission room. The effect of the edge conditions and of the room configuration on the sound insulation properties of a party wall can therefore be investigated.

The purpose of this chapter is to show that low frequency sound pressure level difference across a party wall is strongly dependent on the edge conditions. The sound level difference was calculated for three different types of boundary condition: simply supported, clamped and mixed. The mixed condition is defined as two simply supported edges in the vertical direction and two clamped edges in the horizontal direction. For a fixed room pair volume ($40m^3$ and $35m^3$), the party wall thickness was varied for each condition. Finally, for a fixed wall thickness, the room pair volume was varied, leading to a study of the effects of room configuration and size of the party wall on the sound level difference.

9.2 REVIEW

Sound insulation measurements at low frequencies in the field or in the laboratory, produce poor reproducibility [Roland (1991)] caused by edge conditions of the party wall [Kihlman (1970), Kihlman et al (1972)], niche effects [Sewell (1970-b), Guy et al (1985)] and laboratory design [Kihlman & Nilsson (1972), Bhattacharya (1972), Guy (1985), Roland (1991), Craik (1992)], even for room volumes greater than 50m³.

The effects of the room dimensions on the sound insulation properties of the party wall were highlighted by the works of, Josse and Lamure [1964], Utley [1968], Kihlman [1967 & 70], Kihlman et al [1972], Bhattacharya et al [1972], Nilsson [1972], Crocker and Price [1975], Michelsen [1983], Guy et al [1985], Craik [1992]. The sound reduction index measured for a party wall in a transmission room of equal volumes is lower than that measured in transmission rooms of unequal room volumes. Room configurations were found to influence the sound reduction index data below but not above the coincidence frequency [Kihlman et al (1972)]. When differences occur above the coincidence frequency, they were attributed to incorrectly estimated loss factor [Kihlman (1970)]. Bhattacharya [1972] investigated the effect of the volume of the source room on the sound insulation properties of the party wall. It was found that the large source room decreases the sound reduction index by 5 to 6dB compared with that measured with a source room of small volume. In order to account for such significant differences he suggested a formula taking into account the room dimensions. However, his work is contradicted by that of Guy et al, who showed that sound transmission loss is lower over all the frequency range from 125Hz to 4kHz, when the larger room acts as the receiving room [Guy et al (1985)]. The work of Guy was based on measurements carried out in the transmission room of 94m³ and 37m³, whereas Bhattacharya's work was on rooms of dimensions of 120m³ and 75m³. The absolute and relative difference in room volumes could be the explanation for the two findings.

Most of the work discussed above, however, was carried out by using room volumes greater than 50m³ and the lowest frequency of interest was 100Hz. It is only recently that the effect of smaller room dimensions and lower frequencies has been investigated [Kropp (1994), Pietrzyk (1996 & 97), Osipov (1997-a&b)]. Pietrzyk [1996] examined

189

the effects of room configuration on a limp wall and on a simply supported heavyweight wall [Pietrzyk (1997)]. The position of the party wall was varied from its original position in the middle of the two rooms and then moved a total of 1m from its original position in both directions in 0.05m steps, for 16 different room configurations for which the length and the width were varied. In the case of a limp wall, a spread of data of 18dB was obtained at the lowest frequency and 10dB with increasing frequency.

Equal room configurations provided the lowest sound level difference. For a simply supported heavyweight concrete wall, a large spread of results was recorded for the different room dimensions. The sound reduction index displayed alternating of maxima and minima. The equal room configuration was however not the worst configuration for the sound reduction index [Pietrzyk (1997)]. This was obtained when the partition was at 0.75m far from the central position. The eigenfrequencies of the room modes and of the structural mode were then the same.

Mulholland [1973], Gargliadini [1990 & 91], Osipov[1997-a] and Pietrzyk [1996 & 97] highlighted that the sound transmission at low frequencies is controlled by acoustic-acoustic coupling, and acoustic-structural coupling. When the number of acoustic modes is large in the frequency band, e.g. 20 in a 1/3 octave band [Mulholland (1973)], with at least 3 structural modes [Gargliadini (1991)], the effects of the different couplings are reduced. Osipov [1997-a] also showed that a wall with a low bending stiffness and with a high modal density reduces the strong acoustic-structural couplings.

Few workers have investigated the effects of the edge conditions on single walls. Maidanik [1962], Sewell [1970-a&b], Kihlman [1970], Kihlman et al [1972] and Nilsson [1972] looked at the effects of simply supported and clamped conditions on a thin wall placed in a diffuse sound field. The clamped thin wall was shown to insulate less than when simply supported. Kihlman [1970] also investigated the edge conditions of heavyweight walls which were found to have no effect. Recently, the edge conditions of double walls were investigated using FEM [Kang et al (1996)]. The clamped conditions were found to insulate more than the simply supported conditions.

9.3   SOUND LEVEL DIFFERENCE PREDICTION

As demonstrated in Chapter 6, one acoustic FEM model can be used to represent the source and receiving room to simulate the sound transmission between them. An infinite impedance wall, of zero thickness was defined at the proposed position of the party wall as seen in Chapter 8. The room modes were then processed according to Table 3.2 which define the upper eigenfrequencies to have a modal overlap factor of 1. The sound field was generated by a point source at a position, near a corner opposite to the party wall, to excite the maximum number of room modes. A finite thickness party wall of dimensions 4x2.5m was defined at the same position of the infinite impedance wall, with the material properties of brickwork [Gibbs (1974)]: Young 's modulus 1.1 10^{10} N.m^{-2}, density 1860 kg.m^{-3} and Poisson's ratio 0.4. Three thicknesses were selected in order to investigate the effect of bending stiffness: 0.05m, 0.1m and 0.2m. Three edge conditions were defined, leading to the creation of three structural models. The simply supported (SSSS) was defined by zero translational motion at the edges in the (x, y, z) directions. The clamped conditions (CCCC) was defined by zero translational and rotational motion in the three directions (x, y, z). The mixed boundary condition (SCSC) was defined by assigning zero translational motion along the vertical edges, and zero translational and rotational motions along the two other edges. When material properties, thickness and boundary conditions were defined, the structural modes were then processed. The sound transmission between the two rooms was then modelled by linking the acoustic model with the structural model as described in Chapter 8. Coupled modes and the frequency response were processed from 25Hz to 200Hz in 1 Hz step increments.

Two field point volumes were defined at 0.5m from the walls in the x and y directions and at 0.3m in the z directions. Each co-ordinate axis was subdivided by 5, which create 150 Quad 4 field elements connecting 152 field points (see Appendix 1). 152 field point values in each room were spatially averaged to the average frequency response of the source room and receiving room. To do so, a short program was written for Unix to select the values of mean pressure at each point. Those files then were transferred to a PC where EXCEL macros were used to calculate the narrow-band average sound pressure levels inside the source room and the receiving room, and hence the third

octave band values.

9.4   EDGE CONDITIONS

The selected volume was 40m³ for the source room and 35m³ for the receiving room, both rooms having the same width and height. The number of room and structural modes per 1/3 octave band are given in Table 9.1 and 9.2, respectively. The eigenfrequencies of the wall are given in Table 9.3. The effect of change of structural modal density was investigated by observing the frequency response of the source room and receiving room and the sound pressure level difference.

9.4.1 Source room-party wall

As demonstrated in Chapters 7 and 8, the predicted sound level inside the source room includes the effect of coupling between the source room and the party wall. Such fluid-structural interactions were now investigated by changing the bending stiffness and boundary conditions of the wall. Figures 9.1-3 display the difference between the sound level in the source room with respect to the predicted sound level with six hard surfaces. The wall resonances affect the frequency response of the room. Figure 9.1 shows that the resonance of the 0.05m clamped wall can affect more strongly the frequency response of the source room than a simply supported wall. Conversely, resonances of the 0.1m and 0.2m simply supported brick wall are more influential than the clamped. Figure 9.3, however, shows that the 0.2m wall has nearly no effect on the sound field. The room can be regarded as a room of 6 hard surfaces except around 98Hz and 139Hz which correspond to the first structural mode and to three room modes of the enclosure (139, 139 and 140Hz). These room modes are evident at all thickness when the wall is simply supported. Not only is the sound field inside a source room affected by the loudspeaker position, as seen in Chapter 3, but also by the party wall which acts as a secondary sound source. The wall effect is controlled by thickness and edge condition.

9.4.2 Party wall - receiving room

36 receiving room modes are present in the frequency range of 25Hz - 160Hz. The

sound field is processed when the party wall is simply supported and when the party wall is clamped. To observe any effects of edge conditions on the sound field, Figures 9.4-6 show the difference between the sound pressure level of the clamped case and of the simply supported case for the three wall thickness.

A 0.05m clamped wall provides a greater sound level than the simply supported wall. The 0.1m clamped wall provides a lower sound level than the simply supported and a 0.2m wall does not display a consistent difference. The greatest fluctuations in Figure 9.4 are explained by the large differences in the panel resonances of the simply supported and clamped walls. Those effects are however diminished when the wall thickness is 0.2m, where only two structural resonances affect strongly the sound field. One is at 53 Hz, corresponding to first mode of the simply supported wall and the other is at 98Hz, corresponding to the first mode of the clamped wall. Consequently, the sound level inside the receiving room is controlled by the bending stiffness and edge conditions, which control the modal density of the wall. The sound field is also affected by the low modal density of the room modes. Only 36 room modes and between 4 to 7 structural modes for the 0.1m and 0.2m walls are present in the frequency range of interest.

9.4.3 Source room – party wall– receiving room

The narrow band averaged sound pressure level difference between rooms is shown in Figures 9.7-8 for the 0.05m and 0.2m clamped walls, respectively. Figure 9.7 displays pronounced peaks and dips, with some negative values. At those frequencies, the sound level inside the receiving room is greater than that in the source room, due to strong structural resonances and structural-acoustic couplings. This confirms the observations of Osipov [1997-a]. For example, in the 60-100Hz range, two structural modes of the clamped 0.05m wall, 65.9Hz and 98.5Hz, are excited while one acoustic mode, a z-axial mode at 68 Hz is excited in the source room and in the receiving room. The signature of the simply supported and clamped 0.05m walls show similar trends, but present many different peaks and dips attributed to the different structural modal densities (see Table 9.2) and therefore different resonances, different acoustic-acoustic and acoustic-

structural couplings.

The sound level difference of the 0.2m wall exhibits less alternating maxima and minima. The small dip observed at 42Hz corresponds to a coupling of two acoustic modes in the source room and one acoustic mode in the receiving room. The dip at 53Hz corresponds to the first structural mode. Acoustic couplings and resonances increase the sound transmission through the wall and thus reduce the sound level difference. Despite the thickness of the wall the sound transmission is affected by acoustic couplings. However, the dips and peaks vary with the wall mass and with the number of structural modes excited in the frequency range of interest. The number of structural modes in the frequency range of interest is small: four modes in total for the simply supported wall and two modes for the clamped wall. The change from four to two structural modes causes an increase in sound level difference and reduce the dips, giving a better control of the acoustic-structural and acoustic-acoustic couplings. Despite the different number of modes, the signature of the simply supported and clamped 0.2m walls display a better agreement than that of the 0.05m wall.

The narrow band phenomena, so far described, will not be observed in normal measurements. Figures 9.9-11 display the sound level difference in 1/3 octave bands in order to compare practically the simply supported and clamped sound pressure level differences. Both display alternate maxima and minima, due to acoustic-structural couplings and acoustic-acoustic couplings. Figure 9.9 shows that for a 0.05m wall, the sound pressure level difference is greater when simply supported rather than clamped.

A mass law trend is observed above 40Hz, which corresponds to a coupling of the first acoustic modes with structural modes, with the weaker simply supported wall giving a slightly higher value. The simply supported 0.05m wall appears mass controlled whereas the clamped wall appears to stay stiffness like, up to 80Hz. Such trend is also observed on sound reduction index measurements of a brick wall carried out by Josse and Lamure [1964] at low frequencies.

The maximum sound pressure level difference of the 0.05m wall is 35dB. The maximum values for the 0.05m brick wall found by Josse and Lamure [1964] was 35dB.

194

However, their lowest sound insulation value is far above than the predicted ones. That can be due to the room dimensions which are greater than 50m^3 and the fact that no structural damping was modelled. The maximum sound level difference of a simply supported 0.2m thick wall (see Figure 9.10) is 45 dB. Measured data by Parkin [1960], Josse and Lamure [1964], and Kihlman [1970] give similar values. They are, not greater than 51dB. The sound level difference decreases with increasing frequency about -6dB/octave. This supports the findings of Parkin [1960], Bergassoli [1970], Gargliadini [1991], Gibbs et al [1991] and Osipov [1997-a]. The predicted minimum values are however much lower than the measured ones. This is due to the same explication given for the 0.05m wall. The 0.2m wall appears stiffness controlled (see Chapter 2) and therefore the clamped condition gives the highest value.

The sound level difference of the simply supported 0.1m wall (see Figure 9.11), however, tends to increase with the frequency, while the sound level difference of the clamped wall decreases with increasing frequency.

In order to understand these two different trends, the simply supported 0.1m wall curve is presented with the clamped 0.05m wall in Figure 9.12 and the clamped 0.1m wall is presented against the simply supported 0.2m wall in Figure 9.13. Both curves in each figure present similar trends, but with a 10dB difference in Figure 9.12 compared to 5-15 dB in Figure 9.13.

The similar trends can be explained by the position of the first structural mode of the two walls. In the case of the simply supported 0.1m wall and the clamped 0.05m wall, both have their first structural modes excited below the first acoustic mode. The sound transmission is mass law controlled. In the case of the clamped 0.1m wall and the 0.2m wall presented in Figure 9.13, the first structural modes are excited above the first acoustic modes. The sound transmission is stiffness controlled. The sound level difference of the 0.1m wall displays a transition between stiffness and mass law control.

Consequently, the classic monotonic decrease and increase with frequency for the stiffness controlled and mass controlled regions, respectively, are not observed. However, despite the fact that the sound fields in the source room and in the receiving

room are not statistical, the curves display trends, which can be interpreted by the classical mechanisms.

Mixed edge conditions (SCSC) are shown in Figures 9.9-11. The altering maxima and minima are also observed on measurements carried out by Bergassoli [1970], which then tend to settle down with increasing frequencies representing the mass law. The critical frequency is hidden by the strong resonances which only take place at low frequencies [Bergassoli (1970)]. The fact that the sound insulation is only investigated in the limited frequency range from 31.5Hz to 160Hz, means that the mass law is not applicable.

The sound level difference of the mixed edge condition 0.05m wall is greater than that of the simply supported 0.05m wall (see Figure 9.9), whereas the sound level difference of the 0.1m and 0.2m walls tends to lie between the simply supported and clamped values. For the three thickness, the mixed edge conditions give values which tend towards those of the simply supported case, with a difference of ± 5-10dB. The selection of the simply supported condition seems closer to the real boundary conditions than a clamped condition.

To summarise; at low frequencies, the party wall response is influenced by the modal characteristics of rooms and of the party wall. Large variations in sound level difference can therefore be observed. However, the frequency trends may still be explained in terms of classical mechanisms. A thin masonry wall is likely to be mass controlled above 50Hz. A thick wall, typical of accepted domestic dwelling construction, will be stiffness controlled, below 160Hz. The edge conditions are found to have an effect on the sound pressure level difference since they change the structural modal density and the trend of the sound level difference curves. Mixed edge conditions gave results similar to that of the simply supported.

9.5   EFFECT OF ROOM CONFIGURATION

The different room configurations existing in dwellings in U.K. are looked at to

investigate their effect on the sound level difference of a 0.2m wall with different edge conditions, by presenting the data in 1/3 octave bands.

9.5.1 Dwellings

9.5.1.1 Transmission paths

Two or three bedroom houses and one or two bedroom flats are the most popular form of dwelling in England [Karn et al (1994)]. Floor layouts for both single and multiple occupancy dwellings were studied to establish a range of room-pair configurations. Many dwellings are constructed according to the Handing and Stacking principle, yielding identical dwelling plans [BRE (1993)]. This is to ensure that habitable noise sensitive spaces (living rooms, bedrooms and dining rooms) are not placed next to kitchens or bathrooms, which normally are the noise producing spaces.

Between attached houses, noise is transmitted from bedroom to bedroom or from living room to living room (handing). In high-rise accommodations, the sound is mainly transmitted vertically between the bedrooms or between living rooms. Therefore the design for the ground floor is reproduced and living rooms lie above living rooms and bedrooms above bedrooms (stacking).

Sound transmission occurs mainly in symmetric room configurations. However, there are cases where the sound is transmitted in asymmetric room configurations, such as between living rooms and bedrooms, where the dimension of the wall of the bedroom is smaller than that of the living room.

9.5.1.2 Room dimensions

In case studies by Fothergill [1980-a], it was confirmed that living rooms and bedrooms in Victorian Houses were large; 67m^3 for living rooms and 55m^3 for bedrooms. In modern dwellings, rooms are more modest [Jackson et al (1972)]. Houses built since 1975 have, typically, lounges and bedrooms of 28m^3 and 26m^3, respectively with floor

to ceiling height of 2.5m. Minimum floor areas are recommended for living rooms and kitchens [Karn et al (1994)]. 13m^2 is the minimum required for a living room without kitchen (Peabody standards), although Karn et al [1994] estimates that 7% of houses have living room areas less than this. That means living room volumes can be less than 33m^3 without taking into account the amount of space taken by stairs. Table 9.4 shows groupings of volumes of bedrooms and living rooms likely in the UK.

It shows that airborne sound is mainly transmitted between bedrooms, between living rooms or between living rooms and bedrooms. The living rooms are bigger than the bedrooms. All room volumes are much less than 50m^3 except for un-converted Victorian houses. All volumes are smaller than those required for laboratory measurements [ISO140, part 3 (1995)]. Houses with three bedrooms have even their third bedroom with a room volume much less than 19m^3, being sometimes 13m^3.

In England and Wales, there are no minimum requirements for habitable rooms [Karn et al (1994)] and no requirements for the height of the room. In other countries, there are minimum requirements; 20.7m^3 in France with a ceiling height of 2.3m, 24m^3 in Germany [Sheridan (1999)].

Most rooms are rectangular, but with a minority of L shaped [Fothergill, (1980-b)]

To summarise; volumes of domestic rooms were found to be much smaller than the minimum volume required in laboratories. They varied between 20m^3 and 40m^3. The effects of those room volumes on sound insulation at low frequencies were investigated by defining two categories of transmission rooms for which the width (4m) and the height (2.5m) are kept constant. The first one is the equal room configuration and the second is the unequal room configurations. They are presented in Table 9.5. The 10 room configurations obviously does not represent the entire population, but will still provide information on their effects on the sound insulation of 10m^2 party wall for which different edge conditions are assigned.

198

9.5.2 Symmetric rooms

The mean sound pressure level difference is investigated in a transmission room as shown in Table 9.5 and was calculated for the three different boundary conditions in 1/3 octave bands from 31.5Hz to 160Hz for equal room configurations and for unequal room configurations. The data are presented in Figures 9.14-15. At 31.5Hz, the sound level difference lies between 50-53dB. No acoustic modes are excited in this band. The edge conditions have practically no effects on the sound level difference. The sound level difference then fluctuates over the frequency range 40Hz-160Hz. The dips in sound level difference at 40Hz correspond to the couplings of the first acoustic y-axial modes of each room. The dips at 50Hz and 100Hz for the simply supported case correspond to the first and second structural resonances of the simply supported wall. The dip at 63Hz of the mixed edge conditions wall corresponds to the first structural resonance.

The effects of resonance can be controlled by the type of excited acoustic modes in each room. For example, the first resonance frequency of the clamped wall is only visible when rooms are unequal. This demonstrates that the acoustic modes control the resonances, leading to an acoustic-structural coupling. The different couplings and resonances tend to control the shape of the sound level difference curves. When the room configuration is unequal, the shape of the curve of the flexible party wall presents less peaks and dips than that of the simply supported and clamped walls. The structural modal pattern is modified by non-homogeneous edge conditions and therefore reduces the strength and the number of acoustic-structural couplings. Despite the numerous couplings, the sound level difference still decreases with increasing frequency at about - 6dB/octave. The sound level difference is stiffness controlled. The clamped values are therefore greater than the simply supported values. The mixed boundary conditions case lies between the simply supported and clamped cases.

The effects of edge conditions on the sound transmission direction were investigated by calculating the level difference between the predicted sound level difference obtained with the source room having the largest volume then with the source room having the smallest volume. The data are presented in Figures 9.16-18. The boundary conditions

199

are found to have practically no effect on the sound direction up to 100Hz for any room configuration with the exception of the mixed edge conditions in the 40-20m³ room configuration at 63Hz. The first structural resonance and the presence of one excited acoustic mode in the 20m³ room and two excited acoustic modes in the 40m³ can explain the behaviour of the 40-20m³ room configuration. From 125Hz, the boundary conditions have a strong influence on the sound direction, mainly when one of the room volumes is 40m³ and when the party wall is simply supported or clamped. The mixed edge conditions tend to reduce those effects, but the difference is still in the order of 5-10dB. The presence of the second structural mode of the mixed edge conditions wall might well explain that phenomenon.

Values of the sound level difference predicted for 10 different room configurations are presented in Figures 9.19-21. The spread of data for the simply supported wall varies between 5-54dB and is much larger than that of the mixed edge conditions and clamped conditions. In the case of the mixed edge conditions (see Figure 9.20), the spread is reduced to 30dB or 20dB when the data for equal room configuration are removed before the 63Hz 1/3 octave band. In the 63Hz and 125Hz band, the spreads are 40dB and 30dB, respectively, whereas the spread is 20dB and 25dB when not including data for equal room configuration. Similar phenomena are observed for the clamped wall (see Figure 9.21) at 100Hz, where the spread is 10dB without the equal room configuration data or 30dB with. These variations are explained by the presence of the first and second structural modes for which the strength of the acoustic-structural coupling varies with the room configuration. Strong acoustic-acoustic couplings take place when the room configuration is equal and therefore the spread of data is increased. The spread of data is small when no structural modes are present, recalling the work of Kropp et al.[1994] and Pietrzyk[1996] on a limp wall [Maluski et al (1998-b)].

The effects of equal room configuration vary also with the edge conditions as seen in Figures 9.22-25. The simply supported wall insulates less than the clamped wall and the mixed edge conditions lie between these two. However, different peaks and dips are taking place every time a set of equal room configuration is used, due to different acoustic-acoustic couplings and acoustic-structural couplings. Figure 9.25 shows that when the wall is placed between two rooms of volume equal to 50m³, the sound level

difference is equal to 10-28dB at 31.5Hz depending on edge conditions. That is explained by the acoustic-acoustic coupling of the first mode, x-axial mode.

Figures 9.26-9.28 show the sound level difference obtained for each edge condition, and each figure displays the sound level difference obtained for each room configuration. The two curves for the 20m^3 and 40m^3 equal configurations display the same trend. The two other curves for the 30m^3 and 50m^3 equal room configurations also display the same trend. The length of the 20m^3 room is 2m i.e. half of the length of the 40 m^3. The x-axial modes are only half of the x-axial modes of the 40 m^3 and so on. Changing the edge conditions of the party wall reduces the spread of data (see Figures 9.26-28). The mixed edge conditions lie between simply supported and clamped conditions.

The sound level difference data of the three different edge conditions are averaged for equal and unequal room configuration in Figure 9.29. As expected, a decrease in sound level difference with increasing frequency has been observed for both equal and unequal room configurations. The mean sound level difference in equal rooms is lower than that in unequal room configurations. Such behaviour is expected as strong acoustic-acoustic couplings take place between modes of identical shapes and eigenfrequencies [Kropp et al (1994), Pietrzyk (1997), Maluski et al (1998-b)]. The effects of the equal room configuration, which cause the decrease in the sound level difference, are therefore true not only for the mid and high frequencies [Bhattacharya (1972), Nilsson (1972)], but also for low frequencies in small rooms.

The effects of the source room volume on the sound level difference are presented in Figure 9.30. $V_{SR} > V_{RR}$ means that the larger room acts as the source room. $V_{SR} < V_{RR}$ means that the smaller room acts as the source room. Discrepancies of only a few dBs are obtained with the exception of 125Hz, where there are 9 acoustic modes in the 40m^3 enclosure. The sound level difference can then be reduced by the excitation of large number of acoustic modes in the receiving room compared with the number in the source room. At 160Hz, the difference is decreased to 3dB. The number of modes in each room is equal to or greater than 9 over the range of room volumes, but it is practically the same when the rooms are 30m^3 (14 modes) and 40m^3 (15 modes). The acoustic modal density of each room controls, therefore, the effects of room

configuration on sound insulation.

To summarise, the sound level difference is affected by the acoustic-acoustic couplings and acoustic-structural couplings, due to the non-statistical behaviour of the sound fields and to the structural modal density. Edge conditions of the party wall therefore affect the sound level difference. A masonry heavyweight wall, when clamped insulates more than when simply supported. Values of sound level difference for mixed edge conditions lie between those for simply supported and clamped conditions. The sound pressure level difference also varies with the room configuration. The values for equal rooms are lower than for unequal rooms. The trend of the curves display stiffness control at low frequencies. The mass law was not observed due to the narrow frequency range investigated.

9.5.3 Asymmetric rooms

The airborne sound is usually transmitted between two symmetric rooms of equal volume, but domestic dwellings also show that the sound is transmitted between two asymmetric rooms of equal volumes as seen in Figure 9.31.

To investigate the effects of asymmetric room configuration on the sound insulation of the 0.2m wall, the area of the party wall could not be maintained at $10m^2$, otherwise the room volumes would have to be in excess of $50m^3$. In the present study, only transmission rooms with volumes of $20m^3$ and $30m^3$ were investigated. Two party walls of different area of $2x2.5m^2$ and $3x2.5m^2$, respectively, were then defined. Two symmetric room configurations thus had to be defined with the corresponding dimensions of the wall in order to understand the effects of the asymmetric room configuration on the sound insulation of the party wall.

In line with the reduction in surface area of the party wall, the number of structural elements was decreased along the y-axis. 50 structural elements were defined for the wall of $2x2.5m^2$ and 90 elements were defined for the wall of $3x2.5m^2$. The transmission rooms were then redefined in order to have the same number of structural elements as

the acoustic elements at the interface. Two other symmetric transmission rooms of $20m^3$ and $30m^3$ were modelled to compare the predicted level differences with those of the asymmetric transmission rooms (see Figure 9.32). The loudspeaker position and field point mesh boxes were defined as earlier.

The different effects of the asymmetric and symmetric configurations on the sound level difference were investigated by calculating the level difference between the sound pressure level difference of the asymmetric and of the symmetric room configurations. The level differences are presented in Figure 9.33 for the $20m^3$ configuration and in Figure 9.34 for the $30m^3$ configuration. The sound insulation of the party wall placed in an asymmetric $20m^3$ configuration was found to be 3dB greater than that in the symmetric configuration, except at 125Hz. The sound insulation of the party wall placed in an asymmetric $30m^3$ configuration was found 9-12dB greater than that in the symmetric room configuration in the frequency band [31.5- 63Hz] and then 3dB greater for the remaining other 1/3 octave frequency bands. The effects of the asymmetric room configuration tend to improve the sound insulation of party wall. The couplings of the modes of same shape and same eigenfrequencies are indeed more difficult due to the geometry of the transmission rooms. The drops in sound insulation due to acoustic couplings are therefore controlled by the geometry of the room. Figures 9.35-36 illustrates this phenomenon by displaying only the first acoustic mode in the source room and in the receiving room of the asymmetric and symmetric room configuration, respectively. Figures 9.33-34 also shows that the edge conditions have negligible effect. The wall area is small and therefore few structural modes are excited in the frequency range of interest, presented in Table 9.6. Thus only a limited number of acoustic-structural couplings take place. The room configuration has therefore negligible influence. The sound level difference for the three different types of edge conditions for the $20m^3$ and $30m^3$ asymmetric room configurations are shown in Figures 9.37-38, respectively.

The signatures of the curves are the same as those obtained with the symmetric configuration. The sound insulation of the party wall is stiffness controlled. The simply supported case insulates less than the clamped case and the case of mixed edge conditions insulate as well as the clamped case.

203

In summary, the effect of the asymmetric room configuration improves the sound insulation by reducing the strength and the number of acoustic-acoustic couplings and acoustic-structural couplings. The effect of the edge conditions are generally the same whatever the room configuration, but the mixed edge conditions case was observed to behave more as a clamped wall than a simply supported wall.

9.5.4 Wall size

The sound level difference of two party walls $5m^2$ and $10m^2$ in area were investigated when the party wall was placed in the $20m^3$ equal room configuration. Two other party walls of $7.5m^2$ and $10m^2$ in area were investigated in the $30m^3$ equal room configuration. The level difference was calculated between the sound level difference of the smallest and largest area wall. The data are presented in Figures 9.39-40.

Both figures show that the sound level differences vary with the size of the wall and with the conditions applied along the edge of the wall. The value is greater for small wall area than for large wall area. This phenomenon also is observed by other authors [Josse and Lamure (1964), Sewell (1970-b), Nilsson (1972), Michelsen (1983), Guy et al (1985)]. The sound insulation of the $5m^2$ area wall is improved by roughly 8dB when clamped and 12dB when the wall has mixed edge conditions. The simply supported $5m^2$ wall displays the worst case being less rigid than the other cases. For any edge conditions, the sound insulation of a $7.5m^2$ wall is again better than the $10m^2$ wall except at 40Hz and 80Hz corresponding to acoustic couplings [Table 9.1].

According to BRE [1993], the sound insulation of a party wall of area of 2 LxL is lower than that for a wall of area LxL; where L corresponds to one dimension of one equal room configuration, as shown in Figure 9.41. A 3dB improvement is obtained when the party wall has an area LxL.

Compared to the present work, the corresponding length, l, of the $5m^2$ and $10m^2$ walls is 2.23 which lies between 2m (length of the room) and 2.5m (height of the room). An

improvement of 8dB for the clamped wall and 12dB for the mixed edge conditions is obtained. The 8dB improvement is greater than predicted BRE [1993]. The conditions given by BRE [1993] are therefore not only applicable for the mid and high frequencies but also at low frequencies.

9.6   DISCUSSION

The sound level difference at low frequencies was observed to be strongly influenced by both acoustic-acoustic and acoustic-structural couplings leading to a large spread of data for each type of wall. Such behaviour can be attributed to the non statistical behaviour of the sound field and the small structural modal behaviour of the party wall thus explaining the poor reproducibility of the field measurements at low frequencies [Roland (1995), Goydke (1998)].

The sound level difference was found to be dependent on the boundary conditions whatever the thickness of the party wall, a phenomenon already observed by many other workers [Maidanik (1962), Kihlman (1970), Kihlman et al (1972), Nilsson(1972)]. The sound level difference of the thin clamped lightweight wall is lower than the simply supported case, while structural eigenfrequencies are shifted upwards and the rigidity of the wall increased (see Section 2.4.7) [Berry et al (1994)]. Maidanik [1962], Utley [1968], Sewell [1970], Kihlman [1970] and Nilsson (1972) have previously demonstrated this when considering a thin wall positioned in a diffuse sound field. They have shown that 3dB difference separates simply supported from clamped until the coincidence region. Such differences, however, are not observed with the present work. That is due to the small acoustic modal density in the frequency range of interest. For walls with a thickness equal to or greater than 0.1m, the sound level difference for clamped conditions is greater than for the simply supported case. This confirms the work of Kihlman [1970] again, where the sound field was assumed diffuse. However, in this case, Kihlman attributed that difference to the loss between the two rooms and not to the edge conditions. Thus the effects of edge conditions might be negligible in front

of the flanking sound transmission which takes place at a T-junction [Kihlman (1998)].

The shape of the sound level difference curve of the 0.2m mixed boundary conditions tends however to be flat when the room configurations are unequal. The presence of two clamped sides and two simply supported sides are the main causes of such a response. The alternating edge conditions could change the wall from isotropic to orthotropic.

The small number of excited modes at low frequencies leads to a greater spread of sound level difference data. However, the sound level difference with a resolution in the third octave band leads to an increase in the number of excited modes in the band and therefore a decrease in the spread of data. Such behaviour can explain the comment made by Osipov [1997], that the accuracy of the sound insulation is improved when presented with a resolution in octave bands. However, such resolution in 1/3 octave bands of the sound level difference can mislead the real effects of the party wall and room configuration on the sound transmission. With regard to the sound pressure level difference values, a resonance can give a negative value in a narrow band, whereas it can give a positive value in a third octave band. The same remark can be made when the dip in sound level difference is set between two 1/3 octave bands. A 1/6 or 1/12 octave band resolution would seem more appropriate for sound insulation at low frequencies to have the maximum of information on sound insulation

The use of FEM to investigate the sound transmission at low frequencies in dwellings was observed to predict sound level difference data, which agree with data obtained in laboratory conditions [Maluski and Gibbs (1998-a)]. The non-introduction of acoustic and structural damping in the model seem therefore negligible when calculating the sound level difference. However, the spread of data obtained in this present study when investigating the effects of room configuration is much greater than that obtained by Pietrzyk [1996 & 97] or Osipov [1997]. The reason for this is that an acoustic damping was defined in their model by setting a reverberation time value in the source room and in the receiving rooms. This damping results in a reduction of the peak response of each mode excited in each room and therefore reduces the spread of data. The acoustic damping as well as the structural damping need further investigation.

The sound level difference was found to be lower when the volumes of the two rooms are equal. Such a configuration is typical in domestic dwellings in the U.K. and other European countries [see Chapter 10]. According to Fothergill [1998], if rooms were staggered, it is already enough to decrease the number of acoustic couplings and therefore improve the sound insulation.

The sound pressure level difference is stiffness controlled because of the small structural modal density and the first structural mode which is excited after the first acoustic mode. The control of sound insulation is thus controlled by the real dimensions. According to Osipov [1997-a], a wall of surface area less than $9m^2$ i.e. a wall placed between two rooms of volumes greater than $36m^3$ and smaller than $54m^3$ will present a sound transmission which is stiffness controlled. When the room volume and when the area of the party wall are increased, the sound transmission tends to be mass controlled.

9.7   CONCLUDING REMARKS

The sound level difference at low frequencies is strongly influenced by the structural mode density of the party wall. Walls having their first structural modes excited before the first acoustic modes will tend to be mass controlled, while walls having their first structural mode excited after will tend to be stiffness controlled. The sound level difference at low frequencies of a 0.2m brick wall is stiffness controlled, presenting alternative maxima and minima due to structural-acoustic and acoustic-acoustic couplings. Varying the room configuration and the edge conditions varies the different couplings and thus the sound level difference. The sound level difference is found to be the lowest when the party wall is simply supported and when the room configuration is of equal volumes. A large spread of sound pressure level data was therefore obtained in the frequency range 31.5-160Hz. Such a spread needs to be quantified in order to predict the sound pressure level difference of a party wall at low frequencies. A correction factor is therefore needed to account for these variations and an attempt is made in Chapter 10.

9.8   REFERENCES

Bhattacharya, M.C. and Guy, R.W., (1972): '*The influence of the measuring facility on the measured sound insulating property of a panel*', Acustica, Vol.26, 344-348

Bergassoli, A. et Brodut, M., (1970): '*Transparence des murs et des cloisons*', Acustica, Vol.23, 315-322

Berry, A. and Nicolas, J., (1994): '*Structural acoustics and vibration behaviour of complex panels*', Applied Acoustics, Vol.43, 185-215

BRE & CIRIA, (1993): '*Sound control for homes*', Ed. Crown

Craik, R., (1992): '*The influence of the laboratory on measurements of wall performance*', Applied Acoustics, Vol.35, 25-46

Fothergill, L.C., (1980-a): '*Case studies of attempts to improve the sound insulation between dwellings*', Applied Acoustics, Vol.13, pp. 291-311

Fothergill, L.C., (1980-b): '*Recommendations for the measurements of sound insulation between dwellings*', Applied Acoustics, Vol.13, 171-187

Fothergill, L.C., (1998): Private communication, December

Gargliadini, L., (1990): '*Simulation numerique de la mesure en laboratoire de l'indice d'affaiblissement acoustique: Effets des sources et de la geometrie de la paroie*', Colloque de Physique, Colloque C2, Supplement n⁰ 2, Tome 51

Gargliadini, L., Roland, J. and Guyader, J. L., (1991): '*The used of functional basis to calculate acoustic transmission between two rooms*', Journal of Sound and Vibration, 145 (3), 457-478

Gibbs, B.M. and Lewis, J., (1991): '*Sound insulation of brick diaphragm walls Part I: Scale model measurements and statistical energy analysis*', Building and Environment, Vol.26 (2), 165-172

Gibbs, B.M., (1974): '*The direct and indirect transmission of vibrational energy in building structures*", PhD Thesis in The University of Aston in Birmingham

Goydke, H., (1998): '*Investigations on the precision of laboratory measurements of sound insulation of building elements according to the revised Standard ISO 140*', Proceeding of Inter-Noise 98, 480

Guy, R.W., De Mey, A and Sauer, P., (1985): '*The effects of some physical parameters upon the laboratory measurements of sound transmission loss*',

Applied Acoustics, Vol.18, 81-98

Jackson, G M and Leventhall, H G, (1972): *'The acoustics of domestic houses'*, Applied Acoustics, Vol.5, 265-277

Josse, R. and Lamure, C., (1964): *'Transmission du son par une paroie simple'*, Acustica, Vol.14, 267-280

Kang, Y.J. and Bolton, J.S., (1996): *'A Finite Element model for sound transmission through foam lined double panel structures'*, Journal of Acoustical Society of America, Vol.99 (5), 2755-2765

Karn, V. and Sheridan, L., (1994): *'New Homes in the 1990s: A study of design, space and amenity in housing association and private sector housing'*, Joseph Rowntree Foundation and the University of Manchester

Kihlman, T., (1967): *'Sound radiation into a rectangular room. Applications to airborne sound transmission in buildings'*, Acustica, Vol.18, 11

Kihlman, T., (1970): *'Report on the influence of boundary conditions on the reduction index'*, Report N0 ISO/TC43/SC2/WG2, Chalmers Tekniska Hogskila, Goteborg, Sweden

Kihlman, T and Nilsson, A.C., (1972): *'The effects of some laboratory designs and mounting conditions on reduction index measurements'*, Applied Acoustics, Vol.5

Kihlman, T., (1998): Private communication

Kropp, W., Pietrzyk, A. and Kihlman, T., (1994) *'On the meaning of the sound reduction index at low frequencies'*, Acta Acustica, 2, 379-392

Maidanik, G., (1962): *'Response of a ribbed panels to reverberant acoustic fields'* Journal of Acoustical Society of America, Vol.34, 809-826

Maluski, S. and Gibbs, B.M., (1998-a): *'The influence of partitions boundary conditions on sound level difference between rooms at low frequencies'*, Proceeding of Euro-Noise 98, V.2, 681-686

Maluski, S. and Gibbs, B.M., (1998-b): *'Variation of sound level difference in dwellings due to room modal characteristics'*, Proceeding of Acoustics Performances of Medium-Rise Timber Buildings, 3rd&4th December 1998, Dublin

Michelsen, N., (1983): *'Effect of size on measurements of the sound reduction index of a window or a panel'*, Applied Acoustics, Vol.16, 215-234

Mullholland, K.A. and Lyon, R.H., (1973): *'Sound insulation at low frequencies'*,

Journal of Acoustical Society of America, Vol.54 (4), 867-878

Nilsson, A.C., (1972): *'Reduction index and boundary conditions for a wall between two rectangular rooms', Part I and II,* Acustica, Vol.26, 1-23

Osipov, A., Mees, P., and Vermeir, G., (1997-a): *'Low frequency airborne sound transmission through single partitions in Buildings',* Applied Acoustics, Vol.52 (3-4), 273-288

Osipov, A., Mees, P., and Vermeir G., (1997-b): *'Numerical simulation of airborne sound transmission at low frequencies: the influence of the room and the partition parameters',* Proceeding of Inter-Noise 97, Vol.2, 759-762

Parkin, P.H., Purkis, H.J., and Scholes, W.E., (1960): *'Field and measurements of sound insulation between dwellings',* Her Majesty's Stationery office, London

Pietrzyk, A. and Kihlman, T., (1997): *'The sensitivity of sound insulation to partition location - Case of heavyweight partitions',* Proceeding of Inter-Noise 97, Vol.2, 727-730

Pietrzyk, A., (1996): *'Optimisation of sound insulation at low frequencies by selecting partition location',* Nordic acoustical Meeting, 71-76

Roland, J., (1995): *'Adaptation of existing test facilities to low frequency measurements',* Proceeding of Inter-Noise 95, Vol.2, 1113-1116

Sewell, E.C., (1970-a): *'Transmission of reverberant sound through a single leaf partition surrounded by an infinite rigid baffle',* Journal of Sound and Vibration, Vol.12, 397-409

Sewell, E.C., (1970-b): *'Exact solution for transmission of reverberant sound through a circular panel in a waveguide',* Journal of Sound and Vibration, Vol.12, 397-409

Sheridan, L., (1998): *'A Comparative Study of the Control and Promotion of Quality in Housing in Europe Department of the Environment',* Transport and the Regions

Utley, W.A., (1968): *'Single leaf transmission loss at low frequencies',* Journal of Sound and Vibration, Vol.8, 256

Volume (m^3)	Frequency (Hz)								
	31.5	40	50	63	80	100	125	160	Total
20	0	1	0	1	3	3	5	9	22
30	0	1	0	3	3	3	6	14	30
35	0	1	1	2	3	5	6	18	36
40	0	2	0	2	4	5	9	15	37
50	1	1	1	2	5	6	9	22	47

Table 9.1. Number of room modes per 1/3 octave bands

Thickness (m)	0.05m			0.1m			0.2m		
Frequency (Hz)	SSSS	SCSC	CCCC	SSSS	SCSC	CCCC	SSSS	SCSC	CCCC
25	2	2	1	1	1	0	0	0	0
31.5	0	1	0	0	1	0	0	0	0
40	1	0	1	0	0	0	0	0	0
50	2	1	0	1	0	1	1	0	0
63	0	2	2	0	1	0	0	1	0
80	2	1	1	1	1	1	0	0	0
100	3	2	2	2	0	0	1	0	1
125	2	3	0	0	2	2	0	1	0
160	2	1	4	2	1	1	2	1	1
Total	15	13	11	7	7	5	4	3	2

Table 9.2. Number of structural modes per 1/3 octave bands

| Thickness (m)	0.05m			0.1m			0.2m		
Mode	SSSS	SCSC	CCCC	SSSS	SCSC	CCCC	SSSS	SCSC	CCCC
1	13.5	16.1	26.2	26.8	32.0	51.8	52.7	62.3	98.9
2	25.3	33.0	39.5	50.2	65.1	77.8	97.1	123.8	146.7
3	44.0	45.2	65.9	86.9	89.3	128.6	166.3	170.4	235.9
4	47.1	60.3	68.5	92.9	118.3	133.2	176.6	221.0	
5	55.5	61.6	80.0	109.2	120.4	155.3	206.1	222.0	
6	76.5	87.4	103.0	149.7	169.7	198.5			
7	82.5	100.6	110.3	161.3	195.9	212.0			
8	99.8	107.4	140.5	194.6	206.3				
9	110.7	113.9	143.0	214.7	220.8				
10	110.8	131.3	150.9						
11	130.8	138.4	170.9						
12	138.5	178.8	182.9						
13	163.0	181.0	205.9						
14	164.6	190.4							
15	189.9	202.2							
16	200.1	202.2							

Table 9.3. Structural modes predicted for a brick wall
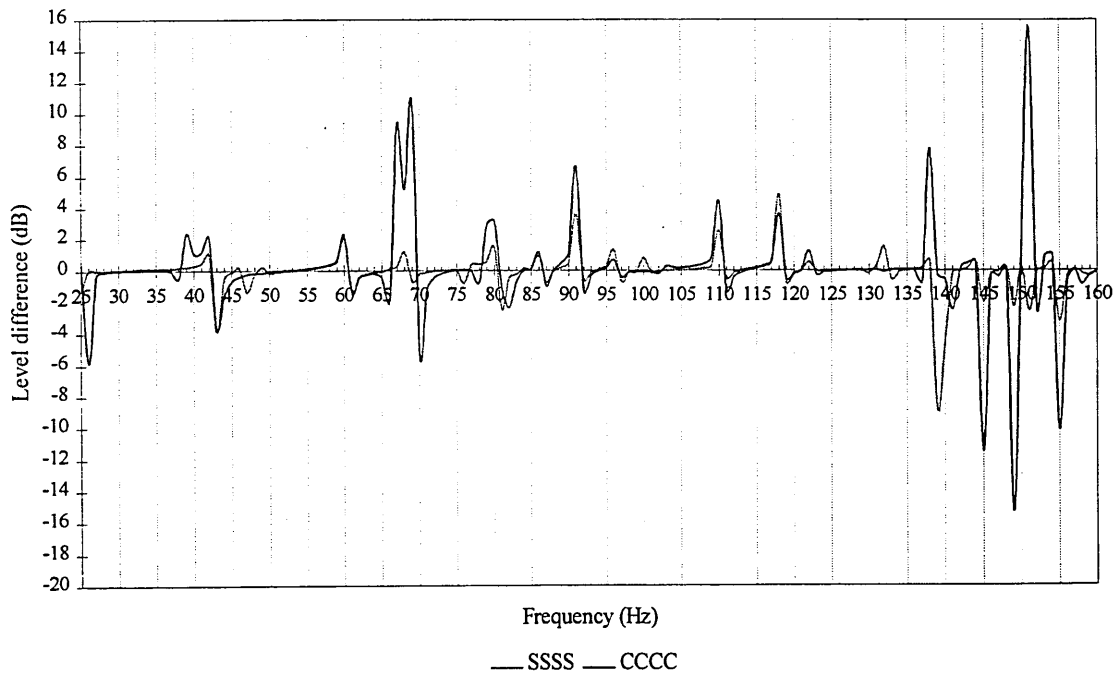
Figure 9.1. Level difference in the source room with a 0.05m thick party brick wall
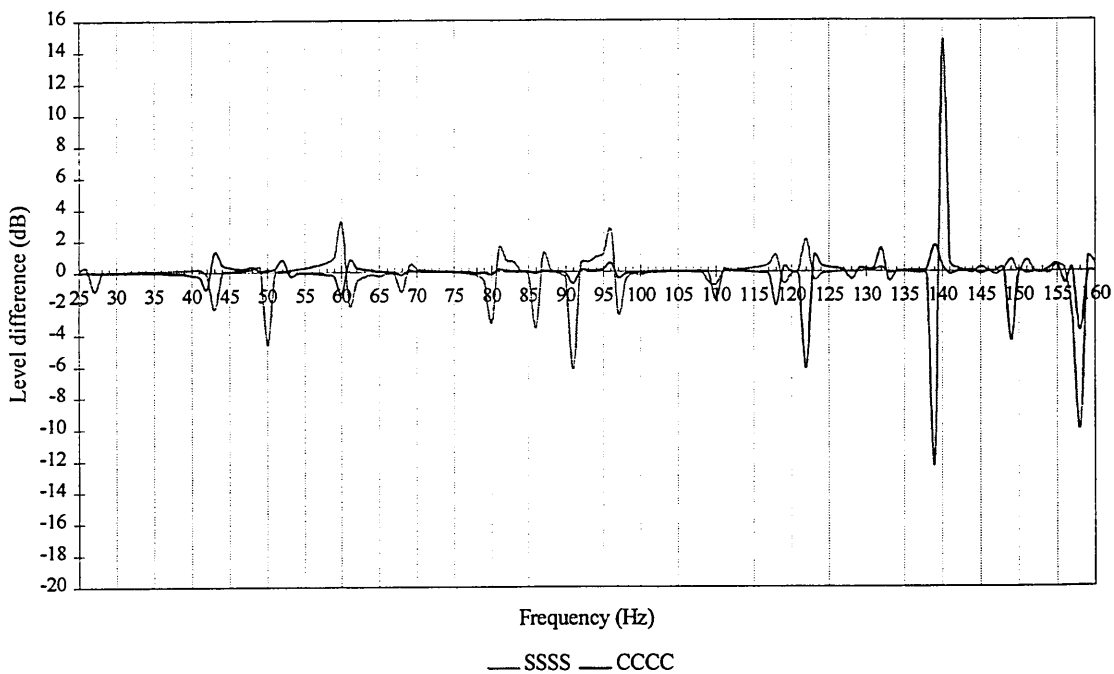

Figure 9.2. Level difference in the source room with a 0.1m thick party brick wall

214
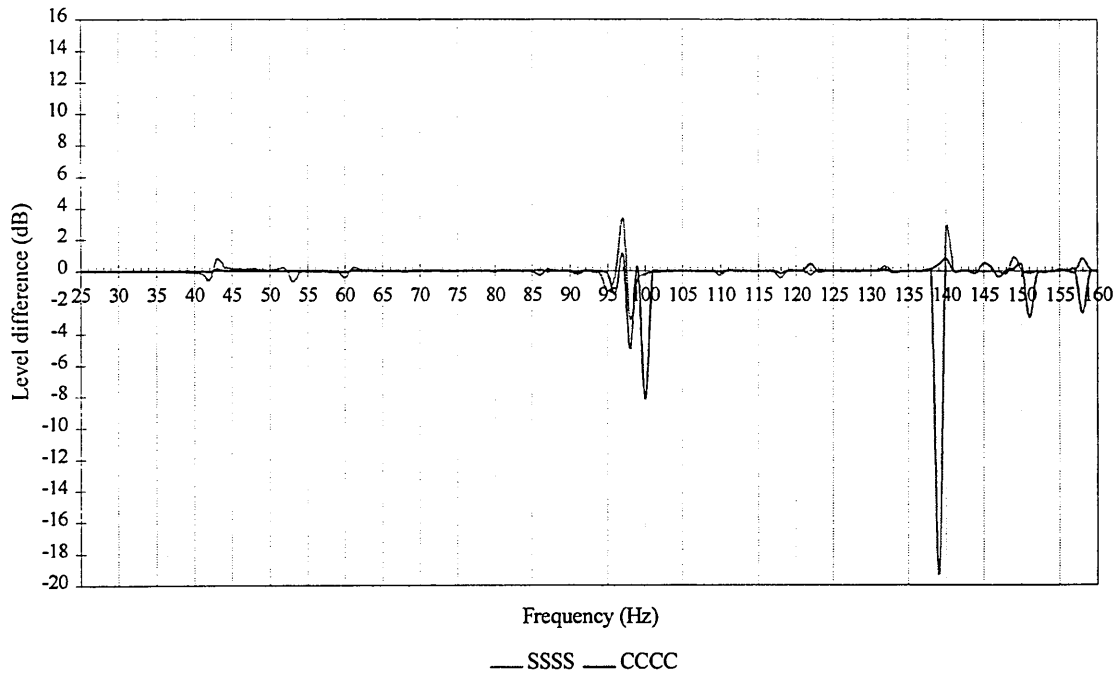
Figure 9.3. Level difference in the source room with a 0.2m thick wall
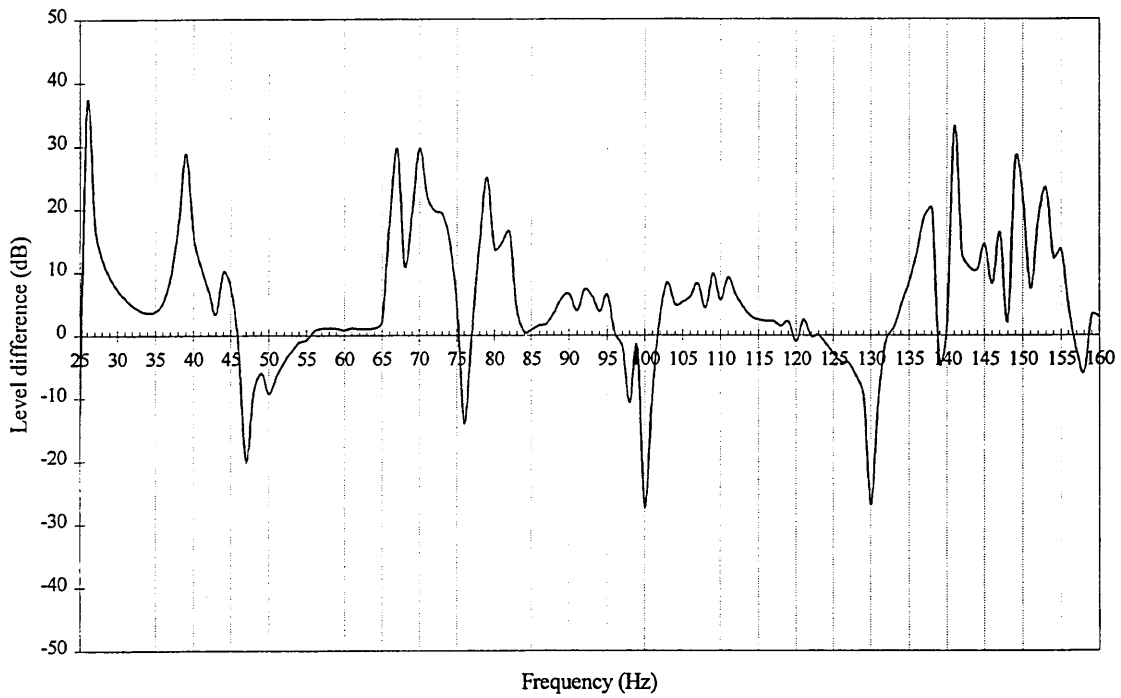
Figure 9.4. Level difference between the clamped and the simply supported 0.05m wall

215
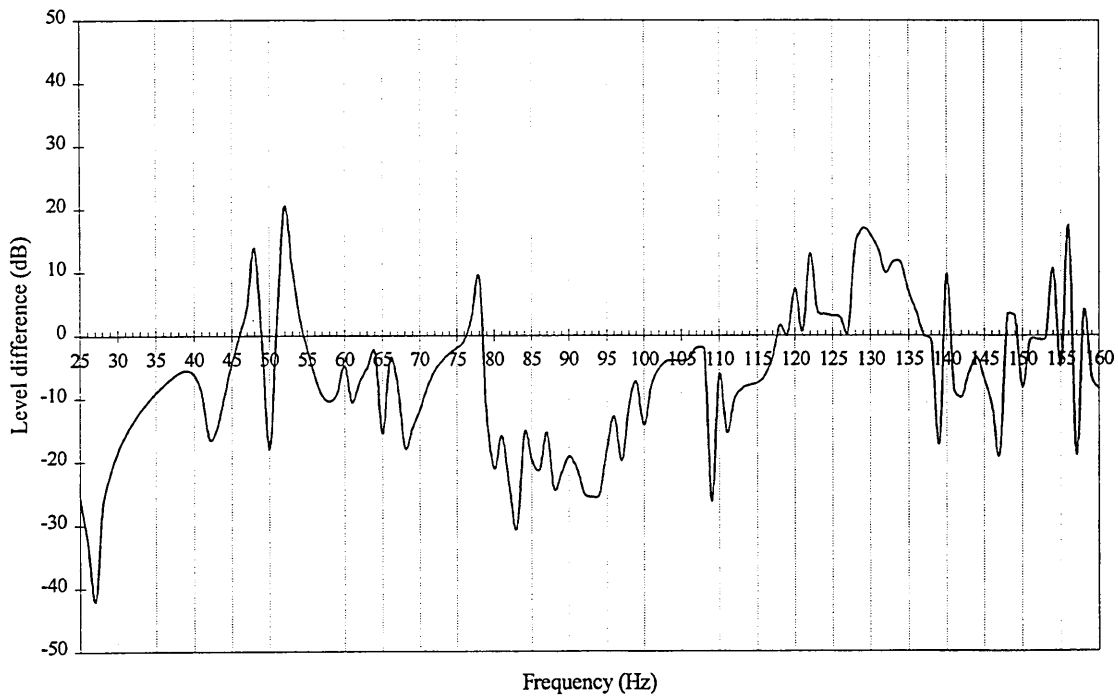
Figure 9.5. Level difference between the clamped and the simply supported 0.1m wall
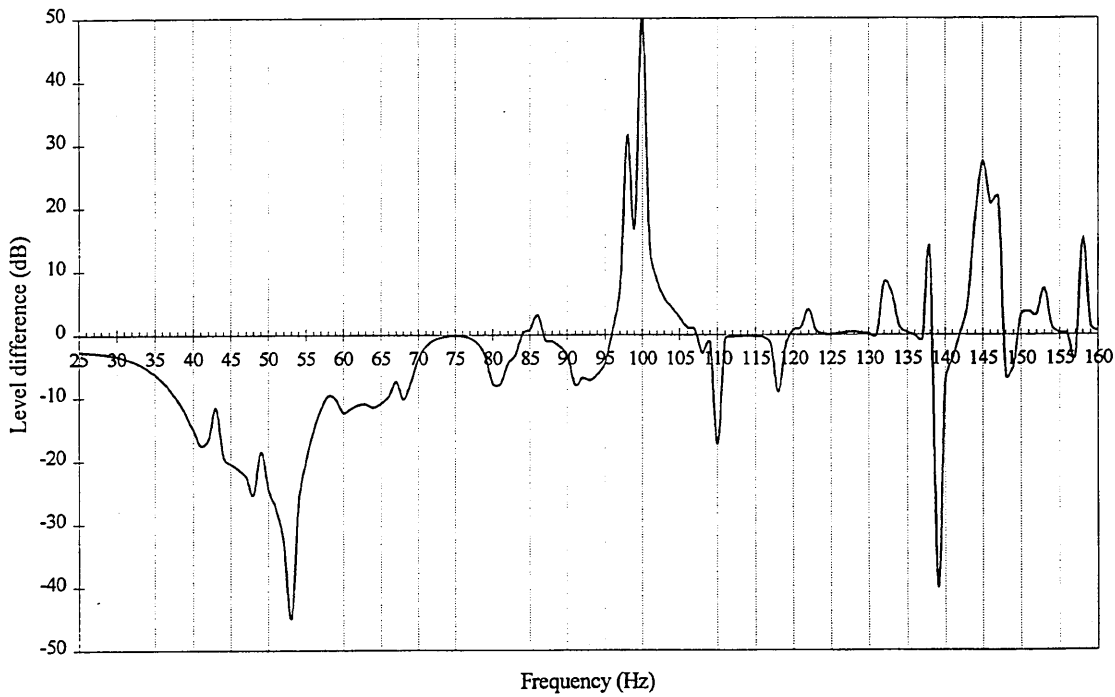
Figure 9.6: Level difference between the clamped and the simply supported 0.2m wall

216
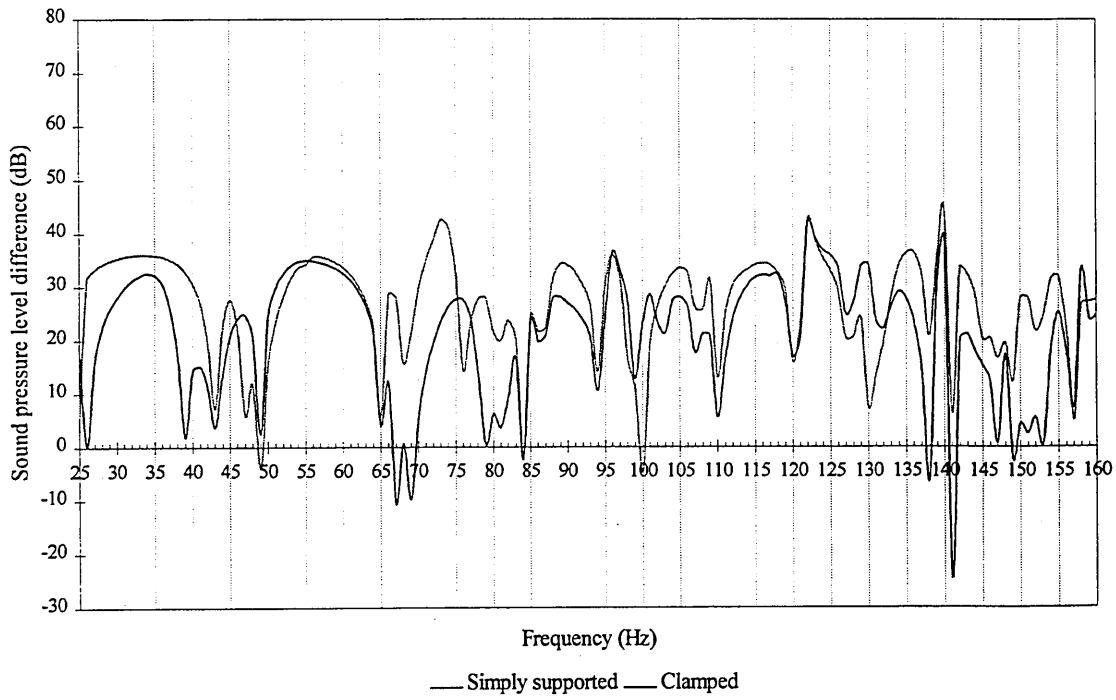
Figure 9.7. Sound pressure level difference of the 0.05m wall in narrow bands
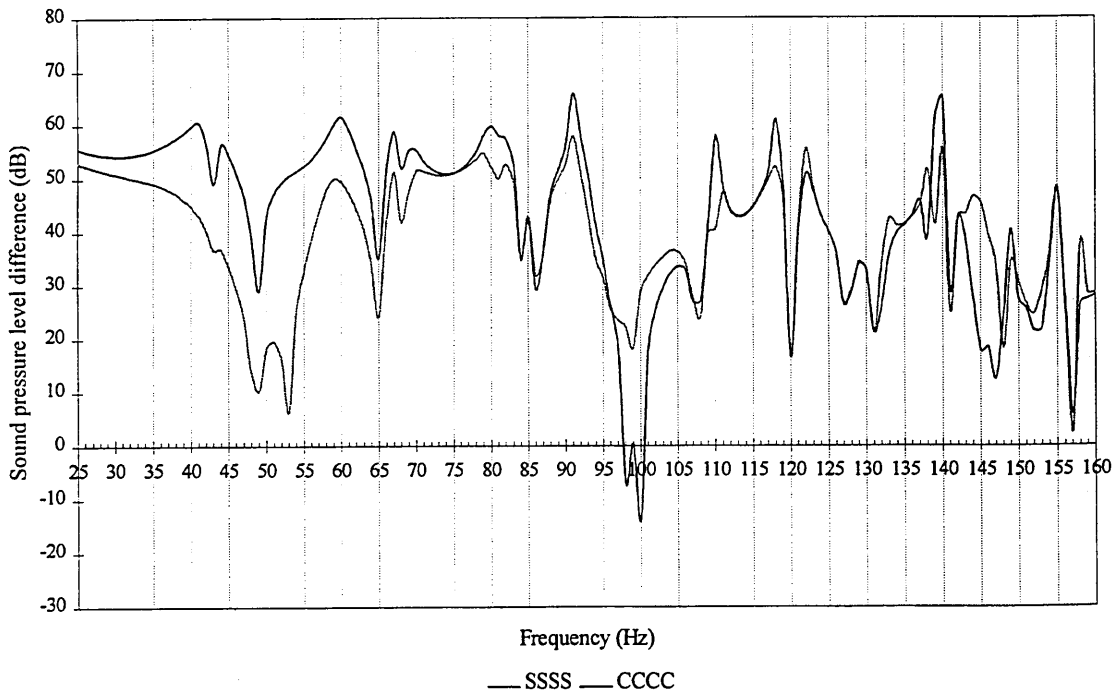
Figure 9.8. Sound pressure level difference of the 0.2m wall in narrow bands

217
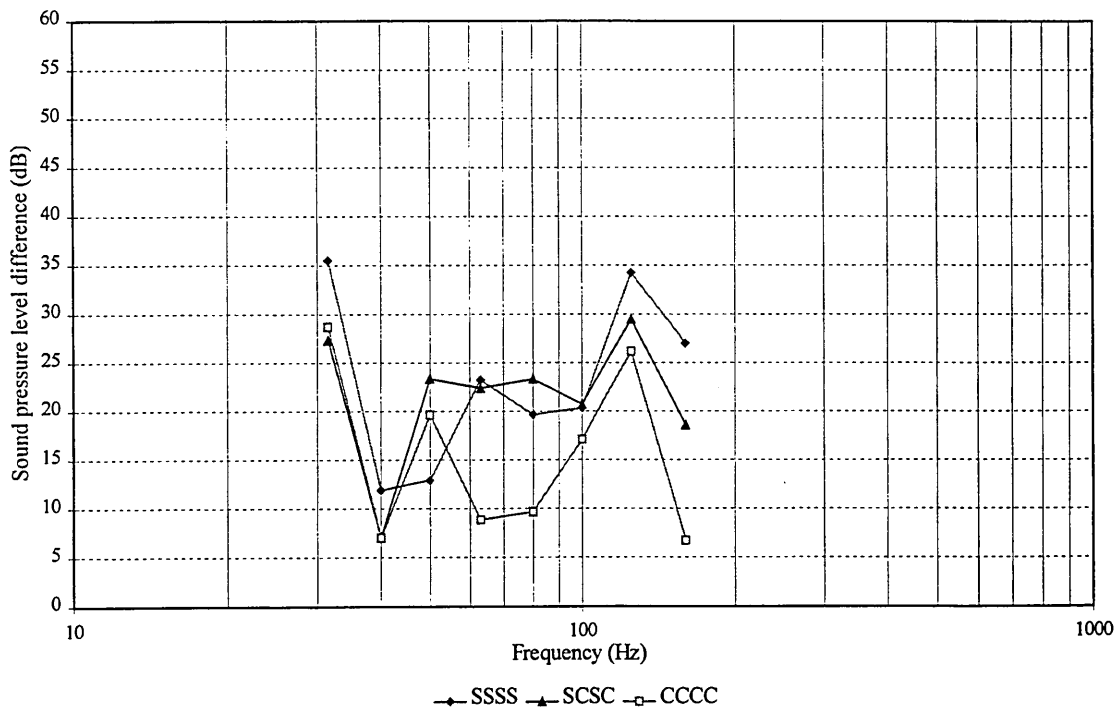
Figure 9.9. Sound pressure level difference of the 0.05m wall in 1/3 octave bands
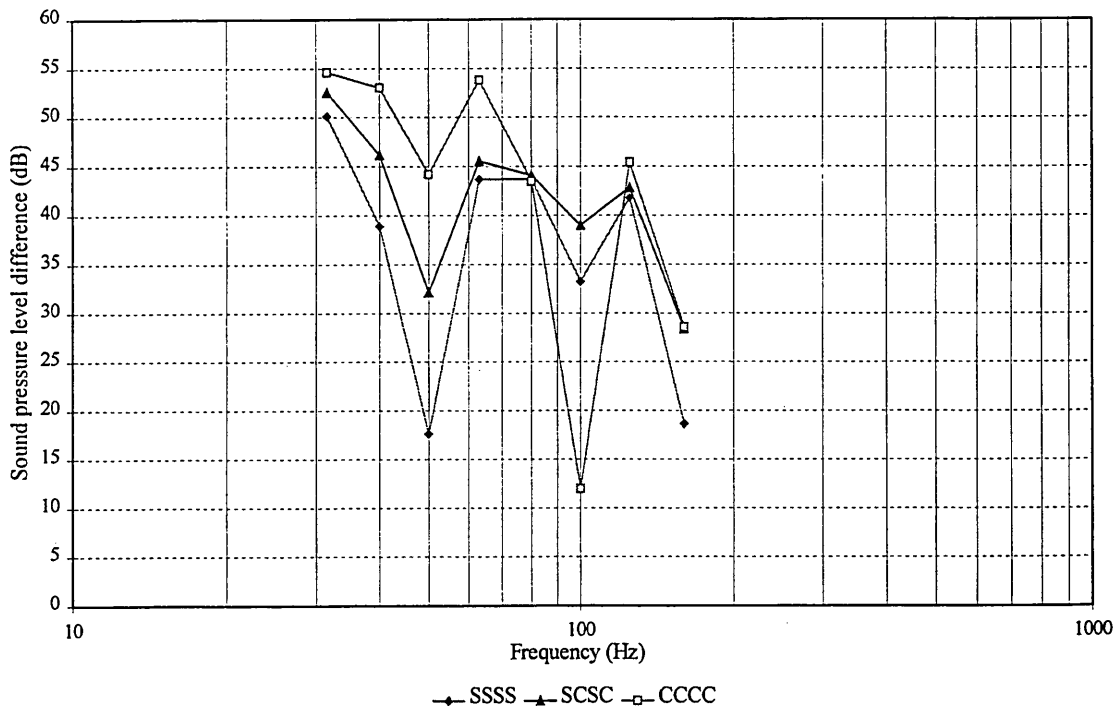
Figure 9.10. Sound pressure level difference of the 0.2m wall in 1/3 octave bands

218
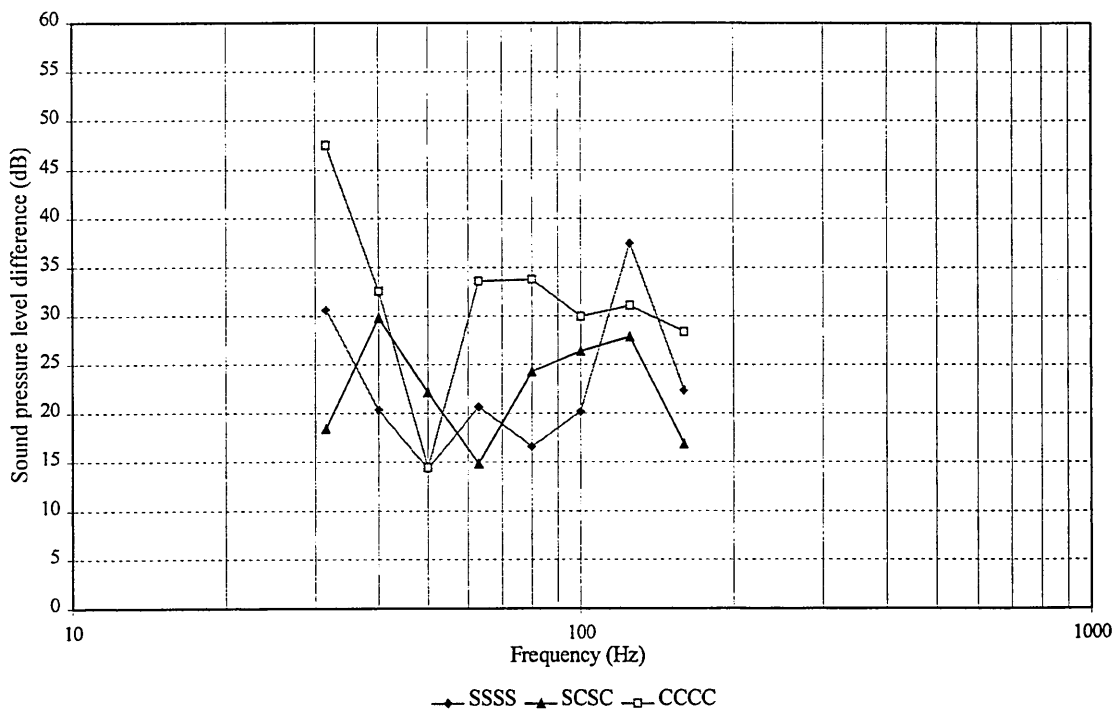
Figure 9.11. Sound pressure level difference of the 0.1m wall in 1/3 octave bands
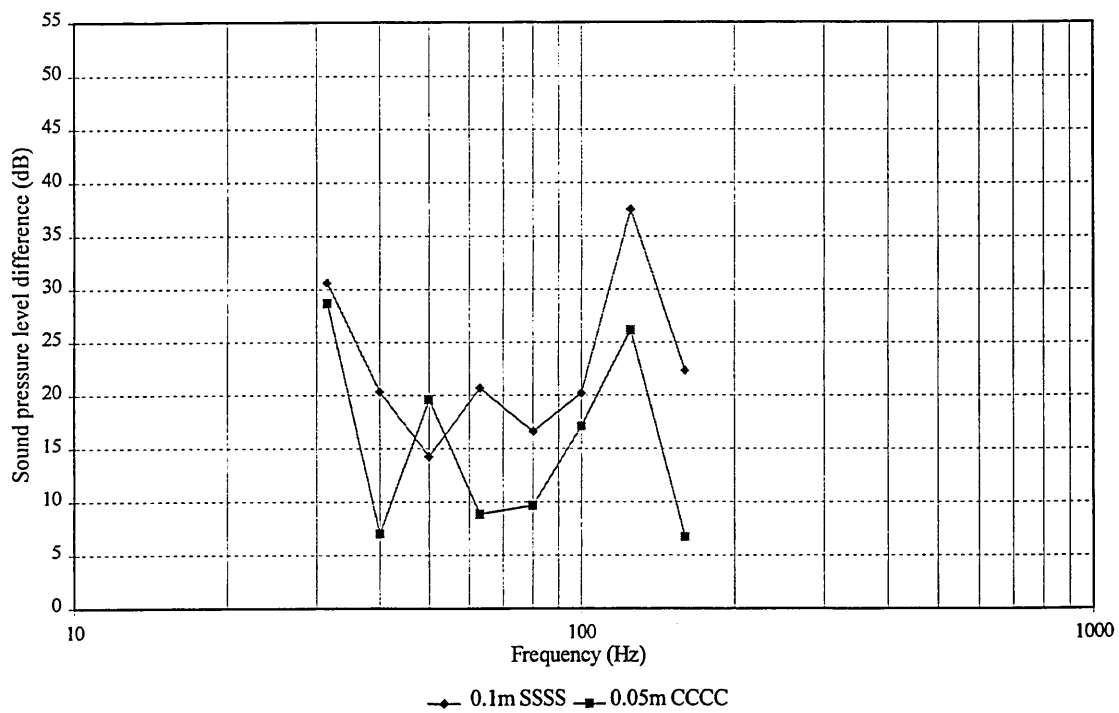
Figure 9.12. Sound pressure level difference of the clamped 0.05m wall and simply supported 0.1m wall in 1/3 octave bands
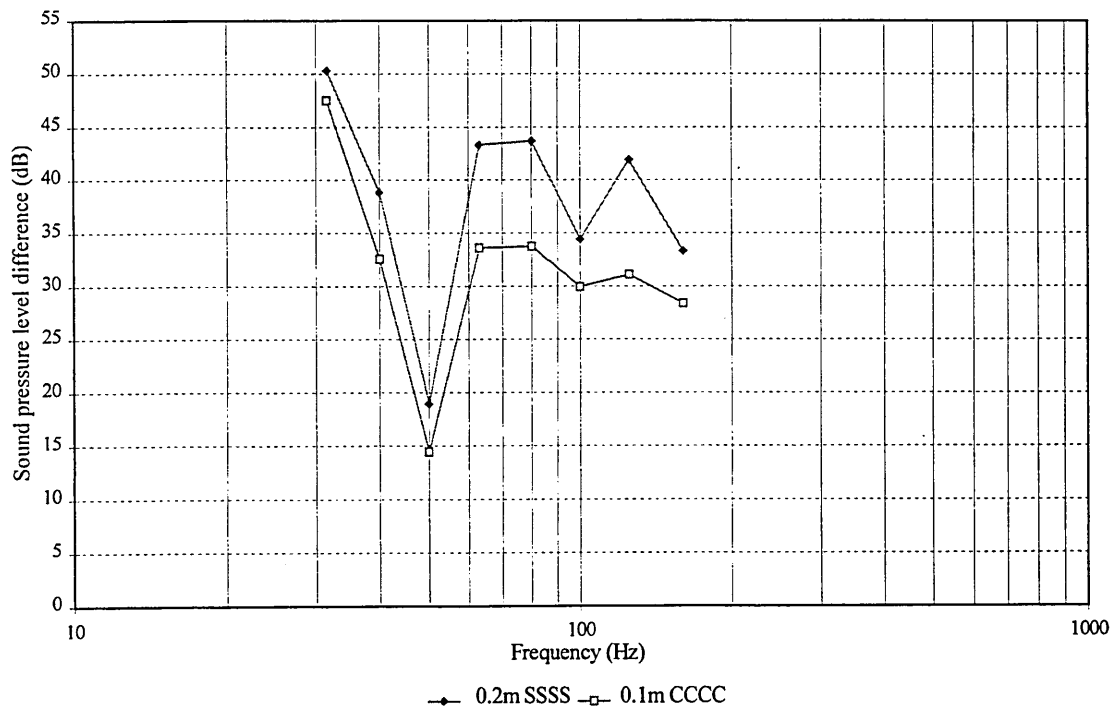
Figure 9.13. Sound pressure level difference of the clamped 0.1m wall and simply supported 0.2m wall in 1/3 octave bands

Type of Rooms	Bedroom 1	Bedroom 2	Bedroom 3	Living room	Living room + dining room
Room volumes in semi detached houses	25, 24, 32, 27, 34, 41, 55[3]	17, 19, 19.5, 19.5, 20, 22.6, 26	14, 13, 18.4	30, 31, 34	45, 44[1], 67[2]
Room volumes in storey blocks	28.2, 25, 28.6, 28.6, 20.4, 24, 21.4	15.7		37.5, 30, 37, 35	44, 44.8, 43.3

[1]: Leventhall [1972]: averaged living room size in domestic houses

[2]: Fothergill [1980-a] giving the volume for $67m^3$ for lounge room in Victorian Houses

Table 9.4. Typical room volumes found in dwellings

Equal Room Configurations		Unequal Room Configuration	
Source room m^3	Receiving room m^3	Source room m^3	Receiving room m^3
20	20	20	30
30	30	20	40
40	40	30	20
		30	40
		40	20
		40	30
		40	35

Table 9.5. Room configurations
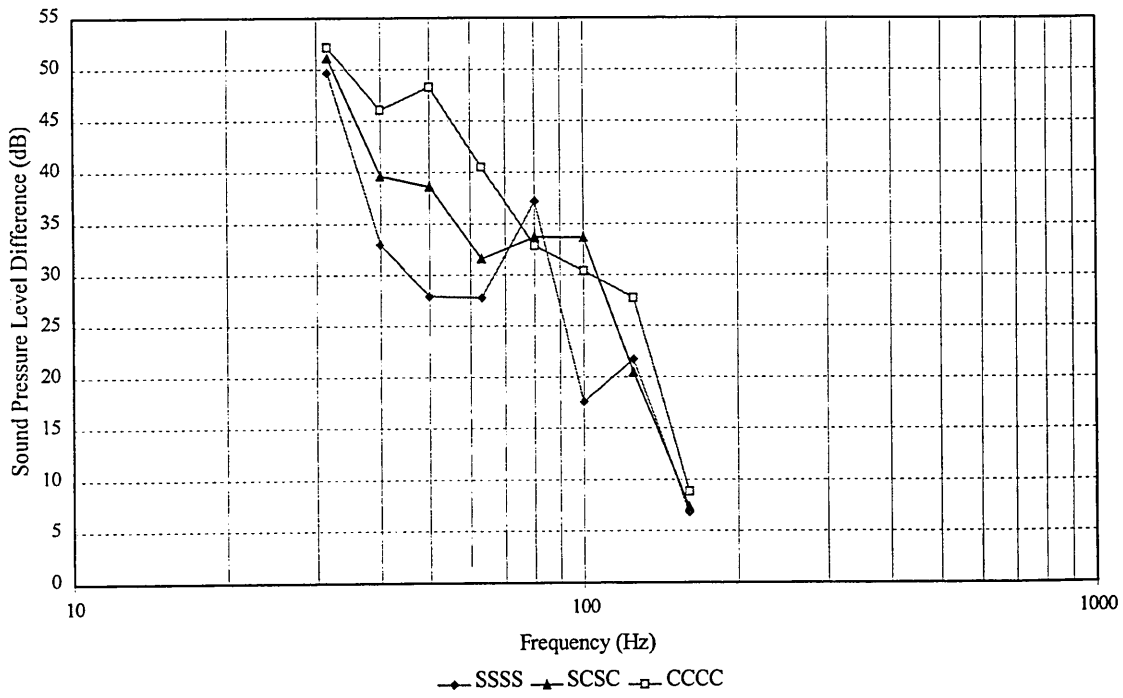
Figure 9.14. Effects of edge conditions on equal room configurations
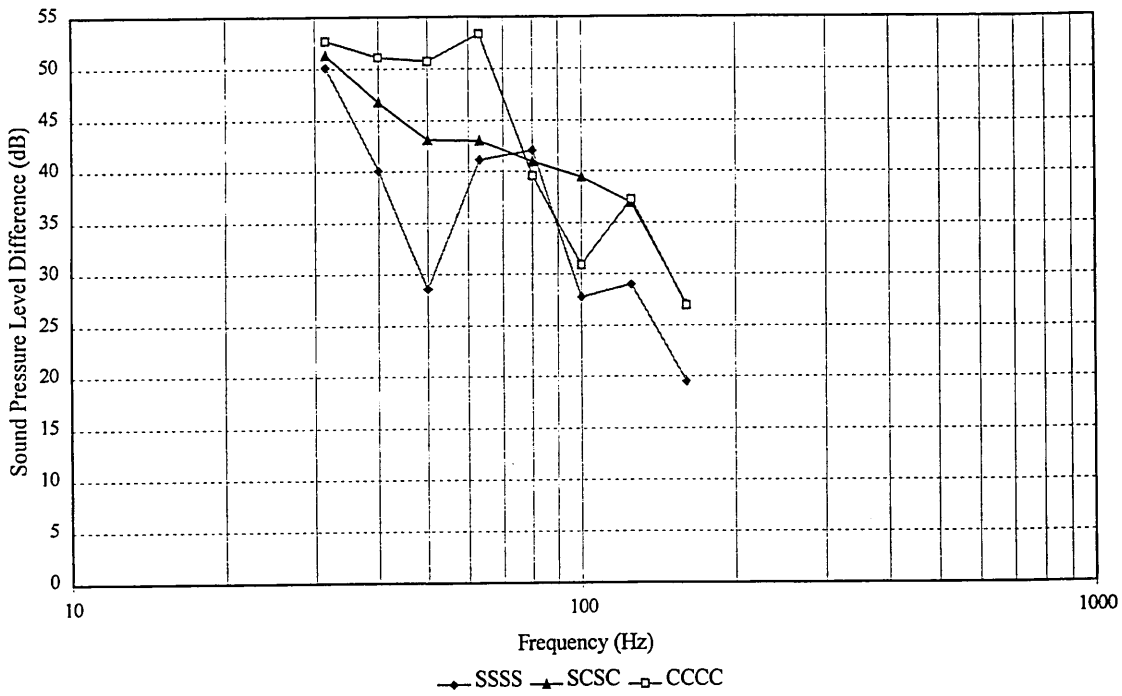
Figure 9.15. Effects of edge conditions on unequal room configurations
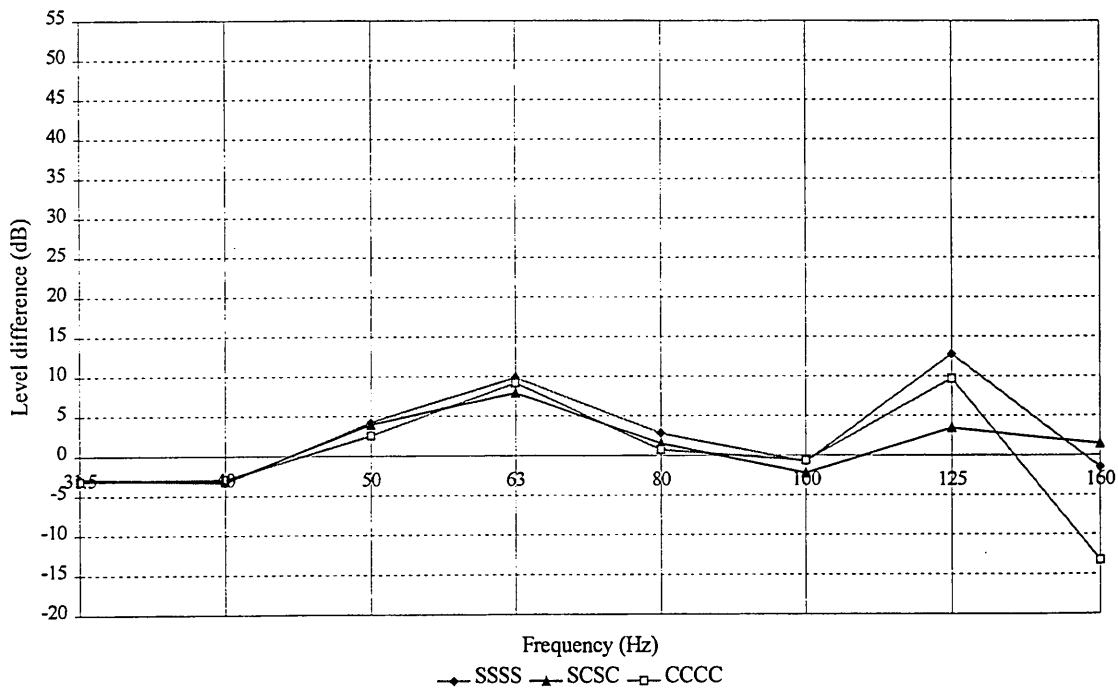
Figure 9.16. Effect of the edge conditions when the sound transmission direction is interchanged. Transmission room 30-20m^3 and 20-30m^3
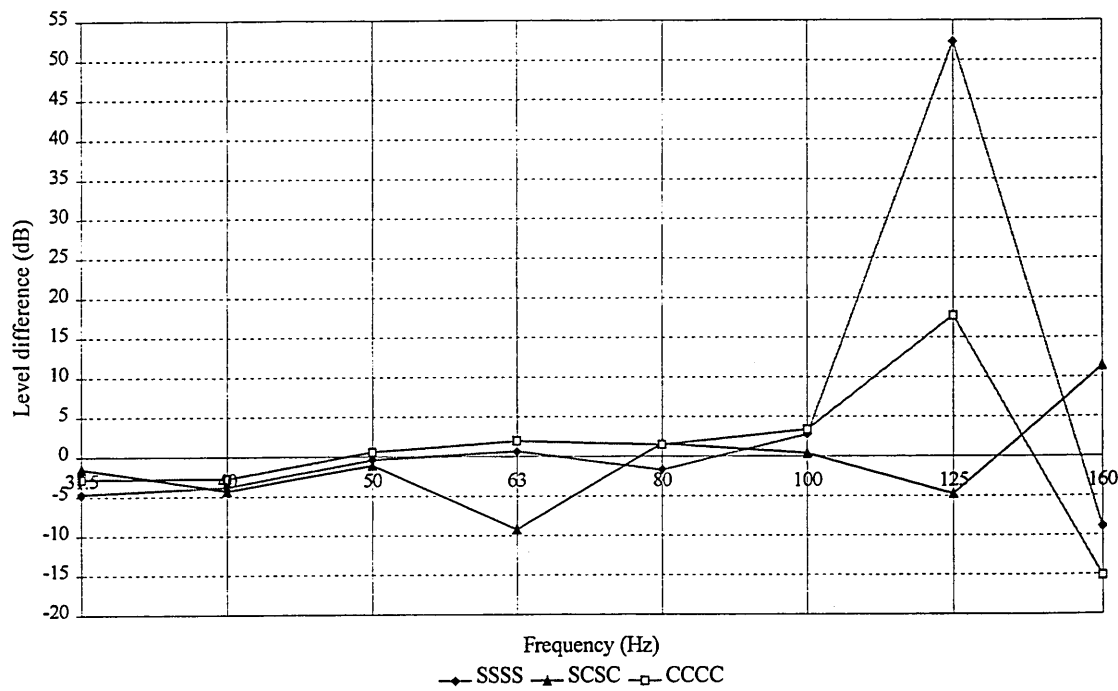
Figure 9.17. Effect of the edge conditions when the sound transmission direction is interchanged: 40-20m^3 and 20-40m^3
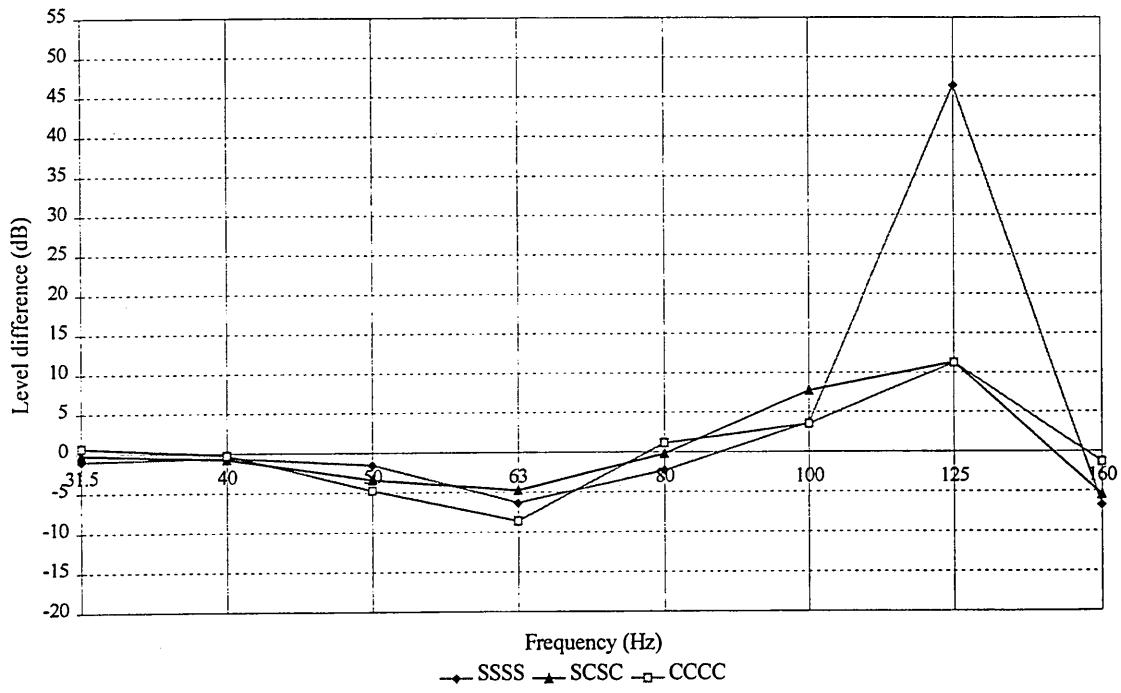
Figure 9.18. Effect of the edge conditions when the sound transmission direction is interchanged: $40\text{-}30\text{m}^3$ and $30\text{-}40\text{m}^3$
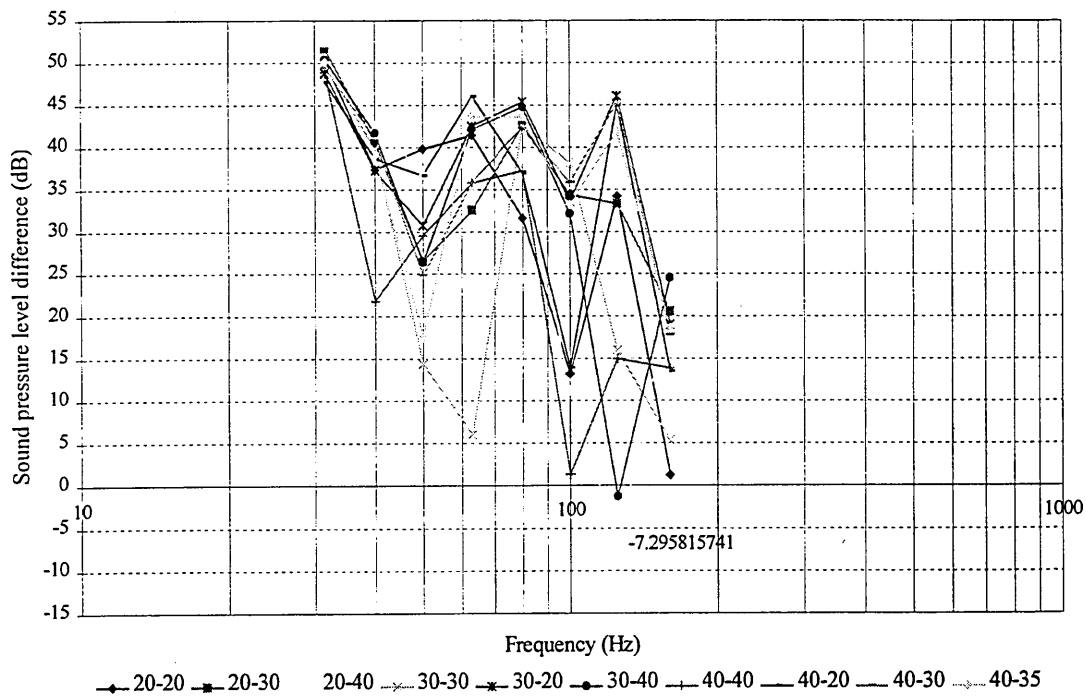
Figure 9.19. Effects of room configuration on a simply supported wall
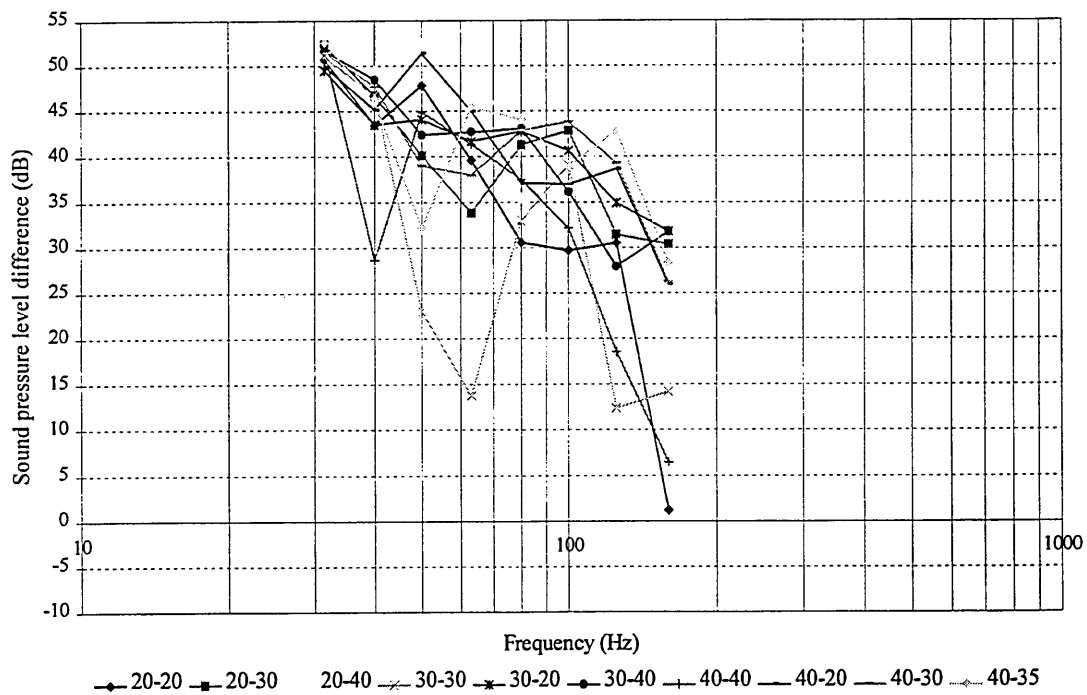
Figure 9.20. Effects of room configuration on a mixed edge conditions

225
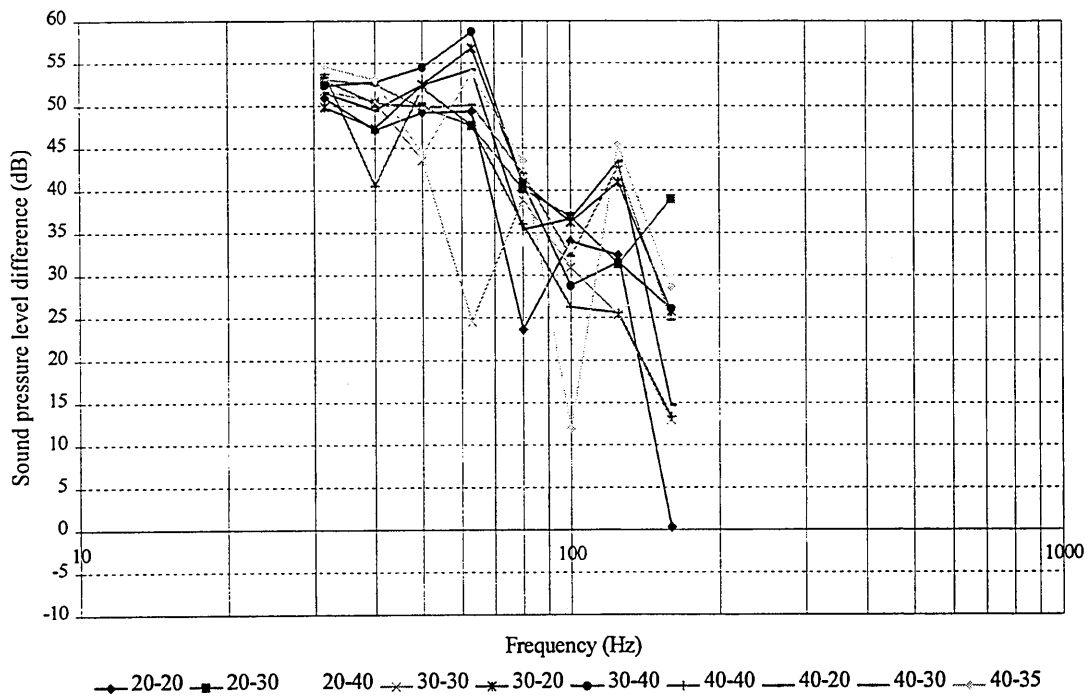
Figure 9.21. Effects of room configuration on a clamped wall
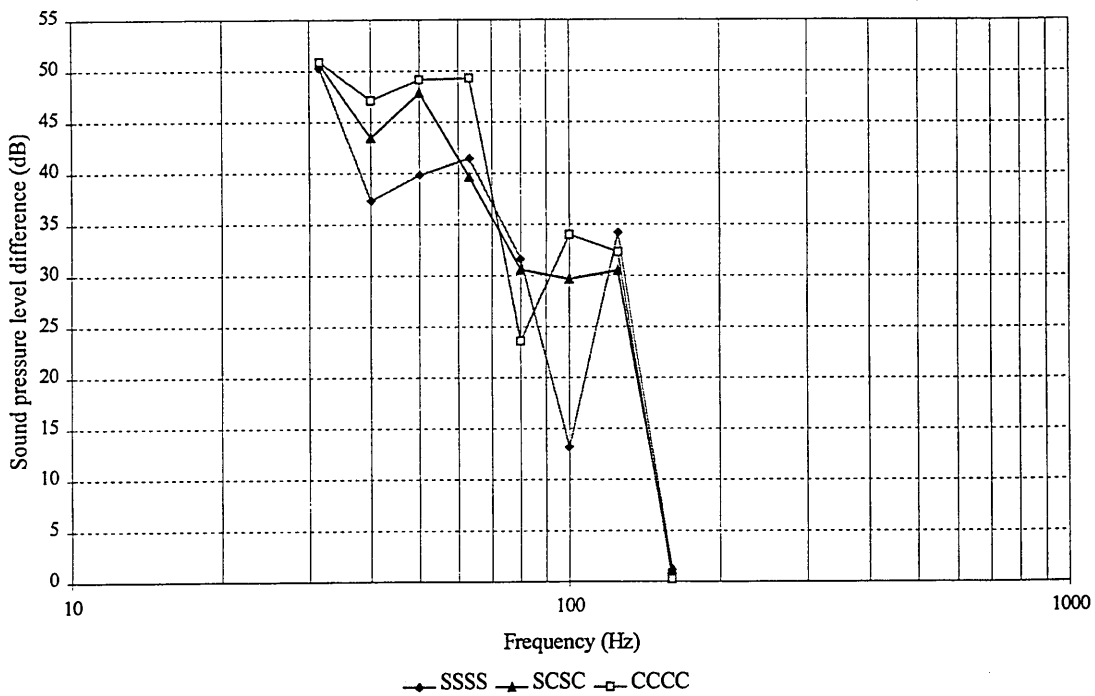
Figure9.22. Effects of 20-20m³ equal room configuration on sound level difference

226
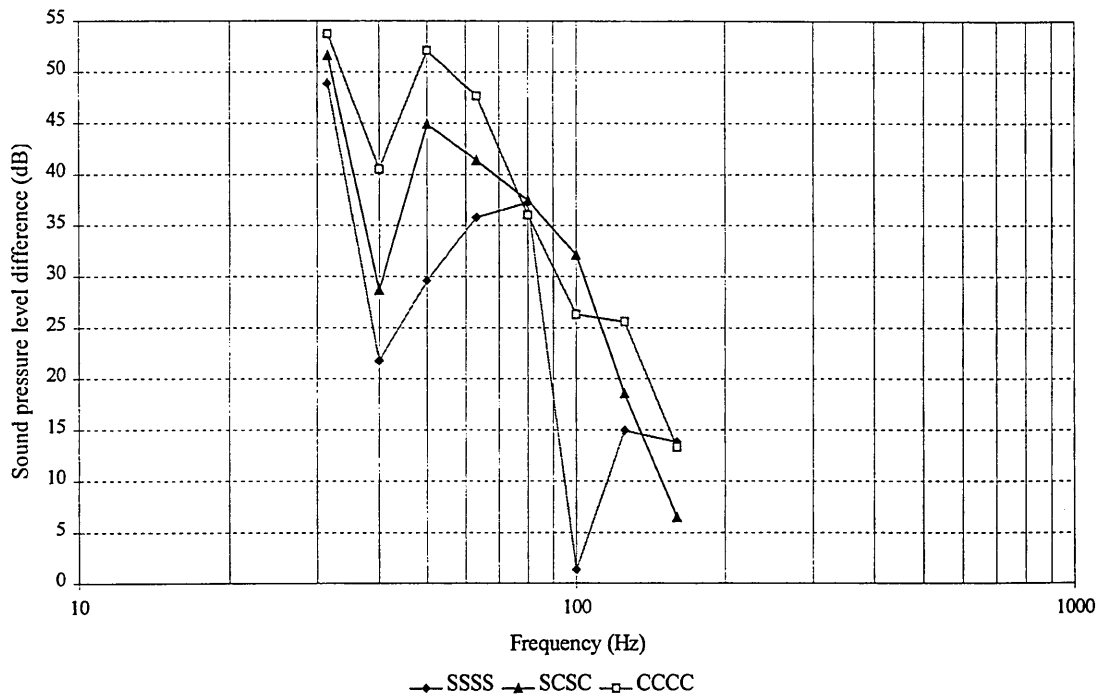
Figure 9.23. Effects of 40-40m³ equal room configuration on sound level difference
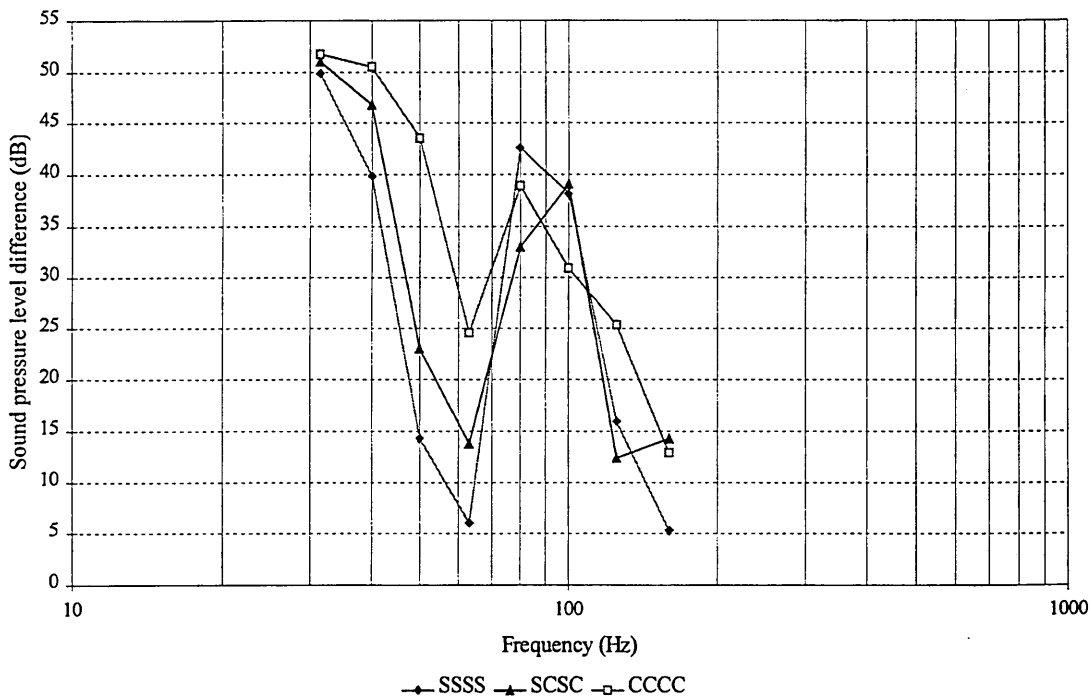
Figure 9.24. Effects of 30-30m³ equal room configuration on sound level difference

227
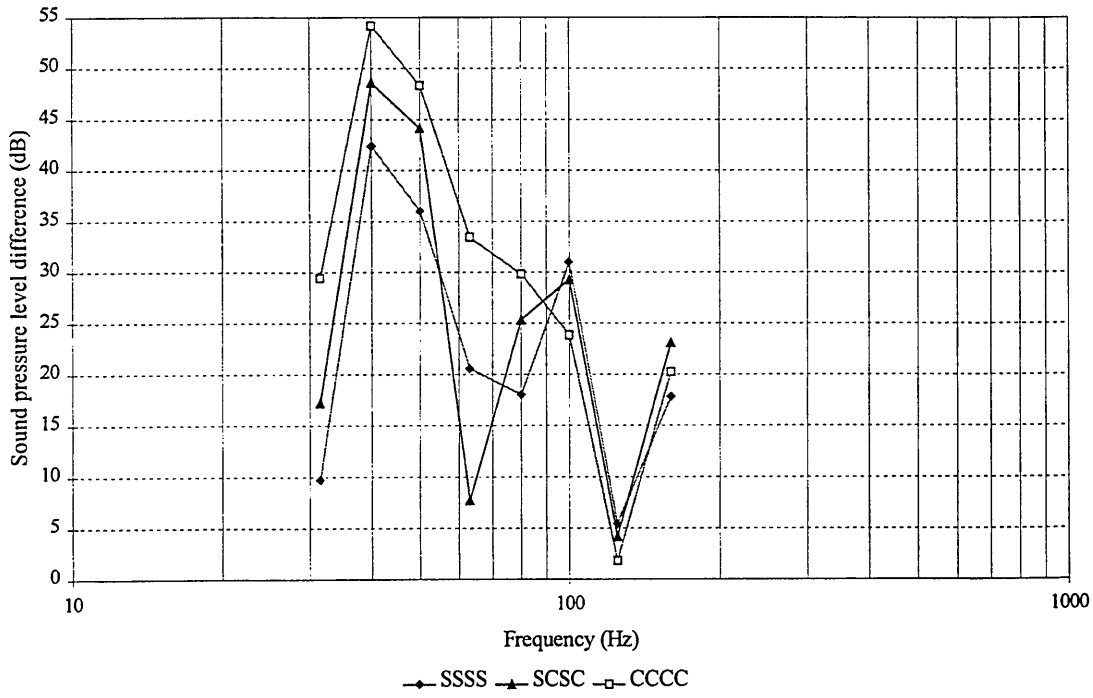
Figure 9.25. Effects of 50-50m³ equal room configuration on sound level difference
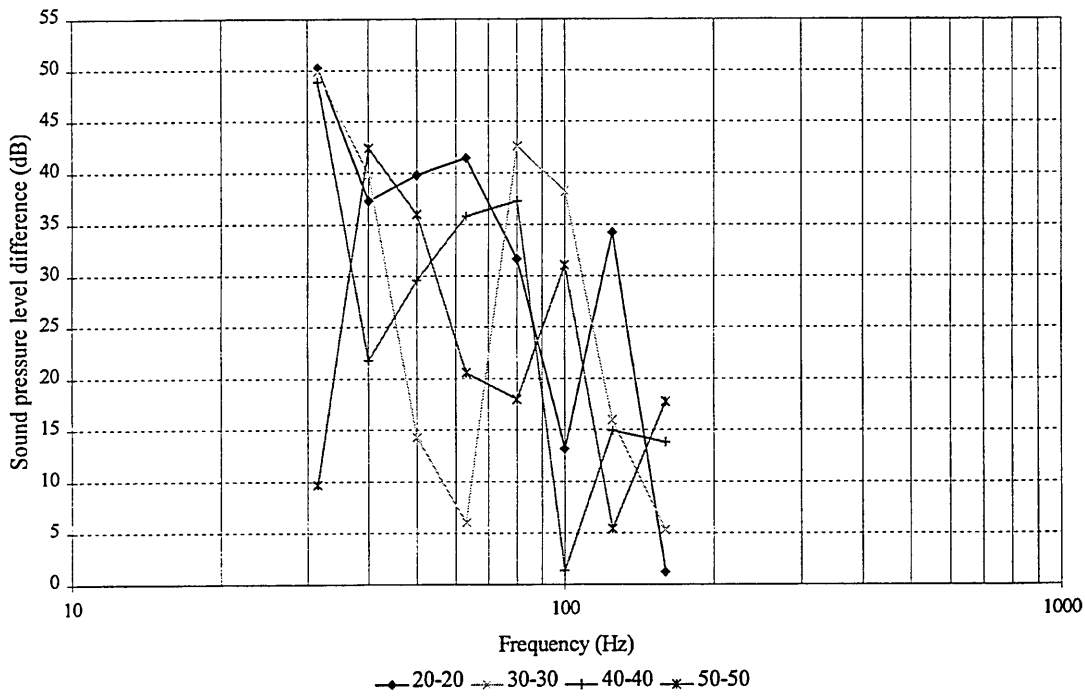
Figure 9.26. Sound level difference of a simply supported wall when placed in different equal room configuration
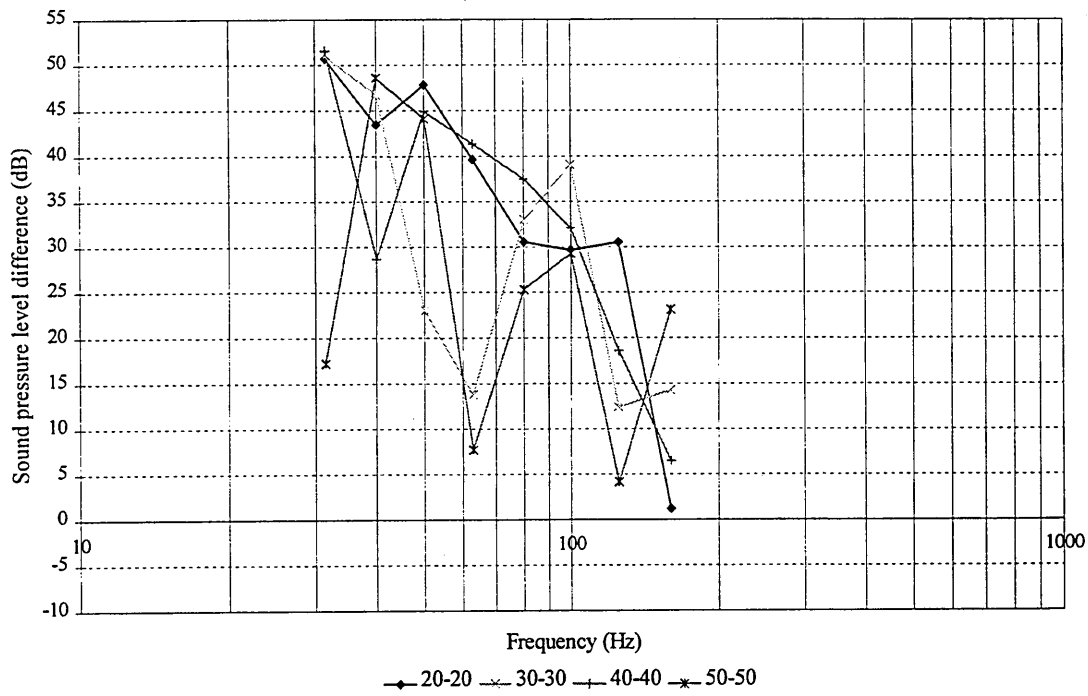
Figure 9.27. Sound level difference of a mixed edge conditions wall when placed in different equal room configuration
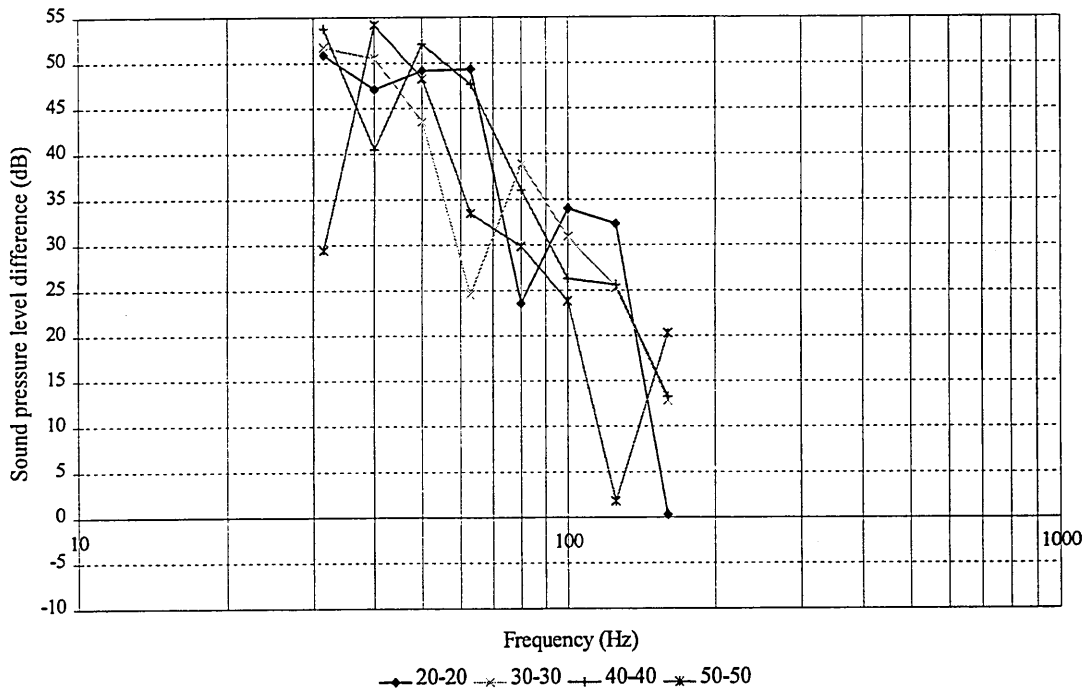
Figure 9.28. Sound level difference of a clamped wall when placed in different equal room configuration
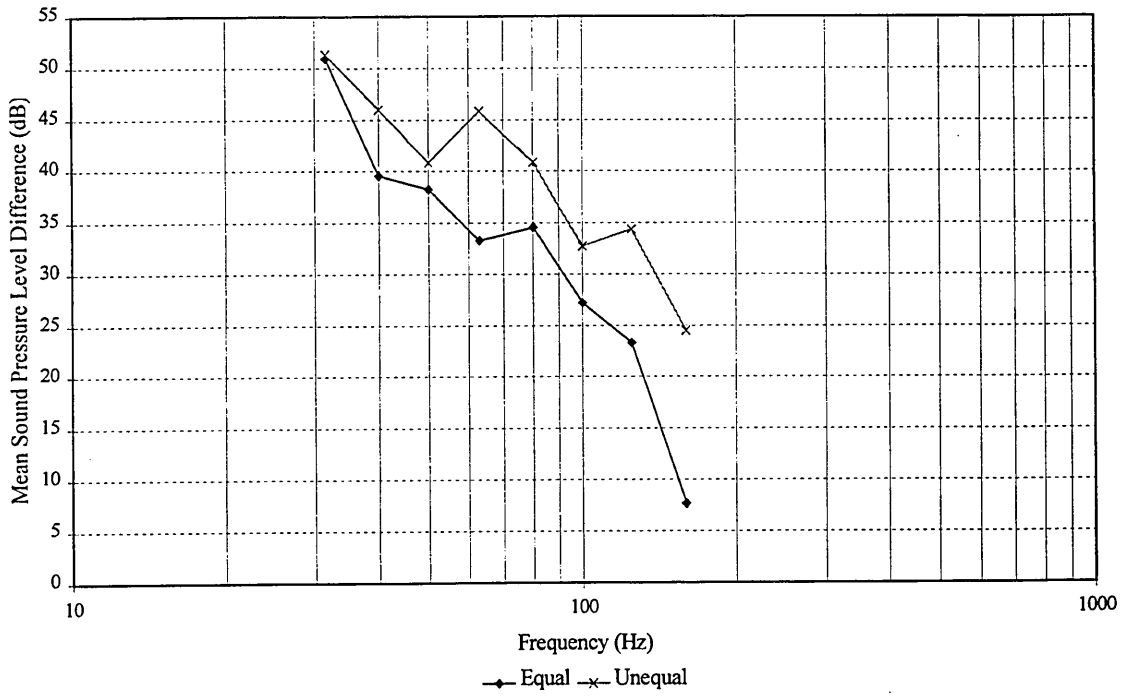
Figure 9.29. Effects of room configuration on the sound level difference
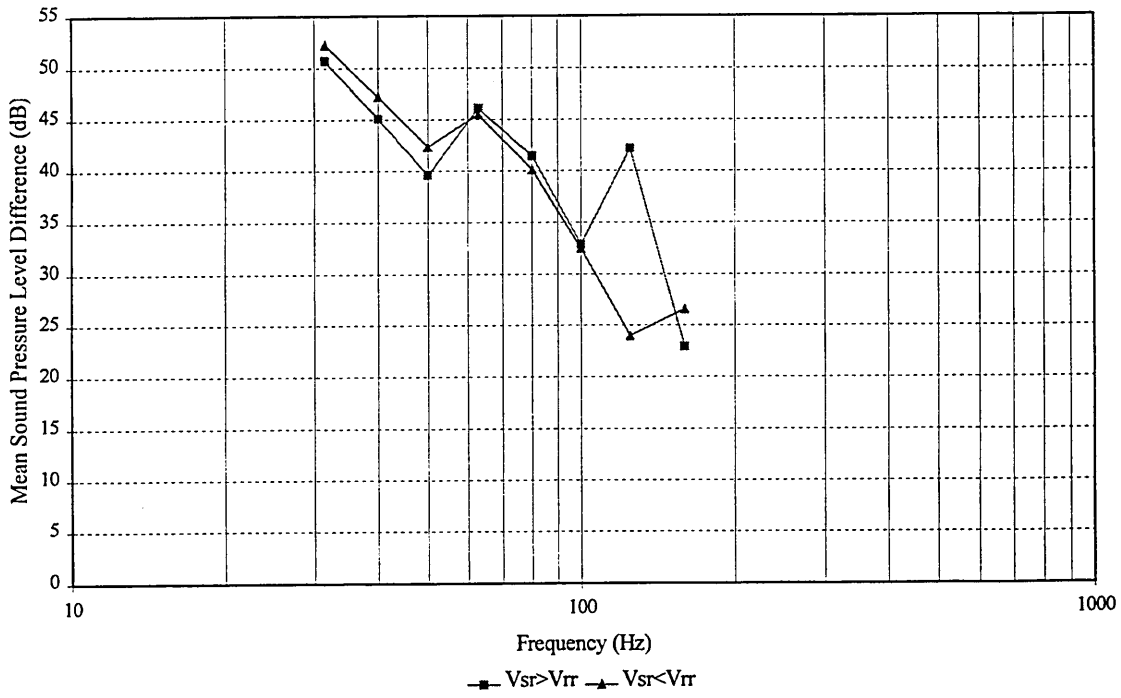
Figure 9.30. Effects of the source room volume on the sound level difference

Source room   Receiving room

Asymmetric transmission rooms

Source room

Receiving room
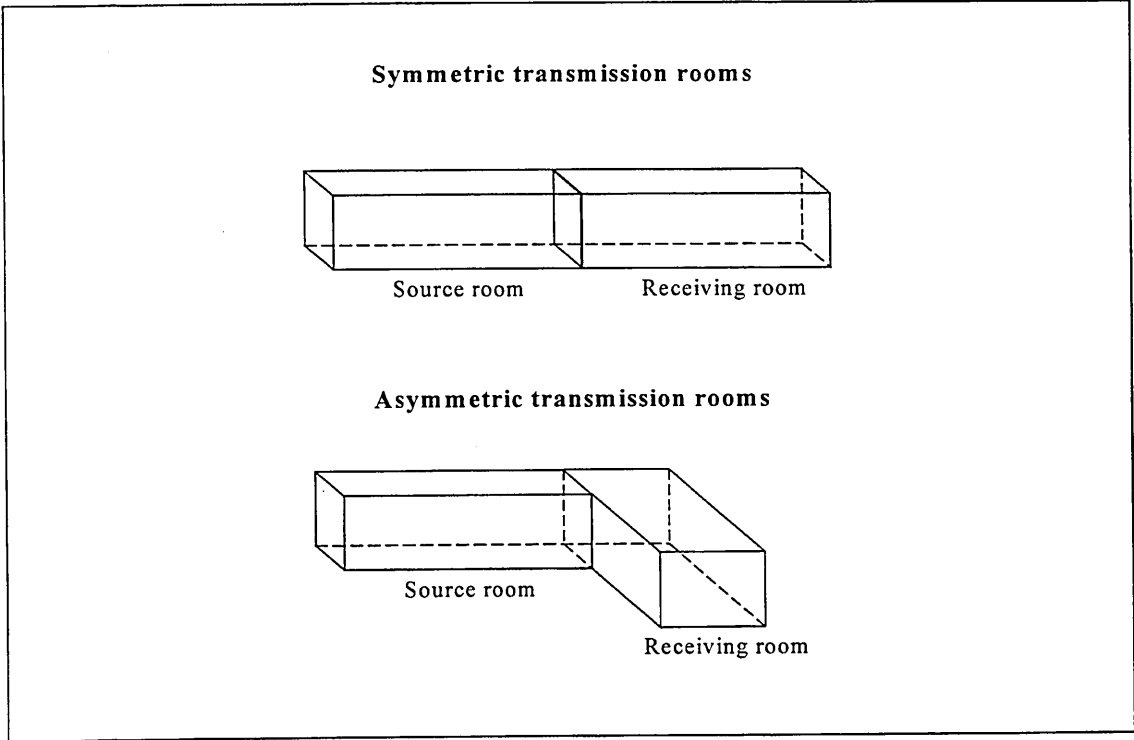
Figure 9.31. Symmetric and asymmetric transmission rooms

SYSNOISE - COMPUTATIONAL VIBRO-ACOUSTICS   party_3x25
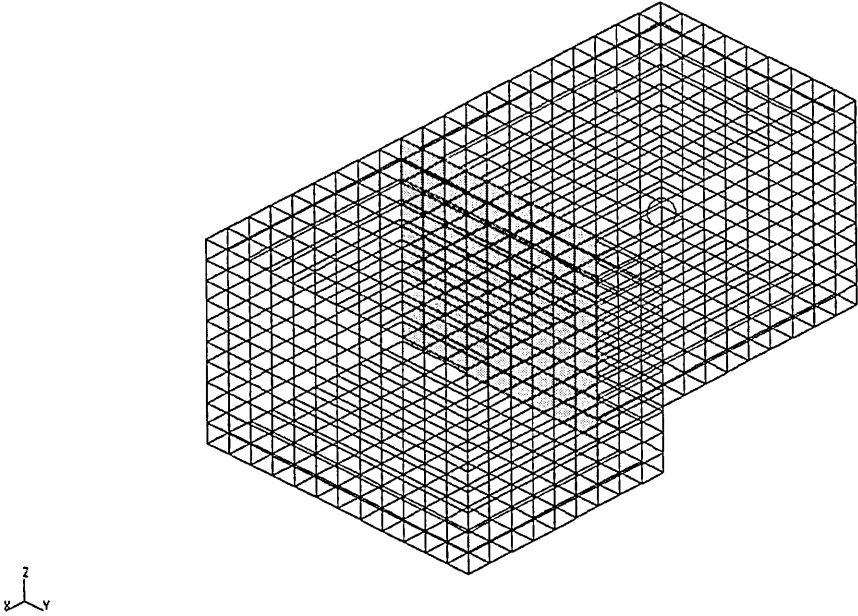
Figure 9.32. Model of the asymmetric rooms configuration of 30m^3

231
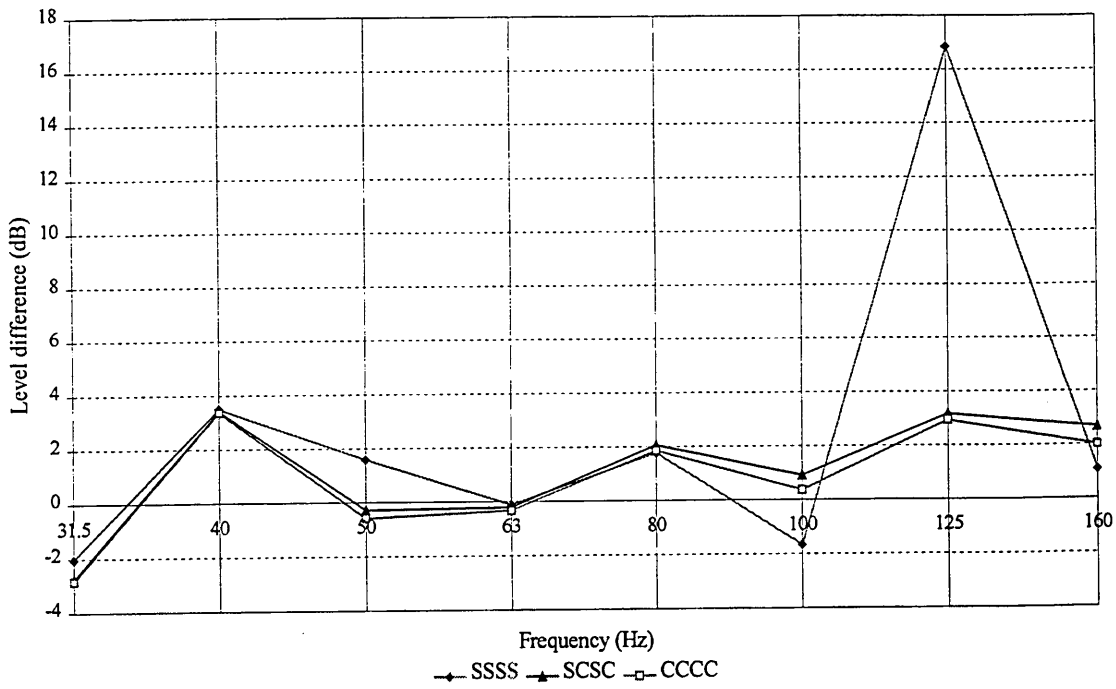
Figure 9.33. Effects of 20m³ asymmetric and symmetric equal configuration on the sound level difference.
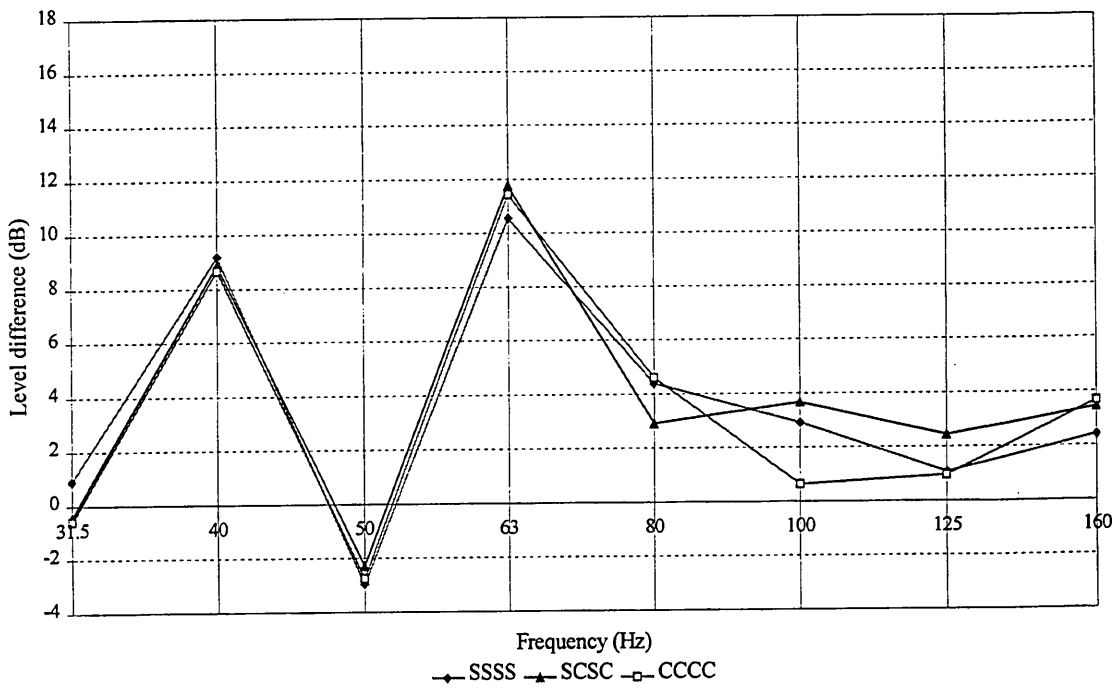
Figure 9.34. Effects of 30m³ asymmetric and symmetric equal configuration on the sound level difference
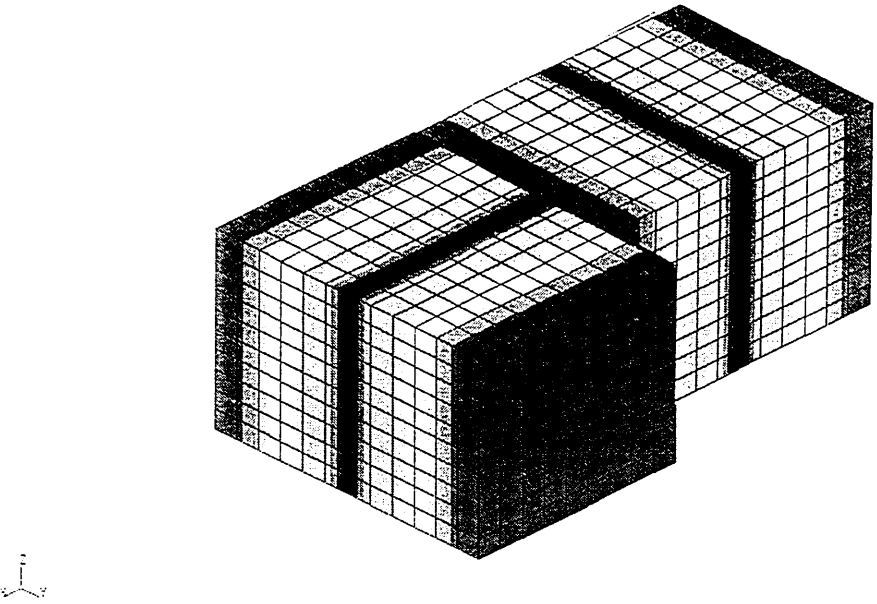
Figure 9.35. Excitation of the first acoustic axial mode in the asymmetric transmission rooms
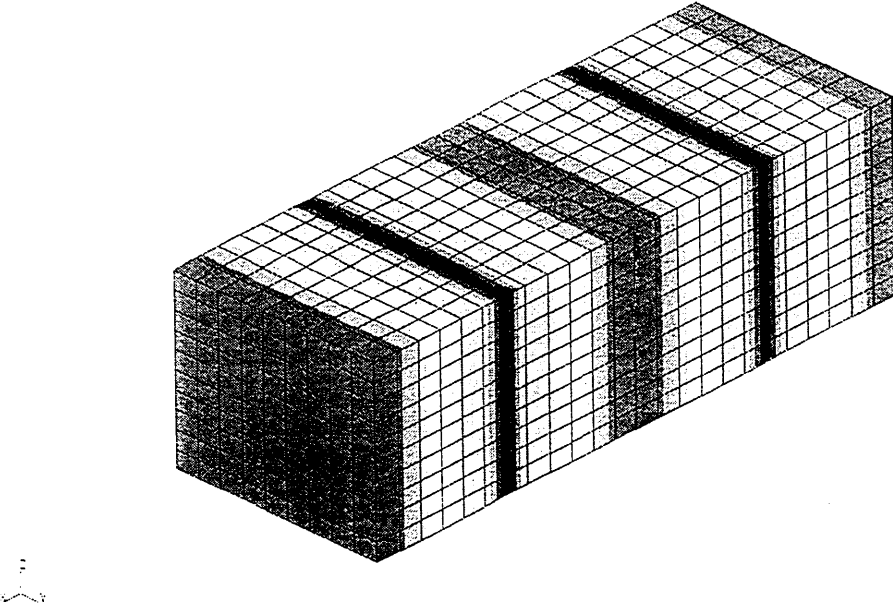
Figure 9.36. Excitation of the first acoustic axial mode in the symmetric transmission rooms

Thickness (m)	0.2			0.2		
Dimensions (m x m)	5 x 2.5			3 x 2.5		
Mode	SSSS	SCSC	CCCC	SSSS	SCSC	CCCC
1	97	159	177	64	97	115
2	206	240	295	143	200	209
3				176	218	253
4				247		

Table 9.6 Eigenfrequencies of the $5m^2$ and $7.5m^2$ party walls
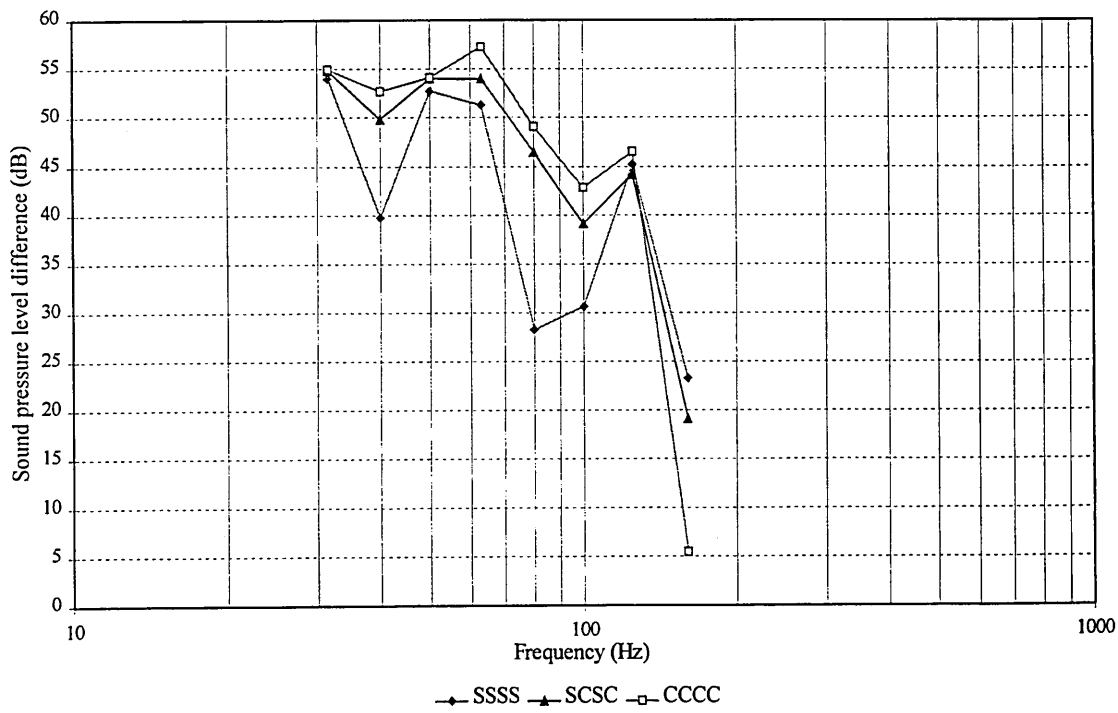
Figure 9.37. Sound level difference of the 0.2m wall of different edge conditions placed in a 20m³ asymmetric equal room configuration.
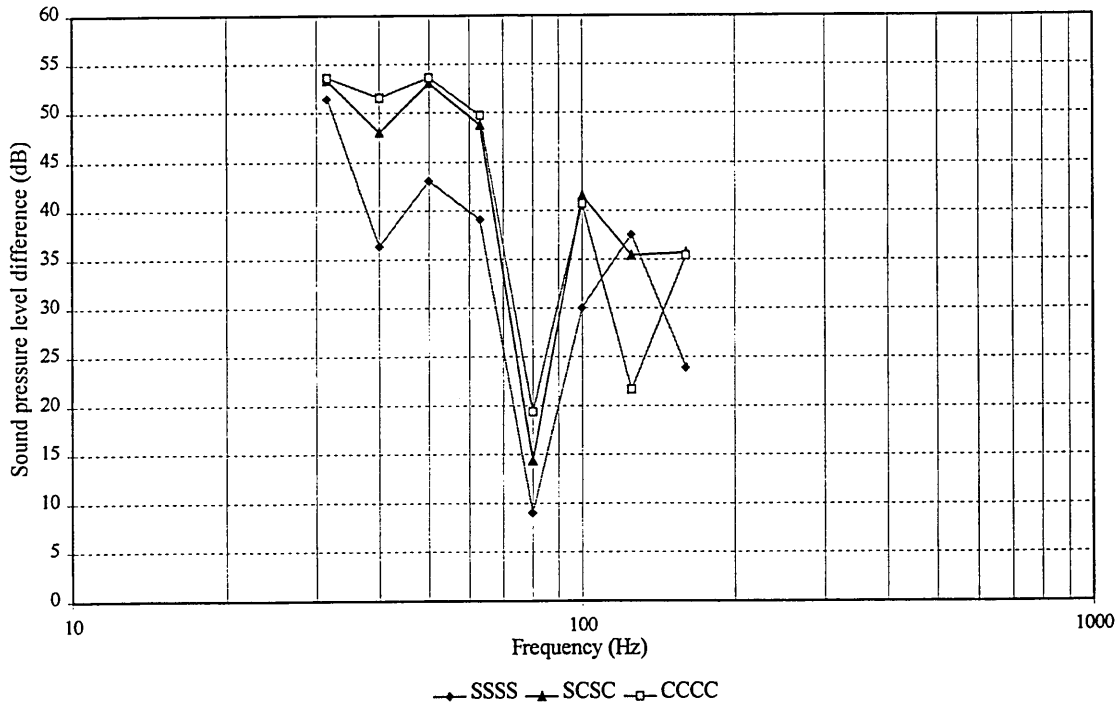
Figure 9.38. Sound level difference of the 0.2m wall of different edge conditions placed in a 30m³ asymmetric equal room configuration
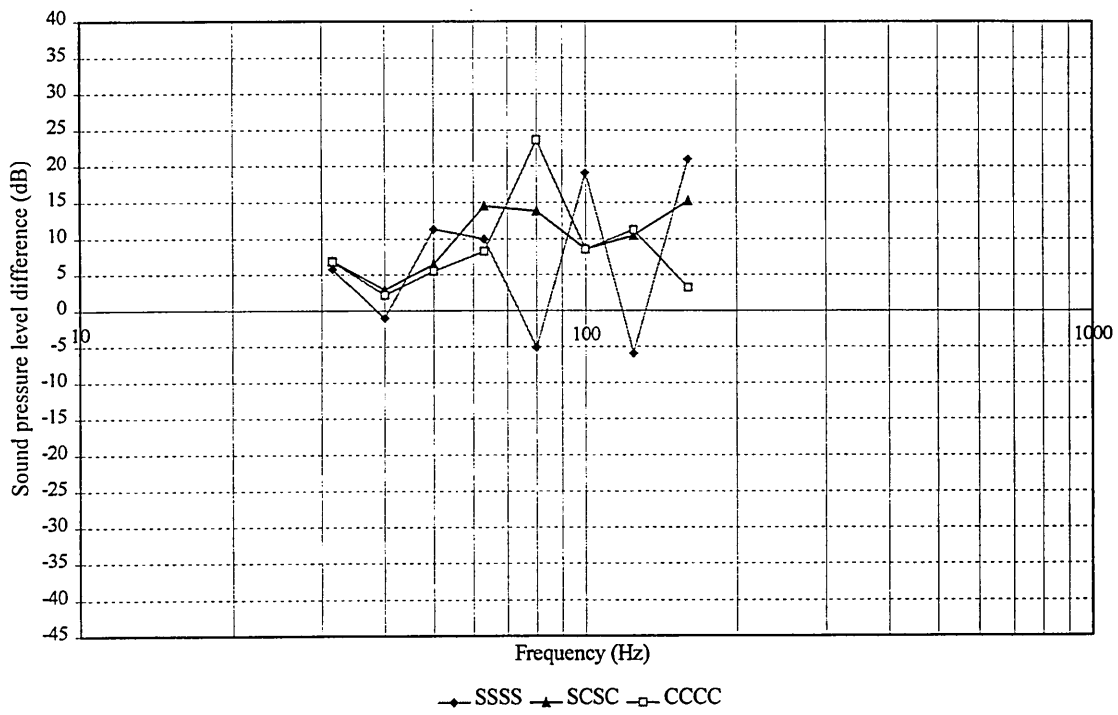
Figure 9.39. Effects of the size of the wall placed in a 20m³ equal room configuration on the sound level difference
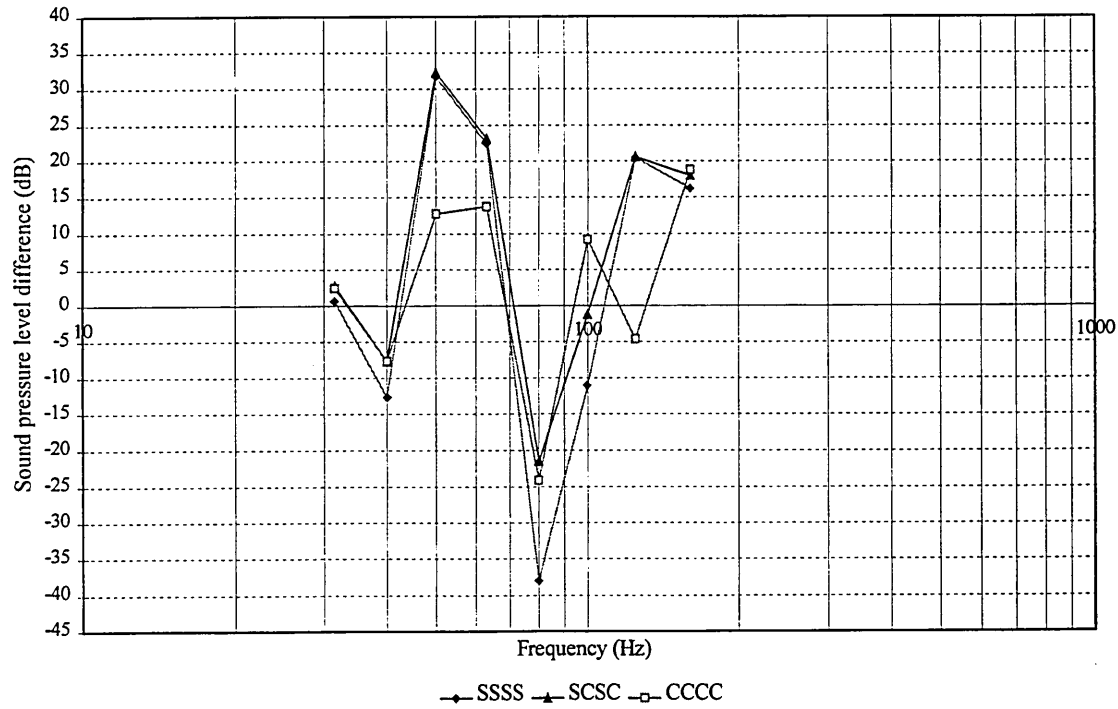
Figure 9.40. Effects of the size of the wall placed in a 20m³ equal room configuration on the sound level difference

236
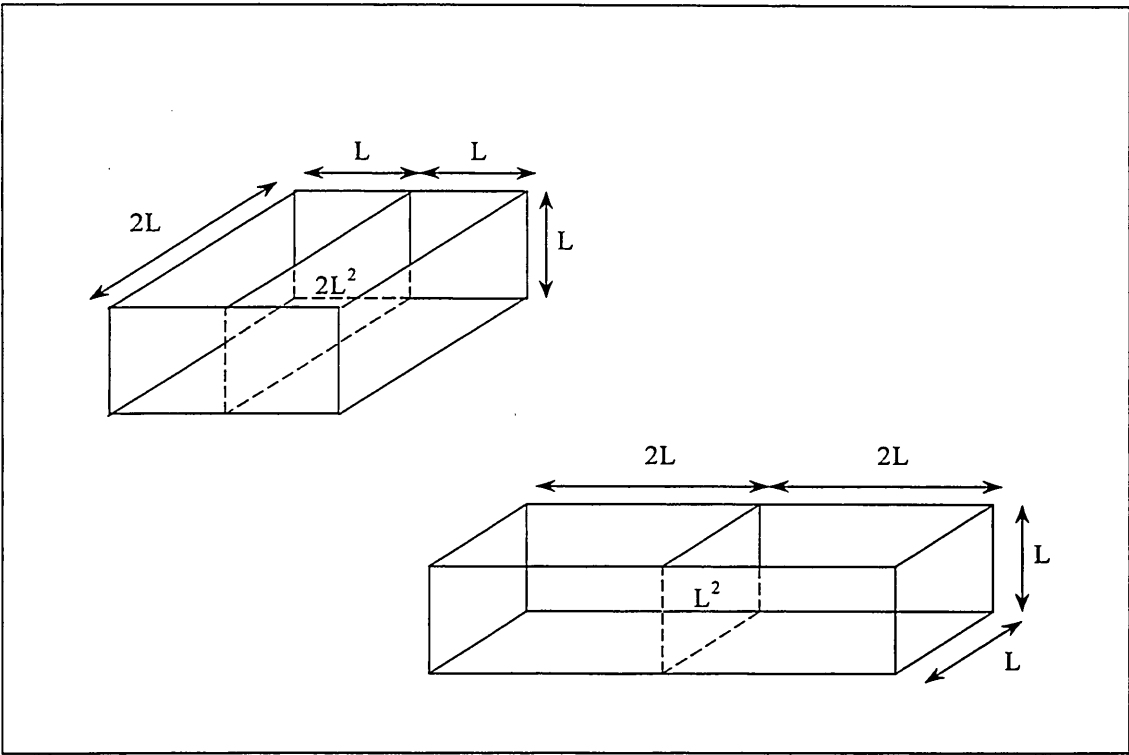
Figure 9.41. Size of the party wall

10 CORRECTION FACTOR FOR SOUND INSULATION IN DWELLINGS

10.1 INTRODUCTION

The deterministic study of the sound transmission at low frequencies in dwellings in Chapter 9 highlighted that room configurations and edge conditions influence considerably the sound level difference. Also, the sound level difference of a real wall installation is likely to be between that of an idealised simply supported and clamped wall. The variability of the sound insulation of a wall needs therefore to be taken into account by defining a correction factor since laboratory measurement does not provide the correct values.

The objectives of this chapter therefore is to make some attempts to predict the sound insulation of a $10m^2$ party wall when built into the range of domestic buildings.

10.2 REVIEW

Kihlman et al [1972], Utley [1968], Bhattacharya et al [1972] investigated the effects of the room configuration on the sound reduction index data of the party wall placed in laboratories using the traditional method of measurements described in Chapter 4. All show experimentally that the room configuration affects the measurements. In particular it was demonstrated that equal room configurations provide the lowest measured sound level difference and hence implied sound reduction index. Bhattacharya [1972] suggested a new correction factor to take into account the room dimensions.

Kropp et al [1994] and Pietrzyk et al [1997] investigated the effect of partition position by calculating the sound level difference of 16 room combinations. Limp and simply supported solid walls were investigated. The effects of boundary conditions were not taken into account. The mean sound pressure level difference in equal rooms is found to

238

be lower than that in unequal room configurations and it is also observed that the sound level differences vary more with volume change for the equal room configurations. For the simply supported solid wall, the expected drop of sound level difference when the two rooms are identical was not observed. A greater reduction in sound insulation was obtained when the partition was moved 0.75m from its original position due to the close matching of the room and wall modes.

In addition, Kropp et al [1994], Pietrzyk [1997] and Osipov [1997] have generated standard deviations and minimum and maximum deviations, but no attempts to define a correction factor.

10.3   STATISTICAL CORRECTION FACTOR

We would like to predict the sound level difference values of a 0.2m thick brick wall when built in domestic buildings ie the likely sound insulation value, the flexible wall will take when placed in a certain room configuration. A statistical analysis of the sound level difference data [Gibbs at al (1998)] obtained for the simply supported, the clamped and the mixed edge conditions is required in order to state, with a fair measure of confidence, the sound level difference of the party wall.

A statistical analysis can only be applied if the events cannot be predicted with certainty, but the relative frequency with which they occur in a long series of trials are often remarkably stable [Godfrey (1988)]. Such events possessing this property are called random or stochastic. In this case, the event is the room configuration, as the sound level difference is dependent upon the room configuration.

Are we in the presence of random events? If a transmission room with a volume of $20m^3$-$30m^3$ is considered, a specific sound level difference is processed for each third octave band. As the frequency range of interest is 31.5Hz to 160Hz, 8 values of the sound level differences are processed. If the simulation was repeated, the same sound level difference would be obtained. Consequently, we are in the presence of events,

which are not random as the room configurations were chosen among the full room configurations found in dwellings. Moreover, the events generate sound level difference values which can be predicted. Therefore, we are in the presence of an ordered, rather than a random population.

Even if the population was random, the sample of studied room configurations is also too small for a correct prediction of the sound level difference. The minimum required sample for a statistical study is 30 in order to have accurate standard deviations and confidence limits [Godfrey et al (1988)].

To summarise, statistical analysis strictly should not be applied to predicted sound level difference data, because the studied population of room configurations is not random. However, in the presence of a large sample, a statistical study would allow us to observe and quantify the acoustic-structural coupling effects on the sound level difference. The statistical study could then be compared with the deterministic study to see if the two studies come to the same conclusion.

Although the sample in this study is small, attempts were made to define a correction factor using the worst case i.e. the lower limit given by the standard deviation, as a preliminary study. The standard deviation was calculated from the sound pressure level difference of 10 room configurations, for each edge condition. The data are presented in Figure 10.1. The standard deviations are greatest for simply supported and mixed edge conditions, in the 40 to 63Hz third octave bands. In this case the standard deviations of the mixed edge conditions and the clamped tend to be the same.

As the edge conditions of real party walls were found to lie between simply supported and clamped as seen in Chapter 9, the highest standard deviation was selected to predict what likely values the sound insulation of a $10m^2$ party wall will take in the different third octave bands. The correction values are given in Table 10.1.

If equal room configurations only are considered (see Figure 10.2 and Table 10.2), different standard deviations are obtained. They cannot be compared with those in Table 10.3 as the sample size was 3. The data can be compared with Figure 10.3, which

240

displays the standard deviations of the same party wall when placed in unequal rooms where the source room volume is greater than the receiving room volume. The standard deviations for equal rooms are seen to be greater than those for unequal rooms. Equal room configurations therefore provide the worst sound insulation as seen in Chapter 9.

The standard deviations obtained for the three edge conditions are displayed in Figure 10.4. They might be more appropriate as correction factors, because the sample is 30, but cannot be compared with values given in Table 10.2.

To this point, the correction factors were defined for sound insulation measurements in dwellings of room volumes smaller than 40m³. No correction factor was defined for a specific room configuration. Although the population is not random, and the sample is only 3, the standard deviation was calculated for each room configuration for the three different edge conditions. The results are given in Table 10.3. The standard deviations are different for each room configuration except at 31.5Hz and 40Hz. There is no reciprocity between room configurations of same volume. All values are collapsed to give Table 10.4. Again, differences between standard deviations are obtained for the different room configurations.

Consequently, correction factors were defined from the standard deviations calculated from the sound level differences obtained for the three different edge conditions. This statistical study was only a preliminary study and is not correct to use, because the samples of room configurations or edge conditions are smaller than 30. It therefore needs further work with a much larger sample of room configurations.

10.4   DETERMINISTIC CORRECTION FACTOR

Since the statistical analysis is not reliable, attempts were made to define a deterministic correction factor in each third octave band frequency. The parameters responsible for variations of sound pressure level difference when varying the room configuration are presented below;

1. The height of the room is 2.5m and remains constant whatever the dwelling room as shown in Section 9.5.1. The axial mode along the z-axis therefore is likely to be the same whatever the room configuration. The structural mode along the z-axis is the same when the party wall is of same material properties and thickness.

2. Width in this present study was kept constant when investigating equal and unequal room configurations. The width of the rooms and also the length of the party wall are constant at 4m. Identical acoustic and structural modes take place along the y-axis.

3. y- and z- axial modes and yz-tangential modes are identical in each room configuration, giving couplings of modes of same shape and eigenfrequencies.

4. Acoustic and structural couplings are the same, when the party wall placed in the different room configurations have the same structural modal distribution.

5. Wall size, $10m^2$, is a reasonable value for dwellings. However, there is a high chance to find party walls of other dimensions. The change in size will lead to different resonances, acoustic-structural couplings, and thus different sound pressure level difference values

6. Thickness of the wall will change the strength and position of the acoustic-structural couplings

7. Double and single masonry walls have different structural modal distributions and thus acoustic-structural couplings.

8. Edge conditions of party walls are likely to vary with the building design and workmanship and thereby modify the structural modes in the frequency range of interest, giving rise to different acoustic-structural couplings.

9. The length of the room is modified when modifying the room configuration. The acoustic modal density is changed as the position of the excited acoustic modes in the frequency range of interest.

Consequently, the correction factor for sound insulation of a masonry wall must include the effects of acoustic and structural modal densities.

Three attempts were made for each third octave band. The first attempt was to calculate the mean value of the sound level difference data obtained for simply supported and

clamped and also select the maximum and the minimum sound level difference in each band to evaluate the spread of the data. The results for the simply supported and the clamped are presented in Figures 10.5-6. As expected the spread of data is not constant when the party wall is simply supported, but then tends to be when the party wall is clamped. The maximum values for the simply supported case are greater than for the clamped wall. As the edge conditions of real walls lie between simply supported and clamped, the sound level difference is going to lie between the minimum values of the simply supported and the maximum values of the clamped. The mean sound level difference was calculated accordingly and displayed in Figure 10.7, including the maximum and minimum deviations. The maximum and minimum deviation curves therefore set the limits. The limits are small at 31.5Hz and 40Hz, then increase greatly with increasing frequency. However, those limits do not provide information when the party wall is placed in a specific room configuration.

The second attempt was to look at the sound level difference of the simply supported, clamped and mixed edge conditions, as well as, the mean sound level difference for each room configuration. The data are presented in Figures 10.8-15. It is observed that for each third octave band, the four curves representing the simply supported, mixed edge conditions, clamped and the mean, often display the same trend for fixed source room volume.

The spread of data, the dB range, is then calculated for each room configuration as shown in Figures 10.8-15. It will be observed that the mixed edge conditions can set the maximum value or the minimum value instead of the simply supported and clamped (see Figures 10.13-15), due to weak acoustic-structural couplings. Consequently, the dB range is not only calculated from the minimum and maximum values given by the simply supported and clamped, but also from the values set by the sound pressure level difference obtained with the mixed edge conditions. The results are shown in the Table 10.5. 160Hz band is not considered, because there are poor agreement between the measured and predicted sound level difference as seen in Chapter 8.

The spread of data is identified for each room configuration. It is likely that at 31.5Hz, the sound insulation will vary within 2-4dB, with room volume change. At 40Hz, it will

vary within 10dB due to the acoustic couplings. Such observations are only applicable for rooms of volumes equal to or smaller than 40m³. If the room is 50m³, the spread would have increased due to the excitation of the first acoustic mode of the room. When the party wall is in resonance, e.g. at 50Hz, large dB ranges are obtained. At 125Hz, the sound insulation in room configuration 40-20m³ varies within a range of 5dB, while for the configuration 20-40m³, it varies within 23dB. There is no reciprocity when the source room becomes the receiving room as seen in Section 10.3. The ranges defined for room configuration 20-30m³ and 30-20m³ are then collapsed to give new ranges for the room configuration 30/20m³. The same was done for the room configuration 30/40 and 40/20m³. The data are presented in Table 10.6.

This table allows an estimation of the spread of sound insulation when the party wall is placed in a specific room configuration. It shows that when one of the rooms is 40m³, large dB ranges are obtained, a phenomenon which is emphasised when the two rooms are 40m³. This is explained by the identical length and width, which give identical x- and y axial modes and identical xy-, xz- and yz- tangential modes. Those modes then create strong couplings.

The defined dB ranges do not consider room configurations which strongly are coupled with the structural mode leading to poorer sound insulation than that in equal room configurations. Indeed Pietrzyk [1997] showed that in particular room configurations, a strong coupling can take place between three modes (a structural mode, an acoustic mode of the source room and an acoustic mode of the receiving room) presenting the same eigenfrequency. They have matching modeforms creating a drop in sound insulation.

Only one speaker position, the corner opposite to the party wall, was investigated in the study. Other loudspeaker positions will probably give different sound insulation values. Moreover, a traditional living room with a hi-fi will have at least two loudspeakers. The excitation of the sound field is then different from that given by one loudspeaker. Different maximum and minimum sound level difference data will be obtained.

The acoustic and structural damping were not included for any model of the room

configuration. If the acoustic damping has real effects on the sound field at low frequencies, the peaks and dips of the sound transmission loss will decrease [Kropp et al (1994), Osipov et al (1997), Pietrzyk et al (1997), Maluski et al (1998-b)] and therefore reduce the spread of data. The maximum and minimum deviations will then be different, giving different range of values. However, those new ranges will be automatically found within the ranges defined in Table 10.6.

Flanking transmission might change the sound pressure level difference curve for each different room configuration. New range values might be obtained.

The range values given in Table 10.6 are the double of the values given in Table10.4. That reinforces the argument of the sample, which is too small for statistical study.

The defined dB ranges is not a function of the length of the room only. Attempt to define a correction factor which includes the axial and tangential modes along the length of the two rooms was not successful due to the small sample.

To summarise; the correction factor defined here was only an attempt. It was defined for rooms, which are unfurnished and do not have windows and doors and there is no flanking transmission between rooms.

10.5 CONCLUDING REMARKS

Statistical and deterministic studies were undertaken to define a correction factor to predict the likely value of sound level difference when the party wall is built in a specific room configuration. The statistical study was found not relevant as the sample is too small. It needs further development.

The deterministic study gave a range of correction factors which provide information on room configuration. Again, it is likely that this range will be modified with a greater sample.

10.6 REFERENCES

Bhattacharya, M.C. and Guy, R.W., (1972): *'The influence of the measuring facility on the measured sound insulating property of a panel'*, Acustica, Vol.26, 344-348

Gibbs, B.M. and Maluski, S., (1998): *'Sound level difference between dwellings at low frequencies'*, Proceeding of Inter-Noise 98, 240

Godfrey, M.G., Roebuck, E.M. and Sherlock A.J., (1988): *'Statistics'*, Ed. Concise

Kihlman, T and Nilsson, A.C., (1972): *'The effects of some laboratory designs and mounting conditions on reduction index measurements'*, Applied Acoustics, Vol.5

Kropp, W., Pietrzyk, A. and Kihlman, T., (1994): *'On the meaning of the sound reduction index at low frequencies'*, Acta Acustica, 2, 379-392

Maluski, S. and Gibbs, B.M., (1998): *'Variation of sound level difference in dwellings due to room modal characteristics'*, Proceeding of Acoustics Performances of Medium-Rise Timber Buildings, 3rd&4th December 1998, Dublin

Osipov, A., Mees, P., and Vermeir, G., (1997): *'Low frequency airborne sound transmission through single partitions in Buildings'*, Applied Acoustics, Vol.52 (3-4), 273-288

Pietrzyk, A. and Kihlman, T., (1997): *'The sensitivity of sound insulation of partition location - case of heavyweight partitions'*, Proceeding of Inter-Noise 97, 727 –730

Utley, W.A., (1968): *'Single leaf transmission loss at low frequencies'*, Journal of Sound and Vibration, Vol.8, 256
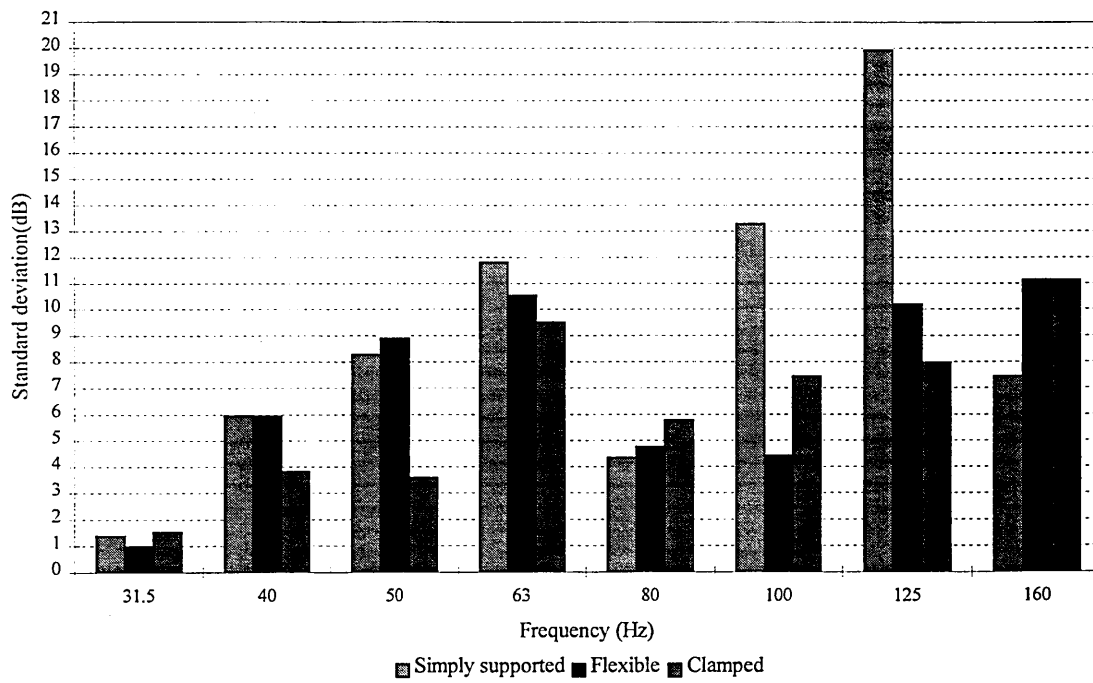
Figure 10.1. Standard deviation for a 10m² party wall placed in room configurations of volumes smaller than 50m³

Frequency (Hz)	Correction factor (dB)
31.5	-2
40	-6
50	-9
63	-12
80	-6
100	-13
125	-20
160	-11

Table 10.1. Correction factor for sound level difference data of a 10m² party wall

247
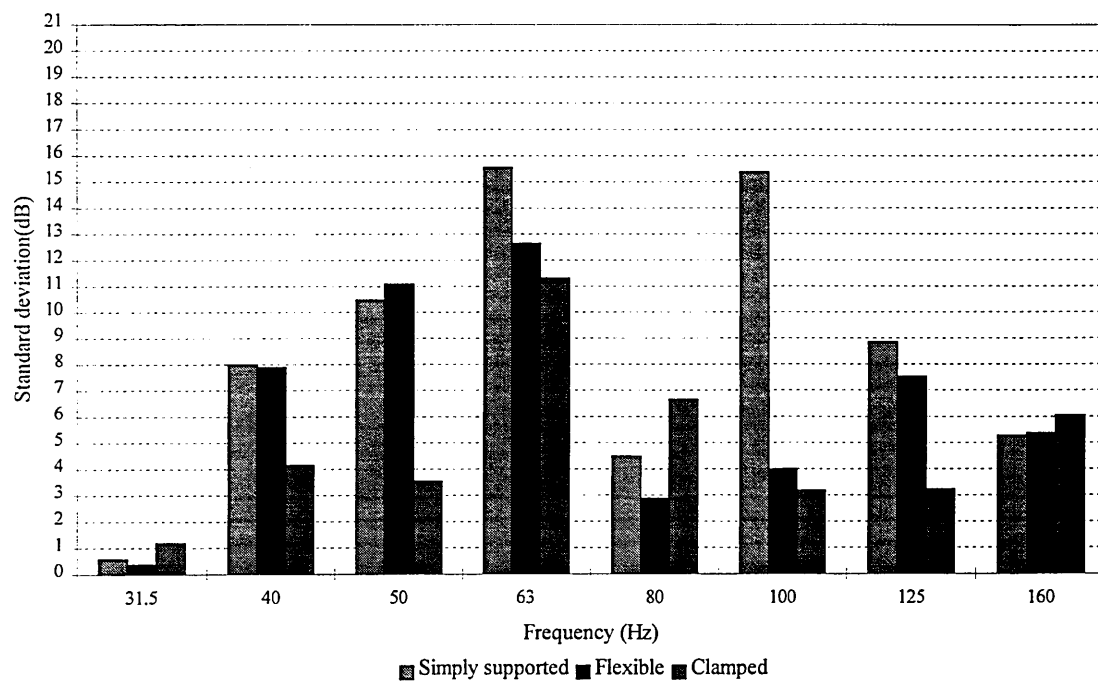
Figure 10.2. Standard deviation for the three different edge conditions of a 10m² wall placed between two identical rooms

Frequency (Hz)	Correction factor (dB)
31.5	-1
40	-8
50	-11
63	-16
80	-7
100	-15
125	-9
160	-6

Table 10.2. Correction factor for sound level difference data of a 10m² wall placed in equal room configuration
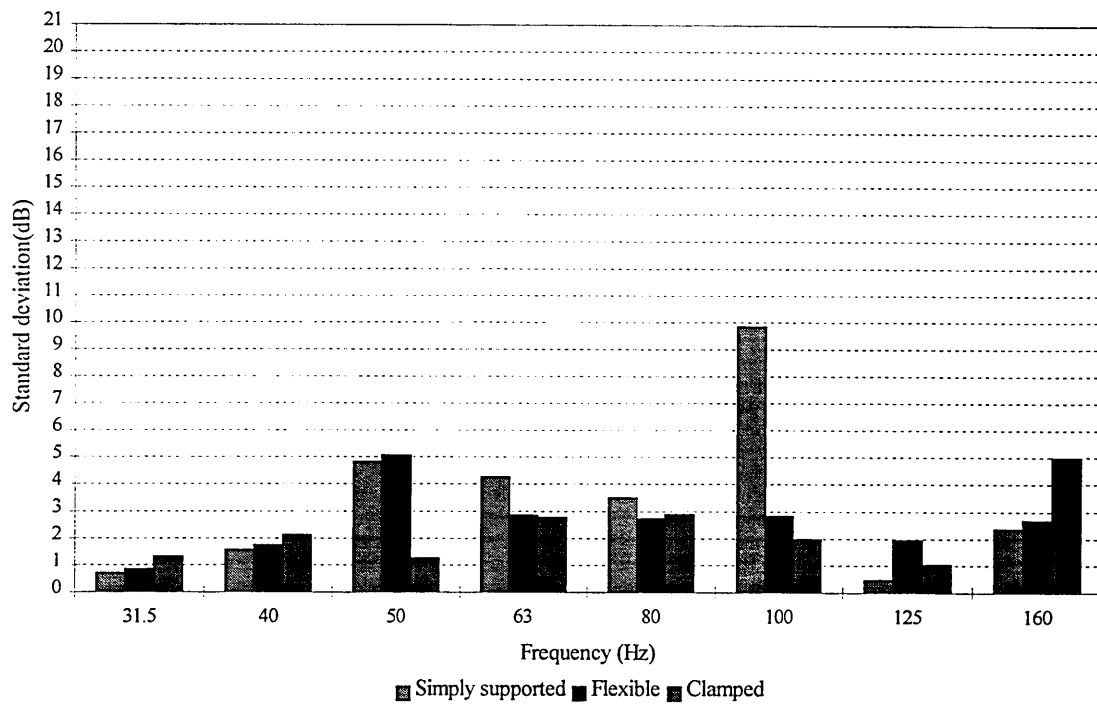
Figure 10.3. Standard deviations for the three different edge conditions of the 10m² party wall placed in unequal room (Source room volume > Receiving room volume)
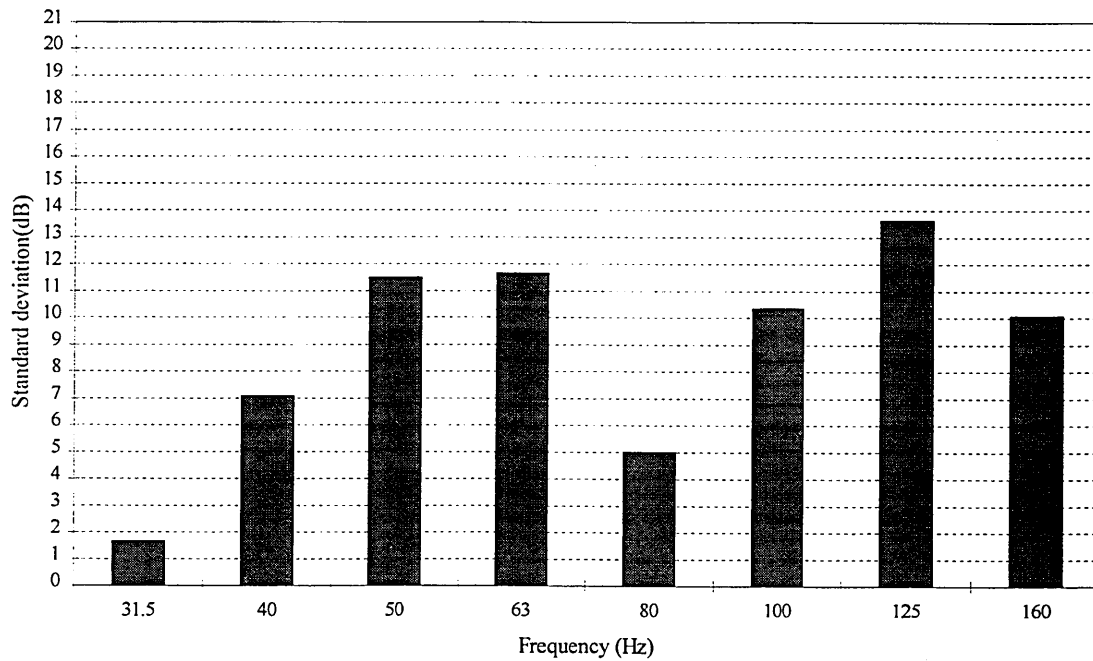
Figure 10.4. Standard deviation of a 10m² party wall of any edge conditions placed in room configuration of volumes smaller than 50m³.

249

Room configurations:		Third octave band (Hz)							
Source room (m³)	Receiving room (m³)	31.5	40	50	63	80	100	125	160
20	20	0	-5	-5	-5	-4	-11	-2	-1
20	30	-1	-5	-12	-8	-1	-4	-1	-9
20	40	-1	-5	-9	-5	-2	-14	-26	-8
30	20	-1	-5	-11	-8	-2	-4	-6	-6
30	30	-1	-5	-15	-9	-5	-4	-7	-5
30	40	-1	-6	-14	-9	-2	-4	-18	-4
40	20	-2	-5	-9	-9	-9	-13	-9	-9
40	30	-2	-6	-12	-8	0	-6	-3	-5
40	35	-2	-7	-13	-5	0	-14	-2	-6
40	40	-2	-9	-12	-6	-1	-16	-5	-4

Table10.3. Correction factor for each room configuration

Room configuration		Third octave band (Hz)							
Volume (m³)	Volume (m³)	31.5	40	50	63	80	100	125	160
20	20	0	-5	-5	-5	-4	-11	-2	-1
30	20	-1	-5	-12	-8	-2	-4	-6	-9
30	30	-1	-5	-15	-9	-5	-4	-7	-5
40	20	-2	-5	-9	-9	-9	-14	-26	-9
40	30	-2	-6	-14	-9	-2	-6	-18	-5
40	40	-2	-9	-12	-6	-1	-16	-5	-4

Table 10. 4. Corrections when the party wall is placed in a specific room configuration
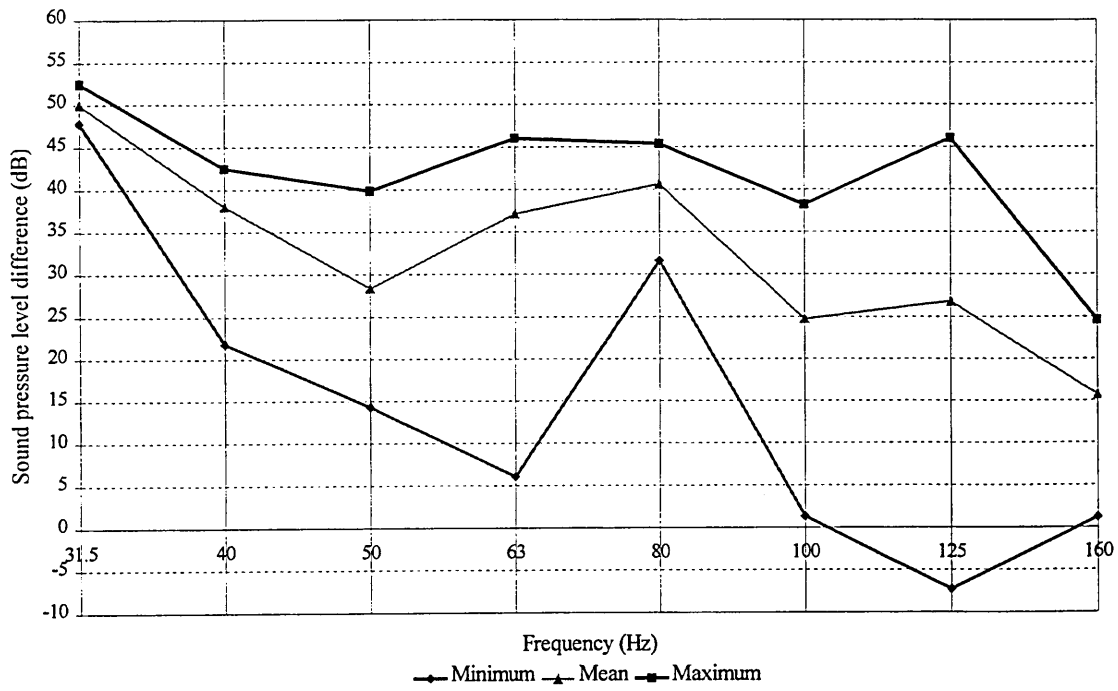
Figure 10.5. Spread and mean sound pressure level difference of a simply supported wall
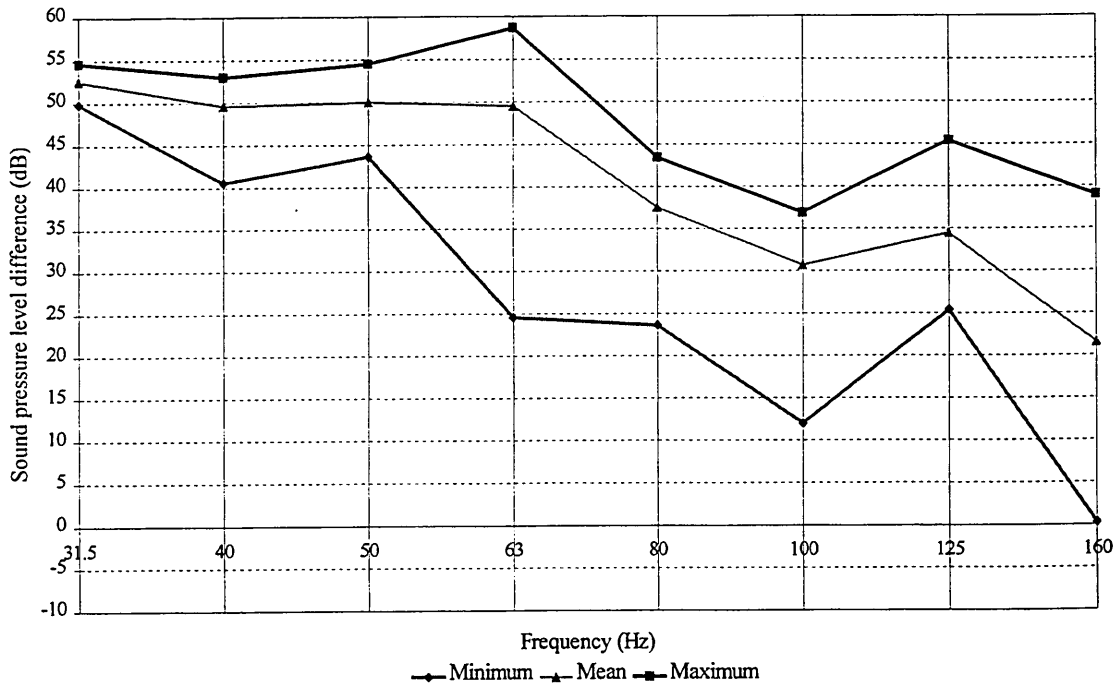
Figure 10.6. Spread and mean sound pressure level difference of a clamped wall

252
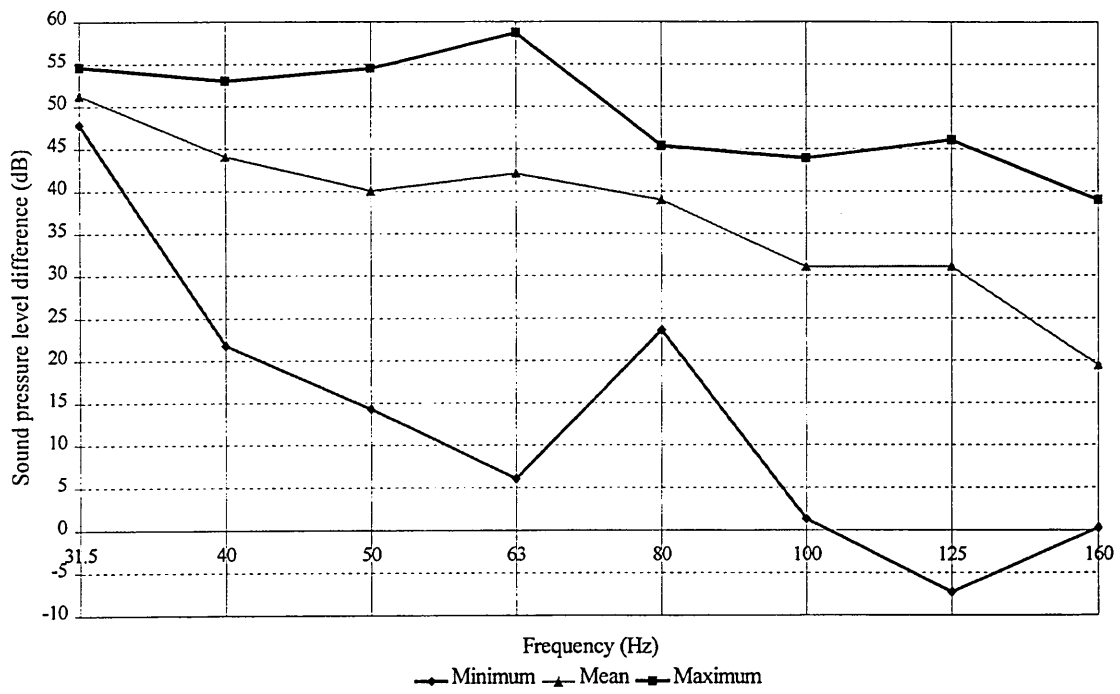
Figure 10.7. Spread and mean pressure sound level difference of a wall
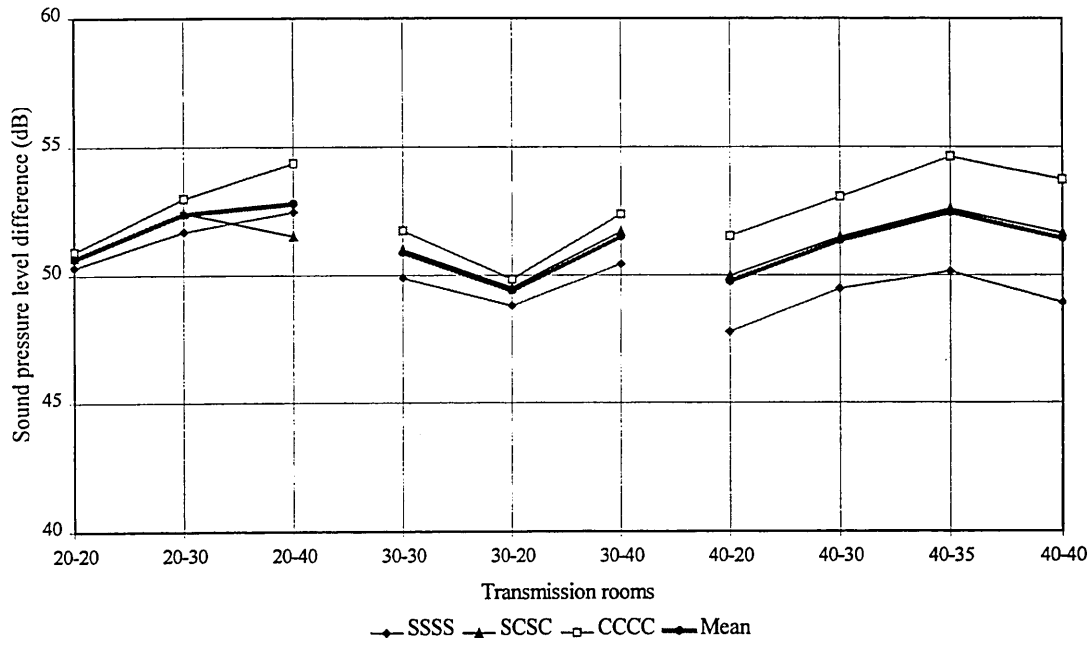
Figure 10.8. 31.5Hz

Figure 10.9. 40Hz

254
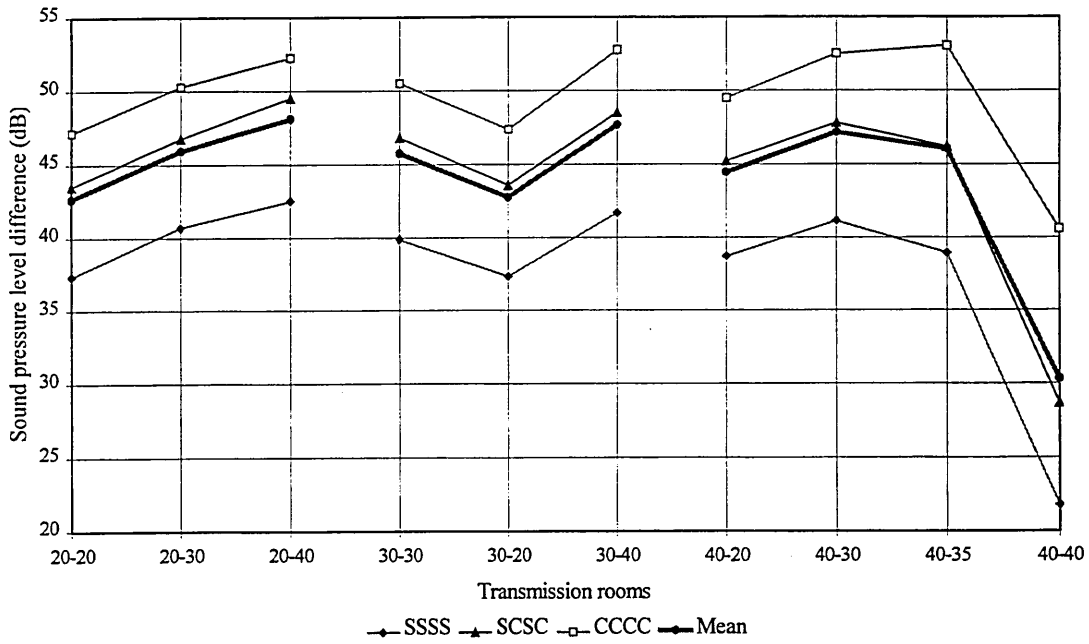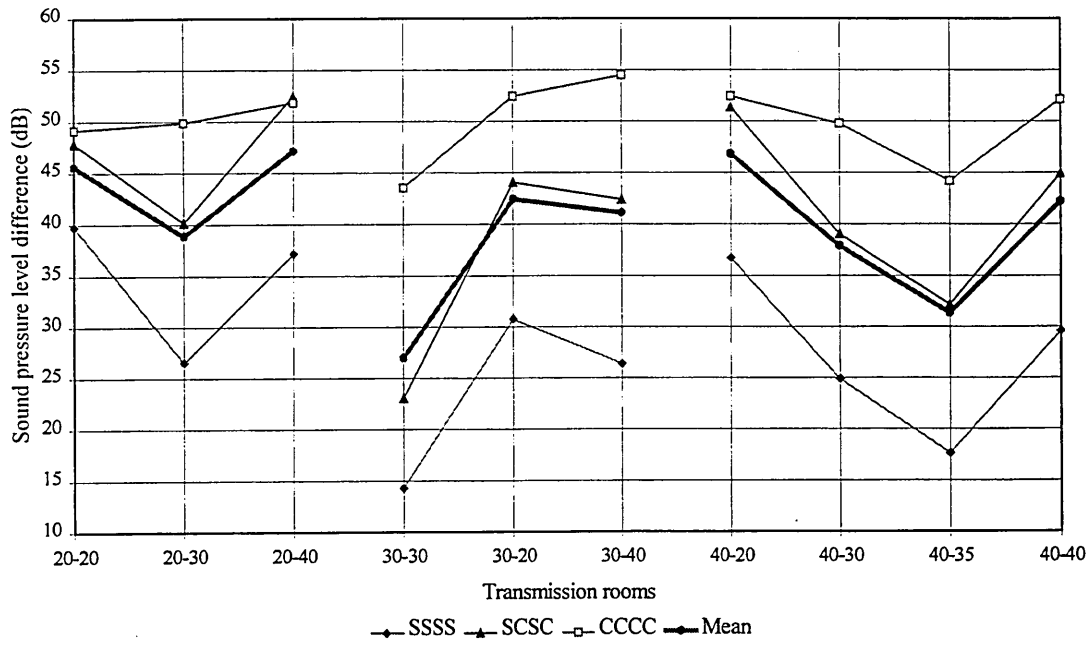
Figure10.10. 50Hz

Figure10.11. 63Hz

255
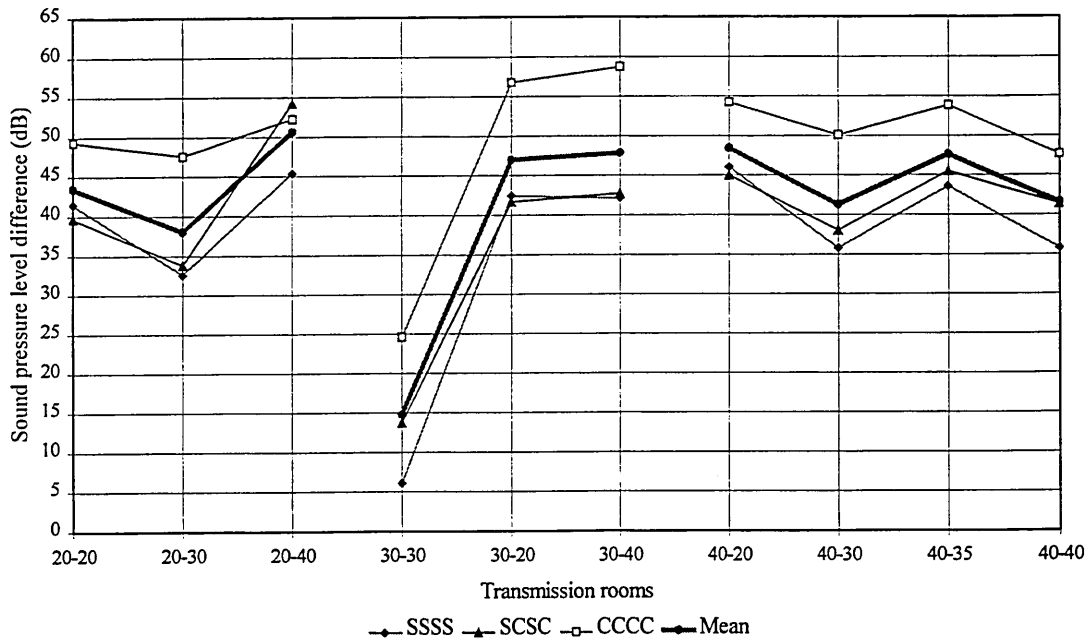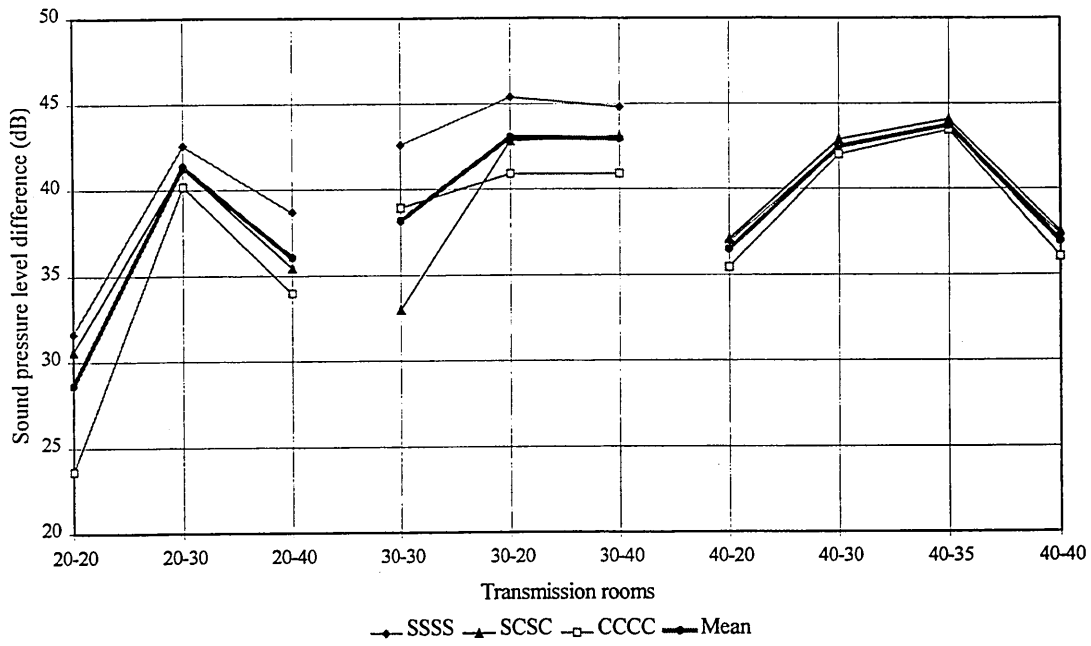
Figure10.12. 80Hz
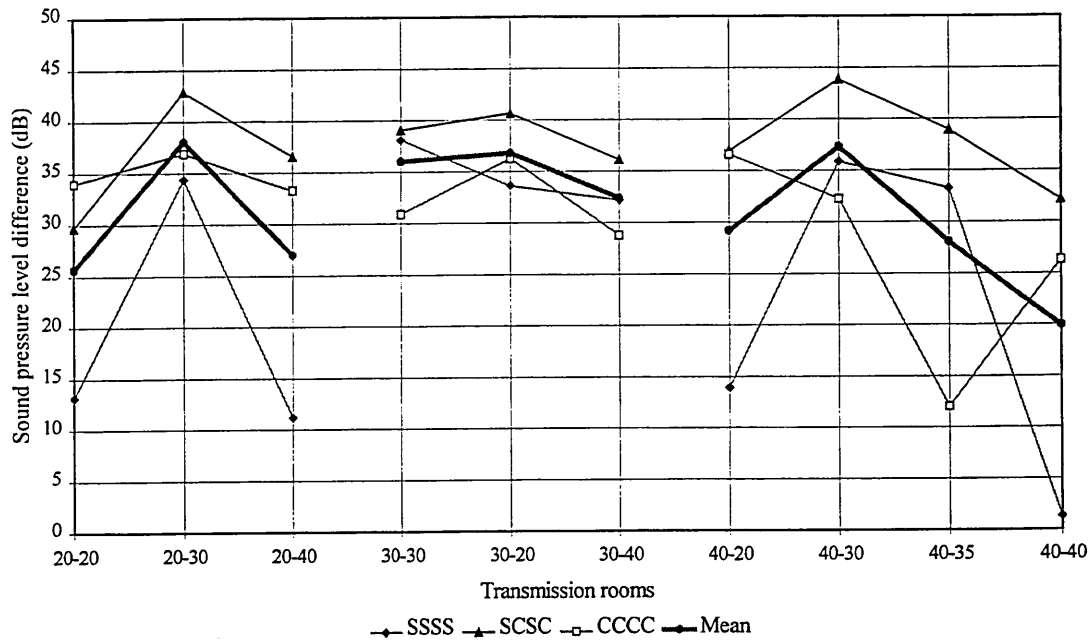
Figure10.13. 100Hz
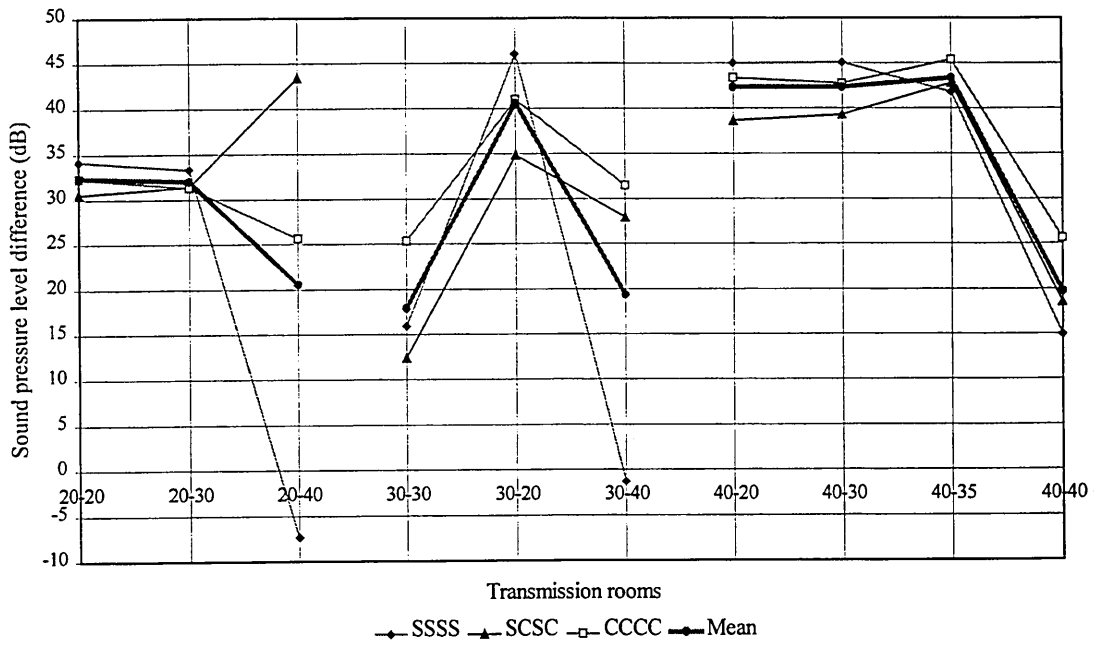
Figure 10.14. 125Hz
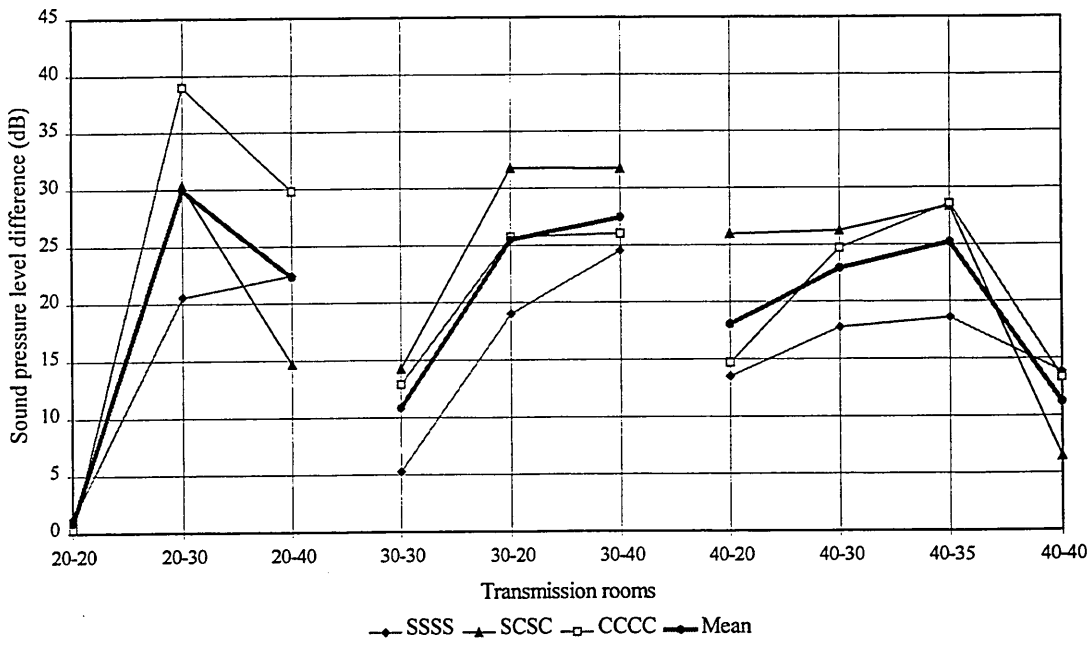
Figure 10.15. 160Hz

257

Room configuration		Third octave band (Hz)						
Source Room (m³)	Receiving room (m³)	31.5	40	50	63	80	100	125
20	20	1	10	9	9	8	21	3
20	30	1	10	23	15	2	9	2
20	40	2	10	15	9	5	26	56
30	20	1	10	22	14	4	7	11
30	30	2	11	29	19	10	8	13
30	40	2	11	28	17	4	7	32
40	20	4	11	16	8	2	23	6
40	30	4	11	25	14	0	12	6
40	35	4	14	27	10	0	27	3
40	40	5	19	23	12	1	31	11

Table 10.5. Wall of 10m²: dB ranges for different room configurations in dwellings

Room configuration		Third octave band (Hz)						
Volume (m³)	Volume (m³)	31.5	40	50	63	80	100	125
30	20	1	10	23	15	4	9	11
40	20	4	11	16	9	5	26	56
40	30	4	11	28	17	4	12	32
40	35	4	14	27	10	0	21	4
20	20	1	10	9	9	8	21	3
30	30	2	11	29	19	10	7	13
40	40	5	19	23	12	1	31	11

Table 10.6. Wall of 10m²: dB ranges for different room configurations in dwellings

11   CONCLUDING REMARKS

The work reported in this thesis has been concerned with the use of a Finite Element Method model to investigate the sound insulation between dwellings at low frequencies.

The sound field in enclosures of volumes corresponding to those in dwellings, at low frequencies, is non diffuse. In addition, masonry walls in the low frequency range have only a few structural modes. Therefore the classical room acoustic and insulation theories are not applicable.

The sound transmission process is actually governed by the interaction of acoustic and structural modes. Any change in the acoustic and/or structural modal distributions lead to a change in the sound level difference between rooms. Mode distribution is controlled by room dimensions, particularly in small rooms. Wall vibration modes are controlled by the bending stiffness and edge conditions. The edge conditions of a party wall are likely to lie between simply supported and clamped conditions.

A review of different existing standard and non standard methods for sound insulation measurements at low frequencies shows that they were defined primarily with the assumptions that the sound field is diffuse and are not appropriate for investigating sound insulation at low frequencies. A numerical method is proposed which describes the modal characteristics of both rooms and the party wall. A Finite Element model is employed where an appropriate element number was selected by optimising prediction accuracy and computation time. It is shown that the simulation of sound field discretized with 10^3 cubic elements and the party wall discretized with 10^2 surface elements had their eigenfrequencies processed with an error of 8%.

It was found that the predicted frequency response gave an overestimate when compared with scale model measurement due to errors in assigning source power, in positioning of the source and by not including the effects of absorption. The errors tended to cancel when calculating sound pressure level difference between rooms. The predicted sound

level difference gives an underestimate of 4-8dB from 31.5Hz to 125Hz in one third octave bands. This was due to incorrect modelling of the edge conditions of the party wall and also by not including structural damping, amplifying the effects of wall resonances. This was circumvented by considering three different edge conditions on three different masonry brick wall thickness. Simply supported, clamped and mixed edge conditions. The mixed edge conditions consisted of two vertical sides simply supported and two horizontal sides clamped.

The walls were assumed placed between two rooms of 40m³ and 35m³. The non statistical sound fields of the two rooms make the sound level difference vary between maximum and minimum values due to acoustic couplings. A thin 0.05m wall is mass law controlled whatever the edge conditions. The simply supported case insulates more than the clamped case.

A 0.2m wall is stiffness controlled, but is strongly affected by acoustic-acoustic and acoustic-structural couplings and structural resonances. The simply supported conditions insulate less than the clamped case.
The 0.1m wall is a transition between the 0.05m wall and the 0.2m wall.

The position of the first structural mode compared with that of the first acoustic modes explained those different trends. Walls having their first structural modes excited before the first acoustic modes will tend to be mass controlled, while walls having their first structural mode excited after will tend to be stiffness controlled.

The effects of room volume change were then investigated on the sound insulation of the 0.2m wall, for which the three different edge conditions were applied. The room volume was varied between 20 and 40m³, which are the extreme volumes for living room and bedroom in dwellings. The sound level difference is found to be the lowest when the party wall is simply supported and when the room configuration is equal. The changes in volume and edge conditions created a large spread of sound level difference data. The largest spread was obtained for the simply supported conditions, and the smallest for the clamped condition.

An attempt was made to define a correction factor to include the variation of the sound level difference with the room configuration and the edge conditions. However, the studied room configuration sample is too small for a statistical study. It is only possible to conclude that equal room configuration in dwellings should be avoided as strong acoustic and acoustic-structural couplings take place.

The present work poses and in part, answers the following questions;

1. *Is the numerical method a good tool for the study of the sound insulation at low frequencies?*

The Finite Element Method selected was appropriate for the study of sound transmission at low frequencies. It provided much of information, which would have been difficult to obtain by measurement. However, fast computers are required. The present study could have been simplified by investigating just the symmetry of the model when using a single and identical loudspeaker position and uniform absorption if included.

2. *Has the present numerical model resolved the problem of sound transmission at low frequencies?*

The answer to the question is negative. The present model forms only a preliminary study of sound transmission between dwellings and has the following limitations;

I. The wall was modelled as a shell. Despite the agreement with the results of other authors, the wall also should be modelled as a solid and compare it with the shell.

II. No damping was included for the acoustic field or for the vibrating party wall. Their introduction is likely to decrease the strength of the couplings between the two sound fields and between the sound field and the structural field.

III. No windows were modelled, while window resonances are known to influence the sound field.

IV. Only one wall of the source room and receiving room was modelled as flexible panel; the other walls were assumed to be hard surfaces. A better approximation to a real system might include six flexible walls for each room. Many more acoustic-structural couplings then can be considered. However, measurements using the quarter physical scale model have shown that predicted and measured sound level differences did not differ greatly. That could signify that after all, the numerical model might be sufficient

V. Domestic rooms are furnished. Although carpets might not have great influence on the sound field, the presence of furniture should be investigated since the room volume will be altered and the sound field changed by damping or shifting the acoustic modes. Will the sound field thus become more diffuse?

Only masonry walls were investigated, while double party walls made of wood or lightweight constructions, are popular in many dwellings.

11.1 TOPICS FOR FURTHER RESEARCH

Consequently, future research should be to develop the present model to approximate more closely sound transmission in dwellings. In particular, there is a need to:

1. Increase the frequency range of interest to observe the mass law controlled region by having more powerfull computer
2. Model the party wall as a solid and compare the predicted sound insulation with the predicted sound insulation of the party wall modelled as a shell.
3. Consider flanking transmission, by modelling the six walls of each enclosure as flexible walls.
4. Investigate the effects of stacking/handing designs and L-shaped rooms on the sound insulation
5. Investigate the effect of the introduction of furniture corresponding to living rooms and bedrooms
6. Investigate the effects of position of the loudspeakers and their number

7. Investigate the effects of double walls on the sound insulation

8. Define a correction factor from a large sample of case studies using statistical analysis.

9. Investigate a new method for field measurements

APPENDIX 1

Field points are defined after the sound field was evaluated inside the Acoustic Finite Element model. They process the pressure data by using the Finite Element shape functions to perform an interpolation between the known nodal values. They are transparent and therefore do not affect the predicted sound field when defined in the model. They are equivalent to the simulation of microphones and therefore can be placed at any chosen position.

Two types of field points were defined. They were an individual field point and a box-field point mesh.

1. The individual field point

They are defined by their co-ordinate values in the (x,y,z) planes.

2. The box field point mesh

It is a box whose its edges are parallel to the XYZ coordinate axes. They are defined by two diagonally opposite corner points, which also are defined by their coordinates. A number of subdivisions is determined by m_x, m_y, m_z, integer values, which then create $2 \times (m_x.m_y + m_x.m_z + m_y.m_z)$ Quad 4 field elements connecting $2 \times (m_x.m_y + m_x.m_z + m_y.m_z + 1)$ field points.

The transmission room model can be produced by creating a link between the Acoustic Finite Element model and the Structural Finite element model. Coupling modes are then processed by re-using the processed acoustic and structural eigenfrequencies of the Acoustic Finite Element model and the Structural Finite Element model. It was recommended to process the acoustic eigenfrequencies and then the nodal pressure by defining a specific loudspeaker position before creating any link.

A new set of equations is created. The sound transmission is calculated by processing the acoustic and structural response i.e. the displacement and the nodal pressures according to the following equation;

$$\begin{bmatrix} [K_S] - \omega^2[M_S] & C^t \\ C & [K] - \omega^2[M] \end{bmatrix} \begin{Bmatrix} w \\ p \end{Bmatrix} = \begin{Bmatrix} F \\ Q \end{Bmatrix}$$

where C is the geometrical coupling matrix,, w is the vector of nodal displacement, p is the vector of the nodal pressure.

The sound transmission was calculated by using the modal co-ordinates in order to have a faster simulation. Indeed, the size of a set of equations is reduced by having the different matrices projected in a modal basis and w and p replaced by the structural and acoustic modal participation factors [Sysnoise V5.3 (1996)]

Published papers:

Maluski, S. and Bougdah, H.,: *'Predicted and measured low frequency response of small rooms'*, Journal Building Acoustics (1997)

Maluski, S., Gibbs, B., and Bougdah, H.,: *'Predicted and measured low frequency response of small rooms'*, I.O.A. Proceeding (1998)

Maluski, S. and Gibbs, B.M., *'The influence of partitions boundary conditions on sound level difference between rooms at low frequencies'*, Proceeding of Euro-Noise 98 (1998)

Gibbs, B.M. and Maluski, S., *'Sound level difference between dwellings at low frequencies'*, Proceeding of Inter-Noise 98 (1998)

Maluski, S. and Gibbs, B.M., *'Variation of sound level difference in dwellings due to room modal characteristics'*, Proceeding of Acoustics Performances of Medium-Rise Timber Buildings (1998)

Predicted and Measured Low Frequency Response of Small Rooms

Sophie Maluski and Hocine Bougdah

School of Construction, Sheffield Hallam University, Sheffield S1 1WB

ABSTRACT

The sound level difference of party walls at low frequencies [25–200 Hz] has been shown to be strongly dependent on the modal characteristics of the sound fields of the separated rooms. The modal characteristics can be modelled by numerical methods and a Finite Element Method has been selected to model sound transmission between adjacent rooms separated by a party wall. The numerical eigenfrequencies were compared with the theoretical eigenfrequencies to select a mesh model for which the eigenfrequencies are processed within an acceptable error range.

As a prelude to the study of sound transmission between dwellings, the simulation of one single room, modelled with the selected mesh model, was validated by predicting the frequency response and comparing values with measured frequency response of a 1:4 scale room model. Results show promising agreement and establish the reliability of the work.

1. INTRODUCTION

Increasingly, it is recognised that noise from adjoining dwellings occurs at low frequencies, below 100 Hz.[1,2] The recommended method of measurement of sound insulation, ISO 140/BS 2750/Part 4 (1980), is limited to frequencies above 100 Hz and therefore may lead to an underestimate of likely complaints. Despite an Annex F in ISO 140/Part 3 (1995) for sound insulation measurements at low frequencies, there is a poor repeatability between measurements[3,4] and Roland[5] shows that a problem remains of poor reproducibility between laboratories for sound insulation measurements from 50 Hz. No method of measurements below 100 Hz has been agreed yet.[5]

Recent investigations show that the sound insulation properties of a party wall at low frequencies are strongly dependent upon the modal characteristic of the two rooms,[6] a phenomenon also confirmed by computer simulation.[7] The utilisation of numerical techniques in building acoustics becomes therefore a very useful method in order to identify the influential room and partition characteristics with respect to low frequency sound transmission.

The work reported in this paper is divided into two parts. In the first part, using a Finite Element Method (FEM), the number of elements required to model a transmission suite was specified from a comparison of the theoretical and numerical eigenfrequencies. In the second part, as a prelude to an investigation of sound transmission between dwellings at low frequencies, the selected mesh model was validated by considering a single room,

where the predicted frequency response was compared with the measured frequency response of a 1:4 scale model.

2. MODELLING THE ACOUSTICAL AND STRUCTURAL FIELDS

To estimate the sound transmission between two rooms, the pressure field in each room and the vibrational velocity of the party wall has to be known.[8] This requires the determination of the effect of the sound source on the source room acoustic volume, the effect of the pressure field on the vibration of the separating wall and response of the receiving room acoustic volume to the vibration of the party wall.

2.1 Acoustic Field

The sound pressure throughout the volume of an enclosure with the dimensions L_x, L_y and L_z is governed by the wave equation[9]

$$\delta^2 p/\delta x^2 + \delta^2 p/\delta y^2 + \delta^2 p/\delta z^2 = 1/c^2 \, \delta^2 p/\delta t^2 \tag{1}$$

where p is the pressure, t is the time and c is the speed of sound in air.

Equation (1) can be rewritten as an Helmotz equation:

$$\nabla^2 p + k^2 p = 0 \text{ where } k = 2\pi f/c \tag{2}$$

In order to obtain the normal modes of the enclosure, the 6 walls were considered as hard surfaces, i.e. the air particle velocity is equal to zero and the variation of the pressure normal to the surface of the walls also is equal to zero:

$$\delta p/\delta n = 0 \tag{3}$$

Using separable functions, the boundary condition is satisfied by the form:

$$p = p_0 \cos\left[\pi n_x x/L_x\right] \cos\left[\pi n_y y/L_y\right] \cos\left[\pi n_z z/L_z\right] \tag{4}$$

where n_x, n_y, n_z are integers and $0 \le x \le L_x$, $0 \le y \le L_y$, $0 \le z \le L_z$.

The corresponding wavenumber components are

$$k_x = \pi n_x/L_x, \; k_y = \pi n_y/L_y, \; k_z = \pi n_z/L_z \tag{5}$$

with

$$k^2 = k_x^2 + k_y^2 + k_z^2 \tag{6}$$

The eigenfrequencies can then be calculated from Equation (6), where

$$f_{n_x n_y n_z} = (c/2)[(n_x/L_x) + (n_y/L_y) + (n_z/L_z)]^{1/2} \tag{7}$$

The acoustic field can be discretised into finite elements,[10] by considering the pressure function p in each element as

$$\{p\} = [N]_e \{p\}_e \tag{8}$$

where $\{p\}_e$ are the nodal values of the pressure function associated with the element, and [N] is a listing of so-called shape functions of the co-ordinates only.

Using a Rayleigh-Ritz method, which considers the total acoustic sound energy as the sum of the acoustic potential energy and the acoustic kinetic energy,[11] and Equation (8), then Equation (2) can be discretised to give a matrix equation of the form,

$$M\{\ddot{p}\} + K\{p\} = \{q\} \tag{9}$$

where K is the acoustic stiffness matrix and M is the acoustic mass matrix; $\{\ddot{p}\}$ is the second time derivative of the nodal pressure and $\{q\}$ is the acoustic force, resulting from a loudspeaker or/and an oscillating fluid-structure interface at the boundary of an acoustic domain.

For the frequency domain analysis, $\{p\}$ and $\{q\}$ are assumed to be time harmonic functions, $\{p\} = \{P\}\exp\{j\omega t\}$ and $\{q\} = \{Q\}\exp\{j\omega t\}$ where $\{P\}$ and $\{Q\}$ are the amplitude of nodal pressures and flows, respectively. The Equation (9) can therefore be rewritten as the following:

$$([K] - \omega^2 [M])\{P\} = \{Q\} \tag{10}$$

The resonance frequencies of the enclosure are obtained when there are no acoustic force $\{Q\} = 0$:

$$[K] - \omega^2 [M] = 0 \tag{11}$$

The numerical method used to define the acoustic modes and the pressure variation of an acoustic field is called the Acoustic Finite Element (AFE) method.[12]

2.2 Structural Field

The wall separating the two rooms is modelled as a finite isotropic panel of dimensions L_y and L_z. In order to model the surface displacement, we had to distinguish between thin plate and thick plate theories to characterise the selected wall. In this study, the chosen panel was a brick wall of a thickness of 100 mm, with a surface area of 10 m^2. Such a wall has a critical coincidence frequency of approximately 152 Hz.[13] Also, according to Cremer,[13] the wall can be considered as a thin plate when $\lambda_b \geq 2h$, where λ_b is the governing bending wavelength and h is the wall thickness. Thus, the wall can be assumed to be a thin plate below 1100 Hz, condition also confirmed by Llungren.[14] Therefore thin plate theory applied to the frequency range of interest [25–200 Hz]. The vibration displacement w of the wall [8,15] is expressed as

$$B \ (\delta^2 w/\delta y^2 + \delta^2 w/\delta z^2)^2 = -\rho_x \delta^2 w/\delta t^2 \tag{12}$$

where ρ_s is the mass per unit area, B is the bending stiffness where $B = Eh^3/12(1 - v^2)$, E is the Young Modulus, and v is the Poisson's ratio.

A solution of this equation is

$$w(y,z,t) = \tilde{w} \ \exp[j(\omega t - k_y y - k_z z)] \tag{13}$$

in which

$$k_y^2 + k_z^2 = k_b^2 = (\omega^2 \rho_s/B)^{\frac{1}{2}} \tag{14}$$

where k_b is the free bending wavenumber at angular frequency ω.

The rectangular wall initially, was assumed simply supported, i.e. no displacement at the edges. The normal vibration velocity distribution takes the form

$$v(y,z) = v_{n_y n_z} \sin[\pi n_y y/L_Y] \sin. \ [\pi n_z z/L_Z] \tag{15}$$

where n, p are integers and $0 \le y \le Ly$, $0 \le z \le Lz$, and $k_y = \pi n/L_y$, $k_z = \pi p/L_z$.

Substituting k_y and k_z into the Equation (14), the natural frequencies of a simply supported wall is given by[15]

$$f_{ny,nz} = (B/2\rho_s)^{\frac{1}{2}}[(n_y/L_y)^2 + (n_z/L_z)^2] \tag{16}$$

At a specific frequency, the bending wavelength matches the acoustic wavelength. The latter is called the critical frequency of the panel, which is determined when the acoustic wavenumber $k = \omega/c$ is equal to k_b

$$k = k_b$$

$$\omega_c = c^2(\rho_s/B)^{\frac{1}{2}} \tag{17}$$

Using variational method,[11] the thin panel is also discretised into finite elements and gives an equation of a form

$$[K_s - \omega^2 M_s]\{w\} = \{q'\} \tag{18}$$

where K_s and M_s are the stiffness and the mass matrices, $\{w\}$ is the displacement vector and $\{q'\}$ is the force applied on the surface of the panel.

As for the acoustic modes, the numerical eigenfrequencies of the party wall are obtained when $\{q'\} = 0$:

$$[K_s - \omega^2 M_s] = 0 \tag{19}$$

The numerical method used to define the structural modes and the displacements is called the Structural Finite Element (SFE) method.[12]

2.3 Sound Transmission between Rooms

To model the airborne sound transmission from one room to another, an AFE model representing the sound field of the two rooms was linked to a SFE model, representing the party wall. In order to create the source and receiving room, the acoustic nodes situated on the party wall position were duplicated to create an infinite hard wall[12] of zero thickness. Two volumes were created and the room modes were calculated for the whole system by superimposing the modes of the source room and of the receiving room. After the normal modes of the structural model were computed, coupled modes were processed when the acoustic model was linked to the structural model. The modal formulation of the stiffness, mass of the coupled systems were then calculated from the acoustical and structural stiffness matrices of the uncoupled models.

3. MESH ERROR

3.1 Discretization of the Acoustic Fields

Each model is subdivided into connected finite elements to model the pressure field or the displacement field of the party wall. The number of elements is dependent upon the upper frequency of interest with the initial assumption that 6 elements would be required to properly represent the pressure/displacement over the governing wavelength. An incorrect selection of the number of elements can result in numerical errors and consequently affects the accuracy of the simulation.[16] The time taken for the simulation (CPU time) can be very long, depending upon the number of finite elements and on the processing power of the computer. In the investigation described, the simulation run was longer than CPU time, since the network system was shared with other users. It was also foreseen that the CPU time for simulating the transmission, obtained by coupling the acoustic finite element (AFE) and the structural finite element (SFE), would be large also. Consequently, an optimum between accuracy of simulation and required CPU power had to be determined.

The dimensions selected for the transmission room represented typical rooms in attached dwellings, 4 m × 4 m × 2.5 and 3.5 × 4 × 2.5. The size of the mesh depends upon the maximum frequency of interest, which, in this study, was 200 Hz, corresponding to a wavelength of 1.7 m. Compared with the longest room dimension, 4 m, 14 elements ideally are required to represent the pressure variation over a wavelength. In the case of a three dimensional model, 14^3 elements were required to model the sound field of one room. Such a model was known as 14 mesh model.

It was found that three days of processing were required for the simulation of the room modes for 12 mesh and greater models and therefore, it was necessary to reject the 6 elements per wavelength condition. Seven acoustic models were constructed from 5 meshes to 11 meshes in order to select a mesh model for which the CPU time is acceptable, and for which data would be processed within an acceptable error. To evaluate the error due to the finite element discretisation, a ratio ε was calculated by comparing the theoretical

eigenfrequencies given by Equation (7) with the finite element eigenfrequencies processed for each mesh model.

$$\varepsilon = \frac{\text{numerical eigenfrequency} - \text{theoretical eigenfrequency}}{\text{theoretical eigenfrequency}} \times 100 \qquad (20)$$

Figure 1 shows the error from a 5 mesh to a 11 mesh model plotted against the number of modes, which corresponds with a frequency range of 0 to 220 Hz. The room mode calculation for a 5 mesh model has a maximum error of 17%, which occurs in the upper part of the frequency range of interest, whereas the calculated modes for a 11 mesh model are within an error of 6%. The observed peaks are not only due to the mesh size, but also the calculation procedure when the room modes of the transmission suite are processed. By duplicating the nodes along the position of the party wall, the calculation procedure gives an increased error when identical modes in the source room and in the receiving room are processed. The errors for the 10, 9 and 8 mesh models were also acceptable as they were below 10%.
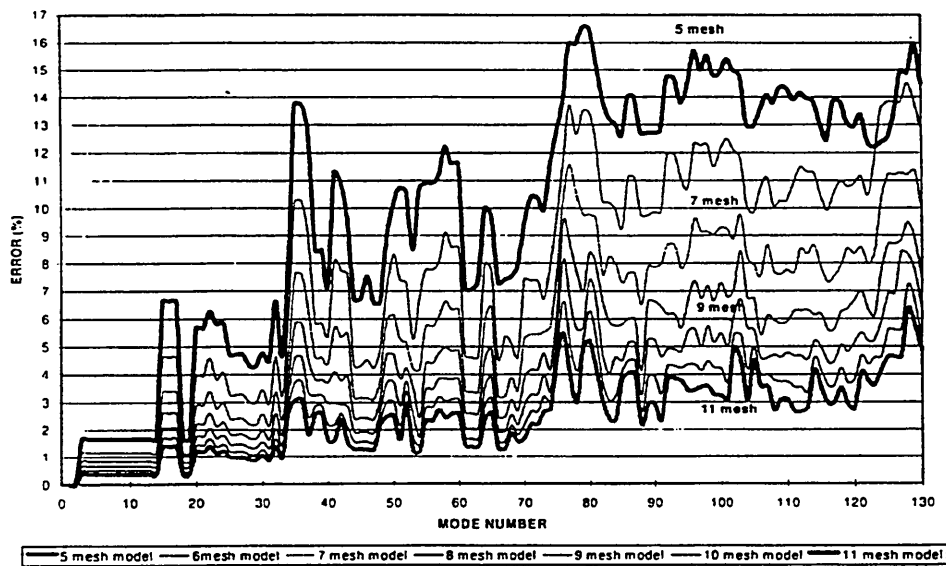
Figure 1.   Acoustic model: Error versus Mode.
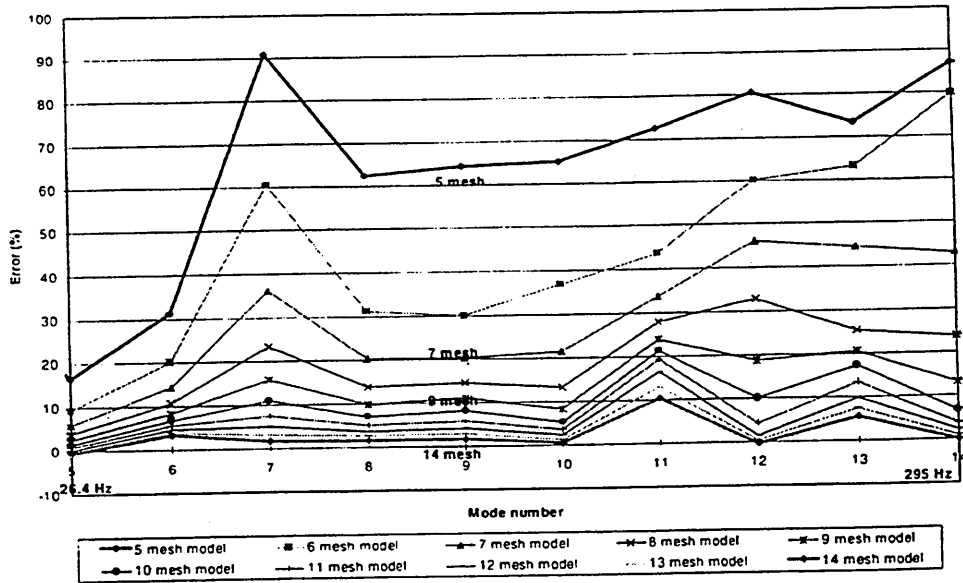
Figure 2. Structural model: Error versus Mode.

Mode 1 (1,1) = 26.77Hz
Mode 2 (2,1) = 49.33Hz
Mode 3 (1,2) = 84.52Hz
Mode 4 (3,1) = 86.93Hz
Mode 5 (2,2) = 107.08Hz
Mode 6 (4,1) = 139.57Hz
Mode 7 (3,2) = 144.68Hz
Mode 8 (1,3) = 180.78Hz
Mode 9 (4,5) = 197.32Hz
Mode 10 (2,3) = 203.34Hz
Mode 11 (5,1) = 207.25Hz
Mode 12 (3,3) = 240.94Hz
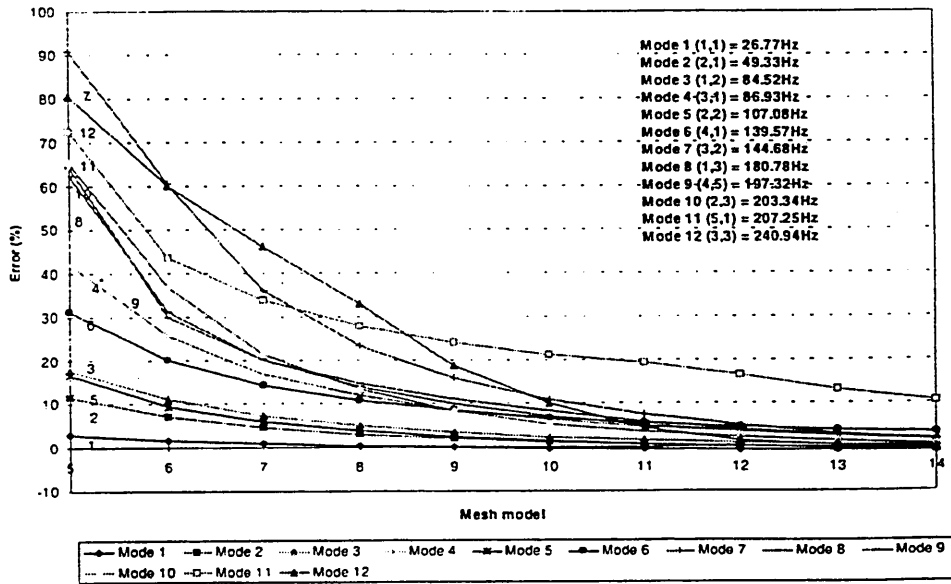
Figure 3. Structural model: Error versus Mesh Model.

3.2 Discretization of the Wall Response

In a similar manner, the eigenfrequencies of a simply supported party brick wall were obtained. Again, the error of the estimate was expressed as in Equation (20) with respect to theoretical eigenfrequencies calculated from Equation (16). Results are shown in Figure 2. The wall mode calculation for a 5 mesh model has a maximum error of 91%, which occurs in the low and upper part of the frequency range of interest, whereas the calculated modes for a 9 to 14 mesh model are within an error of 20%. Only the 14 mesh model gives errors within an initial target of 10%. Instead of displaying error versus mode number, the results can be displayed as error versus mesh model. Figure 3 shows that panel modes 7, 8, 9, 11 and 12 of the 9 mesh model and modes 7, 11 and 12 of the 10 mesh model have an error equal or greater than 10%, but the eigenfrequencies of the modes 11 and 12 are outside of the frequency range of interest. The 11 to 14 mesh models have their eigenfrequencies processed within an error less than 9% except for the mode 11.

The intention for future studies was to link the AFE model of the rooms, with the SFE model of the partition. In order to do so, both mesh sizes have to be the same.[12] By selecting the 10 AFE mesh model, the simulation ran within an error of 7%. When the panel was modelled with 10^3 elements, the simulation ran within an error of 8% except at 144 Hz where the error was 10%. The coupled system was therefore modelled using a 10 mesh model for room and party wall.

4. VALIDATION

As a prelude of the investigation of the sound transmission between dwellings at low frequencies, the simulation was compared with measurements of a 1/4 scale model, of one room of dimensions 1.2 × 1.2 × 0.6 m and with 6 hard walls, i.e. infinite acoustic impedance. The maximum frequency range was [100–800 Hz] corresponding to [25–200 Hz] full scale. The enclosure mesh was designed using Patran3,[17] then transferred into SYSNOISE 5.3 where the values of mass density and sound velocity were assigned to the sound field of the enclosure. Damping and absorption were not included in the model. 90 room modes, 30 of which had eigenfrequencies above the frequency range of interest, were then processed. A point source with a specified power level was assigned to one corner opposite to the party wall, in order to excite the maximum room modes. The frequency response was obtained with a resolution of 1 Hz. A field point mesh was processed to produce the sound pressure levels at position 1 (0.4, 0.5, 0.6 m) and at position 2 (0.8, 0.8, 0.2 m), to allow a comparison with measurements.

An enclosure with the same dimensions as given above was made of 24 mm blockwood, with one side of 10 mm perspex. The perspex was to form the party wall in later measurements of sound pressure level difference, not reported here. The physical scale model was placed in a small sound transmission suite where the background noise level was low and was positioned on resilient foam to reduce vibration from the floor. A photograph of the physical scale model and scale modelling set up is shown in Figure 4. The set up for measurements is shown in Figure 5. To provide a sound source, which approximated a point source, a loudspeaker was placed outside of model room and radiated through a 10 mm hole in one corner (Figure 5). Two 1/2 inch B&K microphone type 4165 were placed at the same positions as selected in the simulation. A maximum length sequence
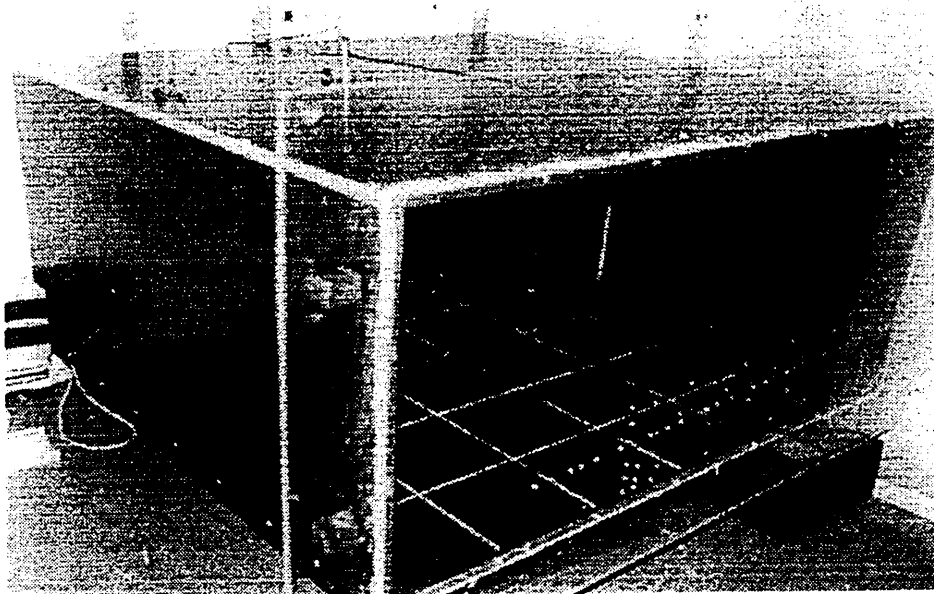
Figure 4.   Physical scale model.
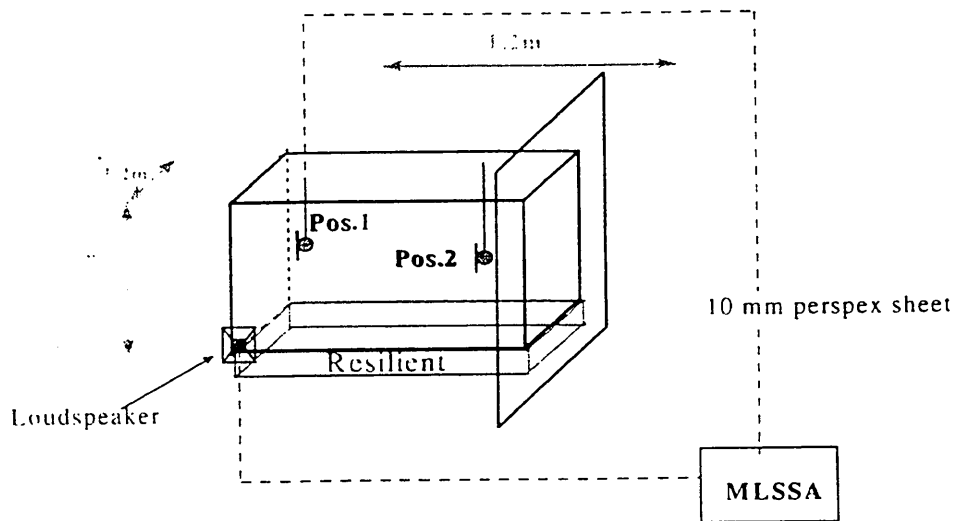
Figure 5.   Set up for sound pressure level measurements at microphone positions 1 and 2.
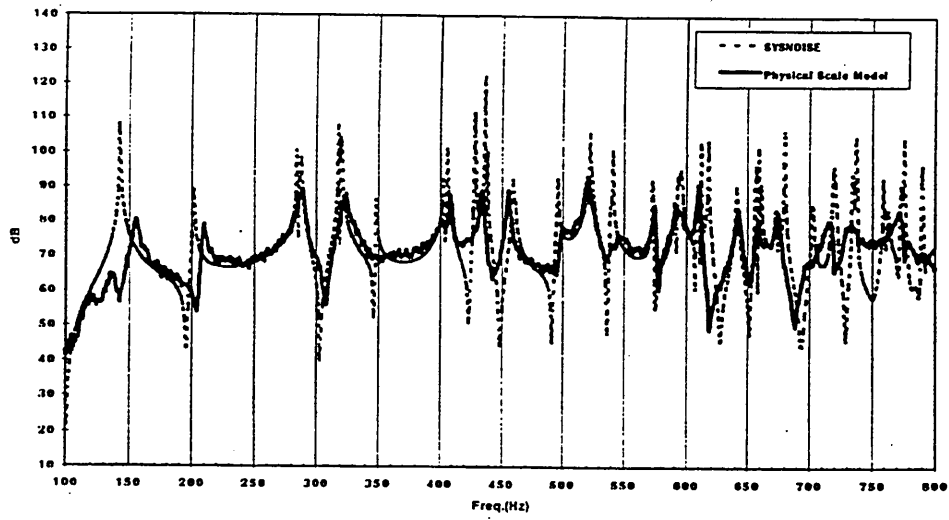
Figure 6.   Sound level at position 1.
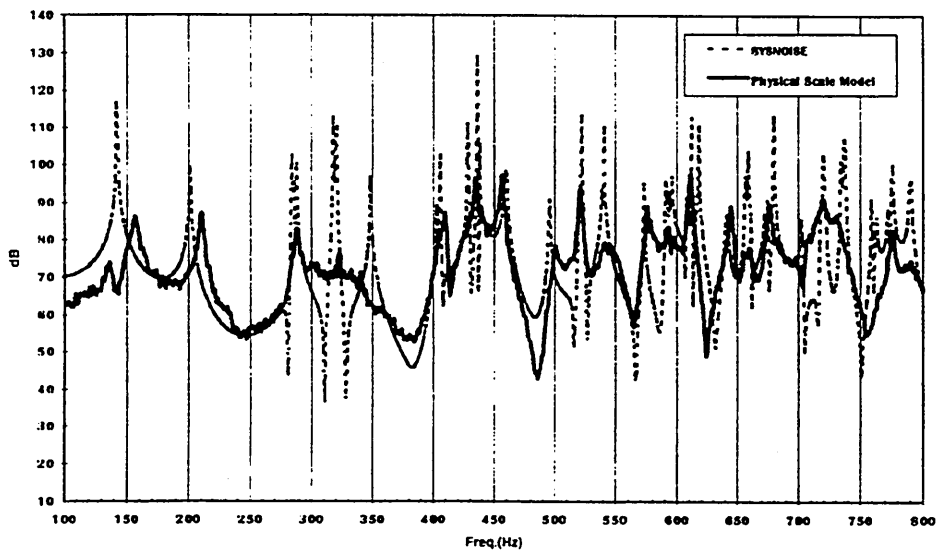
**Figure 7.**   Sound level at position 2.
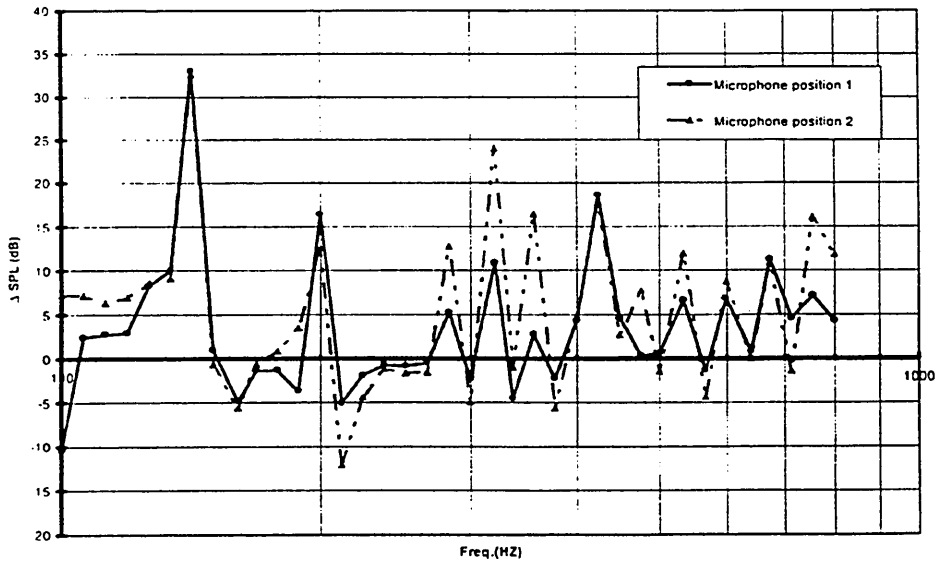
**Figure 8.** Simulation compared with measurements in a 12th octave band.
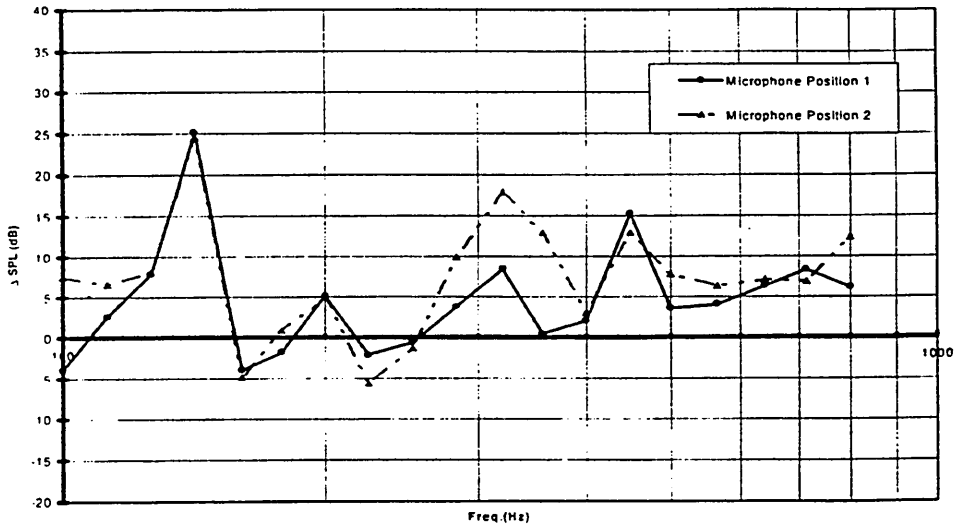
Figure 9. Simulation compared with measurements in a 6th octave band.

(MLS) signal was used as a source of excitation.[18] The spectra of the sound levels at two microphone positions were obtained for a bandwidth of 100 Hz to 800 Hz, with a resolution of 0.5 Hz in order to record all dips and peaks in the response.

Figures 6 and 7 show the predicted and measured sound pressure levels at positions 1 and 2, respectively. As expected, the sound field shows peaks and dips, corresponding to the modes of the enclosure. The magnitude of the measured peaks and dips are not as great as predicted. This was expected since the computer model did not include absorption. At high frequencies, the agreement between prediction and measurement is less good because of the limited number of elements used to describe the frequency response. The simulation also indicates the effect of the perspex panel resonances on the sound field at 350 Hz, 430 Hz and 630 Hz while the measured frequency response did not show such effects.

Due to two different frequency resolutions for prediction and measurements, sound levels were calculated with a 12th octave band resolution in order to compare data. Results are presented as a level difference (simulation-measurements) in Figure 8. The large differences are the results of often quite small shifts in observed with respect to expected resonant frequencies. Again, the numerical model does not include surface or air absorption and therefore the simulation emphasises peaks and dips. Figures 9 and 10 show the level difference calculated with a 1/6 and 1/3 octave band resolution, respectively. In real measurements, the data are commonly presented in a 1/3 octave band. The two figures, compared with Figure 6, show that the discrepancy between simulation and measurement decreases when calculated within a larger bandwidth. A peak at 141 Hz, which corresponds to the 1st room mode, is evident in all curves. The maximum discrepancy between simulation and measurements is 18 dB when calculated within a 1/6 octave band and 15 dB within a 1/3 octave band. The discrepancy is less for the microphone position 1 than for position 2. This can be explained by the fact that the former was closer to the loudspeaker than the latter, and was therefore less affected by the absorption of the room.

The simulation overestimates the overall sound level by approximately 5–10 dB. This could be for two reasons. The first is that the sound power of the point source may have been incorrectly assigned. Secondly, as stated earlier, damping was not included in the FEM model as it is difficult to quantify at low frequencies. The simulation therefore overestimates the sound field when processed inside any room of hard walls. This is confirmed in Figure 11, which shows the measured and simulated sound level difference between two rooms in third octave bands.[19]

5. CONCLUDING REMARKS

Although the size of the element is less than a 1/6 of the governing wavelength, the comparison between simulation and measurements for one room is promising and validates the choice of the mesh number to model the rooms and party wall. Three sources of error were identified: incorrect assignment of sound power to the source, non inclusion of absorption in the FEM model and shifts in the predicted resonance frequencies with respect to measured, which produce larger discrepancies than is indicated by visual inspection of the frequency response curves. However, in the prediction and measurements
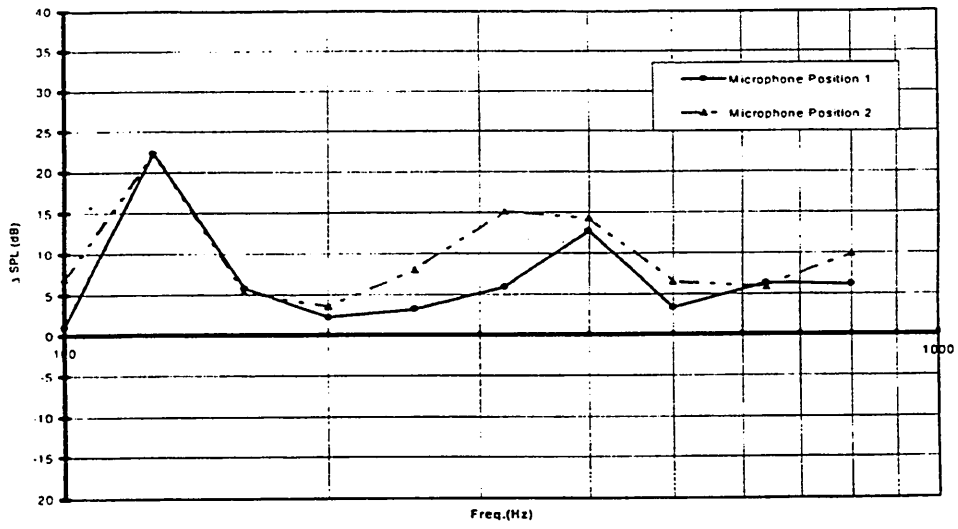
·**Figure 10.**   Simulation compared with measurements in a 3rd octave band.
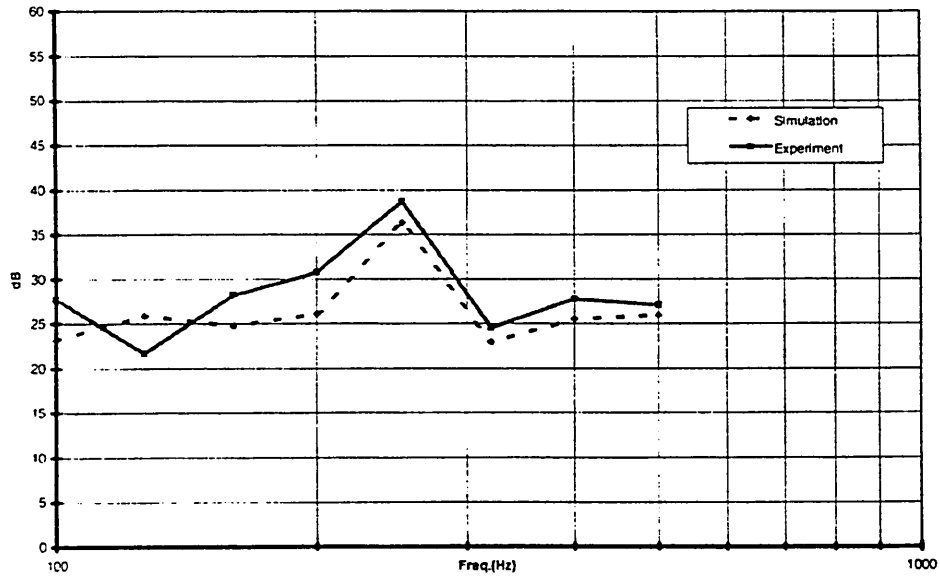

Figure 11.   Sound pressure level difference calculated for a 10 mm perspex sheet.

of the sound level difference between two rooms, the effect of the first two sources of error tends to cancel. The third error may be due to resonances of the blockwood panels, which made up the model.

REFERENCES

1. Brooks, J.R. and Attenborough, K., 1989, "The implication of measured and estimated domestic source levels for insulation requirements", *Proceedings of IOA*, Vol. 11 (11), 19–27.
2. Grinwood, C., 1995, "Complaints about poor sound insulation between dwellings", *IOA Acoustics Bulletin*, Vol. 20(4), 11–16.
3. Kropp, W., Pietrzyk, A. and Khilman, T., 1994, "On the meaning of the sound reduction index at low frequencies", *Acta Acustica*, Vol. 2, 379–392.
4. Farina, A., Fausti, P., Pompoli, R. and Scamoni, F., 1996, Intercomparison of laboratory measurements of airborne sound insulation of partitions pompoli, *Proceedings of Inter-Noise*, 881–886.
5. Roland, J., 1995, "Adaptation of existing test facilities to low frequencies to low frequencies measurements", *Inter-Noise*, 1113–1116.
6. Osipov, A., Mees, P. and Vermeir, G., 1997, Low-frequency airborne sound transmission through single partitions in buildings, *Applied Acoustics*, V.52(3/4), 273–288.
7. Kropp, W., Pietrzyk, A. and Khilman, T., 1994, "On the meaning of the sound reduction index at low frequencies", *Acta Acustica*, Vol. 2, 379–392.
8. Fahy, F., 1985, Sound and structural vibration: radiation, transmission and response, Edition Academic Press.
9. Morse, P.M., 1948, Vibration and Sound, 2nd edition: McGraw-Hill.
10. Petyt, L., Lea, J. and Koopman, G.H., 1976, A finite element method for determining the acoustic modes of irregular shaped cavities, *Journal of Sound and Vibration*, V.45(4), 495–502.
11. Zienkiewicz, O.C., 1971, The Finite Element Method in Engineering Science, Edition: McGraw-Hill.
12. SYSNOISE, 1993, User Manual, Version 3.5.
13. Cremer, Heckl and Ungar, 1988, Structure Borne Sound, 2nd edition: springer-Verlag, p. 104.
14. Llungren, 1991, Airborne Sound Insulation of Thick Walls, *Journal of Acoustical Society of America*, Vol. 89(5), 2338–2345.
15. Leissa, A., 1993, Vibration of plates, Edition: Acoustical Society of America.
16. Atalla, N. and Bernhard, R.J., 1994, Review of Numerical Solutions for Low Frequency Structural-Acoustic Problems. *Applied Acoustics*, V.43, 271–294.
17. P3/Patran User Manual, 1993, PDA Engineering.
18. MLSSA, Version 9.01.
19. The effect of party wall edge conditions on the sound level difference between rooms at low frequencies, in preparation for Applied Acoustics.

PREDICTED AND MEASURED LOW FREQUENCY RESPONSE OF SMALL ROOMS

S Maluski (1), B Gibbs (2), H Bougdah (1)

(1) School of Construction, Sheffield Hallam University, Sheffield S1 1WB.
(2) Acoustics Research Unit, The University of Liverpool, Liverpool L69 3BX.

1. INTRODUCTION

Increasingly, it is recognised that noise from adjoining dwellings occurs at low frequencies, below 100Hz[1,2]. The recommended method of measurement of sound insulation, BS 2750 /Part 4 (1980), is limited to frequencies above 100 Hz and therefore may lead to an underestimate of likely complaints. Despite an Annex F in ISO 140/ part 3 (1990) for sound insulation measurements at low frequencies, Roland[3] shows that a problem remains of poor reproducibility between laboratories for sound insulation measurements from 50Hz and no method of measurements below 100Hz has been agreed. Some recent investigations[4], employing computer simulation, show that the sound insulation of party walls at low frequencies is strongly dependant upon the modal characteristics of the sound fields of the separated rooms. The utilisation of numerical techniques becomes therefore a very useful method in order to identify the influential room and partition characteristics with respect to low frequency sound transmission.

The work reported in this paper was to validate the simulation as a prelude to an investigation of sound transmission between dwellings at low frequencies. A Finite Element Method (FEM) was selected to model a room and the predicted frequency response was then compared with the measured frequency response of a 1:4 scale model.

2. MODELLING

In order to model the airborne sound transmission from one room to another room, two models had to be defined: an acoustic model representing the sound field of the two rooms using an Acoustic Finite Element method (AFE)[5] and a structural model, representing the radiation of the party wall, using a Structural Finite Element method (SFE)[5]. Each model is subdivided into connected finite elements to model the pressure field or the displacement of the surface of the party wall. The number of elements is defined from the upper frequency of interest on the assumption that 8 elements are required to properly represent the pressure/displacement over the governing wavelength. An incorrect selection of the number of elements can result in numerical errors and consequently affects the accuracy of the simulation.

The time taken for the simulation (CPU time) can also be very long, depending upon the number of finite elements and on the processing power of the computer. In our case, the simulation run was longer than CPU time, since the network system was shared with other users. It was also foreseen that the CPU time for simulating the transmission, obtained by coupling the acoustic finite element (AFE) and the structural finite element (SFE), would be greater than the CPU time required for the room modes only. Consequently, an optimum between accuracy of simulation and required CPU power had to be determined.

The dimensions selected for the transmission room represented typical adjacent dwellings, 4m x 4m x 2.5 and 3.5 x 4 x 2.5. The size of the mesh depends upon the maximum frequency of the interest. In this study, the upper frequency was 200 Hz corresponding to a wavelength of 1.7m. Compared with the longest room dimension, 4m, 14 elements ideally are required to represent the pressure variation over

a wavelength. In the case of a three dimensional model, 14^3 elements are required to model the sound field of one room. Such a model is called a 14 mesh model.

It was found that three days of processing were required for the simulation of the room modes for 12 mesh and greater models and it was necessary to reject the 6 elements per wavelength condition. Seven models were constructed from 5 meshes to 11 meshes in order to select a mesh model for which the CPU time is acceptable, and for which data are processed within an acceptable error. To evaluate the error due to the finite element discretisation, a ratio ε was calculated by comparing the theoretical eigenfrequencies[6] with the finite element eigenfrequencies processed for each mesh model.

$$\varepsilon = \frac{\text{theoretical eigenfrequency} - \text{numerical eigenfrequency}}{\text{theoretical eigenfrequency}} \times 100$$

Figure 1 shows the error from a 5 mesh to a 11 mesh model plotted against the number of modes, within a frequency range of 0 to 220Hz.
The room mode calculation for a 5 mesh model has a maximum error of 17%, which occurs in the upper part of the frequency range of interest, whereas the calculated modes for a 11 mesh model are within an error of 6%. The errors for the 10, 9 and 8 mesh models were also acceptable as they were below 10%.

3. MESH MODEL SELECTION

The intention in this study was to link the AFE model of the transmission room with the SFE model of the partition. In order to do so, both mesh sizes have to be the same[5]. By selecting the 10 AFE mesh model, the simulation ran with an error of 7%. When the panel was modelled with 11^3 elements, the simulation ran within an error of 8% except at 144Hz where the error was 10% The error was expressed with respect to calculated eigenfrequencies of a simply supported panel[6].
For validation, the simulation was compared with measurements of a 1/ 4 scale model, room with dimensions 1.2 x 1.2 x 0.8m. The maximum frequency range was [100- 800 Hz] corresponding to [25- 200 Hz] full scale.
The enclosure mesh was designed using Patran3[7], then transferred into SYSNOISE 5.3 where the values of mass density and sound velocity were assigned to the sound field of the enclosure. 90 room modes, a number of eigenfrequencies above the frequency range of interest, were then processed assuming that the enclosure had 6 hard surfaces. The frequency response was obtained with a resolution of 1 Hz. A field point mesh was processed to produce the sound pressure level at position 1 (0.4, 0.5, 0.8m) and at position 2 (0.8, 0.8, 0.2m) to allow a comparison with sound pressure level measurements.

4. EXPERIMENT

An enclosure with the same dimensions as given above was made of 24mm thick blockwood, with one side of 10mm perspex. This physical scale model was in a small sound transmission suite where the background noise level was low and was placed on resilient foam to reduce vibration from the floor. A loudspeaker radiated through a 10mm hole in one corner opposite to the perspex sheet. Two microphones were placed at the same positions as selected in the simulation. MLSSA was used to obtain the spectrum of the sound level at two microphone positions from 100 Hz to 800 Hz with a resolution of 0.5Hz in order to record all dips and peaks in the response.

---

5. VALIDATION

Figure 2 and 3 show the numerical and measured sound pressure levels at positions 1 and 2, from 100 Hz to 800 Hz. The trend and the characteristics of the curves for each position are the same. Due to two different chosen resolutions for prediction and measurements, sound level was calculated with a 12th octave band resolution in order to inspect the discrepancy between simulation and measurement for positions 1 and 2. Results are presented as a level difference (simulation-measurements) in Figure 4. The large differences are the results of often quite small shifts in observed with respect to expected resonant frequencies. In addition, the numerical model does not include surface or air absorption and therefore the simulation emphasises peaks and dips. Figures 5 and 6 show the level difference calculated with a 1/6 and 1/3 octave band resolution, respectively. In real measurements, the data are commonly presented in a 1/3 octave bands. The two figures, compared with Figure 4, show that the discrepancy between simulation and measurement decreases when calculated within a larger bandwidth. A peak at 141Hz (1st mode) is evident in all curves. The maximum discrepancy between simulation and measurements is 18dB when calculated within a 1/6 octave band and 15dB within a 1/3 octave band. The discrepancy is less for the microphone position 1 than for position 2. This can be explained by the fact that microphone position 1 was closer to the loudspeaker than microphone position 2, and was therefore less affected by the absorption of the room. The simulation overestimates the overall sound level by approximately 5-10dB. This could be for two reasons. The first is that the sound power of the point source may have been incorrectly assigned. Secondly, as stated earlier, damping was not included in the FEM model. as it is difficult to quantify at low frequencies.

6. CONCLUDING REMARKS

Although the size of the element is less than a 1/6 of the wavelength, the comparison between simulation and measurements for one room is promising and validates the choice of the mesh number to model the rooms and party wall. Three sources of error were identified: incorrect assignment of sound power to the source, non inclusion of absorption in the FEM model and shifts in the predicted resonance frequencies with respect to measured, which produce larger discrepancies than is indicated by visual inspection of the frequency response curves. However, in the prediction and measurements of the sound level difference between two rooms, yet to be reported[8], the effect of the first two sources of error tends to cancel.

7. REFERENCES

1. Brooks, J. R., Attenborough, K, 1989, "The implication of measured and estimated domestic source levels for insulation requirements", Proceedings of I.O.A., Vol.11 (11), 19-27.
2. Grinwood, C, 1995, "Complaints about poor sound insulation between dwellings", IOA Acoustics Bulletin, Vol.20 (4), 11-18
3. Roland, J., 1995, "Adaptation of existing test facilities to low frequencies to low frequencies measurements", Inter-Noise, 1113-1116
4. Kropp, W., Pietrzyk, A., Khliman, T, 1994, "On the meaning of the sound reduction index at low frequencies", Acta Acustica, Vol.2, 379-392
5. SYSNOISE, 1993, User Manual, Version 3.5
6. Beranek, Noise and Vibration Control Engineering
7. P3/Patran User Manual, 1993, PDA Engineering
8. In preparation for Applied Acoustics

PREDICTED AND MEASURED LOW FREQUENCY RESPONSE OF SMALL ROOMS

Figure 3: Sound level at position 2
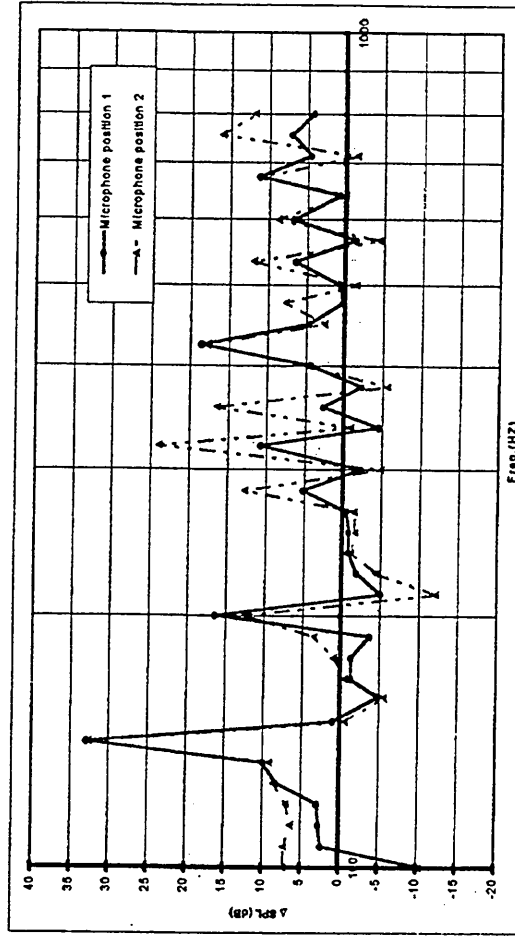
Figure 4: Simulation compared with measurements in a 12th octave band.

PREDICTED AND MEASURED LOW FREQUENCY RESPONSE OF SMALL ROOMS

Figure 1. Error versus mode number

Figure.2: Sound level at position 1

NUMERICAL TECHNIQUES FOR SOLVING ACOUSTIC TRANSPARENCY PROBLEMS

Dr J-P Coyette, C Lecomte, C F McCulloch MIOA, Dr J-L Migeot

Virtual Prototype Refinement, LMS International, Leuven, Belgium

SUMMARY

This paper deals with numerical techniques for solving acoustic transparency problems. This kind of p...
encountered in the design of all major transportation systems, such as ground vehicles, aircraft and s...
noise penetration through fairings, windows and doors, and break-out from engine compartm...
Applications in structural engineering such as the cladding of buildings can also be foreseen.
Acoustic transparency means the assessment of the transmissibility of sound by vibro-acoustic interacti...
one side of a (part of a) structure to the other. This is addressed using a hybrid numerical technique...
finite element (structure) and boundary element (fluid) formulations.
Particular attention is given to the handling of specific boundary conditions and/or operating condition...
are encountered in test procedures and working environments: notably, installation in an infinite rigid t...
also excitation by a diffuse or random acoustic field.
Numerical examples show verifications of the approach which is presented.

1. INTRODUCTION

The question of vibro-acoustic transparency appears in a wide range of problems. Examples in...
transmission of noise through a car door or double-glazed window, and the acoustic energy applied to...
inside the fairing of a launch vehicle. An experimental analysis can be performed by placing a structur...
partition wall between a reverberant chamber, where a diffuse field is generated, and an anechoic cha...
purpose is then to measure which part of the power is transmitted through the structure from one cha...
other. However, such experimental tests are quite expensive, so for this reason, and in order to...
information on performance and any need for engineering design changes earlier in the design and de...
process, predictive methods are attractive.

This paper presents an innovative technology to perform predictive transparency analysis, using...
modelling. The method is based on a baffled boundary element formulation which can handle...
geometries lying outside the plane of the baffle, as well as co-planar with it. Numerical results are c...
analytic results and results obtained by an Infinite-Finite Element Method (IFEM). Some special a...
given to the handling of diffuse field acoustic excitation and to the prediction of the transmitted power.

2. THEORETICAL BASIS

2.1 Description of the problem

A thin structure lies in an infinite homogeneous fluid domain V which is divided into two parts V_+ a...
infinite plane baffle P_∞. By definition this plane is a plane where the acoustic normal velocity is equal...
it is an infinite rigid plane. The structure can lie inside or outside this baffle plane (ie, it need not b...
with the baffle) and the structure may also have holes through it.

# PREDICTED AND MEASURED LOW FREQUENCY RESPONSE OF SMALL ROOMS
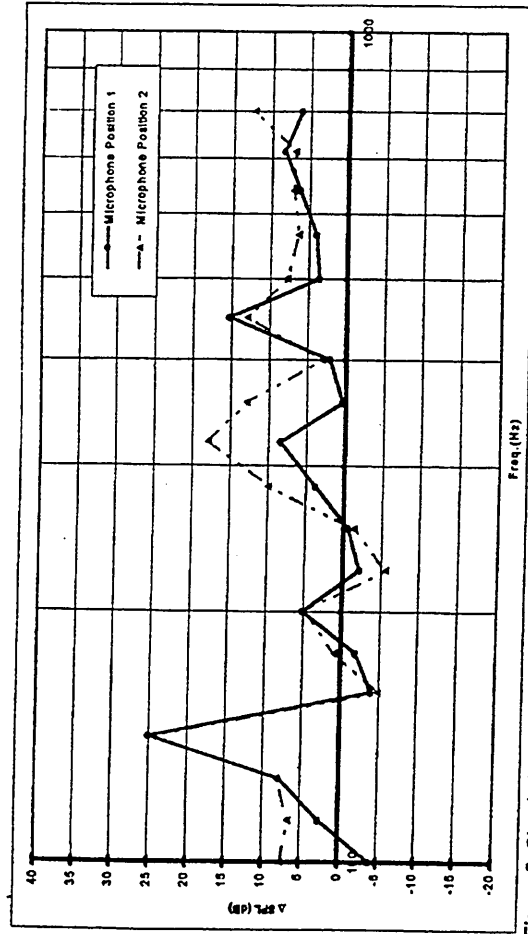
Figure 5: Simulation compared with measurements in a 6th octave band.
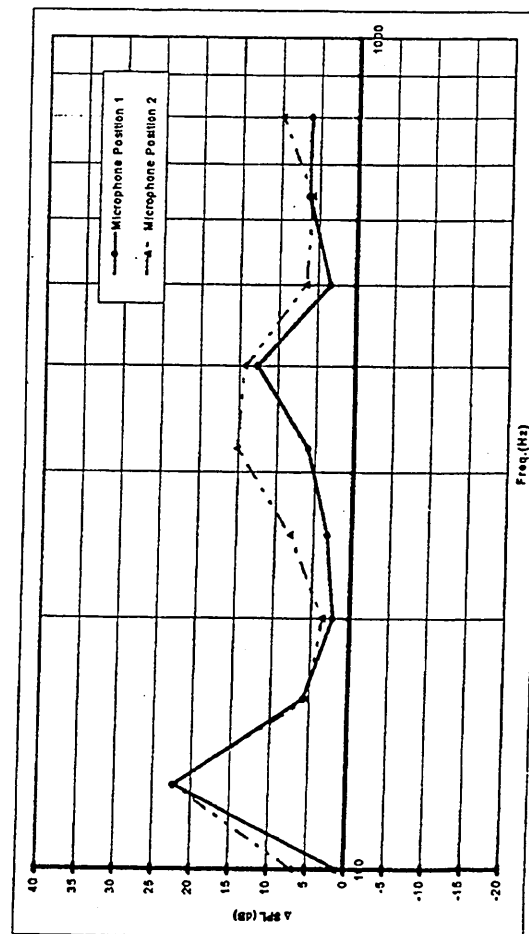
Figure 6: Simulation compared with measurements in a 3rd octave band.

THE INFLUENCE OF PARTITION BOUNDARY CONDITIONS ON SOUND LEVEL DIFFERENCE BETWEEN ROOMS AT LOW FREQUENCIES

S. Maluski[1] and B. Gibbs[2]

1. School of Construction, Sheffield Hallam University, Sheffield S1 1WB, UK
2. Acoustics Research Unit, The University of Liverpool, Liverpool L69 3BX, UK

INTRODUCTION

Noise from adjoining dwellings is increasingly recognised to occur below 100Hz[1,2], but laboratory and field measurements at these frequencies are unreliable and do not produce acceptable reproducibility[3]. The sound field at low frequencies is non statistical. The room modes are well separated and are controlled by the room dimensions. Recent investigations using FEM[4] and analytical methods[5,6,7] have considered the effect of room dimension on the sound insulation of a party wall. The party walls were modelled as simply supported or as mass controlled. In both studies, it was concluded that the sound level difference between rooms is not only a characteristic of the party wall, but also of the room configuration.

The work reported here is of an investigation of the effect of wall edge conditions on the sound insulation of party walls at low frequencies in domestic situations. A Finite Element Method was used to model the sound transmission between two rooms of volume less than 50m³ and to model the edges conditions of the party wall. The sound level difference was calculated for walls of different thickness and edge conditions, placed between two rooms of fixed dimensions.

VIBRATION FIELDS ON REAL WALLS

As a prelude to the computer modelled survey, the vibrational response of real walls was investigated to determine the edge conditions in order to recreate the characteristics of the domestic situations. Two brick walls, (A and B), with dimensions 2.88 x 2.49 x 0.115 m and 1.84 x 2.49 x 0.115m, were studied. An electro-dynamic shaker was bolted at a position which did not correspond to a structural node and a signal was generated by a signal analyser to the shaker with a bandwidth of 0-200Hz. An accelerometer was used to record the acceleration amplitudes at points on a 0.300m x 0.355m grid for wall A and on a 0.305m x 0.250m grid for wall B. The measured signal was displayed on the screen of an oscilloscope and compared with a reference signal. The nodal lines were determined when the measured signal was a minimum or when the measured signal changed from phase to out of phase with the reference signal.

It was possible to identify modes (1,1), (2,1), (3,1) and (1,3) of wall A and modes (1,1), (1,2), (2,1), (2,2) and (1,3) of wall B. In order to identify the likely corresponding edge conditions, the eigenfrequencies and their order along the frequency range were compared with theoretical prediction according to Leissa[x]. Figure 1 and Figure 2 show the frequency error ε, calculated between the theoretical and measured eigenfrequencies of the wall A and B, respectively, for simply supported and simply supported with two clamped edges, where;

$$\varepsilon = \frac{\text{predicted value} - \text{measured value}}{\text{predicted value}} \times 100$$

Large discrepancies were obtained if all simply supported edge conditions are assumed. The smallest discrepancies obtained for each mode is obtained assuming two simply supported with two clamped edges. The edge conditions of a typical party wall therefore lie between simply supported and clamped, a phenomenon already observed by Balike[9]. The walls investigated formed corner junctions and it was recognised that party walls would form a T-junction and thus have a stiffer edge constraint. The approach, therefore, was to investigate the range of possible edge conditions likely, including simply supported, clamped and mixed edge conditions. The real conditions could be assumed to lie somewhere in this range.

ROOM-PANEL-ROOM SIMULATION

The use of FEM to model the sound transmission between rooms was justified in a former work[10]. A fixed room configuration of 40m³ and 35m³ was modelled but did not include surface absorption. The party wall model was of brick with dimensions 4x2.5m², also modelled with no damping. Three wall thicknesses were considered: 0.5m, 0.1m and 0.2m. The sound pressure level difference was calculated from 31.5Hz to 160Hz. A point source was assumed to be in one corner of the 40m³ room, opposite to the party wall. The frequency response in each room was calculated to a frequency resolution of 1Hz. Two field boxes in each room with 152 points each, placed 0.5m from the walls and 0.3m from the ceilings and floors, were defined. The 152 points were then averaged and the narrow band values recalculated to give the 1/3 octave band values.

EFFECT OF WALL THICKNESS AND EDGE CONDITIONS

The sound pressure level difference of a 0.05m, 0.1m and 0.2m thick wall for simply supported (SSSS), clamped (CCCC) and mixed conditions (SCSC) are shown in Figures 3-6. The predicted sound pressure level difference increases with increasing thickness as expected. The presence of alternative maxima and minima clearly observed in the narrow band data in Figure 3, are due to room and wall resonances[7]. When presented as 1/3 octave values, the predicted sound level difference of a simply supported 0.05m wall varies between 20 and 35dB in the range 100Hz to 160Hz. The sound insulation of a simply supported 0.2m thick wall varies between 28 and 45 dB. Measured data by Khilman[11] and Parkin[12] was of similar value. From 40Hz, the sound level difference of the 0.05m thick wall increases at about 6dB/octave. The sound level difference of

the 0.2m thick wall, however, tends to decrease at 6dB/octave. This supports the findings of Gargiadini[5], Parkin[12] and Osipov[13]. Figures 4-6 also show that:

1. The position, with respect to the other edge conditions, of the curve of the clamped wall varies with the thickness of the wall[11,14].
2. The mixed edge values are greater than those of the simply supported 0.05m wall.
3. The mixed edge conditions lie between the simply supported and clamped values for the 0.05m and 0.2m walls.

DISCUSSION

The classic monotonic decrease and increase of sound insulation with frequency corresponding to the stiffness controlled and mass controlled regions, respectively, are not observed in the frequency range of interest. However, although the sound fields in the source room and in the receiving room are not statistical, the curves display trends, which could be interpreted by the classical mechanisms.

The 0.05m wall appears mass controlled from 40Hz with "the limper" simply supported wall giving a slightly higher value. The clamped wall appears to stay stiffness like, up to 80Hz.

The 0.2m wall appears stiffness controlled and therefore the clamped condition gives the highest value. The 0.1m wall displays a transition between stiffness controlled and mass controlled.

For the three thicknesses, the mixed edge conditions give values, which tend toward those of the simply supported case. The selection of the simply supported condition is therefore closer to the real boundary conditions than a clamped condition.

A thin wall seems to reduce the effect of room resonances due to the higher structural modal density than for thick walls[13].

CONCLUDING REMARKS

At low frequencies, the party wall response is influenced by the modal characteristics of rooms and of party wall and large variations in sound level difference can be observed. However, the frequency trends still can be explained in terms of the classical mechanisms. A thin masonry wall likely to be mass controlled above 50Hz. A thick wall, typical of acceptable construction between dwellings, will be stiffness controlled, below 100Hz. The edge conditions are found to have an effect on the sound pressure level difference since they change the structural modal density and the trend of the sound level difference curves. Mixed edge conditions are thought to be a reasonable approximation to typical installations in the field, although one edge of wall A at two edges of wall B are corner junctions and not T-junctions as found in dwellings. Also, the mixed edge conditions gave results similar to that of the simply supported. The effect of edge conditions at low frequencies should be further investigated by introducing absorption inside rooms, damping in the structural model and flanking transmission between the party walls.

Figure 1. Frequency error between theoretical and measured eigenfrequency of wall A

Figure 2. Frequency error between theoretical and measured eigenfrequency of wall B

Figure 3. Sound pressure level difference in narrow bands for simply supported 0.1m wall. Bandwidth containing wall vibration modes

685

REFERENCES

1. Brooks, J. R., Attenborough, K., "The implication of measured and estimated domestic source levels for insulation requirements", Proceedings of I.O.A., Vol.11 (11), 19-27, (1989)

2. Grinwood, "Complaints about poor sound insulation between dwellings", IOA Acoustics Bulletin, 20 (4), 11-16 (1995)

3. J. Roland, "Adaptation of existing test facilities to low frequency measurements", Inter-Noise, 2, 1113-1116 (1995)

4. Pietrzyk and T. Khilman, "The sensitivity of sound insulation to partition location - Case of heavyweight partitions, Inter-Noise 97, 2, 727-730 (1997)

5. L. Gargliadini, J. Roland and J. L. Guyader, "The used of functional basis to calculate acoustic transmission between two rooms", Journal of Sound and Vibration, 145 (3), 457-478 (1991)

6. W. Kropp, A. Pietrzyk, T. Khilman, "On the meaning of the sound reduction index at low frequencies", Acta Acustica, 2, 379-392 (1994)

7. A. Osipov, P. Mees and G. Vermeir, 'Low frequency airborne sound transmission through single partitions in Buildings', Applied Acoustics, 52(3-4), 273-288 (1997)

8. A. Leissa, Vibration of plates. (Edition Acoust. Soc. Amer., 1993).

9. M. Balike, R.B. Bhat and S. Rakheja, "Noise transmission through a cavity backed flexible plate with elastic edge contraints", Third International congress on air- and structure-borne sound and vibration, Montreal, Canada, 335-343, (1994)

10. S. Maluski, H. Bougdah, "Predicted and measured low frequency response of small rooms", Building Acoustics, (1998)

11. T. Khilman, "Report on the influence of boundary conditions on the reduction index", Report ISO/TC 43/SC 2/WG 2 (1970)

12. P.H. Parkin, H.J. Purkis and W.E. Scholes, Field and measurements of sound insulation between dwellings. (Her Majesty's Stationery office, London, 1960).

13. A. Osipov, P. Mees, G. Vermeir, "Numerical simulation of airborne sound transmission at low frequencies: the influence of the room and the partition parameters", Inter-Noise 97, 2, 759-762 (1997)

14. G. Maidanik, "Response of ribbed panels to reverberant acoustic fields", J. Acoust. Soc. Amer., 34 (6), 809-826
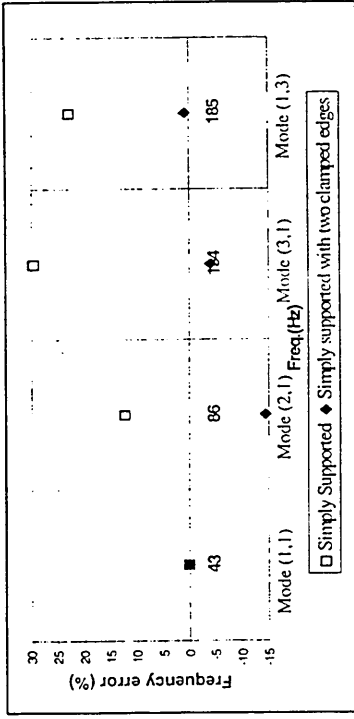
684
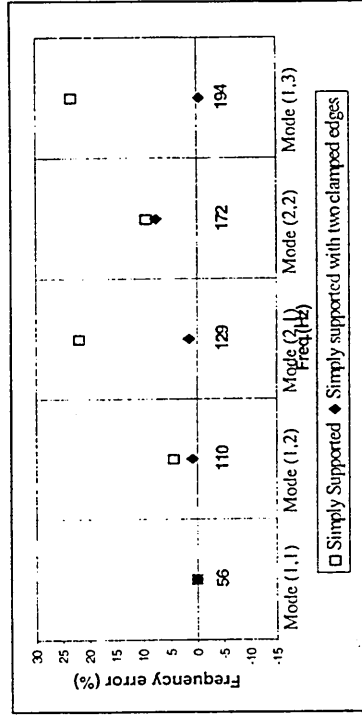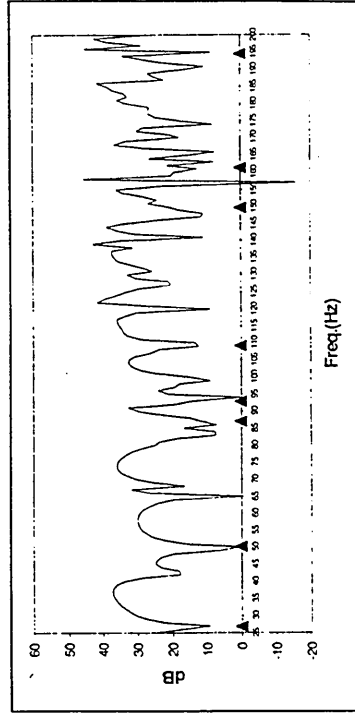
Figure 4. Sound pressure level difference of 0.05m wall

Figure 5. Sound pressure level difference of 0.1m wall

Figure 6. Sound pressure level difference of 0.2m wall

SOUND LEVEL DIFFERENCE BETWEEN DWELLINGS AT LOW FREQUENCIES

B M Gibbs[1] and S Maluski[2]

[1] Acoustics Research Unit, University of Liverpool, Liverpool L69 3BX, U.K.
[2] School of Construction, Sheffield Hallam University, Sheffield S1 1WB, U.K.

1. INTRODUCTION

With the growth in noise problems at low frequencies in dwellings, there is an increasing need to understand sound transmission at frequencies below 100 Hz in order to provide better sound insulation. Wave theory has shown that the sound insulation of a limp or simply supported wall is strongly dependent on the room dimensions due to the non statistical sound fields [1-3]. Field measurements of the vibrational fields of brick walls show that at low frequencies, the wall edge conditions lie between classical simply supported and clamped conditions [4]. Using a Finite Element Method, a parametric study has been conducted on the effect of wall edge condition on the sound level difference between two rooms. It was confirmed that the sound level difference depends upon both the wall bending stiffness and edge condition. For brick walls of 0.1m thickness and more, the sound level difference of a clamped wall is greater than the simply supported.

The aim of this work is to investigate the variance in sound level difference due to the range of wall edge conditions and room configurations likely in the U.K. on the sound level difference at low frequencies. Results are presented as one third octave band values, from 31.5 Hz to 160 Hz, in the form of means and standard deviations from populations of room configurations and wall edge conditions.

2. FEM MODEL

Many plans of houses in the U.K. were looked at and room dimensions were registered. The resultant data base shows that typical domestic room

volumes are lower than 50m³ and equal or greater than 20m³. The most common configuration in storey blocks and attached dwellings is that of equal rooms. Consequently, 20m³, 30m³ and 40m³ equal room configurations and three unequal room configurations using the same three volumes were selected. A FEM model was used of the sound transmission between two rooms. The model had been validated as a result of good agreement between predicted and scale model measurement [5,6].

The model did not include surface absorption in the two rooms or material damping in the separating wall. The source always was placed in the same position whatever the room volume and therefore the effect of loudspeaker location is not included in this paper. In the case of the unequal room configuration, the largest room was selected as the source room. A 0.2m brick wall with three possible edge conditions was investigated: simply supported, clamped and a combination of two simply supported edges and two clamped edges [7].

3. RESULTS

The mean sound pressure level difference for the three wall edge conditions are displayed in Figures 1-4. The sound pressure level difference in unequal rooms is seen to be greater than that in equal rooms and this supports the findings of Pietrzyk [2]. Also, the standard deviations are greater. The level difference decreases with frequency in all cases. As expected, the number of wall vibration modes, in the range of interest, is greater in the simply supported case than the clamped case. In all cases, there are no room or wall modes in the 31.5 Hz band and the sound level difference is of the order of 50 dB, whatever the room configuration and the standard deviation is small. The effects of boundary conditions and room configuration can be considered negligible. This remains true for the clamped wall up to 63 Hz and it can be considered stiffness controlled below this frequency.

From 40 Hz, the room dimensions affect the sound level difference. At least one room mode is excited in each room. In addition, the standard deviations become large when wall vibration modes occur in or near the frequency band of interest. At 63 Hz the standard deviation of the simply supported wall is a maximum due to panel resonance, a phenomenon which is repeated at 100 Hz. The standard deviations for the clamped wall are smaller than for the simply supported and mixed edges walls except at 160 Hz. The wall edge conditions have an effect on the sound level difference when the rooms are equal in volume. The wall resonances give rise to strong coupling with the room modes and edge conditions control the distribution of the panel eigenfrequencies.

The effect of unequal excited room modes in each third octave band reduces the number of strong structural-acoustic couplings, but the simply supported wall still displays strong resonances. This, generally, is not the case for the mixed and clamped edge conditions.

4. CONCLUDING REMARKS

A limited survey has been conducted on the effect on sound level difference between dwellings of room dimensions and wall edge conditions likely in the U.K. Below the standard measurement range of 100 Hz to 3,150 Hz masonry walls of thickness 0.2 m do not display the classical mass law trend but rather a stiffness controlled decrease in value with increase in frequency.

Above 31.5 Hz room modes occur and, depending on the assumed edge condition, wall vibration modes can strongly couple. This will cause large fluctuations in sound level difference due to the variation in room dimension and the method of bonding of the separating wall into the surrounding building structure. These effects can be controlled by having unequal room configurations and mixed or clamped edge conditions. Unfortunately the obtained sound insulation at low frequencies in dwellings is the worst as most of the room configuration encountered are of equal volume. The edge condition of the domestic wall can be assumed to lie between the simply supported and clamped, tending to the former.

REFERENCES

[1]   L. Gargliadini, J. Roland and J. L. Guyader, 'The used of functional bases to calculate acoustic transmission between two rooms', Journal of Sound and Vibration, **145**(3), 457-478, (1991).

[2]   W. Kropp, A. Pietrzyk, T. Khilman, 1994, "On the meaning of the sound reduction index at low frequencies", Acta Acustica, **2**, 379-392, (1994).

[3]   A. Osipov, P. Mees and G. Vermeir, 'Low frequency airborne sound transmission through single partitions in Buildings', Applied Acoustics, **52**(3-4), 273-288, (1997).

[4]   S. Maluski and B. Gibbs, 'The influence of partition boundary conditions on sound level difference between rooms at low frequencies', EURONOISE-98, Munich, (1998).

[5]   S. Maluski, B. Gibbs and H. Bougdah, 'Predicted and measured low frequency response of small rooms', I.O.A. Proceedings, Cranfield, (1998).

[6]   S. Maluski, H. Bougdah, 'Predicted and measured low frequency response of small rooms', accepted for Building Acoustics, (1998).

[7]   M. Balike, R.B. Bhat and S. Rakheja, 'Noise transmission through a cavity backed flexible plate with elastic edge constraints, Third International Congress on air- and structure-borne sound and vibration, Montreal, Canada, 335-343, (1994).
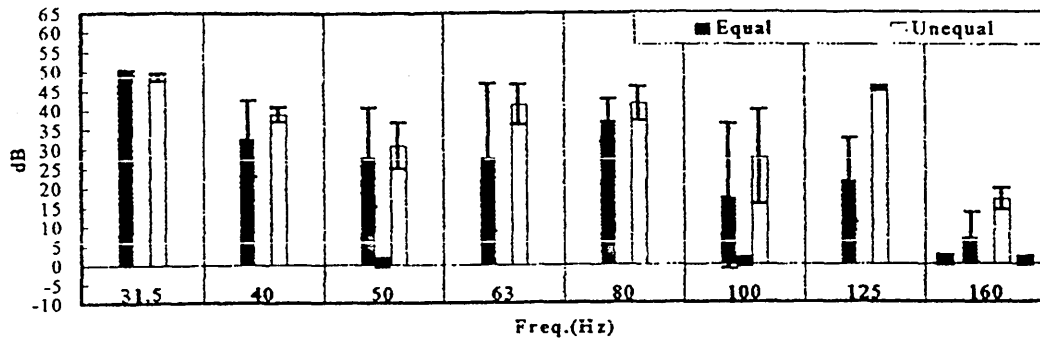
Figure 1.   Sound pressure level difference of a simply supported 0.2m brick wall.
Mean and standard deviations. ☰Bandwidth containing wall modes.
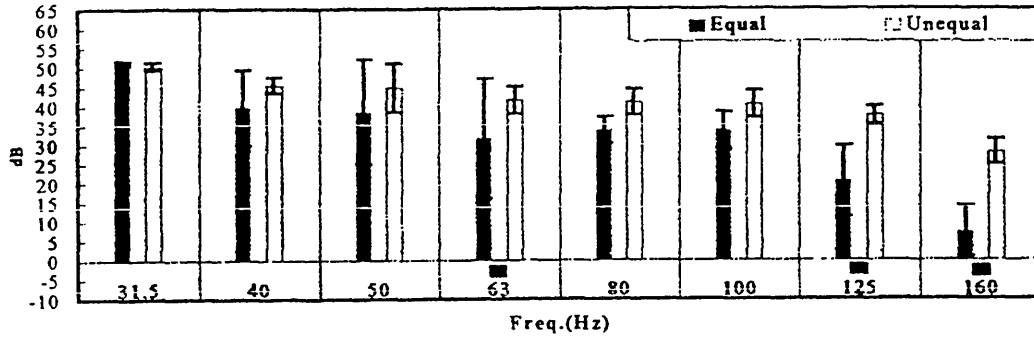
Figure 2.   Sound pressure level difference of the 0.2m wall with mixed
edge   conditions.
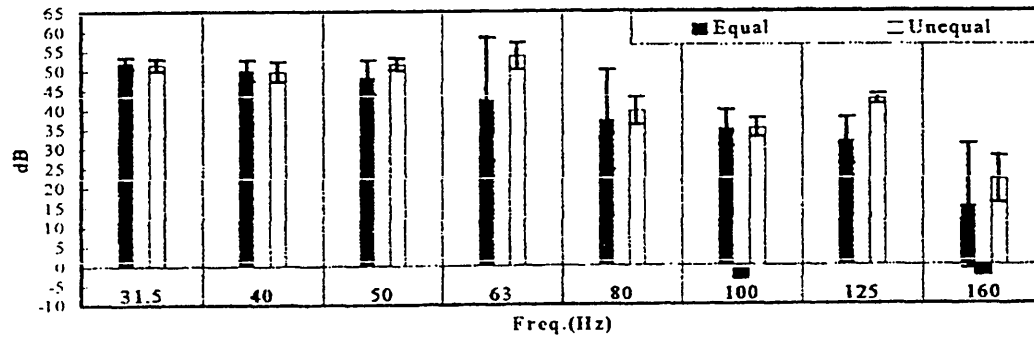
Figure 3.   Sound pressure level difference of the clamped wall.
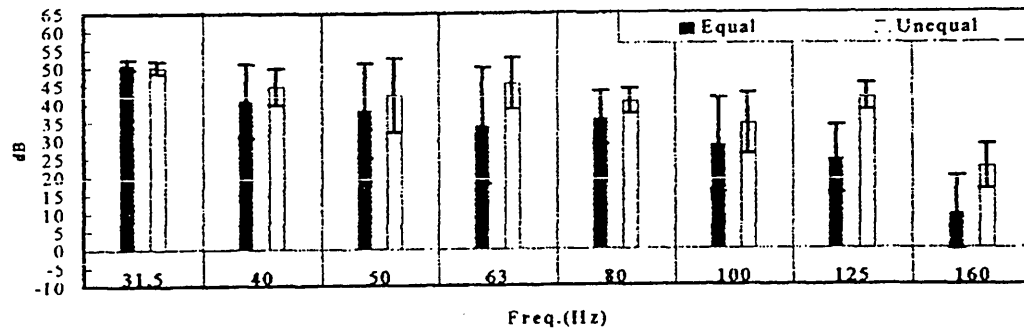

Figure 4.   Sound pressure level difference of the 0.2m brick wall, including all
edge conditions.

VARIATION OF SOUND LEVEL DIFFERENCE IN DWELLINGS DUE TO ROOM MODAL CHARACTERISTICS

Sophie Maluski[1] and Barry Gibbs[2]

1. School of Construction, Sheffield Hallam University, Sheffield S1 1WB, U.K.
2. Acoustics Research Unit, University of Liverpool, Liverpool L69 3BX, U.K.

Sound insulation at low frequencies is known to be difficult to measure accurately and to produce poor reproducibility. The use of numerical or analytical methods with the help of powerful computers allows us to understand the phenomenon of sound transmission at those frequencies. In this review, the sound insulation of party walls are shown to be strongly dependent on the acoustical modal characteristics of the connected rooms and of the structural modal characteristics of the party wall. Equal room configurations give a poorer sound insulation, compared with unequal room configuration. The sound insulation is strongly dependant on room dimensions, as well as size, type and edge conditions of the party wall.

1.1 INTRODUCTION

Increasingly noise from adjoining dwellings occurs below 100Hz, due to powerful modern hi-fi and home cinema systems with enhanced bass response [1,2]. However, the present measurement standards [3,4] are confined to frequencies above 100Hz and therefore there is little field data or prediction methods available for these low frequencies. The introduction of an annex in the standards [3] for laboratory measurements at low frequencies has not solved the problem and at present, no method has been agreed for laboratory measurement [5]. Poor repeatability [6] and reproducibility [5] are explained by the non statistical behaviour of the sound field in the rooms, even for room volumes greater than 50m³ as found in test laboratories. In dwellings, the rooms are much smaller than the standard volumes in laboratories and the problem is exacerbated. Large measurement surveys for frequencies below 100Hz would be expensive and it is not clear yet how the data should be treated.

Recently, analytical and numerical methods have been employed in preliminary studies of the sound insulation of party walls in simulated test and field conditions. The methods are not based on classic statistical sound field assumptions, but take account of the acoustical and structural modal characteristics [5,7-12,14,16,20-23]. The reliability of the methods is strongly dependant on the way the numerical model is defined, but good agreement between prediction and validating measurements has been obtained [7-11].

The present paper is a review of the use of numerical methods for investigation of sound insulation at low frequencies. Effects of room configuration and the size and edge conditions of party walls are examined.

1.2 ANALYTICAL/NUMERICAL METHODS

Analytical or numerical methods are based on the wave theory rather than diffuse field theory. Using the analytical model, the sound transmission between two rooms is modelled by describing the room - party wall - room system with a set of equations for which the boundary conditions are defined. Solutions of the set of equations give the room pressure amplitudes and wall displacements, and the frequency response of the room and party wall. Its utilisation thus gives information not obtainable by classical theory [7-8], but the method is limited to rectangular and cubic shapes to facilitate the decomposition of the modal characteristics. The wall edge conditions also are difficult to model.

Numerical methods and particularly, the Finite Element Method (FEM), are able to describe the interaction between the party wall and the sound fields for all room shapes. The principle of the FEM is to solve a system described by discretising a set of governing differential equations. The elements can have different geometry, and each one is described by a motion equation. They are characterised by a number of nodes, which fulfil continuity conditions between elements. The choice of the number of elements is defined by wavelength and thus the upper frequency of the range of interest. The modelling of the sound transmission between two rooms involves linking the rooms, modelled as Acoustic Finite Elements, and the party wall, modelled as the Structural Finite Elements. The advantages of this method are that the sound field can be predicted in any room shape with or without absorption. The numerical method also provides information not obtainable by classical theory or easily by measurement [12]. Change of parameters such as room dimensions, panel size, edge conditions can be done very easily and observed. The limitations of FEM are that it requires powerful computers, and only the low and mid frequencies can be modelled as more elements are required to model higher frequencies leading to long process times. The more complex the model, the more elements are required. When coupling the acoustic FE and the structural FE, the acoustic meshes need to match the structural meshes, which leads to an underestimation of the panel radiation. The model must also be validated by measurement.

The investigations reviewed here, only modelled airborne sound transmission and modelling flanking transmission between two rooms remains problematical. Acoustic damping has been incorporated in some investigations [7-9,14, 20, 21, 23] by setting a reverberation time of 1s[8,14] or 2.5s [9]. However, it is well known that measurements of absorption at low frequencies are not accurate [13] or easy to interpret and the selected reverberation times might not be representative.

Another issue to be addressed is that of the terminology. Terms such as transmission loss (or sound reduction index) are used to characterise sound transmission at low frequencies. Originally defined for measurement conditions where the sound field was considered statistical, they may not be appropriate for room configurations with volumes smaller than $50m^3$ and where sound wavelengths are large. Consequently, the term sound pressure level difference will only be employed excepts where referenced work indicates otherwise.

1.3 ROOM CONFIGURATIONS

To date, most studies of the effect of the room configurations on the sound level difference involve homogenous masonry walls. Figures 1-2 show the spread of the sound level difference in third octave bands, for a limp wall and for a clamped brick wall, after Pietrzyk [14] and from work of the present authors, respectively. The limp wall, which represents a
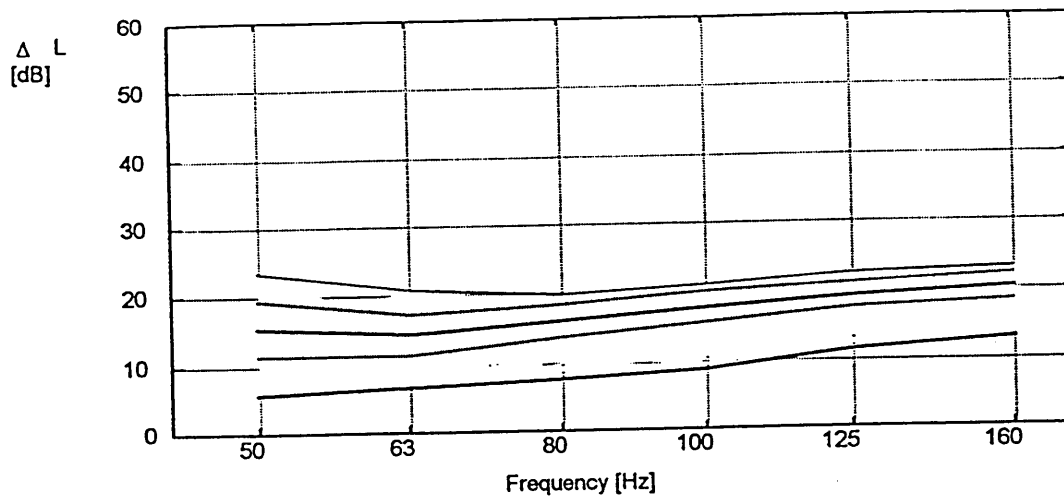
Fig. 1 Effects of varying the room configuration on the sound level difference of a limp wall
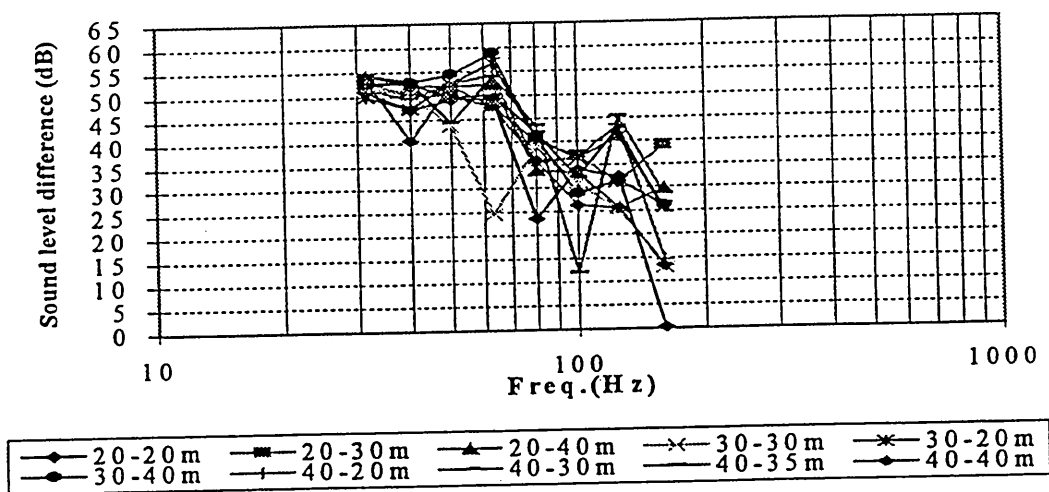

Fig. 2 Effects of varying the length of the two enclosures on the sound level difference of a $10m^2$ clamped heavyweight wall

gypsum board of $20kg/m^2$, is a wall theoretically without resonant characteristics and the clamped brick wall has no resonant characteristics from 31.5Hz to 80Hz 1/3 octave bands. The sound level difference of the limp wall (Fig. 1) is presented as a bandwidth of data from 656 room configurations varying from $15m^3$ to $105m^3$. For the brick wall (Fig. 2), the sound level difference was investigated for a much smaller sample of 10 room configurations, varying from $20m^3$ to $40m^3$. In the first case, the room configuration was modified by changing the length and the width of the rooms, while for the second case, only the length was varied. It is observed that for the limp wall, the spread of results is 18dB at 50Hz and then tends to 10dB as the frequency increases. For the heavyweight wall, the spread is 10dB from 31.5Hz to 80Hz if $40\text{-}40m^3$, $30\text{-}30m^3$ and $20\text{-}20m^3$ equal room configurations are not included in the 40Hz, 63Hz and 80Hz third octave bands, respectively. Then the spread tends to increase above 100Hz due to the presence of the first wall structural mode. The trends of the sound level difference of the limp wall and of the heavyweight wall are different. The sound level difference of the limp wall is mass controlled and increases on average at 6dB/octave, while the sound level difference of the heavyweight wall is stiffness controlled and decreases at -6dB/octave. Room configuration therefore does not affect the 'average' properties of the wall, but introduces variations of sound level difference about the trend line due to strong acoustic

couplings. Those couplings vary with the number of excited acoustic modes in each third octave band. Table 1 shows the number of acoustical modes per 1/3 octave bands for volumes of 20m³, 30m³, 35m³ and 40m³, which are typical room volume in dwellings and used to obtain the data displayed in Figure 2. The room height is 2.5m and the width is 4m.

Volume(m³)	Third Octave Bands(Hz)							
	31.5	40	50	63	80	100	125	160
20	0	1	0	1	3	3	5	9
30	0	1	0	3	3	3	6	14
35	0	1	1	2	3	5	6	18
40	0	2	0	2	4	5	9	15

Table 1 Number of acoustical modes per 1/3 octave band

The number of modes per third octave band is small. The total number of modes in the frequency range of 31.5Hz-160Hz is 22 for a 20m³ room and 37 for a 40m³ room. Thus, no band contains more than 20 modes, which is the minimum required for not having discrepancies in the sound level difference measurements [15]. Also, the 40m³ room has identical length (X) and width (Y) and thus the X- axial modes are identical to Y- axial modes, and the XZ tangential modes are identical to the YZ tangential modes. This also explains why the 40m³ equal room configuration displays a large drop in sound level difference, because of the coupling of four axial modes of wavelength identical to the dimensions of the party wall. The dip at 63Hz and 80Hz corresponding to the 30m³ and 20m³ equal room configurations, respectively are also due to strong acoustic couplings which take place between 3 acoustic modes in each room. Those three identified dips are therefore due to the equal room configurations, which create strong acoustic-acoustic couplings.

The presence of lightweight and heavyweight party walls introduces resonances in the frequency range of interest. Figure 3 shows the sound level difference of a lightweight and heavyweight partition, according to Osipov [9], and Figure 4 shows the sound level difference of another heavyweight partition obtained by the work of the present authors.

In the three cases, the sound level difference varies as alternating maxima and minima, which are more pronounced for the heavyweight walls. The number of excited structural modes can explain that difference. The lightweight wall presents more modes in each third octave band and the first structural mode is excited before the first room resonances. The heavyweight wall presents well-spaced resonances, separated by two third octave bands and the first structural mode is excited above the first room resonances. Acoustic-structural couplings take thus place between the rooms and the partition. Their effects change with the number of room modes and structural modes present in the third octave band. Again the couplings do not affect the trend of the curves of lightweight wall and heavyweight wall.
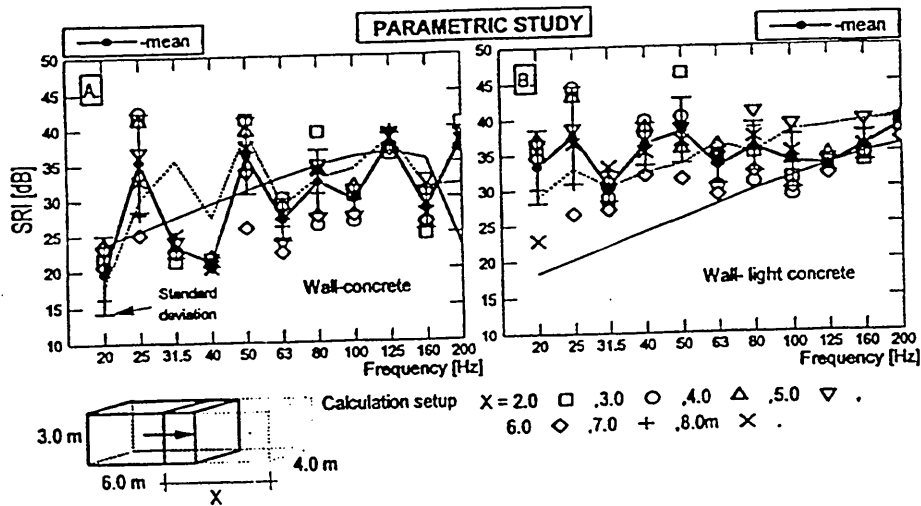
Fig. 3 Effects of varying the length of the receiving room of the transmission rooms (Source room: 72m³) on the sound level difference of a 12m² lightweight and heavyweight party walls
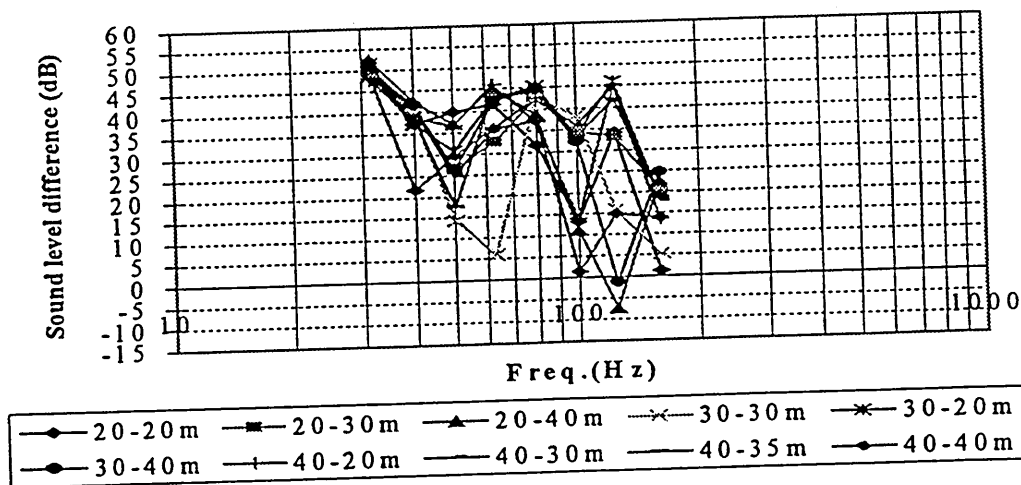

Fig. 4 Effects of varying the length of the two enclosures on the sound level difference of a 10m² heavyweight partition

The spread of values for both the lightweight and heavyweight partitions of Osipov [9] amounts to some 18dB (Fig. 3). The spread for heavyweight party walls can also be very large (Fig. 4). The differences observed between the two heavyweight walls could be explained by the room volumes, which are in general much smaller than those selected by Osipov. The difference can also be explained by the acoustic damping, which is modelled in the source room and in the receiving room of Osipov's model. The effects of high peaks of each mode are then reduced yielding to a smaller spread of the sound pressure level difference. Figure 5 shows the effect on the sound level difference for a gypsum wall placed in 16 different room configurations [14]. The mean sound pressure level difference in equal rooms is found to be lower than that in unequal room configuration, a phenomenon already observed with measurements at higher frequencies [17-19]. The number of couplings is smaller in unequal rooms than in equal rooms. In Figure 5, it is also observed that the sound level differences vary

more with volume change for the equal room configurations. This phenomenon is also observed in Figure 2. It highlights that the sound level difference in a 20m³ equal room configuration is better than in a 30m³ or 40m³ room configuration except in the 80Hz and 100Hz third octave bands, which correspond to acoustic -acoustic and acoustic-structural coupling.
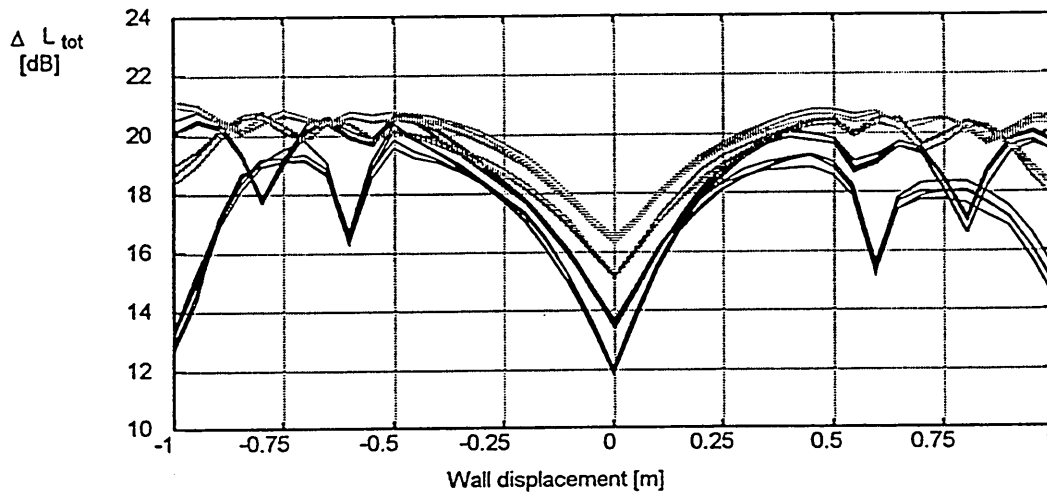

Fig. 5 SPL difference as a function of the displacement of the partition from the original position of equal rooms. - case of single wall partition with 20 kg/m².

The effects of room configuration on the sound level difference of two double walls have been investigated by Pietrzyk [14]. The first was of double gypsum board for each leaf and a cavity of 0.095m, with a mass-spring-mass resonance at 50Hz. The other was of triple gypsum boards for each leaf (30kg/m2) and a cavity of 0.15 and a mass - spring - mass resonance at 33Hz. The sound pressure level difference was obtained for 656 different room configurations and is displayed in Figure 6-8. Figure 6 shows that the spread approaches 20dB and the mean value of sound pressure level difference is close to the analytical results for the infinite wall. Despite the low modal density of rooms, the spread of results is nearly independent of frequency, but decreases significantly at the mass-spring-mass resonance frequency. When the sound pressure level difference is presented in 1/3 octave bands (Fig. 7-8), the spread is reduced to 10dB.
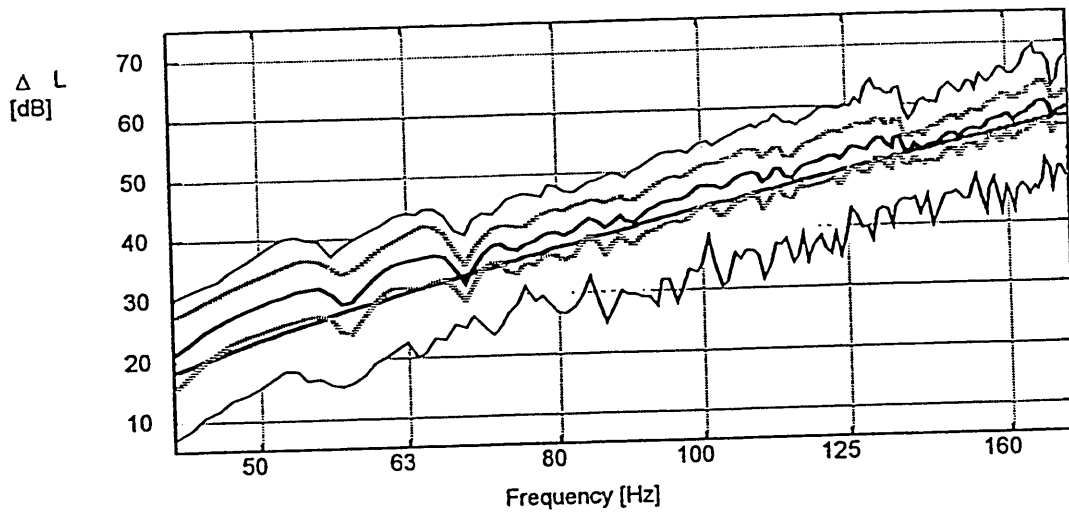
Fig. 6 The narrow band Sound Pressure Level Difference as a function of the frequency for 656 different room configurations.
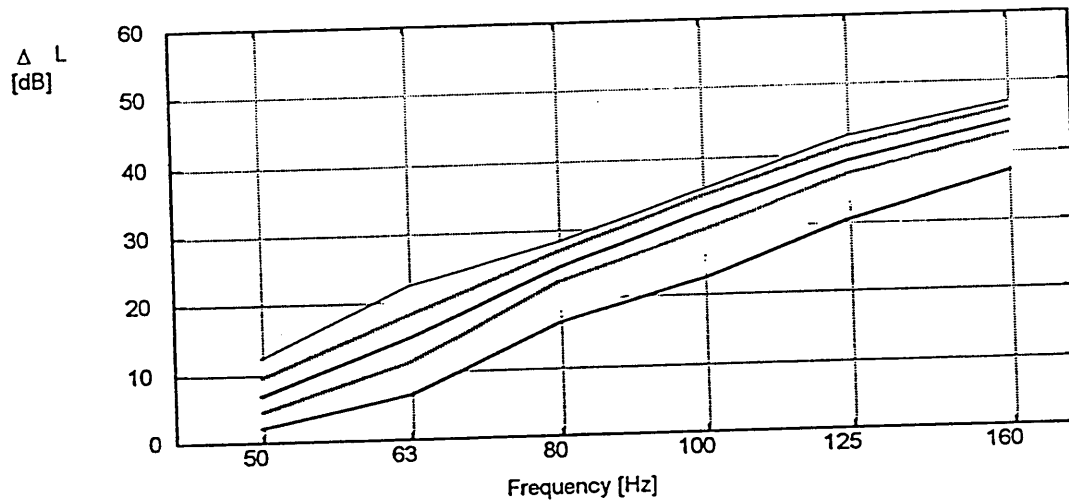

Fig. 7 The 3rd octave band SPL difference as a function of frequency for 656 different room configurations case of first double leaf partition
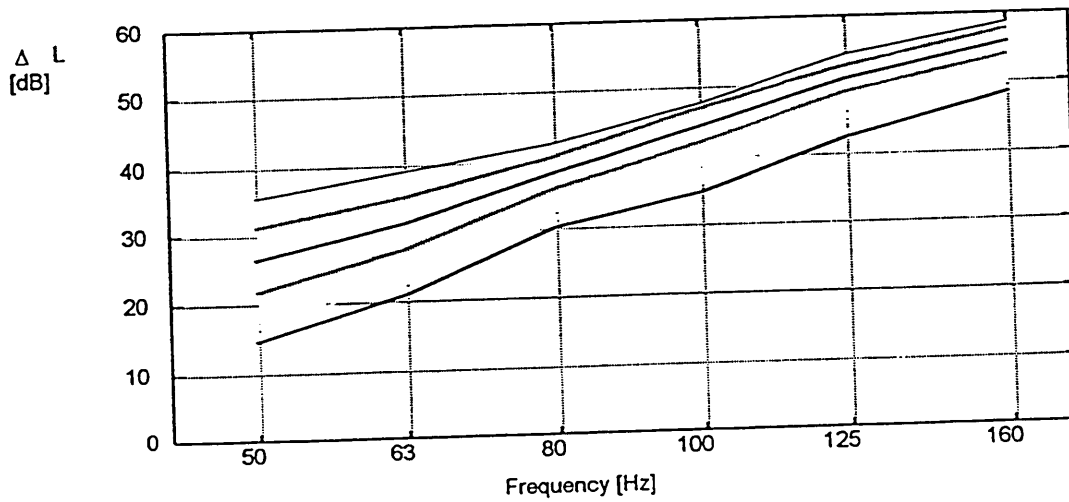

Fig. 8 The 3rd octave band SPL difference as a function of frequency for 656 different room configurations - case of the second double leaf partition.

Figures 9-10 show the sound pressure level difference varying with wall position. Again, the sound level difference is a minimum when the wall is placed in an equal room configuration, but large variations are obtained when the wall is placed in unequal room configurations.
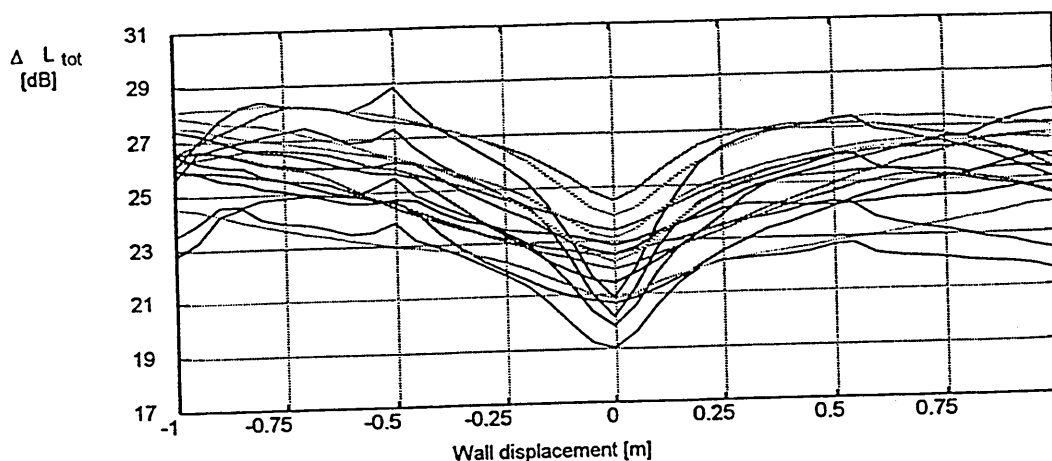

Fig. 9 Sound pressure level difference as a function of the displacement of the partition from the original position of equal rooms. - Case of double leaf partition D 95/70 202 M95.
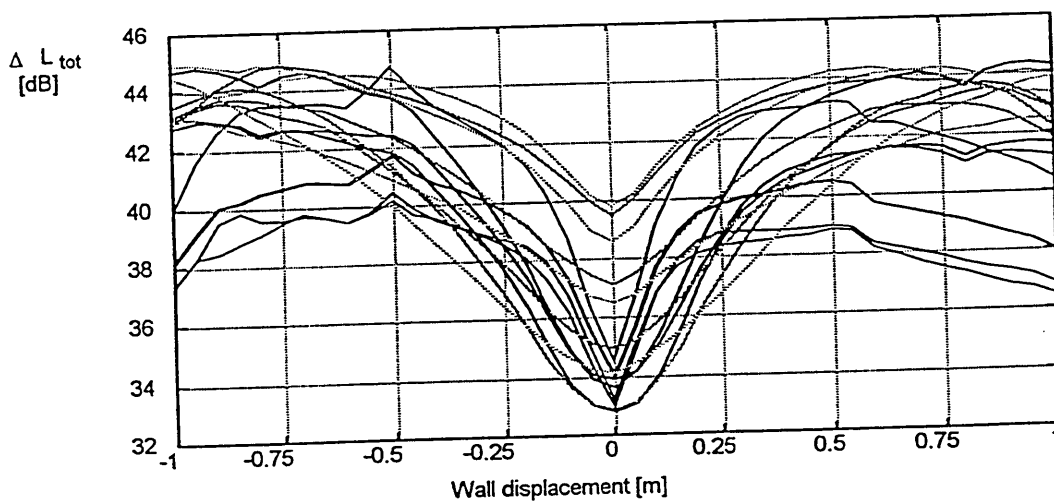

Fig. 10 Sound pressure level difference as a function of the displacement of the partition from the original position of equal rooms. - case of double leaf partition DD 70/70 303 M150.

To summarise, the sound pressure level difference varies with the room configuration, because the sound field is not statistical. Strong acoustical couplings take place, but also structural and structural-acoustical couplings. A correction factor which take account the acoustic coupling and structural-acoustic couplings may be necessary in order to predict the sound level difference of the party wall at low frequencies.

1.4 THE PARTY WALL

In the previous section, it was shown that the sound level difference is dependant on the acoustic couplings which take place between the two rooms. The variations also are affected

when at least one structural resonance is excited in the 1/3 octave band. The structural modes can be shifted in frequency by changing the dimensions and edge conditions of the party wall. The effect of wall size has been investigated by Gargliadini [7,20], Pietrzyk[14], and Osipov[9,21]. Figure 11 shows that the sound level difference of a party wall of different sizes [9]. Again, alternating maxima and minima are observed, but such variations tend to smooth out when the party wall has a large modal density as seen in Figure 3. For a lightweight wall, the sound level difference tends to increase with frequency. The spread is 25 dB, but decreases with increasing frequency and increasing wall size. For thick wall, the sound level difference can be classified into two groups. For walls of sizes smaller than 12m², there is an observed decrease of –6dB/octave. For the less stiffened walls of sizes greater than 12m², there is an increase with frequency. The spread in value is much greater than for lightweight walls. In general, the spread decreases with increase in the number of acoustic and structural modes in the third octave band. Gargliadini [7,20] investigated, analytically, the effects of panel size in one specific room configuration of volumes greater than 50m³. Large variations were also obtained but were shown to be reduced when three structural modes at least are excited in a third octave band. However, Osipov [9] showed that, in the presence of a single acoustical mode in a third octave band, the sound level difference of the partition varies with position in the laboratory wall of the transmission suite. Indeed, the position of the party wall can correspond to a pressure node of for example a tangential mode in the receiving room. The excitation of the sound field in the receiving room will be weak and thus provide a peak in the sound level difference. While the panel placed at the corner of the laboratory wall will correspond to an anti-node pressure and will strongly excite the sound field inside the receiving room. This results in a drop in the sound level difference.
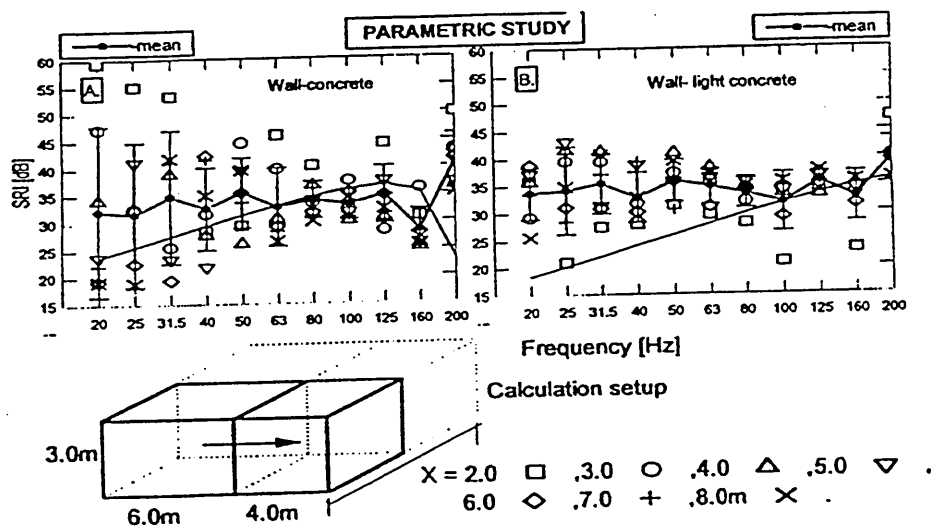

Fig. 11 Predicted Sound Reduction Index averaged over third octave band.
Wall thickness 10cm, ———— Infinite Place theory

The effects of edge conditions including simply supported, clamped and mixed edge conditions (SCSC) were investigated on a masonry wall of 50mm thickness, placed in a room configuration of 40m³ and 35m³ [16]. The edge conditions were applied on the four side of the party wall. The results for a single wall are presented in Figure 12. The change from simply supported to clamped conditions shifts the eigenfrequencies upward. Large variations of sound level difference are then obtained. The structural resonances and the structural-acoustical

couplings are then modified, leading to a different arrangement of peaks and dips of the sound level difference. A large difference between simply supported and clamped conditions is also obtained. Clamped thin walls insulate less than simply supported. Similar observations are found in the work of Khilman [17], but the present difference between simply supported and clamped is not constant due to strong room couplings.

The effects of edge conditions of two types of double walls also have been investigated [22], but the double wall, here, is a panel system of infinite lateral extent and only the normal incidence transmission loss was investigated. Clamped conditions increase the sound insulation at low frequencies owing the mounting stiffness and insulate more than the simply supported. The edge conditions have a strong effect on the sound insulation owing to the strong modal response in the low frequency range. It can be added that a similar phenomenon was observed with heavyweight walls [16]. Gargliadini [23] also has investigated analytically the dynamics of the double wall, but the work is not reported here.

To summarise, the room/wall couplings and thus the sound pressure level difference are strongly influenced by the structural modal characteristic, which can be changed by varying the size and edge conditions of the party wall.
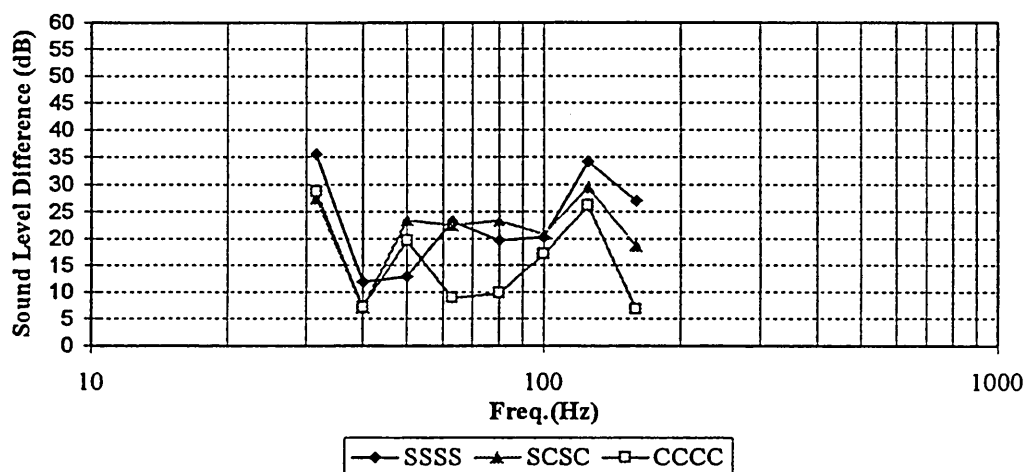

Fig. 12 The effects of the edge conditions of a 50mm brick wall on the sound level difference

1.5 DISCUSSION AND CONCLUSION

Numerical modelling of sound insulation at low frequencies at present is mainly confined to masonry walls, however some observations have relevance to lightweight inhomogenous constructions. Low acoustic modal density of small rooms, at low frequencies causes fluctuations of sound level difference in stiffness or mass control walls. Moreover, those fluctuations increase when there are structural resonances, which are controlled by the size and edge conditions of the party wall. That explains why poor field measurement reproducibility is obtained at low frequencies and the sound insulation of a party wall is difficult to predict when placed between any room pairs. In order to predict the sound pressure level difference of a

party wall at low frequencies, it may be necessary to define a correction factor, which takes account of room and party wall dimensions. In particular, knowledge of the modal density of the party wall and of the enclosures may be required to identify the type of coupling in each third octave bands: acoustical, acoustical-structural couplings, structural resonances.

So far, not much work has been carried out on lightweight panels and the numerical model of sound transmission between rooms needs also further developments, in particular appropriate modelling of damping at low frequencies is required.

1.6 REFERENCES

[1]   Brooks, J. R., Attenborough, K., "The implication of measured and estimated domestic source levels for insulation requirements", *Proceedings of I.O.A.*, vol.11 (11), 19-27, 1989

[2]   Grinwood, "Complaints about poor sound insulation between dwellings", IOA Acoustics Bulletin, 20 (4), 11-16, 1995

[3]   ISO 140, Part 3: 1990, Acoustics - Measurements of sound insulation in buildings and of building elements. Part 3. Laboratory measurements of airborne sound insulation of building elements.

[4]   ISO 140, Part 4: 1978, Acoustics - Measurements of sound insulation in buildings and of building elements. Part 4. Field measurements of airborne sound insulation of building elements.

[5]   J. Roland, "Adaptation of existing test facilities to low frequency measurements", *Proceeding of Inter-Noise 95*, vol 2, 1113-1116, 1995

[6]   Farina, A., Fausti, P., Pompoli, R. and Scamoni, F., 1996, Intercomparison of laboratory measurements of airborne sound insulation of partitions pompoli, *Proceeding of Inter-Noise 97*, 881-886, 1997

[7]   L. Gargliadini, J. Roland and J. L. Guyader, "The used of functional basis to calculate acoustic transmission between two rooms", *Journal of Sound and Vibration*, vol 145 (3), 457-478, 1991

[8]   W. Kropp, A. Pietrzyk, T. Khilman, "On the meaning of the sound reduction index at low frequencies", *Acta Acustica*, 2, 379-392, 1994

[9]   A. Osipov, P. Mees and G. Vermeir, 'Low frequency airborne sound transmission through single partitions in Buildings', *Applied Acoustics*, 52(3-4), 273-288, 1997

[10]   S. Maluski, B. Gibbs and H. Bougdah, 'Predicted and measured low frequency response of small rooms', I.O.A. Proceedings, Cranfield, vol 20(1), 87-92, 1998

[11]   S. Maluski, H. Bougdah, 'Predicted and measured low frequency response of small rooms', *Building Acoustics*, (1997)

[12]   Cutanda, V. and Pietrzyk, A., 1997, Low frequency sound transmission measurements and numerical simulations: A comparative study, *Proceeding of Inter-Noise 97*, vol 3, 1449-1452

[13]   C. Peng, D. Morrey and P. Sanders, "The measurements of low frequency impedance using an impedance tube", Journal of Low Frequency Noise, *Vibration and Active Control*, 1-10, 1998

[14]   A, Pietrzyk, "Optimization of sound insulation at low frequencies by selecting partition location", *Nordic Acoustical Meeting*, Helsinki, 12-14June 1996, 71-76, 1996

[15] K.A. Mulholland and R.H. Lyon, "Sound insulation at low frequencies", *Journal of Acoustical Society of America*, vol 54 (4), 867-878, 1973

[16] S. Maluski and B. Gibbs, "The influence of partitions boundary conditions on sound level difference between rooms at low frequencies", *Proceeding of Euro-Noise 97*, 1997

[17] T. Khilman, "Report on the influence of boundary conditions on the reduction index", Report ISO/TC 43/SC 2/WG 2, 1970

[18] M.C. Battacharya, and R.W. Guy, "The influence of the measuring facility on the measured sound insulating property of a panel", *Acustica*, vol 26, 344-348, 1972

[19] R.W. Guy, A. De Mey, and P. Sauer, "The effects of some physical parameters upon the laboratory measurements of sound transmission loss", *Applied Acoustics*, vol 18, 81-98, 1985

[20] L. Gargliadini, "Simulation numérique de la mesure en laboratoire de l'indice d'affaiblissement acoustique: effects des sources et de la géométrie de la paroie", *Colloque de Physique*, Colloque C2, Supplément au n^{0}2, Tome 51, Février 1990, 1081-1084, 1990

[21] A. Osipov, P. Mees, G. Vermeir, "Numerical simulation of airborne sound transmission at low frequencies: the influence of the room and the partition parameters", *Inter-Noise 97*, vol 2, 759-762 (1997)

[22] Y.J. Kang and J.S.Bolton, " A Finite Element model for sound transmission through foam lined double panel structures, *Journal of Acoustical Society of America*, vol 99(5), 2755-2765, 1996

[23] L. Gargliadini, "Simulation numerique de la transmission acoustique par les parois simples et multiples", Thesis, CSTB, France 1991